ISSN 0021-9673

VOL. 235 NO. 2 JANUARY 29, 1982

THIS ISSUE COMPLETES VOL. 235

HED

NAL OF

HROMATOGRAPHY

NATIONAL JOURNAL ON CHROMATOGRAPHY, ELECTROPHORESIS AND RELATED METHODS

ELSEVIER SCIENTIFIC PUBLISHING COMPANY
AMSTERDAM

JOURNAL OF CHROMATOGRAPHY

Scope. The *Journal of Chromatography* publishes papers on all aspects of chromatography, electrophoresis and related methods. Contributions consist mainly of research papers dealing with chromatographic theory, instrumental development and their applications. The section *Biomedical Applications*, which is under separate editorship, deals with the following aspects: developments in and applications of chromatographic and electrophoretic techniques related to clinical diagnosis (including the publication of normal values); screening and profiling procedures with special reference to metabolic disorders; results from basic medical research with direct consequences in clinical practice; combinations of chromatographic and electrophoretic methods with other physicochemical techniques such as mass spectrometry. In *Chromatographic Reviews*, reviews on all aspects of chromatography, electrophoresis and related methods are published.

Submission of Papers. Papers in English, French and German may be submitted, in three copies. Manuscripts should be submitted to: The Editor of *Journal of Chromatography*, P.O. Box 681, 1000 AR Amsterdam, The Netherlands, or to: The Editor of *Journal of Chromatography, Biomedical Applications*, P.O. Box 681, 1000 AR Amsterdam, The Netherlands. Reviews are invited or proposed by letter to the Editors and will appear in *Chromatographic Reviews* or *Biomedical Applications*. An outline of the proposed review should first be forwarded to the Editors for preliminary discussion prior to preparation. Submission of an article is understood to imply that the article is original and unpublished and is not being considered for publication elsewhere. For copyright regulations, see below.

Subscription Orders. Subscription orders should be sent to: Elsevier Scientific Publishing Company, P.O. Box 211, 1000 AE Amsterdam, The Netherlands. The *Journal of Chromatography* and the *Biomedical Applications* section can be subscribed to separately.

Publication. The *Journal of Chromatography* (incl. *Biomedical Applications*, *Chromatographic Reviews* and *Cumulative Author and Subject Indexes*, *Vols. 221–230*, *231–240* and *241–250*) has 25 volumes in 1982. The subscription prices for 1982 are:

J. Chromatogr. (incl. *Chromatogr. Rev.* and *Cum. Indexes*) + *Biomed. Appl.* (Vols. 227–251):
Dfl. 3625.00 plus Dfl. 500.00 (postage) total *ca.* US$ 1650.00)

J. Chromatogr. (incl. *Chromatogr. Rev.* and *Cum. Indexes Vols. 231–240* and *241–250*) only (Vols. 234–251):
Dfl. 2826.00 plus Dfl. 360.00 (postage) (total *ca.* US$ 1274.50)

Biomed. Appl. (incl. *Cum. Indexes Vols. 221–230*) only (Vols. 227–233):
Dfl. 1050.00 plus Dfl. 140.00 (postage) (total *ca.* US$ 476.00).

Journals are automatically sent by air mail to the U.S.A. and Canada at no extra costs, and to Japan, Australia and New Zealand with a small additional postal charge. Back volumes of the *Journal of Chromatography* (Vols. 1 through 226) are available at Dfl. 156.00 (plus postage). Claims for issues not received should be made within three months of publication of the issue. If not, they cannot be honoured free of charge. For customers in the U.S.A. and Canada wishing additional bibliographic information on this and other Elsevier journals, please contact Elsevier/North-Holland Inc., Journal Information Centre, 52 Vanderbilt Avenue, New York, NY 10017. Tel: (212) 867-9040.

Abstracts/Contents Lists published in Analytical Abstracts, Biochemical Abstracts, Biological Abstracts, Chemical Abstracts, Chemical Titles, Current Contents/Physical, Chemical & Earth Sciences, Current Contents/Life Sciences, Index Medicus, and Science Citation Index.

See page 3 of cover for Publication Schedule, Information for Authors, and information on the News Section and Advertisements.

Printed in The Netherlands

VOL. 235, NO. 2 JOURNAL OF CHROMATOGRAPHY JANUARY 29, 1982

CONTENTS

(Abstracts/Contents Lists published in Analytical Abstracts, Biochemical Abstracts, Biological Abstracts, Chemical Abstracts, Chemical Titles, Current Contents/Physical, Chemical & Earth Sciences, Current Contents/Life Sciences, Index Medicus and Science Citation Index)

(Continued overleaf)

Contents (continued)

Notes

Journal of Chromatography, 235 (1982) 281–288
Elsevier Scientific Publishing Company, Amsterdam — Printed in The Netherlands

CHROM. 14,335

MECHANISM OF PROTEIN RETENTION IN REVERSED-PHASE HIGH-PERFORMANCE LIQUID CHROMATOGRAPHY

R. A. BARFORD*, B. J. SLIWINSKI, A. C. BREYER* and H. L. ROTHBART
*Eastern Regional Research Center**, Philadelphia, PA 19118 (U.S.A.)*
(Received July 1st, 1981)

SUMMARY

The retention of a number of proteins by alkylsilicas with phosphate buffer–isopropanol, buffer–ethanol and buffer–detergent mobile phases (all pH 2.1) was investigated. In each case the percentage of organic component was varied over a wide range without causing appreciable retention. However, a solution composition was reached where very small changes, less than 1 % for the alcohols, caused dramatic increases in protein retention. Retention of proteins decreased with increased temperature. The mobile-phase composition was found to be characteristic of each protein at a given temperature so that separations could be achieved by careful selection of temperature and of buffer–organic component ratios. Calculations of the energy of interaction from surface tension and contact angle measurements supported the concept that protein retention by alkylsilicas may be explained by Van der Waals interactions, and that the interactions may be attractive or repulsive depending on the surface tension of the mobile phase.

INTRODUCTION

The potential of high-performance liquid chromatography (HPLC) for rapidly separating and/or characterizing mixtures of biomacromolecules such as proteins is slowly being realized, as discussed recently in a review by Regnier and Gooding[1]. We envision that a "multidimensional" chromatographic approach with various types of columns will be needed to resolve protein isolates from complex biological matrices. Therefore we have been developing information to understand better the interactions of proteins in chromatographic systems[2,3]. Hearn *et al.*[4], Revier[5] and Mönch and Dehnen[6] have used hydrophilic counterions to form ion-pairs with peptides and proteins and have explored conditions for elution from alkylsilica columns. In general, severe conditions, which may induce structural changes, were necessary for elution of proteins. The present study was undertaken to elucidate further the mechanisms of retention in these systems so that less stringent chromatographic conditions may be developed.

* Present address: Beaver College, Glenside, PA, U.S.A.
** Agricultural Research, Science and Education Administration, U.S. Department of Agriculture.

Theory

The general elution expression for chromatography may be written as:

$$V_R = V_M + V_S K \tag{1}$$

where V_R is retention volume, V_M is the mobile phase or interstitial volume (m), V_S is the volume of stationary phase(s), and K is the distribution coefficient. For considerations of protein–alkylsilica–aqueous mobile phase interactions:

$$-\Delta F_{smp} = RT \ln K \tag{2}$$

where ΔF_{smp} is the free energy of binding of the protein ion-pair (p) to the alkylsilica (s) in the presence of mobile phase (m). It may be assumed that under conditions of chromatography all of the protein exists as the ion-pair. Then the capacity factor, k', a measurable quantity, is given by

$$\ln k' = \ln K + \ln \varphi = (-\Delta F_{smp}/RT) + \ln \varphi \tag{3}$$

The value of φ is a column constant and reflects V_S/V_M. Horváth *et al.*[7] have proposed that the magnitude of the interaction energy is dominated by solute–solvent interactions when hydrocarbonaceous supports are used, and have developed expressions to describe solute retention in such systems. The model is based on comparisons of the energies required to form cavities in the mobile phase for accommodation of the solute and solute–hydrocarbon complex. Analysis of the theory reveals that the magnitude of the non-polar contact area plays a paramount role in retention. Assumptions concerning the relative sizes of the interacting species, particularly that the area of the solute be much less than that of the hydrocarbon, may limit its application to protein containing chromatographic systems.

Van Oss and Gillman[8] have proposed that Van der Waals attractions or repulsions control many biological interactions, particularly those between hydrophobic and hydrophilic molecules. The concept of Van der Waals repulsion emerges from the microscopic treatments of Fowkes[9], and the macroscopic treatments of Israellachvilli[10], and Good and Elbing[11] of the intermolecular forces at interfaces and is shown shematically in Fig. 1. The hydrocarbonaceous surface of the support is viewed as interacting with solute (protein) across a film of mobile phase. Expressions for calculating the forces between two surfaces from considerations of dielectric permittivity were developed, with the general result that the free energy of interaction between substances i and k immersed in a liquid j is expressed by:

$$\Delta F_{ijk} = -A_{ijk}/12\pi D^2 \tag{4}$$

where A_{ijk} is the Hamaker constant of interaction and D is the distance between surfaces, *i.e.* between phases considered as continuous dielectric media. Furthermore:

$$A_{ijk} = \pm B \sqrt{A_{iji} A_{kjk}} \tag{5}$$

where B is constant ($O \leqslant B \leqslant 1$)[10] for a particular system and was found to be close

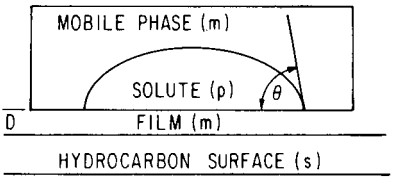

Fig. 1. Schematic of interaction of protein (p) at mobile phase (m)–alkylsilica (s) interface.

to unity for many systems. Thus, the energy of interaction between species i and k acting across medium j may be either attractive or repulsive. The interaction energy is also given by:

$$\Delta F_{ijk} = \gamma_{ik} - \gamma_{ij} - \gamma_{jk} \tag{6}$$

where the γ's are the designated surface tensions. Neuman *et al.*[12] showed that for solids an equation of state may exist between the solid–vapor, liquid–vapor, and solid–liquid interfacial tensions. These authors developed tables for obtaining the solid–vapor and solid–liquid values from the measure of the contact angle (σ) with a liquid of known surface tension. Thus, it is possible to calculate ΔF for the system shown in Fig. 1, where i = s, j = m, and k = p, and the solute is taken as solid, and to predict conditions for either retaining or eluting proteins from alkylsilica supports.

EXPERIMENTAL

Two chromatographs were used in these studies. One was assembled from components as described elsewhere[2] and operated at ambient temperatures. The other was a Spectra-Physics Model 8000B* operated at 25°C unless specified otherwise. Sample sizes were 25–100 μg. Flow-rates were 1 ml/min. In the chromatographs the fixed-wavelength detectors (254 nm) were used in series with a Schoeffel Model 770 fluorescence module equipped with a 370-nm emission filter. Excitation was at 280 nm. The presence of protein in collected fractions corresponding to the chromatographic peaks was confirmed by a dye-binding test[3].

Bovine serum albumin (BSA) and hemoglobin were purchased from Sigma (U.S.A.). The other proteins studied were from Polysciences, (U.S.A.). Their approximate molecular weights were confirmed by size-exclusion chromatography. Protein solutions prepared in mobile phase (1 mg/ml) were filtered through 0.45-μm bacteriological filters.

Mobile phases were prepared with ACS reagent-grade potassium dihydrogen phosphate and 85% phosphoric acid, HPLC grade organic solvents, and water purified with a Continental (U.S.A.) ion-exchange-carbon cartridge circulating system. The pH of 0.05 *M* KH_2PO_4 solutions was adjusted to 2.1 with 85% H_3PO_4 in the presence of the organic component. The non-ionic surfactant used was an ethoxylated alcohol (Neodol 91-6) obtained from Shell (U.S.A.). Sodium azide (0.02%) was added to aqueous solutions as a bacteriostat.

Surface tension measurements were made with a Du Nouy Tensiometer (Cen-

* Reference to brand or firm name does not constitute endorsement by the U.S. Department of Agriculture over others of a similar nature not mentioned.

tral Scientific, U.S.A.) and the appropriate ring corrections applied. Tensions so determined for a number of liquids agreed with published values to within ± 1.5 dynes/cm^2.

A goniometer (Gaertner Scientific, Chicago, IL, U.S.A.) was used to measure contact angles of sessile drops of mobile phases on layers of BSA. Surface tension of the octadecylsilica was approximated from contact angles on layers of octadecane, which was used to simulate the column support. Protein or octadecane layers of increasing thickness were prepared on glass slides by applying 500 μl of solutions containing 20, 30, 35 and 40 mg BSA/ml to clean microscope slides and drying at room temperature.

Partial specific volumes of BSA were calculated from densities[13] measured in a mechanical oscillator density meter (Model DMA02D, A. Paar, K. F. Graz, Austria). Concentrations of 5 mg/ml were used for determinations.

Columns used in these studies were: (I) Partisil-10 ODS, 250 × 4.6 mm I.D. (Whatman, U.S.A.); (II) LiChrosorb RP-8, 250 × 4.6 mm I.D. (Spectra-Physics, U.S.A.); (III) methylsilica, prepared in house by reaction of methyllithium with silica-chloride[14], 500 × 4.2 mm I.D.; (IV) Supelcosil LC-18, 150 × 4.6 mm I.D. plus guard column, (LC-18 Pellicular Packing) (Supelco, U.S.A.).

RESULTS AND DISCUSSION

First studies were conducted with phosphate buffer and isopropanol mixtures (pH 2.1) as mobile phases to obtain data which could be compared with earlier reports[6]. The data (Fig. 2) show that no proteins are retained at isopropanol concentrations above 40%. As the concentration of the alcohol is reduced a composition is reached below which protein cannot be observed to elute. This composition was different for each protein studied. The capacity factor (k') increases from zero to a very large number over a very narrow range of mobile-phase compositions. The

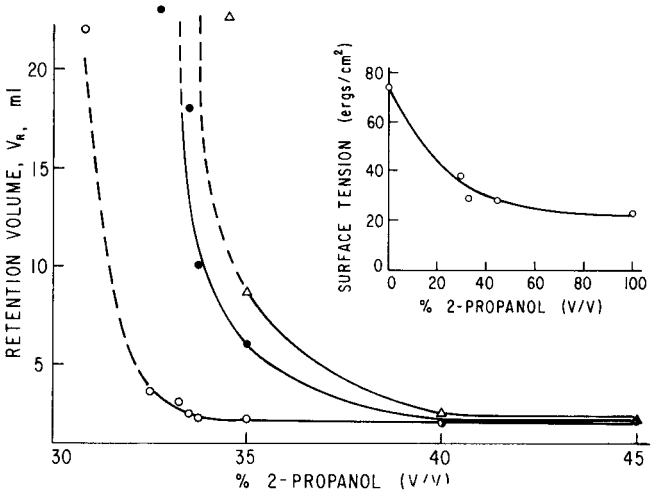

Fig. 2. Effect of isopropanol concentration and surface tension on retention of several proteins: ○, bovine serum albumin; ●, β-lactoglobulin; △, hemoglobin. Mobile phase: 0.05 *M* phosphate buffer–isopropanol (pH 2.1). Column: C_{18} (I).

addition of other additives to the mobile phase to bring about elution was not required, in contrast to other reports. This retention behavior was not peculiar to this particular reversed-phase column but was observed with another octadecylsilica column from a different manufacturer (IV) and with octyl silica (II) and methylsilica (III) columns from other sources (Fig. 3).

Elution of minor non-proteinaceous components of samples and appearance of "solvent peaks" often gave ambiguous results when only UV detection was used. The use of a fluorescence detector with excitation at 280 nm and with a 370-nm long-pass emission filter reduced much of the ambiguity. Fractions of mobile phase corresponding to observed peaks were collected, and the presence or absence of protein was confirmed by a dye-binding test[2].

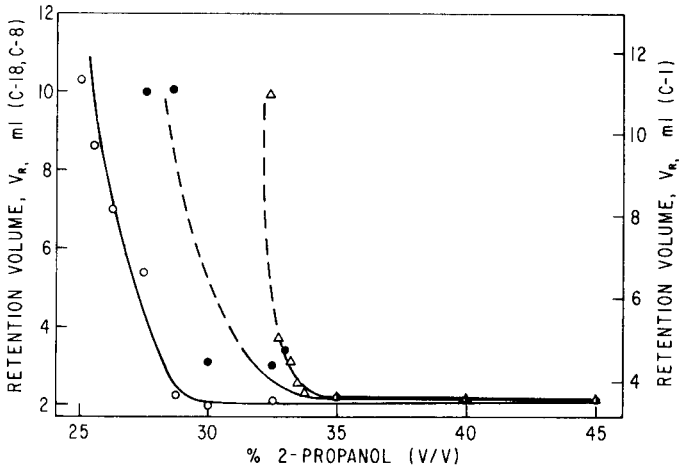

Fig. 3. Variation of retention of BSA with selected reversed-phase columns: △, C_{18} (I); ●, C_8 (II); ○, C_1 (III).

The sudden change in retention characteristics with increasing alcohol concentration could conceivably be the result of an alcohol-dependent change in conformation (denaturation) of the protein molecule. To test this hypothesis, partial specific volumes of BSA in solutions of varying isopropanol concentration were measured. The partial specific volume of BSA increased, but only slightly, over the range of concentrations used in the chromatography experiments (0.72 ± 0.01 ml/g at 40% isopropanol to 0.67 ± 0.01 ml/g at 30% (n = 2)). However, considering the pore diameter of the packings studied (less than 60 Å) and the buffer–isopropanol ratios coincident with the sudden change in retention, elution by a size-exclusion mechanism did not seem likely. Furthermore, elution order of proteins in this and subsequent studies did not correlate with molecular size (see Table I).

Little correlation of elution order with average hydrophobicity was found. The hydrophobicity scale shown in Table I (average hydrophobicity) is one of several in common use. It is based on the number of residues of each amino acid and the experimentally determined free energies of transfer of amino acid moieties from water to ethanol[15]. The average hydrophobicity has correlated well with protein properties such as solubility, aggregation phenomena, structural characteristics and thermal stability.

TABLE I

PROPERTIES OF PROTEINS

	Molecular weight (kD)[15]	*Average hydrophobicity (cal/residue)*[15]	*pI*[16]
Lysozyme (LYZ)	15	970	11[17]
Carbonic anhydrase (CAR)	30	1060	7.3
Bovine serum albumin (BSA)	67	1120	4.8
Hemoglobin (Hb)	68	1120	7.0
β-Lactoglobulin (β-LAG)	17[18]	1230	5.2

Plots of surface tension *vs.* mole fraction of alcohol in the buffer–alcohol mixture were linear over the range used in chromatography. However, when viewed with concentration expressed as volume percent (as usually done in chromatography), greater changes in surface tension were observed in the concentration range where large changes in protein retention occurred. Therefore, surface properties of the system seemed to be important factors in retention. When ethanol replaced isopropanol a larger proportion of ethanol was needed for BSA elution (Fig. 4). Nevertheless, elution in both cases occurred at about the same surface tension of mobile phase (*ca.* 33 ergs/cm^2). Buffer salts precipitated when methanol was used.

Free energies of interaction (ΔF_{smp}) of the mobile phase, stationary phase and BSA systems were estimated from contact angle measurements as proposed by Van Oss *et al.*[19] using the equation-of-state approach and the table based on it as published by Neuman *et al.*[12]. The results of the contact angle and surface tension measurements and the values derived from them are given in Table II. The ΔF_{smp} values predicted that BSA would be eluted when the mobile phase contained less than *ca.* 49% buffer when ethanol was the organic component. This same elution composition was determined by chromatography. Layers of octadecane were used to simulate

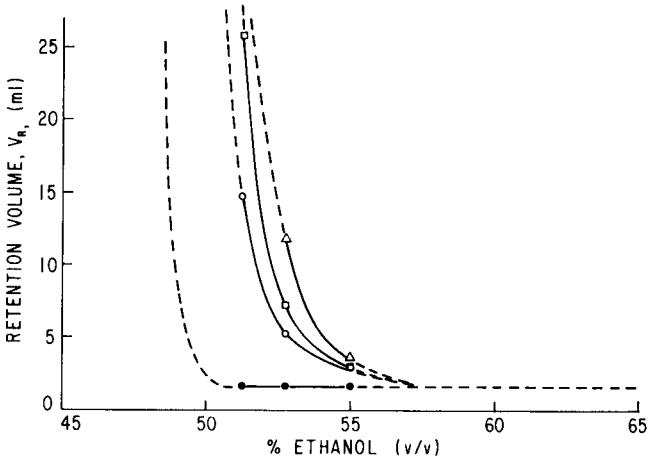

Fig. 4. Effect of ethanol concentration and surface tension on retention of several proteins: ●, bovine serum albumin; □ and ○, lysozyme (two peaks observed); △, carbonic anhydrase. Mobile phase: phosphate buffer–ethanol. Column C_{18} (IV).

stationary phase in the contact angle experiments. There was no measurable difference in contact angle over the solvent compositions used. Some difficulties were encountered in depositing a smooth layer of BSA on the slide, which may account for the large average deviation of the measured angles compared with those obtained for known liquids on teflon, which agreed within $\pm 1^\circ$ of published values. Dissolution of protein into the drop may be another source of error. The average contact angle over layers deposited from all BSA concentrations was used in calculations. Considering these factors, the thermodynamic assumptions made in the equation-of-state approach used for the calculations of ΔF_{smp} are only approximated in these experiments. Nevertheless, consideration of these data, eqn. 3, and the chromatographic result support the concept that protein retention by alkylsilicas may be explained by Van der Waals interactions, and that the interactions may be repulsive or attractive depending on the surface tension of the mobile phase.

TABLE II

ESTIMATION OF INTERACTION ENERGY IN BSA–OCTADECANE*–ETHANOL–BUFFER SYSTEM

Percent buffer in ethanol	*Contact angle BSA (degrees)*	*Surface tension mobile phase (ergs/cm²)*	*Calculated values***			
			γ_{sm} *(ergs/cm²)*	γ_{pm} *ergs/cm²)*	γ_{sp} *ergs/cm²)*	ΔF_{smp} *(ergs/cm²)*
45.6	5 ± 2	32	1.0***	0	1.3	+0.3
48.8	9 ± 3	33	1.1	0	1.1	0
52.5	12 ± 3	34	1.1	0.1	1.0	−0.2
56.3	24 ± 4	35	1.2	0.1	0.5	−0.8
60.0	29 ± 2	36	1.2	0.2	0.4	−1.0

* Contact angles of mobile phases with octadecane were 45 ± 2° over the range of mobile phase compositions studied.

** From tables of ref. 12.

*** Interpolated values.

The retention of all of the proteins studied was observed to decrease with increasing temperature (Fig. 5). It is difficult to assess experimentally the effect of temperature in eqn. 6. For many liquids, surface tension decreases by *ca.* 0.1 ergs/cm² per degree near room temperature[20]. Limited data on contact angle measurements at various temperatures suggests little variation with temperature[21]. Thus, complete reconciliation of the observed temperature effects on protein retention with the surface chemical model cannot be made at present.

Aqueous solutions of alcohols are known to denature proteins, and the kinetics of denaturation increase with increasing alkyl chain length[22]. This denaturation may be reversed in some cases. However, the use of alkylsilicas in the chromatography of proteins to solve important biochemical problems would be enhanced if less drastic mobile phases could be found. The observations reported here suggest that small amounts of surfactants could be added to buffers to lower surface tension sufficiently to bring about elution. The use of such mobile phases may permit separation and recovery of proteins in their native state. Preliminary HPLC experiments indicate retention could be controlled by addition of a non-ionic surfactant to phosphate

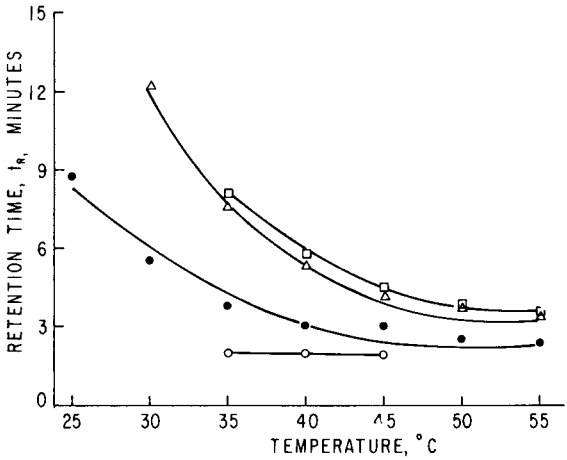

Fig. 5. Variation of protein retention with temperature. Column: C_{18} (I). Mobile phase, 33.8% isopropanol in 0.05 *M* KH_2PO_4 buffer, pH 2.1. ○, Bovine serum albumin; ●, carbonic anhydrase; △, lysozyme; □, β-lactoglobulin.

buffer. More detailed studies of the effects of surfactant, pH and other chromatography variables on the recovery and structure of proteins as well as mechanisms of retention are being conducted.

ACKNOWLEDGEMENTS

A.C.B. was a National Science Foundation Faculty Development Fellow at the Center. The authors thank Betty J. Mays for measuring contact angles.

REFERENCES

1 F. E. Regnier and K. M. Gooding, *Anal. Biochem.*, 103 (1980) 1.
2 R. A. Barford, B. J. Sliwinski and H. L. Rothbart, *J. Chromatogr.*, 185 (1979) 393.
3 R. A. Barford, B. J. Sliwinski and H. L. Rothbart, *Chromatographia*, 12 (1979) 285.
4 M. T. W. Hearn, B. Grego and W. S. Hancock, *J. Chromatogr.*, 185 (1979) 429.
5 J. E. Revier, *J. Liquid Chromatogr.*, 1 (1978) 343.
6 W. Mönch and W. Dehnen, *J. Chromatogr.*, 147 (1978) 415.
7 Cs. Horváth, W. Melander and I. Molnár, *J. Chromatogr.*, 125 (1976) 129.
8 C. J. van Oss and C. F. Gillman, *Phagocytic Engulfment and Cell Adhesiveness*, Dekker, New York, 1975.
9 F. M. Fowkes, in B. R. Weiss (Editor), *Surfaces and Interfaces, I Chemical and Physical Characteristics*, Syracuse University Press, Syracuse, NY, 1967.
10 J. N. Israellachvilli, *J. Chem. Soc., Faraday Trans. II*, 69 (1973) 1729.
11 R. F. Good and E. Elbing, *Ind. Eng. Chem.*, 62 (1970) 54.
12 A. W. Neuman, D. R. Absolom, D. W. Frances and C. J. van Oss, *Separ. Purif. Methods*, 9 (1980) 69.
13 O. Kratky, H. Leopold and H. Stabinger, *Methods Enzymol.*, 27D (1973) 98.
14 P. Magidman, R. A. Barford, D. H. Saunders and H. L. Rothbart, *Anal. Chem.*, 48 (1976) 44.
15 C. C. Bigelow, *J. Theor. Biol.*, 16 (1967) 187.
16 D. Malamud and J. W. Drysdale, *Anal. Biochem.*, 86 (1978) 620.
17 L. A. Decker, *Worthington Manual*, Worthington Biochem. Corp., Freehold, NJ, 1977, p. 185.
18 R. Townend and S. N. Timasheff, *J. Amer. Chem. Soc.*, 79 (1957) 3613.
19 C. J. Van Oss, D. R. Absolom and A. W. Neuman, *Separ. Sci. Technol.*, 14 (1979) 305.
20 A. W. Adamson, *Physical Chemistry of Surfaces*, Wiley-Interscience, New York, 1960, p. 54.
21 H. Schonhorn, *Nature (London)* 210 (1966) 896.
22 H. B. Bull and H. Breese, *Biopolymers*, 17 (1978) 2128.

Journal of Chromatography, 235 (1982) 289–297
Elsevier Scientific Publishing Company, Amsterdam — Printed in The Netherlands

CHROM. 14,312

CHROMATOGRAPHIC STUDY OF OPTICAL RESOLUTION

IX*. OPTICAL RESOLUTION OF MONOVALENT COMPLEX CATIONS ON AN ANION-EXCHANGE COLUMN

SHIGEO YAMAZAKI** and HAYAMI YONEDA*

Department of Chemistry, Faculty of Science, Hiroshima University, Higashisenda-machi, Naka-ku, Hiroshima 730 (Japan)

(Received August 24th, 1981)

SUMMARY

The principle has been established of the optical resolution of a monovalent complex cation on an anion-exchange column using an eluent containing a divalent chiral selector anion. Based on the expressions of two equilibria, ion association and ion exchange, general equations have been derived for the retention volume, the difference in the retention volumes and the separation factor for two enantiomers. These equations have been verified by experimental data for actual complexes eluted with the eluent containing antimony *d*-tartrate.

INTRODUCTION

The chromatographic resolution of racemic cations is usually carried out on a cation-exchange column using an eluent containing chiral selector anions. Many examples of a complete resolution by this technique have been reported[1]. In contrast, there are few papers[2,3] which describe the optical resolution of racemic cations through a column packed with the chiral selector–anionic form of an anion-exchange resin***. This type of chromatography was first attempted by Yoshino *et al.*[2] who succeeded in the resolution of racemic $[Co(en)_3]^{3+}$ on an anion-exchange resin saturated with optically acitve *d*-tartrate or antimony *d*-tartrate (hereafter abbreviated as *d*-$tart^{2-}$ and $[Sb_2$-*d*-$tart_2]^{2-}$ respectively). They also achieved optical resolution of racemic $[Co(EDTA)]^-$ by elution through a cation-exchange column saturated with optically active Λ-$[Co(en)_3]^{3+}$. However, since their interest was focused on finding a substitute for an optically active resin, no consideration on the detailed mechanism of an optical resolution was made either from the stereochemical point of view or from

* Part VIII: see ref. 6.

** Present address: Central Research Laboratory, Toyo Soda Manufacturing Co. Ltd., 4560 Tonda, Shin-Nanyo-shi, Yamaguchi-ken 746, Japan.

*** In ref. 3 the resolution of the octahedral complex cations was achieved by preferential adsorption on an anion-exchange column in the *d*-tartrate form.

0021-9673/82/0000–0000/$02.75

the chromatographic separation theory. Thus, only a partial resolution was obtained. A similar attempt was made by Gaál and Inczédy[4] who reported a complete resolution of racemic aspartic acid on a cation-exchange column saturated with optically active Λ-$[Co(en)_3]^{3+}$. They assumed a preferential ion association of one enantiomeric form of aspartate anion over the other towards Λ-$[Co(en)_3]^{3+}$. However, although they gave no detailed discussion on the separation mechanism, the experimental conditions they used do not seem to be reasonable for the enantiomeric separation based on preferential ion association.

Here we reconsider the separation of metal cations using an anion-exchange resin. This technique was explored as part of the Manhattan Project, and many examples of separations were reported after World War II[5]. In this method, metal ions are adsorbed on an anion-exchange column as negatively charged complex anions and eluted with an eluent containing anionic ligands. It consists of two equilibria, complex formation and ion exchange, and the separation is achieved owing to the difference in their degrees of complex formation. The theory of separation was established along this line. A similar situation can be imagined for the optical resolution of racemic cations on an anion-exchange column.

Consider the case where monovalent complex cations are to be separated into enantiomers with divalent chiral selector anions. Complex cations form ion pairs with chiral selector anions. Since the ion pair thus formed has a single negative charge, it can be retained on an anion-exchange resin. Although the enantiomeric separation on an anion-exchange column is, in principle, carried out in the same way as the metal ion separation, the former has disadvantages compared with the latter. In the metal ion separation, complex formation, such as $M^{2+} + 4Cl^- \rightleftarrows [MCl_4]^{2-}$, is an inner-sphere association and its formation constant is large. However, in the present enantiomeric separation, we are dealing with an outer-sphere association and its formation constant is relatively small. Also, while the charge of the anionic complex in the metal ion separation is higher than that of the anionic ligand, the charge of the ion pair in the present enantiomeric separation is lower than that of the selector anion. Therefore, it is fairly difficult for the complex to be retained on an anion-exchange column. Poor resolution on an anion-exchange column is expected. For good resolution, it is necessary to have a large retention volume for each enantiomer. The dissociation of the ion pair should be depressed with an eluent containing the proper concentration of a chiral selector anion. However, if the concentration is too high, the chiral selector anion will replace the adsorbed ion pair, which results in a decrease in the retention volume. There should be an optimum concentration of the eluent. The situation can be formulated in a quantitative way. This work describes the theory of optical resolution on an anion-exchange column and the experimental data which support the theory.

THEORETICAL

Suppose a monovalent complex cation M^+ is loaded on to an anion-exchange resin of a divalent anionic form X^{2-} and eluted with an eluent containing the anionic ligand X^{2-}. The complex cation M^+ is associated with the anion X^{2-} to form a negatively charged ion pair MX^- which is retained on an anion-exchange resin because of its negative charge. Now, let us consider how the complex M^+ is eluted with

varying concentrations of X^{2-} in an eluent. In the low concentration range, the increase in the concentration in X^{2-} causes an increase in the formation of the ion pair MX^-, which results in an increase in the retention volume of the complex ion. However, above a certain concentration of X^{2-}, another trend becomes predominant. The ion-pair formation reaches a limit. The increased numbers of the anion X^{2-} are directed mainly to exchanging with the adsorbed MX^-. This results in a decrease in the retention volume of the complex ion. Considering two equilibria, ion-pair formation and ion exchange, the situation can be described in a quantitative way.

As the ion-pair formation equilibrium we have

$$M^+ + X^{2-} \rightleftarrows MX^-$$

where the association constant β is defined by

$$\beta = \frac{[MX]}{[M]\,[X]} \tag{1}$$

For the ion-exchange equilibrium on an anion-exchange resin, we have

$$2R(MX) + X^{2-} \rightleftarrows MX^- + R_2X \tag{2}$$

where R is the functional group of the resin. Here, the ion-exchange equilibrium constant K^X involving MX^- and X^{2-} is defined by

$$K^X = \frac{(MX)^2[X]}{[MX]^2(X)} \tag{2}$$

The symbol in parentheses denotes the concentration in the ion-exchange resin, and the symbol in square brackets the concentration in the eluent.

Since the complex ion exists in two forms, M^+ and MX^-, the distribution ratio D_M is given by

$$D_M = \frac{(MX)}{[MX] + [M]} \tag{3}$$

If the total concentration of the complex ion is assumed to be low both in the resin and the eluent phases, *i.e.* $(X) \gg (MX)$ and $[X] \gg [MX]$, the concentration of the divalent anion adsorbed in the resin is, to a good approximation, equal to half of the ion-exchange capacity Q (mequiv./ml), *i.e.*

$$(X) = \frac{1}{2} \cdot Q \tag{4}$$

Using eqns. 1–4, the distribution ratio D_M is expressed by

$$D_M = \frac{\sqrt{K^X Q[X]/2}}{[X] + \frac{1}{\beta}} \tag{5}$$

The adjusted retention volume, V, for the elution of the complex ion can be related to D_M by

$$V = D_M V_r$$

where V_r is the volume of the resin in the column. Substituting V for D_M in eqn. 5, we obtain

$$V = \frac{K\sqrt{[X]}}{[X] + \frac{1}{\beta}} \tag{6}$$

where $K = V_r\sqrt{K^X Q/2}$. As is easily seen from $dV/d[X] = 0$, the retention volume V has a maximum equal to $K\beta/2$ at an eluent concentration [X] of $1/\beta$.

Now that the general equation for elution has been obtained, chromatographic conditions for enantiomeric separation can be examined based on this general equation. The complex ion M^+ exists in two enantiomeric forms, Δ-M^+ and Λ-M^+. We have to discriminate the quantities related to them by putting the symbols Δ and Λ as affixes such as V_Δ, V_Λ, β_Δ and β_Λ. Fig. 1 shows a plot of the retention volumes V_Δ and V_Λ against [X] according to eqn. 6, where β_Λ is assumed to be greater than β_Δ. It must be noted that the maximum in V appears at different values ($1/\beta_\Delta$ and $1/\beta_\Lambda$) of [X] for the two enantiomers.

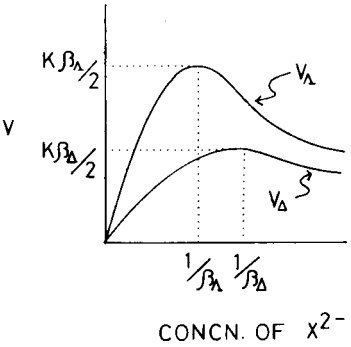

Fig. 1. Theoretical curves of retention volumes, V_Δ and V_Λ, as a function of eluent concentration [X].

If K in eqn. 6 is assumed to be unchanged for the two enantiomers, the difference in the retention volumes ΔV can be expressed by

$$\Delta V = V_\Lambda - V_\Delta = \frac{K\left(\frac{1}{\beta_\Delta} - \frac{1}{\beta_\Lambda}\right)\sqrt{[X]}}{\left([X] + \frac{1}{\beta_\Lambda}\right)\left([X] + \frac{1}{\beta_\Delta}\right)} \tag{7}$$

where the product $K(1/\beta_\Delta - 1/\beta_\Lambda)$ can be regarded as constant and described as K'. Thus, eqn. 7 can be rewritten as

$$\Delta V = \frac{K'\sqrt{[X]}}{\left([X] + \frac{1}{\beta_\Lambda}\right)\left([X] + \frac{1}{\beta_\Delta}\right)} \tag{8}$$

The plot of ΔV against [X] is shown in Fig. 2. Here again, a maximum is obtained. It can be proved mathematically that this maximum in ΔV lies at a smaller value of [X] than either of the two maxima in V for Δ and Λ.

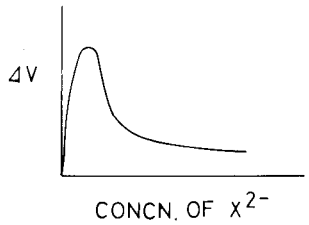

Fig. 2. Theoretical curve of the difference (ΔV) in the retention volumes, V_Δ and V_Λ, as a function of eluent concentration [X].

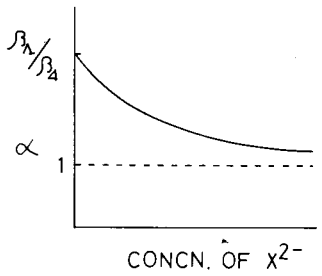

Fig. 3. Theoretical curve of the separation factor as a function of eluent concentration [X].

The separation factor α is defined as the ratio of the retention volumes V_Λ and V_Δ. It is expressed as

$$\alpha = \frac{V_\Lambda}{V_\Delta} = \frac{\beta_\Lambda}{\beta_\Delta}\cdot\frac{\beta_\Delta[X] + 1}{\beta_\Lambda[X] + 1} \tag{9}$$

Inspection of this equation reveals that $\alpha = \beta_\Lambda/\beta_\Delta$ at [X] = 0 and reaches unity at [X] = ∞. The plot of α against [X] is shown in Fig. 3.

EXPERIMENTAL

Sample complexes

Three monovalent complexes, *cis*(O),*cis*(N)-[Co(en)(gly)$_2$]Cl·2H$_2$O (A), *cis*(O),*trans*(N)-[Co(NH$_3$)$_2$(gly)$_2$]Cl·H$_2$O (B) and *cis*-α-[Co(N$_3$)$_2$(trien)]I (C) were used as samples. The preparations of these complexes were described previously[6].

Eluent

The eluent used was water containing potassium antimony *d*-tartrate, K$_2$[Sb$_2$-*d*-tart$_2$], at various concentrations.

Column

A large column (60 × 2.0 cm I.D.) was used for complex A, and a small

column (40 × 1.5 cm I.D.) for complexes B and C. Each column was packed with the $[Sb_2\text{-}d\text{-}tart_2]^{2-}$ form of QAE-Sephadex A-25 anion exchanger.

Procedure

A sample solution was prepared by dissolving 20 mg of complex A and 10 mg of complexes B and C in 2 ml and in 1 ml of eluent, respectively. The flow-rate was set at 0.38 ml/min for complex A and 0.16 ml/min for complexes B and C using a peristaltic pump. The detector was operated at the first absorption band of each complex. Circular dichroism and ultraviolet spectra of the eluate for each run proved that complete resolution was achieved.

RESULTS AND DISCUSSION

To check the validity of the theory, chromatographic separation was studied for three actual complexes, *cis*(O),*cis*(N)-$[Co(en)(gly)_2]^+$ (A), *cis*(O),*trans*(N)-$[Co(NH_3)_2(gly)_2]^+$ (B) and *cis*-α-$[Co(N_3)_2(trien)]^+$ (C) using eluents containing $K_2[Sb_2\text{-}d\text{-}tart_2]$ at various concentrations. Typical elution curves obtained with three different eluent concentrations are shown for complex A in Fig. 4. Comparison of these three elution curves reveals that the separation of the two peaks is greater with 0.01 *M* than with the other two concentrations, 0.0025 and 0.01 *M*. There seems to be an optimum concentration of the eluent for the best separation of the two peaks. A similar situation is seen for complexes B and C. This is as predicted by the theory.

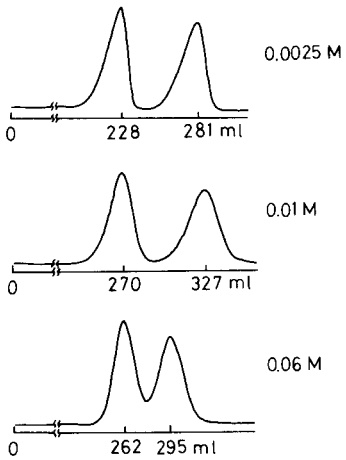

Fig. 4. Typical elution curves of *cis*(O),*cis*(N)-$[Co(gly)_2(en)]^+$ with three concentrations of $K_2[Sb_2\text{-}d\text{-}tart_2]$ solution.

Fig. 5 shows plots of the adjusted retention volumes for the enantiomers of the three complexes against the eluent concentrations. These plots show a close resemblance to those in Fig. 1. As expected from the theory, there is a maximum in the curve of retention volume against eluent concentration in all three cases. At low eluent concentration, a large fraction of the complex ion exists as cations, with only a very small fraction existing as negatively charged ion pairs. Under these circumstances, an in-

crease in the eluent concentration results in an increase in the number of the ion pairs retained by the anion-exchange resin. Thus, it brings about an increase in the retention volume. However, this trend soon reaches a limit. Above a certain eluent concentration, an increase in the numbers of the selector anion no longer brings about an increase in the numbers of the ion pair, but is directed towards expelling the adsorbed ion pairs, so that the retention volume of the complex ion will begin to decrease as the eluent concentration increases. The same trend can be found in Kraus and Nelson's review[5] in which for many metal ions there is a maximum value for the retention volume when plotted against the concentration of the anionic ligands.

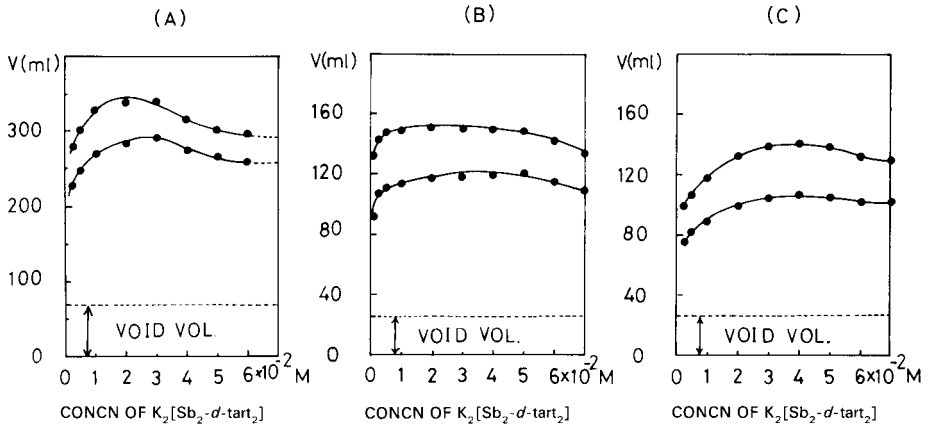

Fig. 5. Dependence of the retention volume on the concentration of $K_2[Sb_2$-*d*-$tart_2]$ for the complexes *cis*(O),*cis*(N)-$[Co(gly)_2(en)]^+$ (A), *cis*(O),*trans*(N),*cis*(NH_3)-$[Co(gly)_2(NH_3)_2]^+$ (B) and *cis*-α-$[Co(N_3)_2(trien)]^+$ (C).

Fig. 6 shows plots of the peak separation, *i.e.* the difference in the retention volumes of the two enantiomers (ΔV) against the concentration of the chiral selector anion. Here again, a maximum is found in the curve. As mentioned in the Theoretical section, the concentration which gives a maximum value of ΔV is definitely lower than that which gives a maximum value of the retention volume. A careful look at these three curves, A, B and C, will reveal that while A and B have their maxima at very low eluent concentrations, C has its maximum at a high eluent concentration. The same situation can be seen in the plots of the retention volume in Fig. 5. Here again, the maximum lies at a higher eluent concentration in C, than in A and B. Since the eluent concentration which gives the maximum retention volume is equal to the reciprocal of the ion-pair formation constant, the above fact means that the tendency towards ion-pair formation in complex C is smaller than that in the other two complexes.

Fig. 7 shows the trend of the separation factor α with increasing eluent concentration. As predicted from the theory separation factor decreases with increasing eluent concentration. Here it must be noticed that the separation factor is always greater in C than in A and B. It is also worth noting that the separation factor in C will not decrease to unity so soon with increasing eluent concentration, contrasting with the cases in A and B. These facts can be understood from eqn. 9. As seen in this equation, the separation factor is a product of two terms, β_A/β_Δ and $(\beta_\Delta[X] +$

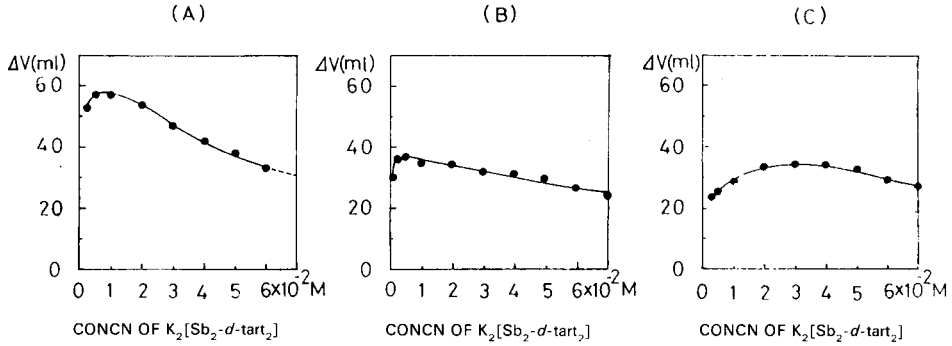

Fig. 6. Dependence of the difference (ΔV) in the retention volumes, V_Δ and V_Λ on the concentration of $K_2[Sb_2$-d-$tart_2]$ solution A, B and C.

1)/(β_Λ[X] + 1). At [X] = 0, the second term becomes unity, so that the separation factor is just the ratio of two ion-pair formation constants. At [X] = ∞, the second term becomes $\beta_\Delta/\beta_\Lambda$, which is just the reciprocal of the first term, so that the separation factor is unity. Between these two extreme cases, the second term varies from 1 to $\beta_\Delta/\beta_\Lambda$. In case β_Δ and β_Λ are small, the second term will not decrease so soon to $\beta_\Delta/\beta_\Lambda$ as [X] increases. Thus, the separation factor also will not decrease so soon to unity. This corresponds to the case in C. It can therefore be concluded that although the degree of ion-pair formation is small in complex C, discrimination between the two enantiomers is large.

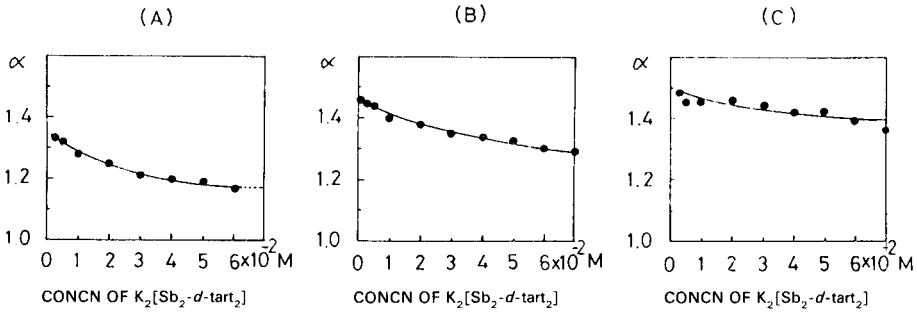

Fig. 7. Dependence of the separation factor α on the concentration of $K_2[Sb_2$-d-$tart_2]$ for complexes A, B and C.

Finally, the advantage of this "ambush-type" chromatography over ordinary chromatography must be mentioned. If racemic cations are resolved on a cation-exchange column, a large amount of a chiral selector must be used as an eluent. Therefore, if we want to obtain the resolved enantiomers as crystals, we have to isolate them from the eluate containing a large amount of the chiral selector. In contrast, in the "ambush-type" chromatography, a fairly dilute solution of the chiral selector is used, so that it is much easier to obtain the resolved enantiomers in pure form.

REFERENCES

1 Y. Yoshikawa, *Coord. Chem. Rev.*, 28 (1979) 205.
2 Y. Yoshino, H. Sugiyam, S. Nagaito and H. Kinoshita, *Sci. Pap. Coll. Gen. Educ., Univ. Tokyo*, 16 (1966) 57.
3 R. D. Gillard and P. R. Mitchell, *Transition Met. Chem. (Weinheim)*, 1 (1976) 223.
4 J. Gaál and J. Inczédy, *Talanta*, 23 (1976) 78.
5 K. A. Kraus and F. Nelson, in W. J. Hamber (Editor), *The Structure of Electrolyte Solutions*, Wiley, New York, 1959, p. 340.
6 S. Yamazaki and H. Yoneda, *J. Chromatogr.*, 219 (1981) 29.

Journal of Chromatography, 235 (1982) 299–308
Elsevier Scientific Publishing Company, Amsterdam — Printed in The Netherlands

CHROM. 14,303

CHROMATOGRAPHIC BEHAVIOUR OF DIASTEREOISOMERS

VI. RELATIVE RETENTIONS OF THE DIASTEREOISOMERS OF 3-HYDROXY-2,3-DIARYLPROPIONATES ON SILICA GEL AND THEIR THEORETICAL INTERPRETATION

M. D. PALAMAREVA* and B. J. KURTEV
Department of Chemistry, University of Sofia, Sofia 1126 (Bulgaria)
and
M. P. MLADENOVA and B. M. BLAGOEV
Institute of Organic Chemistry, Bulgarian Academy of Sciences, Sofia 1113 (Bulgaria)
(First received April 1st, 1981; revised manuscript received August 18th, 1981)

SUMMARY

Separations by thin-layer chromatography on silica gel have been achieved for fifteen diastereoisomeric pairs of the type Ar–CH(X)–CH(COOR)–Ar′ (X = OH, OAc or NHPh; R = Me, iso-Pr, *n*-Bu, iso-Bu or *tert.*-Bu) which have known relative configurations. R_F values of the compounds studied have been measured as a function of the concentration of diethyl ether in mixtures with heptane. Thus, the values of a parameter, related to the adsorption pattern, have been found. The relative retentions of the diastereoisomers $R_{F(erythro)} > R_{F(threo)}$ and $R_{F(threo)} > R_{F(erythro)}$ within those compounds where X = OH and R = *tert.*-Bu have been explained. Four different patterns of adsorption have been discussed. The data and the conclusions permit further outlining of the scope of each of the two retentions; they also support the previously elaborated criteria for thin-layer chromatographic assessment of the relative configurations of other diastereoisomeric pairs of tetrasubstituted ethanes.

INTRODUCTION

Separation of diastereoisomeric compounds by liquid–solid chromatography (LSC) on polar adsorbents such as silica gel and alumina is widely practised[1–23] (see also references cited in the previous papers of the present series[24–28]). The techniques used are thin-layer chromatography (TLC), column chromatography and normal-phase high-performance liquid chromatography, the last being lately of increased importance. The separation itself has been the main problem as it enables isolation of each isomer in pure form. In some cases of related compounds, one isomer moves faster than its diastereoisomer. More comprehensive treatment of this phenomenon is given by Helmchen and co-workers[5–7,17] and by Pirkle and co-workers[2,3]. The most difficult point of this problem is the inversion, *i.e.* a few of the diastereoisomers have a reverse relative retention[8].

0021-9673/82/0000–0000/$02.75

In our series[24–28], diastereoisomeric tetrasubstituted ethanes, >CH–CH< and related cyclic compounds, which have known relative configurations, have been investigated. Our efforts have been directed to performing TLC separation on the same silica gel and thus to establish experimentally the relative retention of the diastereoisomers. The retention orders have been elucidated on the basis of LSC theory[29–35]. As far as tetra-substituted ethanes are concerned, the retention $R_{F(erythro)} > R_{F(threo)}$ and the opposite alternative, $R_{F(threo)} > R_{F(erythro)}$, are both possible, depending mainly on the nature of the substituents. The purpose of our studies is to outline the scope of each pattern of retention. So far, semi-empirical criteria have been given[25,28] for using the order $R_{F(erythro)} > R_{F(threo)}$ to assess the relative configurations of some diastereomeric tetrasubstituted ethanes. Since the diastereoisomeric species investigated showed mainly the latter order, it was of utmost importance to find compounds having the opposite order. This paper reports the TLC behaviour of diastereoisomeric 3-hydroxy-2,3-diarylpropionates and their O-acetyl derivatives which offer such a possibility.

In our opinion, any differences in the chromatographic behaviour of diastereoisomers deserves detailed investigation since they could be highly informative. For instance, the reverse retentions of a given set of diastereoisomers obtained on two separate silica gels[11] are probably due to secondary adsorbance effects (see p. 140 of ref. 29); a study of intramolecular hydrogen bonding in the solutes could be of significance. It is of importance to clarify the factors responsible for the inversion of the retention sequence due only to replacement of CH_3 by C_2H_5 in a mevalonate series[8]. It should be mentioned that the retentions established in the present paper and in refs. 25 and 26 were even more surprising than those in ref. 8. Besides, the interpretation of $R_{F(threo)} > R_{F(erythro)}$ established[18] for eight diastereoisomeric pairs of type I (see the formulae below, X = OH or derivatives, Y = CH_3 or CH_2HgCl, Ar = Z = Ph or 4-$CH_3OC_6H_4$) requires further investigations.

EXPERIMENTAL

Silica gel DG (Riedel-de Haen, Hanover, G.F.R.) was used as previously[24–28]. TLC was performed as reported in ref. 24 on 0.5 mm layers without pre-saturation of the tank with the vapours of the solvent system. The developing distance was 18 cm.

As previously[27,28], the dilution method of Soczewiński *et al.*[32] was also used for elucidation of the adsorption pattern. R_F values of the compounds studied were measured in mixtures of heptane (diluent) and diethyl ether (polar solvent) with increasing concentration, C, of diethyl ether, the latter concentration being proportional to the molar fraction, X_S, of the polar solvent in the equation

$$R_M \left[= \log \left(\frac{1}{\xi R_F} - 1 \right) \right] = \text{constant} - n \log X_S$$

where ξ is a constant depending on the chromatographic conditions. The conversion of R_F into R_M values was done directly by means of the graph shown in Fig. 3 of ref. 32 with $\xi = 1$. The values of the parameter n from the above equation were derived from the slope of R_M *versus* log C plots. The absolute values of n are indicative of the

adsorption pattern[36]. In applying this method, the measurements were performed as in ref. 27 with the same reproducibility.

Erythro- and *threo*-isomers 1–4 and 9–28 (see Table II) have been prepared[37–40] by means of Reformatsky or Ivanoff reactions followed by treatment with diazomethane. The hydroxy-esters 5–8 (m.sp. *ca.* 50°C) were synthesized by Reformatsky reaction as described for other cases[39,40]. The crude mixtures of 5–6 and 7–8 were separated by repeated column chromatography on a 100-fold quantity of silica gel S (Riedel-de Haen) with heptane–diethyl ether–ethanol (98.5:1:0.5), the separation being controlled by TLC (see Table II). The relative configurations were assessed by the NMR spectra[41] as recommended in ref. 42.

The IR spectra of 1–2 and 9–10, in 10^{-3} *M* carbon tetrachloride solution, are very similar for each isomer. The bands for free OH (more intense in 1 and 9) appear at 3625 cm^{-1} and those for OH $\cdots$ O = C and OH $\cdots$ Ar are in the region 3400–3600 cm^{-1} (ref. 41).

The anilino-ester 30 has been prepared by Simova and Kurtev[43]. The diastereoisomeric compound 29, characterized by its NMR spectrum[41], has been isolated from the filtrates of the recrystallization of 30.

The preferred conformations of 1–2, 5–10, 21, 22, and 29–30 in $CDCl_3$ are those with antiperiplanar hydrogen atoms[41,42].

RESULTS AND DISCUSSION

The separation of a number of *erythro*- and *threo*-3-hydroxy-2,3-diarylpropionic acids and their derivatives has been controlled by TLC on silica gel. Table I shows the R_F values. The data have previously been reported in a dissertation[44] without any interpretation of the retention order of $R_{F(erythro)} > R_{F(threo)}$ in all cases.

Some of the compounds in Table I and the esters 5–8 and 29–30 mentioned in the Experimental section were investigated in detail in the present study. Table II presents the R_F values of compounds 1–30, investigated with four different solvent systems, and the values of the parameter n from R_M *versus* log C plots. The latter are shown in Fig. 1a–d. Heptane was used as diluent and diethyl ether as the polar solvent when applying Soczewiński's method[32] since these solvents were used in the usual TLC separations. Only heptane–diethyl ether mixtures were used since it was of importance to compare the TLC behaviour of 1–30 and not to study changes in the values of n owing to difverent solvent systems. The values of n are not exactly 1 or 2 which would correspond to one- or two-point adsorption, respectively[36]. This deviation can probably be attributed to solvation effects participating in the main adsorption mechanism[45].

A separation was achieved in all cases studied. With methylene chloride or methylene chloride–diethyl ether (95:5), the separation was excellent for the majority of cases. Table II shows clearly that the order $R_{F(erythro)} > R_{F(threo)}$ is characteristic for all compounds except the *tert.*-butyl esters 9–10 which have the reverse order. It was surprising that compounds 13–14 and 29–30, which also contain a *tert.*-Bu group, did not behave as 9–10. Treatment of these results requires a review of our previous papers[24,25,27,28], which will be presented retrospectively.

TABLE I

R_F VALUES[44] OF DIASTEREOISOMERIC 3-HYDROXY-2,3-DIARYLPROPIONIC ACIDS AND DERIVATIVES OF THE TYPE Ar–CH(X)–CH(Y)–Ar′

Ar	*Ar′*	*X*	*Y*	*Solvent system**	$R_{F(threo)}$	$R_{F(erythro)}$
Phenyl	Phenyl	OH	COO-iso-propyl	A	0.37	0.45
2-$CH_3C_6H_4$	Phenyl	OH	$COOCH_3$	B	0.16	0.27
4-$CH_3C_6H_4$	Phenyl	OH	$COOCH_3$	B	0.17	0.27
2-ClC_6H_4	Phenyl	OH	$COOCH_3$	B	0.16	0.33
4-ClC_6H_4	Phenyl	OH	$COOCH_3$	B	0.15	0.25
4-$CH_3OC_6H_4$	Phenyl	OH	$COOCH_3$	B	0.07	0.13
α-Naphthyl	Phenyl	OH	$COOCH_3$	B	0.15	0.24
Phenyl	4-BrC_6H_4	OH	$COOCH_3$	B	0.12	0.26
2-$CH_3C_6H_4$	Phenyl	$OCOCH_3$	$COOCH_3$	B	0.34	0.41
2-ClC_6H_4	Phenyl	$OCOCH_3$	$COOCH_3$	B	0.28	0.38
4-ClC_6H_4	Phenyl	$OCOCH_3$	$COOCH_3$	B	0.27	0.39
4-$CH_3OC_6H_4$	Phenyl	$OCOCH_3$	$COOCH_3$	B	0.20	0.27
α-Naphthyl	Phenyl	$OCOCH_3$	$COOCH_3$	B	0.21	0.30
Phenyl	4-BrC_6H_4	$OCOCH_3$	$COOCH_3$	B	0.22	0.31
2-$CH_3C_6H_4$	Phenyl	OH	COOH	C	0.38	0.47
4-$CH_3OC_6H_4$	Phenyl	OH	COOH	C	0.24	0.33
2-ClC_6H_4	Phenyl	OH	COOH	C	0.40	0.50
4-ClC_6H_4	Phenyl	OH	COOH	C	0.37	0.46
α-Naphthyl	Phenyl	OH	COOH	C	0.34	0.40
Phenyl	4-$CH_3C_6H_4$	OH	COOH	C	0.31	0.41
2-$CH_3C_6H_4$	4-$CH_3C_6H_4$	OH	COOH	C	0.37	0.45
4-$CH_3OC_6H_4$	4-$CH_3C_6H_4$	OH	COOH	C	0.23	0.33
2-ClC_6H_4	4-$CH_3C_6H_4$	OH	COOH	C	0.36	0.43
4-ClC_6H_4	4-$CH_3C_6H_4$	OH	COOH	C	0.32	0.41
Phenyl	4-BrC_6H_4	OH	COOH	C	0.36	0.47
2-$CH_3C_6H_4$	4-BrC_6H_4	OH	COOH	C	0.33	0.44
4-$CH_3OC_6H_4$	4-BrC_6H_4	OH	COOH	C	0.28	0.39
2-ClC_6H_4	4-BrC_6H_4	OH	COOH	C	0.34	0.45
4-ClC_6H_4	4-BrC_6H_4	OH	COOH	C	0.35	0.43
Phenyl	2-ClC_6H_4	OH	COOH	C	0.34	0.41
2-ClC_6H_4	2-ClC_6H_4	OH	COOH	C	0.36	0.43

* TLC on silica gel DG (Riedel-de Haen). Solvent systems: A = benzene–diethyl ether (7:1); B = heptane–diethyl ether (2:1); C = light petroleum–benzene–diethyl ether–acetic acid (9:1:10:0.5).

The relation $R_{F(erythro)} > R_{F(threo)}$ on silica gel was established for 60 diastereoisomeric pairs of type 1:

Ar–CH(X)–CH(Y)–Z	X and Y = NH_2, OH, COOH and their derivatives
type 1	Z = Ar′ or R
	Ar and Ar′ = phenyl, 4-alkoxyphenyl, 3,4-dialkoxyphenyl or carbazyl
erythro and *threo*	R = CH_3 or C_2H_5

According to the Snyder–Soczewiński theory[29–35], most widely adopted in LSC, the relative retention of non-ionic compounds depends on the difference between the diastereoisomeric pair of four factors (see eqn. 2 in ref. 25) having the

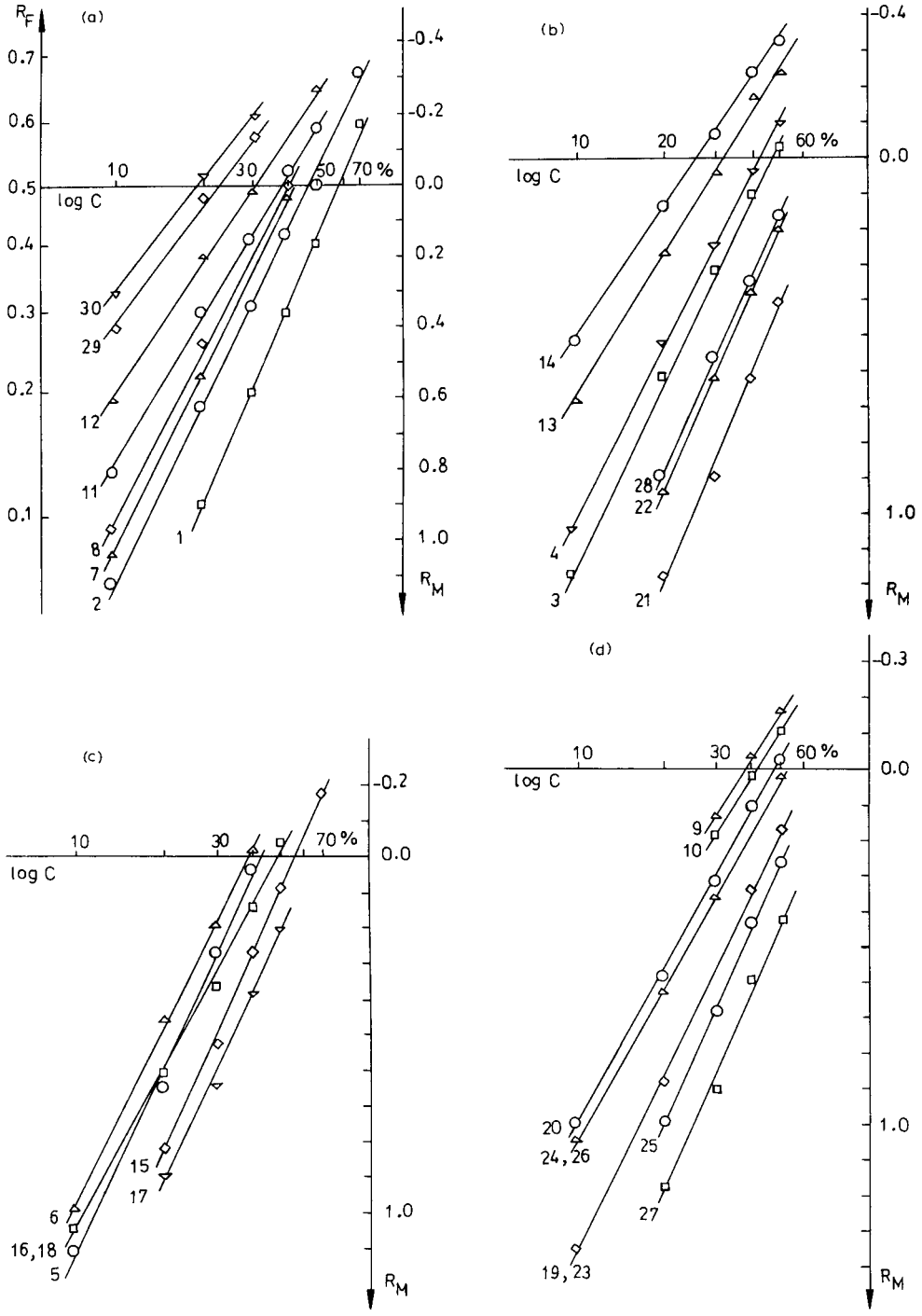

Fig. 1. Plots of R_M *versus* log C (% of diethyl ether) for compounds 1–30 (see formula in Table II). Diluent: heptane.

TABLE II

R_F VALUES AND ABSOLUTE VALUES OF THE SLOPES (n) OF R_M *VERSUS* LOG C PLOTS* FOR COMPOUNDS OF THE TYPE Ar–CH(X)–CH(Y)–Ar′

Ar	*Ar′*	*X*	*Y*	*Configuration*	*Compound No.*	R_F				n
						*Heptane–diethyl ether (2:1)***	*Heptane–acetone (5:1)***	*Methylene chloride–diethyl ether (95:5)*	*Methylene chloride*	
Phenyl	Phenyl	OH	$COOCH_3$	*threo*	1***	0.32	0.30	0.50	0.21	2.0
				erythro	2***	0.46	0.36	0.69	0.39	1.8
Phenyl	Phenyl	OH	COO-*iso*-propyl	*threo*	3	0.48	0.38	0.62	0.29	1.7
				erythro	4	0.53	0.41	0.70	0.39	1.6
Phenyl	Phenyl	OH	COO-*n*-butyl	*threo*	5	0.51	0.41	0.66	0.32	1.8
				erythro	6	0.56	0.41	0.73	0.42	1.7
Phenyl	Phenyl	OH	COO-*iso*-butyl	*threo*	7	0.54	0.42	0.66	0.33	1.7
				erythro	8	0.59	0.42	0.73	0.42	1.7
Phenyl	Phenyl	OH	COO-*tert.*-butyl	*threo*	9	0.56	0.46	0.69	0.36	1.4
				erythro	10	0.53	0.42	0.69	0.36	1.4
Phenyl	Phenyl	$OCOCH_3$	COO-*iso*-propyl	*threo*	11	0.59	0.49	0.80	0.58	1.4
				erythro	12	0.68	0.56	0.85	0.65	1.4
Phenyl	Phenyl	$OCOCH_3$	COO-*tert.*-butyl	*threo*	13	0.66	0.54	0.83	0.62	1.4
				erythro	14	0.72	0.59	0.88	0.68	1.3
2-ClC_6H_4	Phenyl	OH	$COOCH_3$	*threo*	15	0.34	0.29	0.58	0.31	1.9
				erythro	16	0.49	0.33	0.73	0.48	1.6
4-ClC_6H_4	Phenyl	OH	$COOCH_3$	*threo*	17	0.36	0.26	0.53	0.26	1.9
				erythro	18	0.51	0.33	0.74	0.48	1.6
4-$CH_3C_6H_4$	Phenyl	OH	$COOCH_3$	*threo*	19	0.39	0.27	0.49	0.21	1.8
				erythro	20	0.49	0.34	0.70	0.39	1.6
4-$CH_3OC_6H_4$	Phenyl	OH	$COOCH_3$	*threo*	21	0.23	0.18	0.38	0.14	2.0
				erythro	22	0.34	0.23	0.56	0.24	1.9
α-Naphthyl	Phenyl	OH	$COOCH_3$	*threo*	23	0.37	0.26	0.59	0.29	1.8
				erythro	24	0.49	0.31	0.74	0.48	1.6
Phenyl	4-BrC_6H_4	OH	$COOCH_3$	*threo*	25	0.32	0.26	0.49	0.23	1.8
				erythro	26	0.50	0.33	0.73	0.48	1.6
4-$CH_3OC_6H_4$	4-$CH_3C_6H_4$	OH	$COOCH_3$	*threo*	27	0.23	0.19	0.36	0.13	2.0
				erythro	28	0.36	0.24	0.58	0.27	1.9
Phenyl	Phenyl	NHPh	COO-*tert.*-butyl	*threo*	29	0.78	0.54	0.94	0.88	1.2
				erythro	30	0.82	0.54	0.94	0.88	1.2

* See Experimental section and Fig. 1a–d.
** Developed twice.

following physical meaning: electronic and steric effects; localization effects, reflecting the number of the adsorbing groups; solute area effects; and so-called secondary effects. When the same adsorbent is used, as in our cases, the latter effects are only secondary solvent ones which arise from the specific solvent–solute and solvent–adsorbent interactions. Using methylene chloride, which is free from significant solvent effects, instead of solvent systems which exhibit such effects, the relation $R_{F(erythro)} > R_{F(threo)}$ was again established. This shows that the secondary solvent effects are of no importance in deciding the retention order. Adsorption by the same group(s) within any two isomers was derived on the basis of Soczewiński's method. Hence, the localization and the solute areas of the diastereoisomers under adsorption seem to be identical, and thus the corresponding effects are not important for the retention order. The *erythro*-isomer of a diastereoisomeric pair of type 1 (see compounds 1–2 of ref. 27) is a stronger base; however, it is again adsorbed less than the *threo*-isomer. Thus, it is clear that electronic effects are not decisive factors. Consequently, steric effects remain and determine the relationship $R_{F(erythro)} > R_{F(threo)}$ in the cases studied.

This conclusion is equal to the widely used concept (*e.g.* see refs. 2,3,5–8,24 and 46) for interpretation of chromatographic behaviour of diastereoisomers which is derived on the basis of conformational analysis[47] without taking into account details of the retention mechanism. However, bearing in mind the other factors mentioned above, concerning the adsorption mechanism, this makes the treatment more reliable and is of great importance in some cases of inversion[25]★.

The groups X and Y seem to be more strongly adsorbing, and with smaller effective volumes, than the groups Ar and Ar′ in any compound studied (see Table 10-2 of ref. 29 and ref. 49). Having also in mind the values of n[27,28], the two cases presented in Fig. 2a and b should be chosen for interpretation of the order $R_{F(erythro)} > R_{F(threo)}$. It can be seen that the adsorbing groups are less sterically hindered in the *threo*-isomers (case a). The adsorbing group in case b, for instance Y, significantly more adsorbing than X, is in nearly the same environment (between X and H). However, the conformation of the *threo*-isomers has less interaction between the bulky groups.

Let us return to the chromatographic behaviour of the compounds of the present study. Diethyl ether and acetone in the solvent systems used can form hydrogen bonds with the OH groups of the hydroxyesters 1–10 and 15–28 while with methylene chloride such a possibility is negligible. Table II shows that retention of the compounds does not change with the presence or absence of a solvent with secondary solvent effects. The values of n (see Table II) within any diastereoisomeric pair are nearly equal. Hence, the electronic and steric effects only should be responsible for the relative retentions. The hydroxyesters 1–10 and 15–28, including those in Table I, possess intramolecular hydrogen bonds; electronic effects should therefore be discussed. The hydroxyesters, excluding for the moment 9–10, the acetoxyesters 11–14 and the anilinoesters 29–30 have the same retention, $R_{F(erythro)} > R_{F(threo)}$. It should be borne in mind that 11–14 and 29–30 are free from intramolecular hydrogen bonding.

★ The retention order of diastereoisomers in LSC is often treated in analogous manner, as in the case of gas–liquid chromatography (GLC)[46]. However, the main mechanism in GLC is "dissolution of the solute in the bulk of the liquid film"[46] complicated by some types of adsorption[48]. Thus such an analogy requires caution.

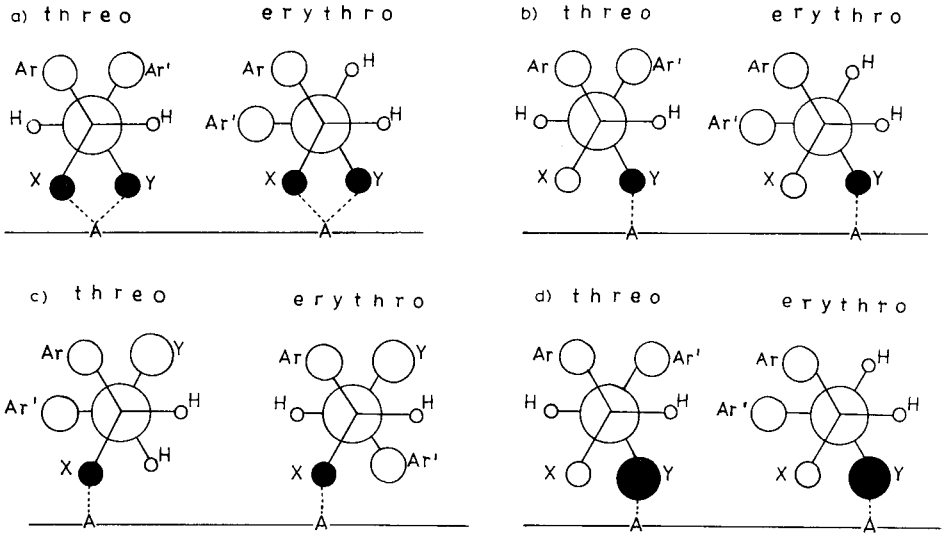

Fig. 2. Illustrative representation of the adsorption patterns for diastereoisomeric compounds of type 1. The full circle denotes the strongest adsorbing group/s of the molecule. A = Active site comprising the different types of the adsorbent surface hydroxyl groups; see p. 157 of ref. 29. (a) Two-point adsorption with X and Y; $R_{F(erythro)} > R_{F(threo)}$. (b) One-point adsorption with Y (or with X via conformations where X is between H and Y, not presented); $R_{F(erythro)} > R_{F(threo)}$. (c) One-point adsorption with X; $R_{F(threo)} > R_{F(erythro)}$. (d) One-point adsorption with Y; $R_{F(erythro)} > R_{F(threo)}$. In (a) and (b) X and Y are smaller than Ar and Ar′; in (c) and (d) X is smaller and Y bulkier than Ar and Ar′.

This means that the electronic effects are of no decisive importance; physically it can be rationalized by the previously adopted concept of cleavage of the intramolecular hydrogen bonds under the action of the adsorbent[24–26,28]. Such a cleavage seems possible only when the distance between the intramolecularly bonded groups of the solute is similar to that between the hydroxyl groups of the active site of the adsorbent (see the interpretation of TLC behaviour for compounds 23–24 in ref. 25). The hydrogen bonding in 1 and 9 and in 2 and 10 is similar, which indicates that the electronic effects in 9–10 can also be neglected. Thus, the steric effects will be discussed below.

The TLC behaviour of the hydroxyesters 1–8 and 25–28, showing two-point adsorption ($n > 1.5$) with the functional groups X and Y, can be explained in Fig. 2a as above. The substituents Cl, Br, CH_3 and CH_3O attached to the phenyl groups, as well as the naphthyl group, in these cases are less adsorbing than X and Y (see Table 10-2 of ref. 29). Thus, the former groups are not directly adsorbed; they are delocalized, which leads to a change in the adsorption of the directly attached groups (see p. 270 of ref. 29). The position (*ortho* or *para*) of these low-adsorbing groups, as expected, does not affect the retention order of the diastereoisomers.

The compounds 1–8 differ in the alkyl group of the ester group only. Its effective volume increases in the order Me, *iso*-Pr, *n*-Bu, *iso*-Bu. The above-mentioned two-point adsorption of 1–8 gradually decreases (see Table II) owing to the increasing hindrance of the adsorbing carbonyl oxygen. Substitution of the *iso*-Bu group by the most bulky[49] *tert.*-Bu group results in one-point adsorption (9–10, $n = 1.4$) and inversion of the retention to $R_{F(threo)} > R_{F(erythro)}$. It is clear that the ester group COO-*tert.*-Bu is not a more adsorbing one and the adsorption of 9–10 occurs by means of the hydroxyl group X. In this case the most favourable position of the latter is that between H and Ar′, as shown in Fig. 2c, because the effective volume of COO-*tert.*-Bu

(Y) is expected to exceed that of Ar′[49]. The conformation of the *erythro*-isomer shown coincides with the energetically preferred conformation in solution of 10. However, the conformation depicted for the *threo*-isomer differs from the preferred conformation of 9. For this reason *erythro*-10 should be and is more strongly adsorbing than *threo*-9. The inversion of the retention order for the butyl esters 5–10 occurs exclusively with compounds 9–10 which have a tertiary butyl group. Consequently, COO-*n*-Bu and COO-*iso*-Bu groups should be considered as groups possessing a smaller effective volume than Ar′.

In the course of isolation of a series of optically active diastereoisomeric hydroxyesters of type 1, X = OH, Y = COO(−)-menthyl, the retention $R_{F(threo)} > R_{F(erythro)}$ was established[50] on the same silica gel as in the present study. The group COO(−)-menthyl could also be assumed to be bulkier than Ar′. Thus, it becomes clear that 9–10 is not an isolated case and the latter retention is normal when the adsorption occurs as shown in Fig. 2c.

The *tert.*-Bu esters 9–10 and 29–30 differ in the group X only. Comparison of the R_F values of these compounds reveals that the adsorptivity of the anilino group NHPh in 29–30 is considerably smaller than that of the OH group in 9–10. Hence, one-point adsorption of the group COO-*tert.*-Bu is expected and is found for 29–30 ($n = 1.2$), as shown in Fig. 2d. This group is in the most favourable position in the conformations shown (between X and H), but only the conformation of the *threo*-isomer coincides with the energetically preferred conformation of 29. Thus it is clear why the retention in this case is $R_{F(erythro)} > R_{F(threo)}$. The same pattern of adsorption (case d) is probably responsible for the TLC behaviour of the acetoxyesters 13–14. In this case one-point adsorption ($n < 1.5$) should also occur with the ester group COO-*tert.*-Bu. The lack of adsorption of the acetoxy group X is not so apparent because it has a greater adsorption than the anilino group (*cf.* the R_F values of 13–14 with those of 29–30).

The retention of the diastereoisomeric acetoxyesters of Table I and 11–12 is probably due to adsorption with the ester group Y (COOMe or COO-*iso*-Pr) which is smaller than Ar′ (see Fig. 2b). The behaviour of the diastereoisomeric hydroxyacids of Table I could be attributed to adsorption with the strongest adsorbing carboxyl group Y, as shown in Fig. 2b, provided there are no considerable complications by the fact that these compounds are not fully non-ionic ones.

CONCLUSIONS

The results of the present study support the criteria given in refs. 25 and 28 for assessing the relative configurations of the diastereoisomers of type 1 on the basis of the relation $R_{F(erythro)} > R_{F(threo)}$. The principle requirement, in such a case, is that the groups X and Y should be more strongly adsorbing, and with smaller effective volumes, than the groups Ar and Ar′, as shown in Fig. 2a and b. The results also provide a further development of the criteria for the case where X is smaller, and Y is bulkier, than Ar and Ar′:

(1) Adsorption with Y (see Fig. 2d) results in retention of the order $R_{F(erythro)} > R_{F(threo)}$.

(2) Adsorption with X leads to inversion, as shown in Fig. 2c.

ACKNOWLEDGEMENT

Thanks are due to Dr. E. Simova for samples of the anilinoesters 29–30.

REFERENCES

1 I. S. Krull, *Advan. Chromatogr.*, 16 (1978) 175.
2 W. H. Pirkle and P. E. Adams, *J. Org. Chem.*, 43 (1978) 378.
3 W. H. Pirkle and P. L. Rinaldi, *J. Org. Chem.*, 43 (1978) 3803.
4 K. Joshioka, D. S. Fullerto and D. C. Rohrer, *Steroids*, 32 (1978) 511.
5 G. Helmchen, G. Nill, D. Flockerzi, W. Schühle and M. S. K. Youssef, *Angew. Chem., Int. Ed. Engl.*, 18 (1979) 62.
6 G. Helmchen, G. Nill, D. Flockerzi and M. S. K. Youssef, *Angew. Chem., Int. Ed. Engl.*, 18 (1979) 63.
7 G. Helmchen and G. Nill, *Angew. Chem., Int. Ed. Engl.*, 18 (1979) 65.
8 B. J. Bergot, F. C. Baker, E. Lee and D. Å. Schooley, *J. Amer. Chem. Soc.*, 101 (1979) 7432.
9 T. Tamegai, M. Ohmae, K. Kawabe and M. Tomoeda, *J. Liquid Chromatogr.*, 2 (1979) 1229.
10 Á. H. Csárnyi, A. Szabolcs, M. Vajda and L. Ötvös, *J. Chromatogr.*, 169 (1979) 426.
11 A. Sunde, P. Stenstad and K. B. Eik-Nes, *J. Chromatogr.*, 175 (1979) 219.
12 M. Jarman and W. J. Stec, *J. Chromatogr.*, 176 (1979) 440.
13 H. H. Wittekind and B. Testa, *J. Chromatogr.*, 179 (1979) 370.
14 H. Berbalk, K. Eichinger and R. Schuster, *J. High Resolut. Chromatogr. Chromatogr. Commun.*, 2 (1979) 535.
15 D. M. Johnson, A. Reuter, J. M. Collins and G. T. Thompson, *J. Pharm. Sci.*, 68 (1979) 112.
16 A. J. Meyers, J. Slade, R. K. Smith and E. D. Mihelich, *J. Org. Chem.*, 44 (1979) 2247.
17 E. Ade, G. Helmchen and G. Heiligenmann, *Tetrahedron Lett.*, (1980) 1137.
18 S. G. Bandaev, Yu. S. Sabarov, A. Hantschmann and M. Weissenfels, *J. Prakt. Chem.*, 322 (1980) 643.
19 T. Okumura, *J. Chromatogr.*, 184 (1980) 37.
20 T. Tamegai, S. Sohda, N. Hirose, M. Ohmae and K. Kawabe, *J. Chromatogr.*, 193 (1980) 483.
21 F. Gasparrini, S. Cacchi, L. Caglioti, D. Misiti and M. Giovannoli, *J. Chromatogr.*, 194 (1980) 239.
22 G. Szókán, F. Ruff and Á. Kucsman, *J. Chromatogr.*, 198 (1980) 207.
23 S. Hara and A. Ohsawa, *J. Chromatogr.*, 200 (1980) 85.
24 M. Palamareva, M. Haimova, J. Stefanovsky, L. Viteva and B. Kurtev, *J. Chromatogr.*, 54 (1971) 383.
25 M. D. Palamareva and B. J. Kurtev, *J. Chromatogr.*, 132 (1977) 61.
26 M. D. Palamareva, B. J. Kurtev and M. A. Haimova, *J. Chromatogr.*, 132 (1977) 73.
27 M. D. Palamareva and B. J. Kurtev, *J. Chromatogr.*, 178 (1979) 139.
28 M. D. Palamareva, B. J. Kurtev, K. B. Faitondzieva and L. D. Zheljazkov, *J. Chromatogr.*, 178 (1979) 155.
29 L. R. Snyder, *Principles of Adsorption Chromatography*, Marcel Dekker, New York, 1968.
30 L. R. Snyder, *Anal. Chem.*, 46 (1974) 1384.
31 L. R. Snyder and H. Poppe, *J. Chromatogr.*, 184 (1980) 363, and references cited therein.
32 E. Soczewiński and J. Jusiak, *Chromatographia*, 14 (1981) 23, and references cited therein.
33 F. Geiss, *Die Parameter der Dünnschicht-Chromatographie*, Vieweg, Braunschweig, 1972.
34 K. K. Unger, *Porous Silica. Its Properties and Use as Support in Column Liquid Chromatography*, Elsevier, Amsterdam, Oxford, New York, 1979, p. 187.
35 M. Jaroniec and J. Piotroska, *J. High Resolut. Chromatogr. Chromatogr. Commun.*, 3 (1980) 257.
36 E. Soczewiński, W. Gołkiewicz and W. Markowski, *Chromatographia*, 8 (1975) 13.
37 B. Blagoev, M. Mladenova and A. Papazov, *Commun. Dep. Chem., Bulg. Acad. Sci.*, 4 (1971) 81.
38 M. Mladenova, J. Stefanovsky and B. Blagoev, *C.R. Acad. Bulg. Sci.*, 24 (1971) 471.
39 M. Mladenova, B. Blagoev and B. Kurtev, *Bull. Soc. Chim. Fr.*, (1974) 1464.
40 M. Mladenova, B. Blagoev and B. Kurtev, *C.R. Acad. Bulg. Sci.*, 28 (1975) 1633.
41 S. L. Spassov, M. Mladenova and B. Blagoev, unpublished results.
42 S. L. Spassov, *Tetrahedron*, 25 (1969) 3631.
43 E. Simova and B. Kurtev, *Commun. Dep. Chem.*, Bulg. Acad. Sci., 3 (1970) 349.
44 M. Mladenova, *PhD Dissertation*, Institute of Organic Chemistry, Bulgarian Academy of Sciences, Sofia, 1977.
45 E. Soczewiński, *Chromatographia*, 11 (1978) 534.
46 E. Gil-Av and D. Nurok, *Advan. Chromatogr.*, 10 (1974) 99.
47 S. Winstein and N. Holness, *J. Amer. Chem. Soc.*, 77 (1955) 5562.
48 F. Riedo and E. sz. Kováts, *J. Chromatogr.*, 186 (1979) 47, and references cited therein.
49 J. Hirsch, in N. Allinger and E. Eliel (Editors), *Topics of Stereochemistry*, Vol. 1, Interscience, New York, 1967, p. 199.
50 M. Palamareva, S. Bojadziev, N. Berova and B. Kurtev, *God. Sofii. Univ., Khim. Fak.*, in press.

Journal of Chromatography, 235 (1982) 309–322
Elsevier Scientific Publishing Company, Amsterdam — Printed in The Netherlands

CHROM. 14,340

ROLE OF COLUMN TEMPERATURE IN OPEN-TUBULAR MICROCAPILLARY LIQUID CHROMATOGRAPHY

TOYOHIDE TAKEUCHI*, MASAYOSHI KUMAKI and DAIDO ISHII
Department of Applied Chemistry, Faculty of Engineering, Nagoya University, Chikusa-ku, Nagoya-shi 464 (Japan)
(Received September 8th, 1981)

SUMMARY

The influence of column temperature on chromatographic performance was examined for reversed-phase, normal-phase and cation-exchange columns in open-tubular microcapillary liquid chromatography. Linear relationships between the logarithm of capacity factor and the reciprocal of column temperature were generally observed. Operation at higher column temperature had the tendency to give higher column efficiency owing to the decrease in the viscosity of the mobile phase.

INTRODUCTION

Column temperature is one of the most significant parameters in gas chromatography (GC) and gradient elution with temperature is a popular and powerful technique in GC. In contrast, it has often been neglected in liquid chromatography (LC), which has sometimes caused poor reproducibility of retention of solutes or incorrect results. Some workers have examined the hydrodynamic and thermodynamic roles of column temperature in LC[1–15]. In reversed-phase chromatography, it has been reported that operation at elevated temperature leads to a decrease in the viscosity of the mobile phase and consequently an increase in column efficiency[3–5,15]. However, a few workers concluded that operation at subambient or low temperature improves the selectivity[8]. However, the logarithm of the capacity factor was proportional to the reciprocal of column temperature in the reversed-phase mode.

In normal-phase LC, the effect of temperature on solute retention and selectivity has been discussed[1,2,12–14]. The direction of the dependence of solute retention on column temperature was reversed with variation of temperature.

Temperature-gradient separations have been tried in LC, and these reduced the analysis time comparable to conventional solvent gradient separations[2,7,15].

The larger difference in diffusion speed in the liquid and gaseous states is the main reason why open-tubular capillary LC has not generally been so successful as glass capillary GC[16]. The employment of a narrow-bore capillary column is necessary in order to solve this problem, as can be appreciated from the following equation:

0021-9673/82/0000–0000/$02.75

$$H = \frac{2D_m}{u} + \frac{2k'd^2u}{3(1 + k')^2 D_s} + \frac{(11k'^2 + 6k' + 1)r_c^2 u}{24(1 + k')^2 D_m} \quad (1)$$

where H is height equivalent to a theoretical plate, u is the linear velocity of the mobile phase, k' is the capacity factor, d is the thickness (or depth) of the stationary phase, r_c is the radius of an open tube and D_m and D_s are the diffusion coefficients of a solute in the mobile and the stationary phase, respectively.

For non-retained solutes ($k' = 0$), eqn. 1 is simplified to

$$H = \frac{r_c^2 u}{24D_m} \equiv H_m \quad (2)$$

Eqn. 1 indicates that a system with larger D_m and D_s can also generate a higher efficiency as the first term in the equation is negligible under the usual conditions. The third term in eqn. 1, based on the resistance of mass transfer in the mobile phase, is dominant in open-tubular capillary LC[17,18]. Hence the viscosity of the mobile phase should be given particular attention in open-tubular capillary LC.

This paper describes the influence of column temperature on chromatographic characteristics for reversed-phase, normal-phase and cation-exchange columns in open-tubular microcapillary LC.

EXPERIMENTAL

All reagents were obtained from Wako (Osaka, Japan), unless stated otherwise.

A liquid chromatograph was assembled from a pumping system, a capillary column, a column oven and a detection system. The pumping system included a Micro Feeder (Azumadenki Kogyo, Tokyo, Japan) and a 100-μl gas-tight syringe (Hamilton, Reno, NV, U.S.A.). The column oven was home-made and consisted of asbestos boards equipped with a heater and a micro fan. The temperature was adjusted by altering the applied voltage with a sliding rheostat, and could be kept within ± 1°C during each chromatographic run. A Uvidec-100 UV spectrophotometer (Japan Spectroscopic Co., Tokyo, Japan) was employed as the detector. A flow cell was arranged for capillary LC, as described previously[19]. A schematic diagram of the apparatus is shown in Fig. 1.

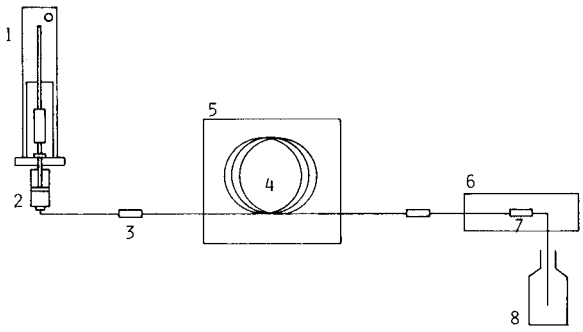

Fig. 1. Schematic diagram of the apparatus. 1 = Micro Feeder; 2 = gas-tight syringe; 3 = inlet; 4 = capillary column; 5 = column oven; 6 = UVIDEC 100 UV spectrophotometer; 7 = micro flow cell; 8 = waste reservoir.

In this work, capillary columns containing octadecylsilane (ODS), γ-aminopropylsilane (NH_2), silica gel (Si) and 2-sulphoethylsilane (CEX) were prepared as described earlier[18,20,21]. The preparation procedures for these columns are presented in Fig. 2. First, soda-lime glass capillaries were treated with 1 *N* sodium hydroxide solution for 2 days at 45–50°C. This treatment produced quasi-silica gel on the surface of the glass capillaries, the properties of which were dependent on the treatment temperature and time[20]. Subsequent to washing and drying, the surface of the glass capillaries was reacted with octadecyltrichlorosilane[18], γ-aminopropyltriethoxysilane and 2-mercaptoethyltriethoxysilane[21] (Tokyo Chemical Industry Co., Tokyo, Japan). For the CEX column, mercato groups were oxidized to sulpho groups by treatment with potassium permanganate solution.

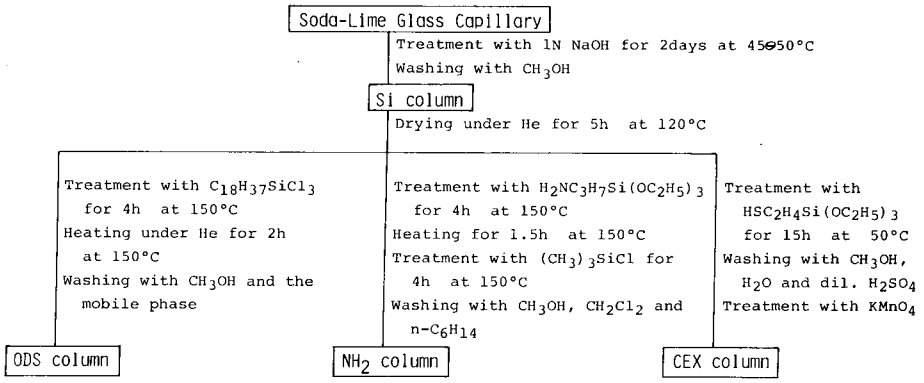

Fig. 2. Preparation procedures for open-tubular capillary columns. ODS = octadecyltrichlorosilane; NH_2 = γ-aminopropylsilane; CEX = 2-sulphoethylsilane; Si = silica gel.

Each column was set in the column oven and the effect of column temperature was studied. The ODS column was examined in both reversed- and normal-phase systems; the Si and NH_2 columns were examined in the normal-phase system and the CEX column in a cation-exchange system.

RESULTS AND DISCUSSION

Reversed-phase system

The diffusion coefficient of a solute in the mobile phase (D_m) is highly dependent on the temperature and composition of the mobile phase. The effect of column temperature and mobile phase composition on H for a non-retained solute is illustrated in Fig. 3. H_m is inversely proportional to D_m, as represented by eqn. 2. In other words, H_m corresponds to the viscosity of the mobile phase. Therefore, Fig. 3 indicates that a methanol solution containing *ca.* 60% of water has the maximal viscosity, whereas the viscosity of acetonitrile solution varies monotonously with mobile phase composition. In both instances, the higher the column temperature, the smaller is H, which suggests that a higher efficiency will be obtained at elevated temperature for retained solutes. However, it should be remembered that the retention of solutes generally decreases with increasing column temperature and therefore a water-rich solution should be employed at elevated temperature.

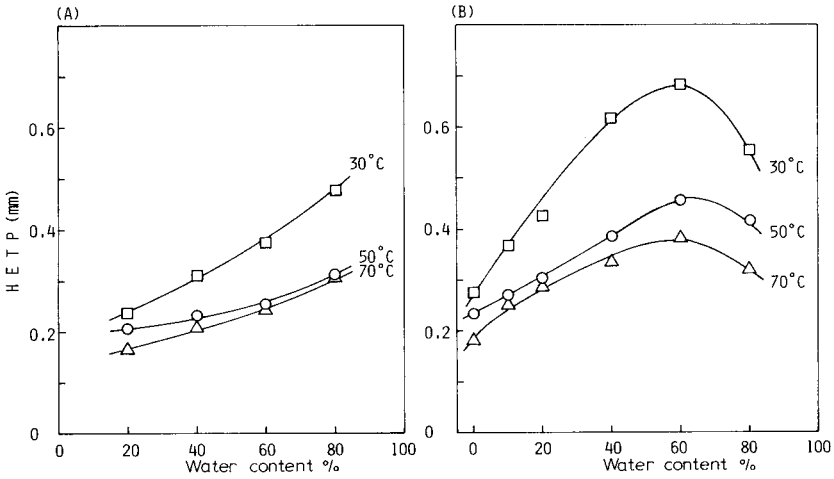

Fig. 3. Effect of column temperature and mobile phase composition on H. Column: 7.6 m × 72 μm I.D. Mobile phase: (A) acetonitrile–water; (B) methanol–water. Flow-rate: 1.7 μl/min. Sample: phenol in the mobile phase.

The dependence of k' on temperature is given by

$$\ln k' = \frac{-\Delta H^\circ}{RT} + \frac{\Delta S^\circ}{R} + \ln\left(\frac{V_s}{V_m}\right) \tag{3}$$

where ΔH° and ΔS° are the enthalpy and entropy, respectively, of transfer of a solute from the mobile phase to the stationary phase, R is the gas constant, T is absolute column temperature, V_s is the total volume of the stationary phase and V_m is the interstitial volume in the column. Eqn. 3 indicates that the logarithm of capacity factor is proportional to the reciprocal of absolute column temperature and ΔH° can be calculated from the slope of $\ln k'$ *versus* $1/T$ plots.

The order of retention of some polynuclear aromatic hydrocarbons reverses with change in column temperature. Fig. 4 demonstrates an example of the change in elution sequence with temperature change. 1,3,5-Triphenylbenzene elutes before 3,4-benzopyrene at low temperature (40°C), whereas the elution sequence is reversed at higher temperature (71°C); this is ascribed to the difference in the enthalpies of the two solutes. The flow-rate depends slightly on column temperature owing to the expansion of the eluent. As only the column was heated, the flow-rate at higher temperature was higher than original value.

Figs. 5 and 6 show the relationship between $\ln k'$ and $1/T$ using acetonitrile–water as the mobile phase. The slope of $\ln k'$ *versus* $1/T$ plots is peculiar to the structure of the solute. Compact solutes such as chrysene, perylene and 3,4-benzopyrene give smaller slopes than non-compact solutes such as *p*-terphenyl, 9-phenylanthracene and 1,3,5-triphenylbenzene. Similar results have been reported for packed column LC[7,15].

Fig. 7 shows the linear relationship between $\ln k'$ and $1/T$ using methanol–water as the mobile phase. Nearly the same tendency was obtained as in the acetonitrile–water system (Fig. 6), except for *p*-terphenyl. *p*-Terphenyl is obviously not

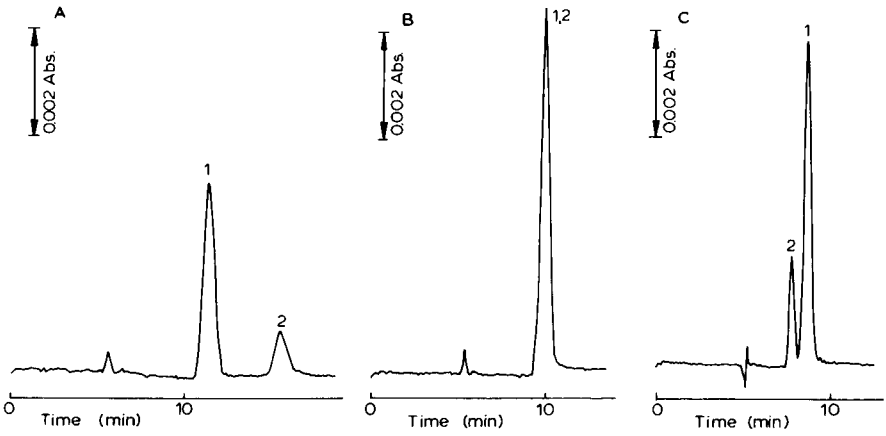

Fig. 4. Change in elution sequence with change in column temperature. Column: ODS, 5.3 m × 46 μm I.D. Mobile phase: acetonitrile–water (1:1). Flow-rate: 1.7 μl/min. Column temperature: (A) 40°C; (B) 50°C; (C) 71°C. Sample: 1 = 1,3,5-triphenylbenzene; 2 = 3,4-benzopyrene. Wavelength of detection (UV): 254 nm.

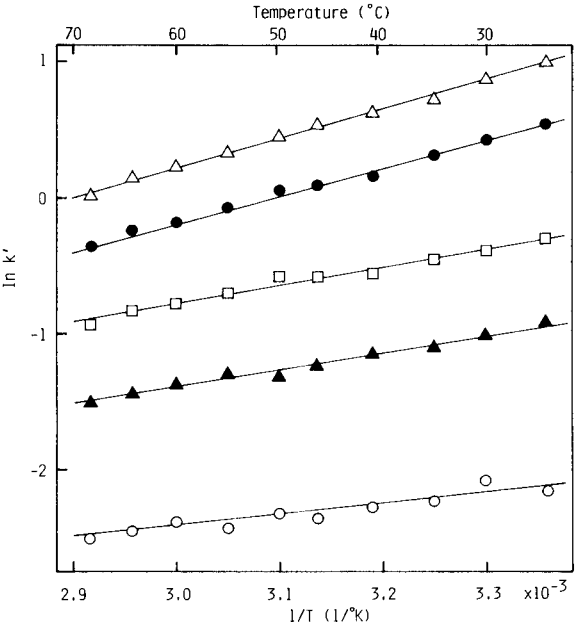

Fig. 5. Relationship between ln k' and $1/T$. Column: ODS, 5.3 m × 46 μm. Mobile phase: acetonitrile–water (35:65). Sample: ○ = benzene; ▲ = naphthalene; □ = biphenyl; ● = anthracene; △ = pyrene.

compact, but has a larger slope than other non-compact solutes. Snyder[9] considered that the common factor for "irregularity" seems to be the relative departure from a flat, straight molecule on the one hand, *versus* a bulky three-dimensional or spherical shape on the other. Hence polyaryls become less flat and become more compact or spherical with increasing intermolecular crowding, which may be dependent on the solvent system.

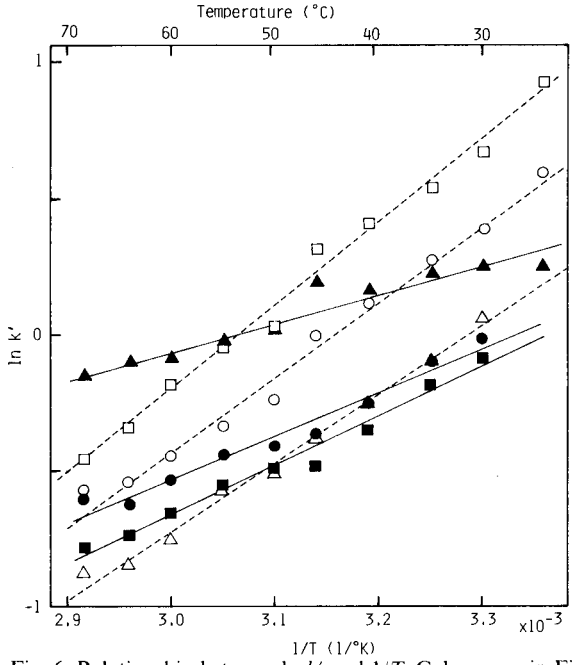

Fig. 6. Relationship between ln k' and $1/T$. Column: as in Fig. 5. Mobile phase: acetonitrile–water (1:1). Sample; ■ = *p*-terphenyl; △ = chrysene; ● = 9-phenylanthracene; ○ = perylene; ▲ = 1,3,5-triphenylbenzene; □ = 3,4-benzopyrene.

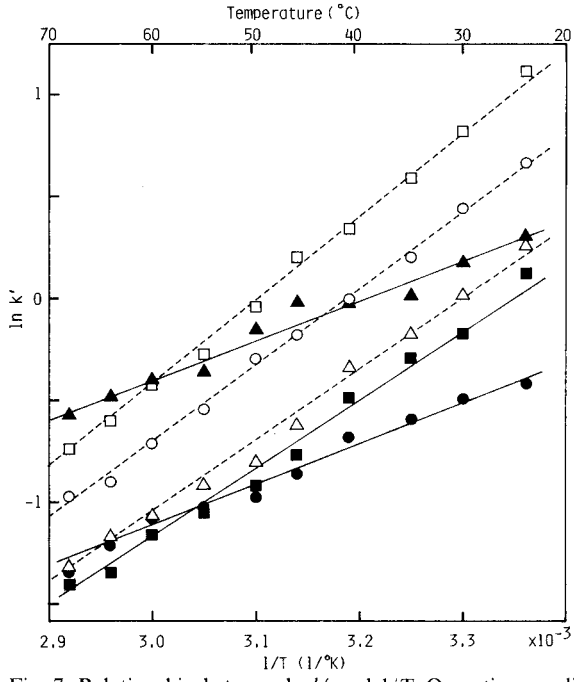

Fig. 7. Relationship between ln k' and $1/T$. Operating conditions as in Fig. 6, except the mobile phase (methanol–water, 7:3).

ΔH° values for polynuclear aromatic hydrocarbons are given in Table I. With the acetonitrile–water system, the ΔH° values obtained were nearly the same as those in the literature[7]. ΔH° is dependent on the kind of organic solvent and the water content. As described above, as the retentions of polynuclear aromatic hydrocarbons are individually dependent on column temperature, the ΔH° values become qualitative and temperature-programmed separation will be favoured in capillary LC as in GC.

TABLE I

ΔH° VALUES FOR POLYNUCLEAR AROMATIC HYDROCARBONS

Column: ODS, 5.3 m × 46 μm I.D.

Solute	*Mobile phase*	$-\Delta H^\circ$ *(kJ/mol)*
Benzene	Acetonitrile–water (35:65)	7.0
Naphthalene		10.3
Biphenyl		11.3
Anthracene		16.0
Pyrene		17.6
p-Terphenyl	Acetonitrile–water (1:1)	15.2
Chrysene		20.7
9-Phenylanthracene		13.0
Perylene		23.2
1,3,5-Triphenylbenzene		8.5
3,4-Benzopyrene		25.7
p-Terphenyl	Methanol–water (7:3)	29.1
Chrysene		29.7
9-Phenylanthracene		17.1
Perylene		31.9
1,3,5-Triphenylbenzene		16.5
3,4-Benzopyrene		34.4

Selectivity is highly dependent on column temperature. Fig. 8 shows the effect of column temperature on the resolution (R_s) of solutes, which is defined by

$$R_s = \frac{2(t_2 - t_1)}{w_1 + w_2} \tag{4}$$

where t_1 and t_2 are retention times of solutes 1 and 2 ($t_2 > t_1$) and w_1 and w_2 are the peak widths (time units) of the two solutes. A pair of solutes can be resolved when $R_s \geqslant 1$ and they overlap when $R_s = 0$.

The effect of column temperature on efficiency is shown in Fig. 9. The theoretical plate number (N) increases with increasing column temperature. N doubles with a temperature increase of 30°C. On the other hand, the effective theoretical plate number (N_{eff}) varies only slightly with temperature because the retention of solutes decreases with increasing column temperature. Operation at temperatures higher than ambient gives higher efficiencies.

A typical separation of polynuclear aromatic hydrocarbons on an ODS capil-

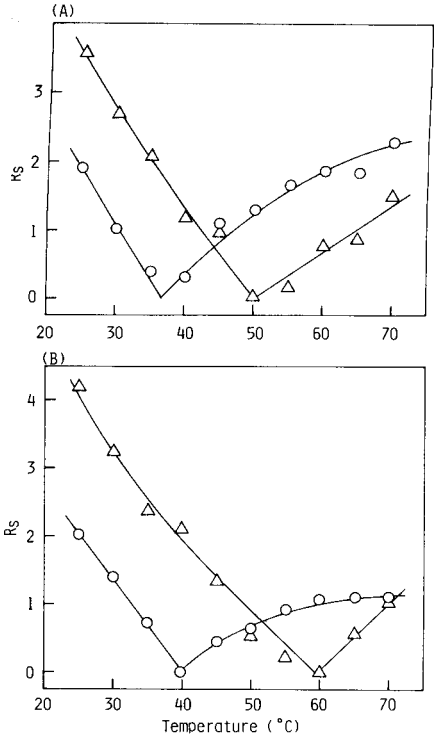

Fig. 8. Effect of column temperature on resolution of solutes. Resolution: ○ = perylene–1,3,5-triphenylbenzene; △ = 1,3,5-triphenylbenzene–3,4-benzopyrene. Flow-rate: 1.7 μl/min. Mobile phase: (A) acetonitrile–water (1:1); (B) methanol–water (7:3).

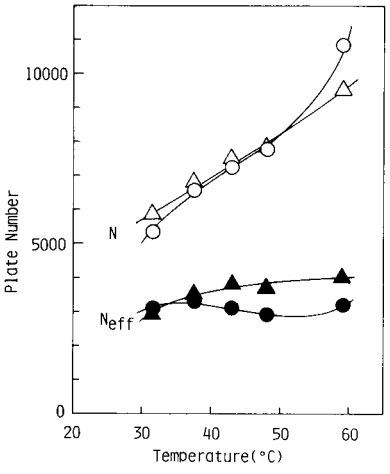

Fig. 9. Effect of column temperature on efficiency. Column: ODS, 7.2 m × 32 μm I.D. Mobile phase: acetonitrile–water (45:55). Flow-rate: 0.42 μl/min. Sample: ○, ● = 3,4-benzopyrene; △, ▲ = 1,3,5-triphenylbenzene.

lary column is shown in Fig. 10. *p*-Terphenyl and chrysene overlapped at 43°C but fourteen compounds could be resolved at 13 or 32°C. A theoretical plate number of 19,000 was attained for 1,3,5-triphenylbenzene (Fig. 10).

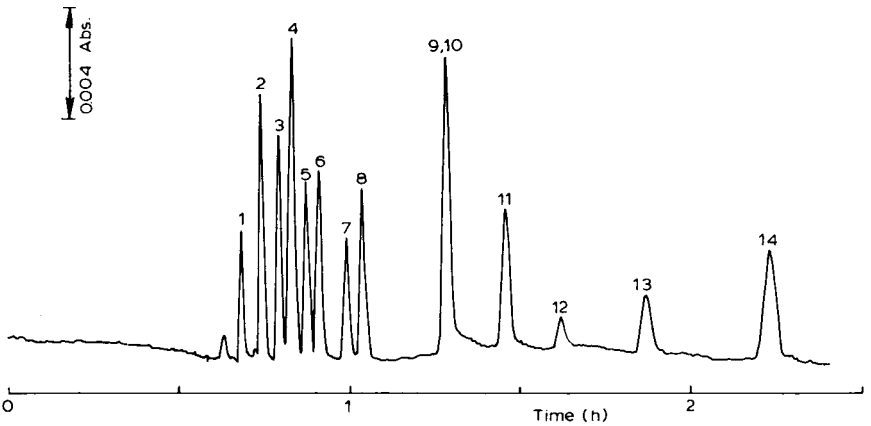

Fig. 10. Separation of polynuclear aromatic hydrocarbons on ODS capillary column. Column: ODS, 7.2 m × 32 μm I.D. Mobile phase: acetonitrile–water (45:55). Flow-rate: 0.14 μl/min. Sample: 1 = benzene; 2 = naphthalene; 3 = biphenyl; 4 = fluorene; 5 = phenanthrene; 6 = anthracene; 7 = fluoranthene; 8 = pyrene; 9 = *p*-terphenyl; 10 = chrysene; 11 = 9-phenylanthracene; 12 = perylene; 13 = 3,4-benzopyrene; 14 = 1,3,5-triphenylbenzene. Column temperature: 43°C. Wavelength of detection (UV): 254 nm.

Normal-phase system

Si, NH_2 and ODS columns were prepared and the effect of column temperature on the retention of aromatic amines was examined in the normal-phase system. Although ODS columns are usually employed in the reversed-phase mode, residual silanol groups in ODS capillary columns worked as adsorbents and permitted separation also in the normal-phase mode.

Figs. 11–13 show relationships between $\ln k'$ and $1/T$ for three types of columns. The mobile phase was *n*-hexane containing 0.5% (v/v) of acetonitrile as the moderator. Linear relationships were observed with the NH_2 and ODS columns, but for the Si column the relationship deviated from linearity. These results are not consistent with results in the literature[12,14]. In normal-phase chromatography using packed columns, the relationship between $\ln k'$ and $1/T$ is complex and far from linear.

Likewise in the reversed-phase system, ΔH° can be calculated from the data in Figs. 12 and 13. The results are given in Table II, which also gives ΔH° values using other solvents as the moderator for the NH_2 column. The ΔH° values are dependent on both the moderator and the stationary phase. In particular the ΔH° values for N-phenyl-α- and N-phenyl-β-naphthylamine obtained on the ODS column and those obtained using *n*-hexylamine as the moderator are characteristic.

The difference in the selectivity with the three types of columns was considered. Separation factors, defined as k_1'/k_2', are given in Table III. The difference in selectivity may be ascribed to the modification of the stationary phase.

The separation of aromatic amines on the ODS capillary column is shown in Fig. 14.

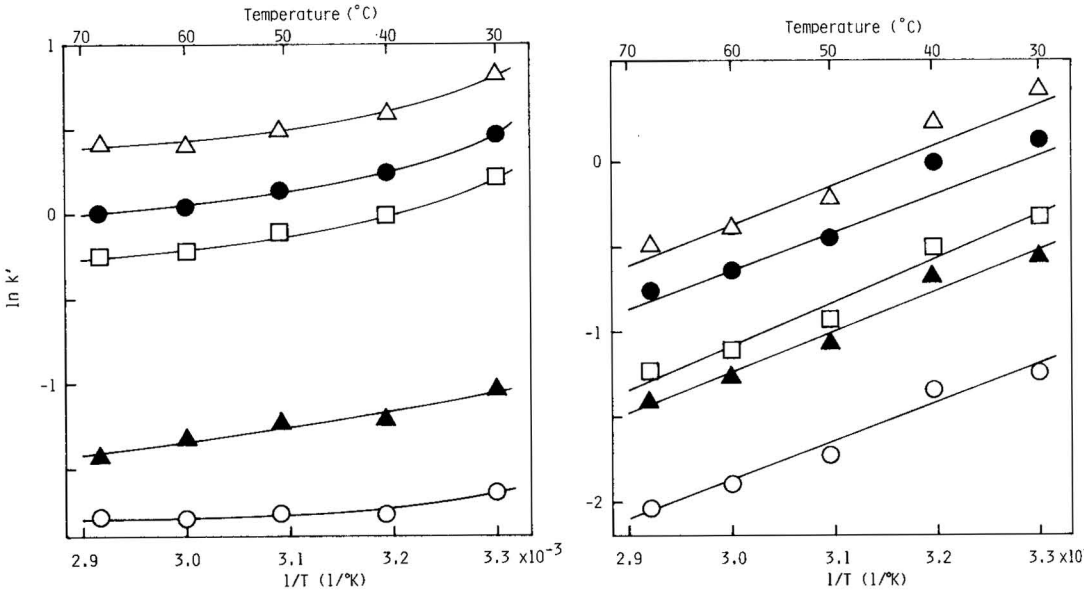

Fig. 11. Relationship between ln k' and $1/T$ for Si column. Column: Si, 5.2 m × 46 μm I.D. Mobile phase: *n*-hexane containing 0.5% of acetonitrile. Sample: ○ = N-phenyl-α-naphthylamine; ▲ = N-phenyl-β-naphthylamine; □ = aniline; ● = α-naphthylamine; △ = β-naphthylamine.

Fig. 12. Relationship between ln k' and $1/T$ for NH_2 column. Column: NH_2, 5.2 m × 55 μm. Other conditions as in Fig. 11.

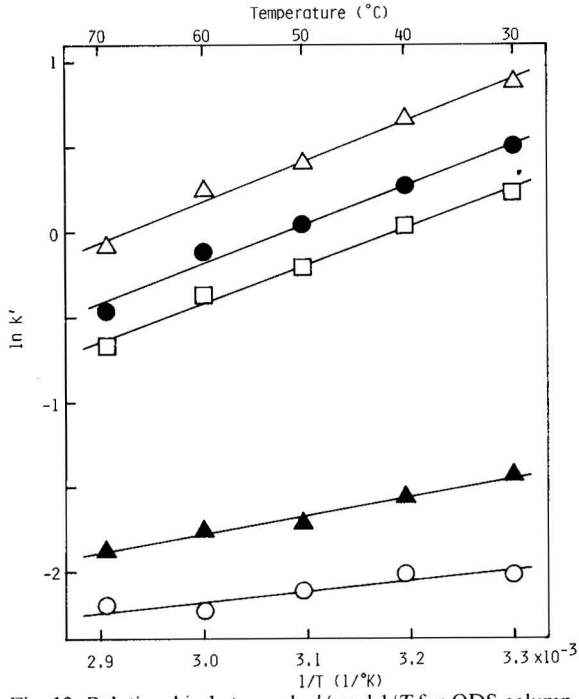

Fig. 13. Relationship between ln k' and $1/T$ for ODS column. Column: ODS, 5.3 m × 46 μm I.D. Other conditions as in Fig. 11.

TABLE II

ΔH° VALUES FOR AROMATIC AMINES

Columns: NH_2, 5.2 m × 55 μm I.D., and ODS, 5.3 m × 46 μm I.D. Mobile phase: *n*-hexane containing the moderator indicated.

Column	*Moderator*	*Solute**	$-\Delta H^\circ$ *kJ/mol*
NH_2	CH_3CN (0.5%)	NPαNA	18.8
		NPβNA	20.1
		A	21.1
		αNA	21.0
		βNA	21.1
NH_2	CH_3CN (0.2%) + CH_2Cl_2 (5%)	NPαNA	12.8
		NPβNA	15.4
		A	19.5
		αNA	18.7
		βNA	19.0
NH_2	*n*-$C_6H_{13}NH_2$ (0.2%)	NPαNA	5.2
		NPβNA	6.4
		A	–
		αNA	6.5
		βNA	6.1
ODS	CH_3CN (0.5%)	NPαNA	5.1
		NPβNA	9.2
		A	19.0
		αNA	19.1
		βNA	20.1

* NPαNA = N-phenyl-α-naphthylamine; NPβNA = N-phenyl-β-naphthylamine; A = aniline; αNA = α-naphthylamine; βNA = β-naphthylamine.

TABLE III

SEPARATION FACTORS OBTAINED IN THE NORMAL-PHASE SYSTEM

Mobile phase: *n*-hexane containing 0.5% of acetonitrile.

Column	*Temperature (°C)*	*Separation factor**		
		k' (A)/k' (NPβNA)	*k' (αNA)/k' (NPβNA)*	*k' (βNA)/k' (NPβNA)*
Si	30	3.5	4.5	6.3
NH_2	30	1.2	2.0	2.6
ODS	30	5.2	6.9	10.0
Si	50	3.0	3.9	5.3
NH_2	50	1.1	1.8	2.4
ODS	50	4.6	5.9	8.6

* Abbreviations in parentheses as in Table II.

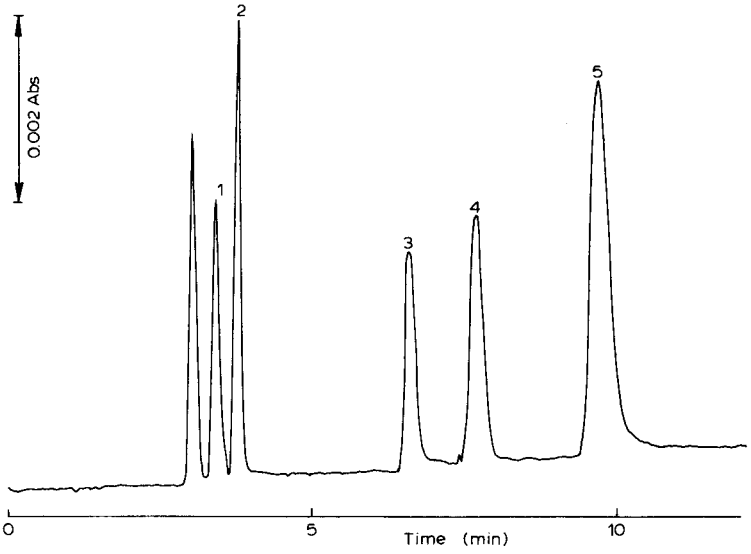

Fig. 14. Separation of aromatic amines on ODS column. Column: ODS, 5.3 m × 46 μm I.D. Mobile phase: *n*-hexane containing 0.5% of acetonitrile. Sample: 1 = 2.2 ng of N-phenyl-α-naphthylamine; 2 = 2.6 ng of N-phenyl-β-naphthylamine; 3 = 3.1 ng of aniline; 4 = 1.7 ng of α-naphthylamine; 5 = 1.5 ng of β-naphthylamine. Temperature: 35°C. Wavelength of detection (UV): 235 nm.

Cation-exchange

Diffusion coefficients of solutes in the mobile phases employed in ion-exchange chromatography are so small that it is preferable to operate at higher temperature. The effect of temperature on column efficiency was examined in this work and previously[21], and a higher efficiency was attained at *ca.* 60°C for retained solutes.

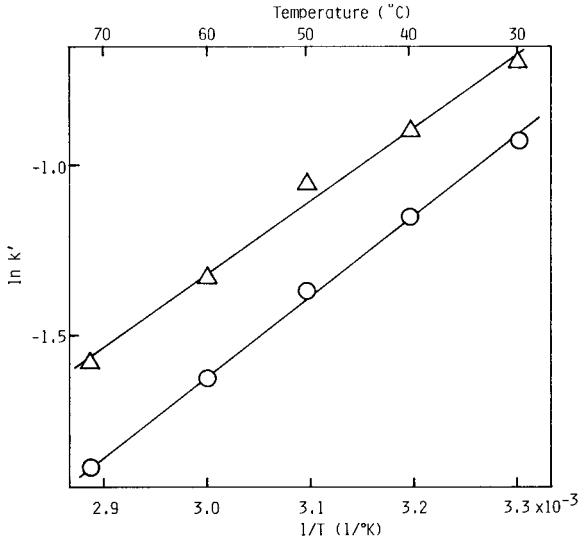

Fig. 15. Relationship between ln k' and $1/T$ for CEX column. Column: CEX, 5.4 m × 47 μm I.D. Mobile phase: $1 \cdot 10^{-3}$ *M* ammonium formate adjusted to pH 3.5 with formic acid. Sample: ○ = adenosine; △ = cytidine.

A linear relationship between ln k' and $1/T$ is also observed in cation-exchange capillary LC. The results are shown in Fig. 15. The ΔH° values for adenosine and cytidine were calculated to be -19.9 and -18.2 kJ/mol, respectively.

The separation of four nucleosides on the CEX column is shown in Fig. 16.

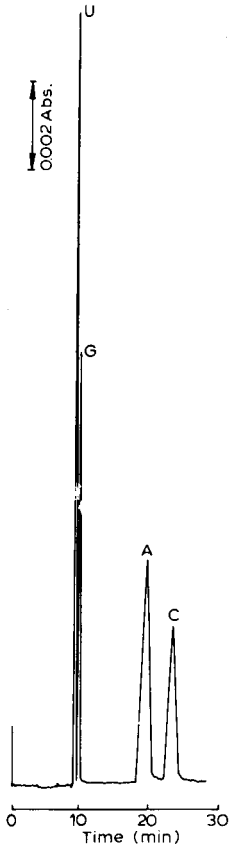

Fig. 16. Separation of nucleosides on CEX column. Column: CEX, 6.0 m × 39 μm I.D. Mobile phase: 2×10^{-3} *M* ammonium formate adjusted to pH 3.4 with formic acid. Sample: U = uridine; G = guanosine; A = adenosine; C = cytidine. Temperature: 43°C. Wavelength of detection (UV): 260 nm.

CONCLUSION

Temperature determines the retention of solutes, selectivity and column efficiency in open-tubular capillary LC. Linear relationships between ln k' and $1/T$ are generally obtained in reversed-phase, normal-phase and cation-exchange capillary LC. Operation at higher temperature leads to a decrease in the viscosity of the eluent, which results in an increase in column efficiency and a decrease in inlet pressure.

REFERENCES

1 R. J. Maggs, *J. Chromatogr. Sci.*, 7 (1969) 145.
2 R. P. W. Scott and J. G. Lawrence, *J. Chromatogr. Sci.*, 8 (1970) 619.

3 C. Burgess, *J. Chromatogr.*, 149 (1978) 233.
4 K. Tsuji and J. F. Goetz, *J. Chromatogr.*, 157 (1978) 185.
5 H. Colin, J. C. Diez-Masa, G. Guiochon, T. Czajkowska and I. Miedziak, *J. Chromatogr.*, 167 (1978) 41.
6 R. J. Perchalski and B. J. Wilder, *Anal. Chem.*, 519 (1979) 774.
7 J. Chmielowiec and H. Sawatzky, *J. Chromatogr. Sci.*, 17 (1979) 245.
8 R. B. Diasio and M. E. Wilburn, *J. Chromatogr. Sci.*, 17 (1979) 565.
9 L. R. Snyder, *J. Chromatogr.*, 179 (1979) 167.
10 W. R. Melander, B.-K. Chen and Cs. Horváth, *J. Chromatogr.*, 185 (1979) 99.
11 J. R. Gant, J. W. Dolan and L. R. Snyder, *J. Chromatogr.*, 185 (1979) 153.
12 W. R. Sisco and R. K. Gilpin, *J. Chromatogr. Sci.*, 18 (1980) 41.
13 K. Jinno, H. Nomura and Y. Hirata, *J. High Resolut. Chromatogr. Chromatogr. Commun.*, 3 (1980) 305.
14 R. K. Gilpin and W. R. Sisco, *J. Chromatogr.*, 194 (1980) 285.
15 T. Takeuchi, Y. Watanabe and D. Ishii, *J. High Resolut. Chromatogr. Chromatogr. Commun.*, 4 (1981) 300.
16 D. Ishii and T. Takeuchi, *J. Chromatogr. Sci.*, 18 (1980) 462.
17 K. Hibi, T. Tsuda, T. Takeuchi, T. Nakanishi and D. Ishii, *J. Chromatogr.*, 175 (1979) 105.
18 D. Ishii and T. Takeuchi, *IVth International Symposium on Capillary Chromatography, Hindelang, West Germany, May 3–7, 1981.*
19 T. Tsuda, K. Hibi, T. Nakanishi, T. Takeuchi and D. Ishii, *J. Chromatogr.*, 158 (1978) 227.
20 D. Ishii, T. Tsuda and T. Takeuchi, *J. Chromatogr.*, 185 (1979) 73.
21 D. Ishii and T. Takeuchi, *J. Chromatogr.*, 218 (1981) 189.

Journal of Chromatography, 235 (1982) 323–336
Elsevier Scientific Publishing Company, Amsterdam Printed in The Netherlands

CHROM. 14,355

IN SITU COATING OF A NARROW-BORE GLASS CAPILLARY COLUMN WITH A HIGH TEMPERATURE NEMATIC LIQUID CRYSTAL

F. JANSSEN* and T. KALIDIN
Chemistry Department, Joint Laboratories and Other Services of the Dutch Electricity Supply Companies (N.V. KEMA), P.O. Box 9035, 6900 ET Arnhem (The Netherlands)
(First received June 19th, 1981; revised manuscript received August 26th, 1981)

SUMMARY

A method for the *in situ* coating of a narrow-bore glass capillary column with N,N′-bis(*p*-phenylbenzylidene)-α,α′-bi-*p*-toluidine (BPhBT) as stationary phase for gas chromatography is presented. The reaction components α,α′-bi-*p*-toluidine and *p*-phenylbenzaldehyde are brought together in the capillary and react with each other during the evacuation step in the static coating technique.

The gas chromatographic behaviour of five- and two-ring polycyclic aromatic hydrocarbons are compared on the two nematic liquid crystal phases BPhBT and N,N′-bis(*p*-methoxybenzylidene)-α,α′-bi-*p*-toluidine (BMBT) respectively. The quality of the columns is evaluated in terms of the effective number of theoretical plates, partition ratio (capacity factor), separation factor and Trennzahl. It is shown that a polar liquid crystal forms a coherent film on a glass surface which has been covered by a layer of barium carbonate or of carbon black. Glass capillaries pretreated in this way exhibit equal or better separation efficiencies than conventional capillary, micro- and packed columns which liquid nematic crystals as stationary phase.

INTRODUCTION

Since 1963, high temperature nematic liquid crystals have been used for difficult separations of isomers such as disubstituted benzenes[1,2], polycyclic aromatic hydrocarbons[3–12], isomers of the anti-inflammatory agent benoxaprofen[13], polychlorinated biphenyls[14] and azaheterocyclic compounds[15].

The theoretical background of liquid crystal systems is discussed in many papers (refs. 16, 17 and references therein). Most of the chromatographic applications of liquid crystals have been to the separations of the above compounds on packed columns. In general, the crystal homologues and analogues of N,N′-bis(*p*-methoxybenzylidene)-α,α′-bi-*p*-toluidine (BMBT) were employed as stationary phase. Only a few papers describe the application of high temperature nematic liquid crystals as stationary phase in capillary columns[18–20].

The use of the liquid crystals BPhBT and BBBT (the *p*-phenyl and *p*-butoxy

0021-9673/82/0000–0000/$02.75

homologues of BMBT) as wall coating substrates in wide-bore (0.75 mm I.D.) stainless-steel capillary columns was recently reported[19,20]. The efficiencies obtained were a factor of 10–20 greater than for packed columns, but much less than those attainable on conventional (0.25 mm I.D.) capillary columns. The properties and preparation of the liquid crystal BBBT and in admixture with a gum phase (SE-52) in a leached and silylated glass capillary (17.5 m × 0.2 mm I.D.) have also been reported.

In the present paper we describe the *in situ* coating of BPhBT in a narrow-bore (0.25 mm I.D.) glass capillary column and its utilization in gas chromatographic (GC) analysis. BPhBT is thermally stable in the nematic phase and also shows a high selectivity for five-ring polyaromatic hydrocarbons (PAHs). The results are compared with those obtained on a conventionally coated (OV-1) capillary column and a capillary with BMBT as stationary phase.

EXPERIMENTAL

Materials

The starting reagents, α,α'-bi-*p*-toluidine (Eastman-Kodak), *p*-phenylbenzaldehyde (Aldrich) and BMBT (Eastman-Kodak), were purified by recrystallization from water–ethanol. The purity of the reagents was checked by IR spectroscopy, solid probe mass spectrometry and thermal analysis.

Standard polycyclic aromatic hydrocarbons (Community Bureau of Reference-BCR of the European Communities, Brussels, Belgium) were used without further purification and were dissolved in glass-distilled cyclohexane. The sample bottles were wrapped in aluminium foil to prevent photolysis. The concentrations of the compounds phenanthrene, anthracene, 1,2-benzopyrene (BeP), perylene (Per), 3,4-benzopyrene (BaP) and benzo[*b*]chrysene [B(b)C] were 250, 250, 245, 100, 255 and 62.5 ng/μl respectively.

Apparatus and procedures

The measurements were performed on a Varian 3700 gas chromatograph equipped with a flame ionization detector. The oven temperature was measured with a mercury thermometer and a digital thermocouple (United Systems, OH, U.S.A.).

A universal capillary injection system (Chrompack, Middelburg, The Netherlands) was used in the splitless injection mode. The splitter was closed for 2 min before injecting a sample; the injection was carried out within 5–10 sec. The sample (1 μl) was introduced using a Hamilton 701 N 10-μl syringe (empty-needle injection).

The columns were installed via Kalrez ferrules (Carlo Erba) at the detector and with graphite ferrules at the injector. Ultra high purity hydrogen was used as carrier gas and nitrogen as make-up gas. The chromatograms were recorded on a Sigma-10 data station (Perkin-Elmer) using a electrometer setting of $8 \cdot 10^{-11}$ A full scale. Scanning electron microscopy (Jeol JSM 35) was applied to study the behaviour of the liquid crystals BPhBT and BMBT on carbon and on barium carbonate.

Preparation of the columns

Barium carbonate. The pre-treatment of borosilicate columns (0.25 mm I.D.) was studied by Grob and co-workers[21–27] and will be commented upon only briefly.

After straightening the ends of the empty glass columns, the surface was leach-

ed with HCl in order to produce a deionized silica gel surface layer. The capillary was filled with 20% HCl solution and both ends were closed in a flame. The capillary was kept overnight at 180°C. The HCl was displaced by deionized water and then dried for 2 h at 250°C with a low helium flow. After the leaching and dehydration, the column was treated by the barium carbonate method according to Grob *et al.*[24,27].

Carbonization. A very thin layer of carbon was deposited on the inner surface of glass capillaries by pyrolysis of methylene chloride. Nitrogen was bubbled through methylene chloride at 0°C and directly brought into the capillary, which was held at 50°C. After 2 h, both ends were closed in a flame and the column was placed in an oven at 550°C. After 1 h the capillary was opened and a solution of 10% diethylamine in methylene chloride was sucked in, in order to remove the HCl.

Static coating. The columns were filled with a solution of α,α′-bi-*p*-toluidine and *p*-phenylbenzaldehyde in acetone–diethyl ether (50:50 v/v) at concentrations of 3.18 and 5.43 g/l respectively (molar ratio 1:2). The concentrations were based on a layer thickness of 0.5 μm and on a reaction efficiency of 100%.

With the mixture acetone–diethyl ether no visible reaction occurs, even after a week. This mixture was chosen instead of pentane or methylene chloride because of the greater solubility of water (a product of the reaction between the aldehyde and the aromatic amine). The hygroscopic solvent ethanol cannot be used because of its low vapour pressure and because of the high reaction rate of the compounds in it. In case of BMBT, methylene chloride was used as solvent.

After filling, one end of the column was closed. Four methods of closing the column were tried, namely: sodium silicate, silicone rubber, rubber of a septum and paraffin (42–44°C). The least time-consuming and most elegant method was the paraffin closing. One column end of the column was then placed in hexane and a low vacuum was applied to the other end to move the meniscus by 4–5 cm. The end with the hexane plug was then placed into the liquid paraffin (50°C) and again a low vacuum (0.1 bar) was applied to the inlet and moved the hexane–paraffin meniscus by 1–2 cm. After cooling the solid paraffin forms a good solid closure. The hexane plug is necessary to avoid reactions between the paraffin plug and the reactants during the evacuation step.

The column was immediately and completely immersed in a water-bath (10 l) at room temperature and evacuated at the open end. After 16–40 h the closed end was cut away and both ends were deactivated with an 0.1% methylene chloride solution of Carbowax (MW 400). The column was placed in the gas chromatograph for conditioning and the oven temperature was raised slowly (0.5°C min^{-1}) from room temperature to 300°C. The columns were kept at this temperature for 24 h.

RESULTS AND DISCUSSION

The coating technique

During work on packed and micro-packed glass columns with BPhBT as stationary phase[5] we observed a yellow film on the silanized glass surface after emptying the column. The origin of this film can be ascribed to column-bleed and/or to diffusion of the pure liquid crystal from the Chromosorb support to the glass wall. So there are intermolecular attraction forces between functional groups on the surface and the stationary phase BPhBT, and/or bleeding.

TABLE I

CAPILLARY COLUMNS USED

Phen = phenanthrene; anth = anthracene.

No.	*Length (m)*	*T (°K)*	*Pre-treatment**	*Liquid phase*	*Film thickness** (μm)*	*TZ*** BaP/BeP*	*N§ BaP*	*TZ Phen/Anth*	*N Phen*	*Flow (cm sec⁻¹)*	
										Measured§§	*Methane§§§*
1	18.5	538.8	$BaCO_3$	BPhBT	0.5	2.85	712	–	–	303.7	38.5
2	17.0	451.5	C	BMBT	0.5	–	–	7.60	818	67.9	34.5
3	32.0	479.5	$BaCO_3$	BMBT	0.5	–	–	7.85	526	67.8	25.2

* See Experimental section.

** In the case of BPhBT, this was calculated on the basis of 100% yield of the reaction α,α′-bi-*p*-toluidine and *p*-phenylbenzaldehyde.

*** Maximum attainable values of TZ, calculated from

$$TZ = \frac{t_{R,BaP} - t_{R,Bep}}{w_{0.5,BaP} + w_{0.5,Bep}} - 1$$

where $w_{0.5}$ is the peak width at half-height.

§ Effective theoretical plate number per metre, $5.54\,(t'_R/w_{0.5})^2$.

§§ The flow measured with a soap-film meter, divided by the cross-sectional area.

§§§ The flow calculated from the retention of methane.

Therefore, in order to study the wettability of the silica framework we had to treat the support surface. This treatment is based on the principles of the so-called geometrical and chemical film stabilization[26].

There are two pre-requisites in making glass capillary columns. First there should be an uninterrupted coherent "liquid crystal" film on the glass surface in order to achieve maximum separation efficiency. Secondly, there should be no active sites on the surface in order to avoid adsorption of sample and catalytic effects on sample and stationary phase degradation. Untreated and HCl-leached/dehydrated glass surfaces are highly reactive, because of the dipole moment of the functional group Si–OH. Such surfaces form good substrates for the semipolar phase BPhBT. However, some active sites remain on the surface which can result in adsorption of polycyclic aromatic hydrocarbons and/or increased retention of some aromatic hydrocarbons, and also give rise to severe peak distortions.

The use of persilylated surfaces[22] is not possible in our case, because of the medium polarity of the liquid crystals. So we applied the barium carbonate deactivation method and carbonization of the glass surface. The barium carbonate layer is less active than the leached surface itself and it roughens the glass wall[28]. Carbonized glass is also suitable for the coating of glass capillaries with polar liquid crystals. Our attempts to spread the BPhBT on the glass surface with the static coating technique did not succeed. The solubility of BPhBT in various solvents is too low to yield a suitable film on the glass wall. Moreover, BPhBT crystallizes during the evacuation step in the static coating technique when working with slurries of BPhBT in methylene chloride. The crystals can move freely through the column after the coating.

To overcome the problems of solubility and film formation from slurries, BPhBT was synthesized directly in the column during the evacuation step of the static coating method. One problem that should not be overlooked is the rôle of water which is generated as a by-product of the reaction between the amine and the aldehyde. The water can destroy or at least influence the barium carbonate layer in a negative sense. The water has to be removed because the reaction

$$\text{amine} + \text{aldehyde} \rightarrow \text{liquid crystal} + \text{water}$$

has to be displaced to the right. We, therefore, chose an acetone–diethyl ether mixture in which water is reasonably soluble. However, we could not find any influence of water on the barium carbonate layer. This could support the fact that the divalent cation (Ba^{2+}) has a considerable crystal lattice energy at the silicate surface and thus resistance to hydrolysis, as pointed out by Pretorius *et al.*[28].

Gas chromatography

Table I lists the columns used. We started this study with mixed phases such as a gum phase OV-1 or a phase like OV-101. In both cases severe bleeding was observed. So we discarded the idea of an "epitactic" layer between the liquid crystal and the glass wall itself. After coating the columns there are small white crystals on the column wall. These crystals disappear after heating in the gas chromatograph to leave a yellow film on the glass surface.

From Table II it can be seen that the surface modification and pre-treatment has a small influence on the molar enthalpy of solutions. The surface area is probably

TABLE II

PARTIAL MOLAR ENTHALPIES OF SOLUTION OF THREE-RING PAHs ON BMBT (COLUMNS 2 AND 3)

Compound	*Carbonized surface*			*Barium carbonate surface*		
	ΔH* ($kJ\ mol^{-1}$)	C**	r^2***	ΔH ($kJ\ mol^{-1}$)	C	r^2
Phenanthrene	−56.84	−8.33	0.95	−50.20	−5.37	0.98
Anthracene	−57.09	−8.14	0.99	−55.50	−6.42	0.98

* Calculated from plots of $\log_e (t_R - t_0)$ *vs.* $1/T$.

** C is the constant (entropy term) of the equation:

$$\log_e (t_R - t_0) = -\Delta H/RT + C$$

*** r^2 is the coefficient of determination:

$$r^2 = \frac{[\Sigma xy - (\Sigma x \Sigma y/n)]^2}{[\Sigma x^2 - (\Sigma x)^2/n]\,[\Sigma y^2 - (\Sigma y)^2/n]}$$

greater in the case of the carbonized surface so the heat evolved increases when a solute is transferred from the gas phase to the solution. Table III summarizes the partial molar enthalpies of solution of five-ring PAHs. Also in this case, the enthalpies are greater on a carbonized surface than on a barium carbonate treated surface[29].

TABLE III

PARTIAL MOLAR ENTHALPIES OF SOLUTION OF FIVE-RING PAHs ON BPhBT (COLUMN 1, BARIUM CARBONATE SURFACE)

For definitions see Table II.

Compound	ΔH ($kJ\ mol^{-1}$)	C	r^2
1,2-Benzopyrene	−63.64	−8.70	0.99
Perylene	−61.72	−8.11	0.99
3,4-Benzopyrene	−61.84	−8.09	0.99
Benzo[*b*]chrysene	−76.53	−10.15	0.99

As the temperature decreases, α, k, TZ and N increase as is seen in Tables IV–VI. So the best separation efficiency and resolution of the liquid crystal can be obtained in the vicinity of the solid nematic transition temperature. Plots of TZ *vs.* $1/T$ in the temperature range 265–282°C for BPhBT and 185–225°C for BMBT are linear with a coefficient of determination of 0.98 and 0.97 respectively (Figs. 1 and 2). The plots of $\log_e t'_R$ *vs.* $1/T$ in Fig. 3 show clearly the solid–nematic transition point of BPhBT. This transition point is sharper than in the case of a micro-packed column as has been shown previously[5].

Fig. 4 combines two chromatograms of five-ring PAHs on a BPhBT and a OV-

TABLE IV

RETENTION, TRENNZAHL, EFFECTIVE NUMBER OF THEORETICAL PLATES, PARTITION RATIO AND SEPARATION OF PHENANTHRENE AND ANTHRACENE AS A FUNCTION OF TEMPERATURE WITH BMBT ON A CARBON SUPPORT AND A BARIUM CARBONATE LAYER (COLUMNS 2 AND 3 RESPECTIVELY)

T (°K)	*Retention (sec)**		*TZ*	*N*		*k***		*α**** *Anth/Phen*
	Phen	*Anth*		*Phen*	*Anth*	*Phen*	*Anth*	
Carbonized column			*Nematic phase*					
499.5	213	247[§]	3.49	6380	9597	4.33	5.56	1.285
490.0	273	355	4.69	9500	11,490	5.56	7.22	1.300
481.0	346	463	5.08	9625	11,425	7.04	9.42	1.339
471.0	462	620	5.95	10,125	14,795	9.39	12.60	1.343
461.5	623	852	6.74	12,920	17,440	12.65	17.32	1.365
			Solid phase					
451.5	842	1171	7.60	13,900	16,295	17.10	23.81	1.393
Barium carbonate column								
496.0	880	1120	5.78	14,619	21,730	6.92	8.80	1.272
489.5	1088	1411	6.18	14,893	19.147	8.55	11.1	1.294
479.5	1354	1803	7.50	16,826	22,636	10.67	14.1	1.331

* Adjusted retention (t'_R) = retention time minus retention time of methane.
** Partition ratio (capacity factor) = $t'_R/t_{methane}$.
*** The separation factor, *i.e.*, the ratio of the corrected retentions of anthracene and phenanthrene.
[§] Mean from two measurements.

TABLE V

RETENTION, TRENNZAHL, EFFECTIVE NUMBER OF THEORETICAL PLATES AND PARTITION RATIO AS A FUNCTION OF TEMPERATURE

BPhBT as stationary phase on $BaCO_3$ (column 1, Table I). For definitions see Tables I and IV.

T (°K)	*Retention (sec)*				*k*				*N*		*TZ* *BeP/BaP*
	BeP	*Per*	*BaP*	*B(b)C*	*BeP*	*Per*	*BaP*	*B(b)C*	*BeP*	*BaP*	
				Nematic phase							
557.2	153	184	188	581	3.19	3.83	3.92	12.1	–	–	–
555.5	161	191	204	–	3.35	3.98	4.25	–	2462	2713	1.04
552.6	174	204	215	699	3.63	4.25	4.48	14.56	4806	6351	1.60
547.0	200	235	247	804	4.17	4.90	5.15	16.76	–	–	–
543.3	219	257	270	898	4.57	5.36	5.63	18.71	7628	7969	2.31
538.8	245	290	302	1022	5.09	6.04	6.29	21.30	9169	13,166	2.85
				Solid phase							
534.2	252	305	305	1043	5.25	6.35	6.35	21.73	7886	4821	1.69
529.3	290	354	354	1212	6.04	7.38	7.38	25.25	7832	5092	1.94

TABLE VI

SEPARATION FACTORS ON BPhBT (COLUMN 1, TABLE I)

T (°K)	Separation factor*			$t_{R,BaP}$ (min)
	BeP	Per	B(b)C	
555.5	0.783	0.930	–	3.40
552.6	0.800	0.942	3.448	3.58
547.0	0.810	0.952	3.257	4.12
543.3	0.808	0.952	3.297	4.50
538.8	0.808	0.957	3.362	5.03
534.2	0.824	1.000	3.394	5.08
529.3	0.823	1.000	3.437	5.90

* $t'_{R,\text{compound}}/t'_{R,\text{BaP}}$.

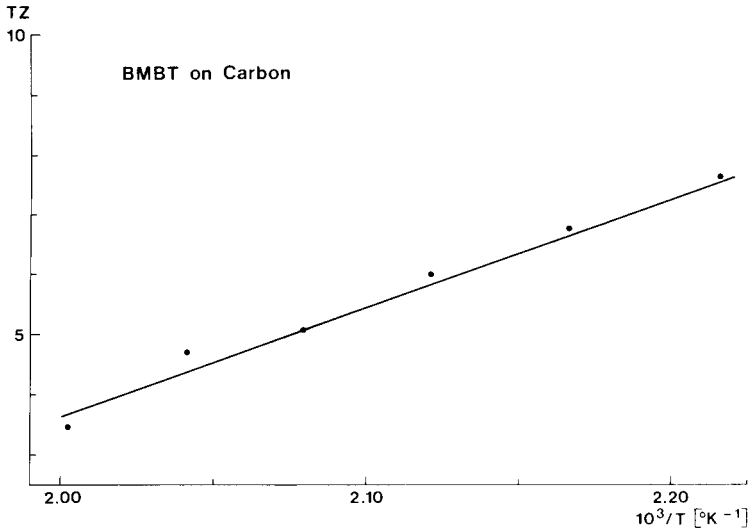

Fig. 1. Dependence of the Trennzahl of phenanthrene and anthracene on $1/T$ of column 2 (Table I).

l column and demonstrates the difference in analysis times. Both columns contain barium carbonate as a surface layer. Fig. 5 shows a chromatogram of three-ring PAHs on a BMBT column (carbonized).

To improve the selectivity and resolution of the capillary systems we studied the possibility of a semibonded phase. The C≡N group of the OV-225 molecule is hydrolyzed to the carboxylic acid and then transformed into the acid chloride, which has to be catalytically hydrogenated via the Rosenmund reaction. The aldehyde formed in this way could react with the α,α′-bi-*p*-toluidine which in its turn reacts with the *p*-phenylbenzaldehyde. So this stationary phase has a polar and an apolar side. The apolar side is necessary for the persilylated glass surface and the polar side for the coating of BPhBT.

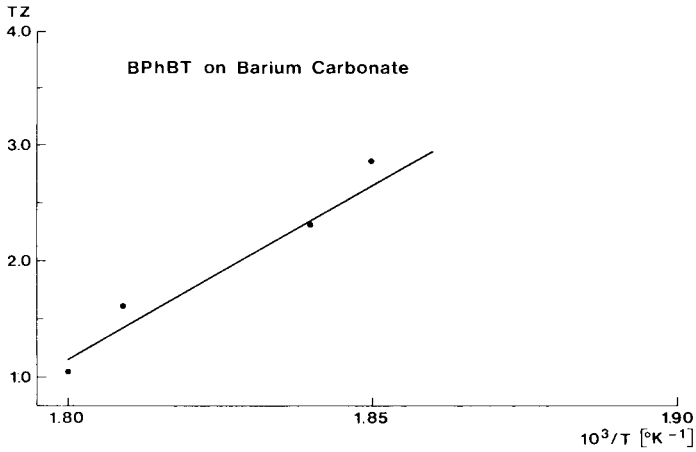

Fig. 2. Dependence of the Trennzahl of 3,4-benzopyrene and 1,2-benzopyrene on $1/T$ of column 1 (Table I).

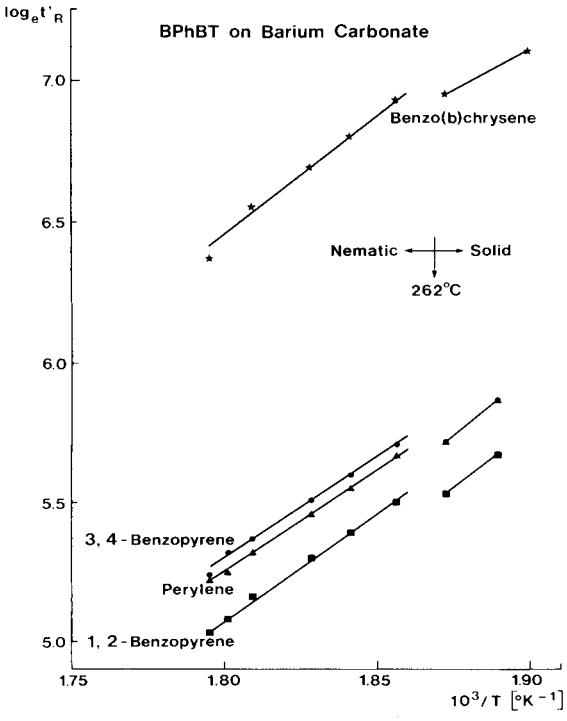

Fig. 3. Dependence of the logarithm of the adjusted retention time (t'_R) on the reciprocal absolute temperature of five-ring PAHs on column 1 (Table I).

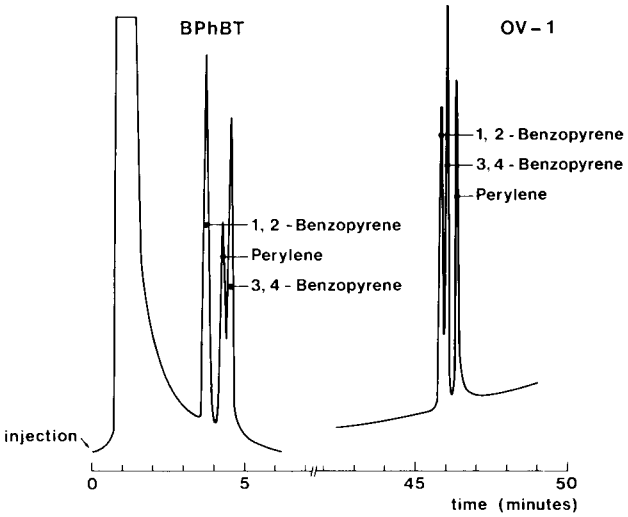

Fig. 4. Glass capillary chromatograms of five-ring PAHs on (left) a 18.5 m × 0.25 mm column coated *in situ* with BPhBT (0.5 μm), pressure 0.60 bar, temperature 280° C and (right) a 27 m × 0.30 mm column coated with 0.15-μm OV-1, programmed from 60 to 300° C at 6° C min^{-1}.

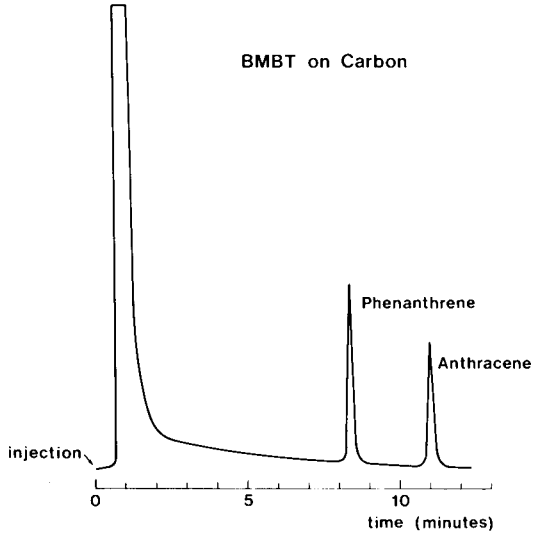

Fig. 5. Glass capillary chromatogram of phenanthrene and anthracene on a 17 m × 0.25 mm column coated with BMBT on carbon; pressure 0.54 bar, temperature 198° C.

Electron microscopy

Fig. 6 shows the BPhBT coating on a barium carbonate layer and on a carbon layer and before and after heating in the gas chromatograph. In Fig. 6A, some unreacted starting compounds is probably present on the surface. After heating, the surface is covered with a layer (probably BPhBT) and also with large crystals, which

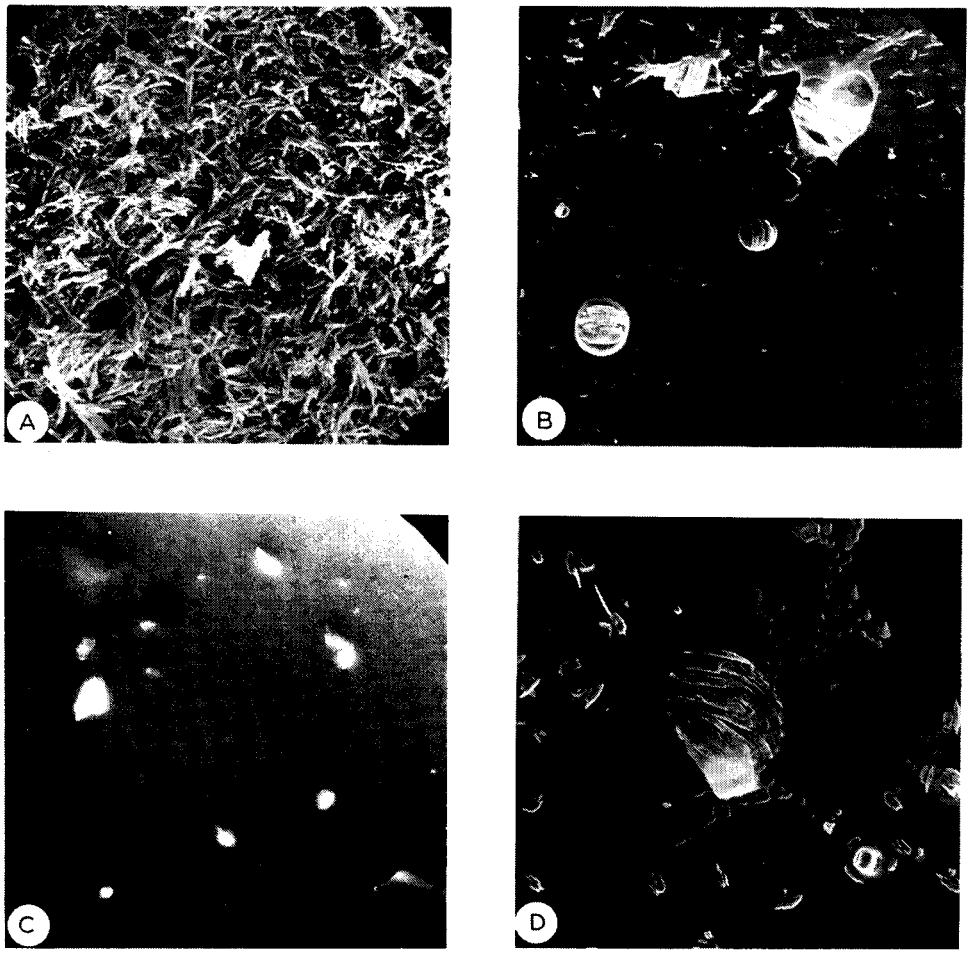

Fig. 6. Scanning electron micrographs of BPhBT: A, on $BaCO_3$ at room temperature (× 3672); B, on $BaCO_3$ after heating for 2 h at 300°C in a helium flow (× 3672); C, on a carbonized surface at room temperature (× 680); D, on a carbonized surface after heating for 2 h at 300°C in a helium flow (× 3672).

have the same shape as BPhBT crystals. The completion of the layer is supported by the fact that the barium carbonate crystals are not longer visible, as in Fig. 7A.

In case of the carbonized surface the BPhBT crystals become visible only after heating (Fig. 6C and D) in the gas chromatograph. So during the heating and the cooling of the columns a recrystallization process takes place. The carbon layer consists of very small spheres (Fig. 7B) surrounded by smaller homogeneously divided carbon particles. We expect the crystals on a carbonized surface to be smaller than on a surface with a barium carbonate layer because the surface area is greater.

In the case of BMBT the situation is different. Fig. 8B shows that there are still barium carbonate crystals left and the integrity of the stationary phase film is being disrupted at room temperature. So the wettability of BMBT is poor in comparison with that of BPhBT on barium carbonate. The BMBT forms droplets on the barium

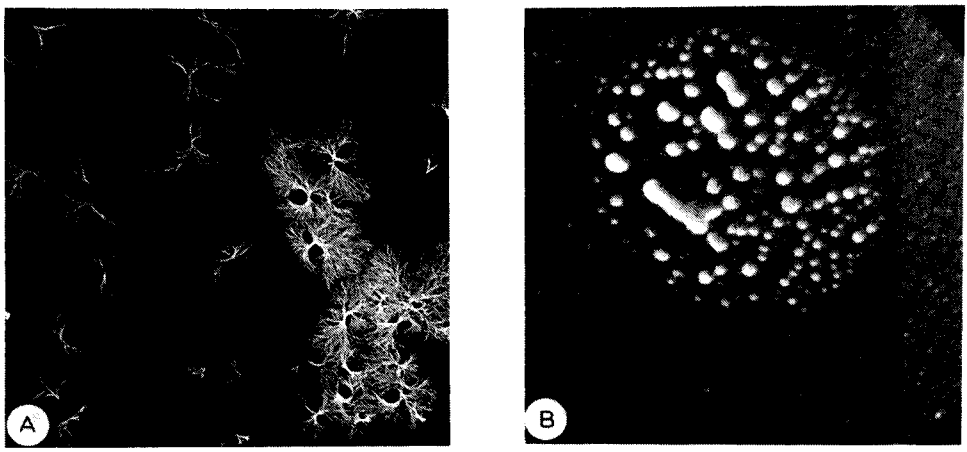

Fig. 7. Scanning electron micrographs (× 680); A, $BaCO_3$ on the wall of a capillary column; B, carbon deposits on the wall of a capillary column.

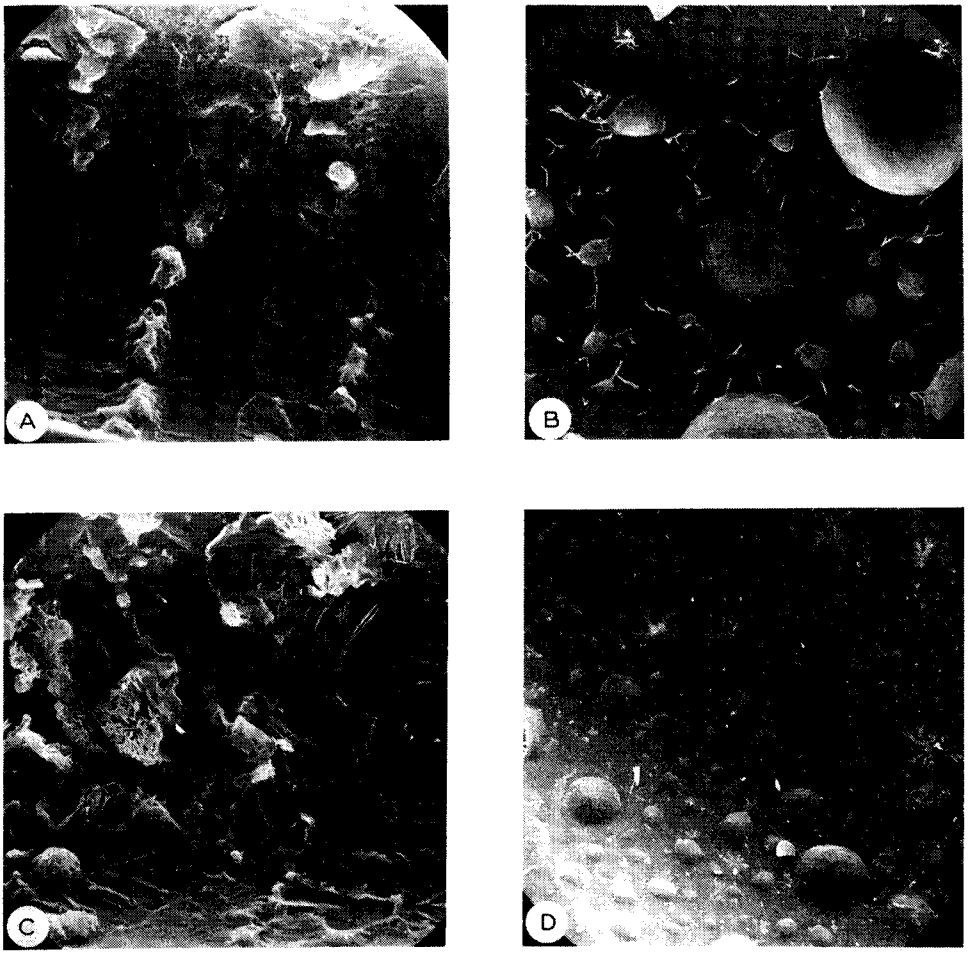

Fig. 8. Scanning electron micrographs of BMBT; A, on $BaCO_3$ at room temperature (× 272); B, on $BaCO_3$ after heating for 2 h at 300°C (× 680); C, on a carbonized glass surface at room temperature (× 272); D, on a carbonized glass surface after heating for 2 h at 300°C in a helium flow (× 367).

carbonate layer as well as on the carbonized layer. However, on the latter these droplets are smaller than on the former.

However, it should be remembered that the electron-microscope investigations were carried out at "room temperature". In future studies we hope to investigate the surface layers at elevated temperatures, especially at the solid–nematic transition point, to approach the actual situation in a capillary column during chromatographic separations.

CONCLUSIONS

A carbonized surface forms a good substrate for BMBT as stationary phase in a capillary column, probably better than that formed by barium carbonate. In contrast, barium carbonate is a better substrate for BPhBT. We could not prepare a carbonized column with comparable qualities to the barium carbonate column.

The film thickness should have a value between 0.05 and 0.5 μm. A 0.05-μm layer improves the selectivity, but the Trennzahl and the number of plates decrease[29] in the case of BPhBT.

The time required for analyses of five-ring PAHs on a BPhBT column is very short, about 3–6 min for 3,4-benzopyrene (Table V). Even a short column shows a good selectivity and resolution.

ACKNOWLEDGEMENTS

The authors are indebted to Mr. D. Wanjon for the scanning electron microscopy and to Mrs. T. de Roos for secretarial aid.

REFERENCES

1 H. Z. Kelker, *Z. Anal. Chem.*, 254 (1963) 198.
2 M. J. S. Dewar and J. P. Schroeder, *J. Amer. Chem. Soc.*, 86 (1964) 5235.
3 W. L. Zielinski, Jr., *Ind. Res.*, Feb. 1980, 178.
4 A. Radecki, H. Lamparczyk and R. Kaliszan, *Chromatographia*, 12 (1979) 595.
5 F. Janssen, *Anal. Chem.*, 51 (1979) 2163.
6 A. Radecki, H. Lamparczyk, J. Grzybowski and J. Halkiewicz, *J. Chromatogr.*, 150 (1978) 527.
7 J. W. Strand and A. W. Andren, *Anal. Chem.*, 50 (1978) 1508.
8 G. M. Janini, Badaruddin Shaikh and W. L. Zielinski, Jr., *J. Chromatogr.*, 132 (1977) 136.
9 G. M. Janini, G. M. Muschik, J. A. Schroer and W. L. Zielinski, Jr., *Anal. Chem.*, 48 (1976) 1879.
10 G. M. Janini, G. M. Muschik and W. L. Zielinski, Jr., *Anal. Chem.*, 48 (1976) 809.
11 G. M. Janini, K. Johnston and W. K. Zielinski, Jr., *Anal. Chem.*, 47 (1975) 670.
12 G. M. Janini, R. I. Sato and G. M. Muschik, *Anal. Chem.*, 52 (1980) 2417.
13 M. Hall and D. N. B. Mallen, *J. Chromatogr.*, 118 (1976) 268.
14 H. Lamparczyk, A. Radecki and J. Falandysz, *J. High Resolut. Chromatogr. Chromatogr. Commun.*, (1980) 301.
15 M. Pailer and V. Hložek, *J. Chromatogr.*, 128 (1976) 163.
16 J. Kelker and R. Hatz, *Handbook of Liquid Crystals*, Chemie Verlag, Weinheim, 1980.
17 H. Kelker, *J. Chromatogr.*, 112 (1975) 165.
18 R. J. Laub, W. L. Roberts and C. A. S. Smith, *J. High Resolut. Chromatogr. Chromatogr. Commun.*, 3 (1980) 355.
19 G. M. Muschik and M. H. Miller, *Abstracts 179th National Meeting of the Amer. Chem. Soc., Houston, TX, March 1980*, Washington D.C., 1980, ANAL 73.
20 W. L. Zielinski, Jr. and G. M. Janini, *J. Chromatogr.*, 186 (1979) 237.

21 K. Grob, G. Grob and K. Grob, Jr., *J. High Resolut. Chromatogr. Chromatogr. Commun.*, 2 (1979) 677.
22 K. Grob, G. Grob and K. Grob, Jr., *J. High Resolut. Chromatogr. Chromatogr. Commun.*, 1 (1979) 31.
23 K. Grob and G. Grob, Jr., *J. High Resolut. Chromatogr. Chromatogr. Commun.*, 2 (1979) 527.
24 K. Grob, Jr., G. Grob and K. Grob, *J. High Resolut. Chromatogr. Chromatogr. Commun.*, 1 (1978) 149.
25 K. Grob and G. Grob, *Chromatographia*, 10 (1977) 181.
26 K. Grob, *J. High Resolut. Chromatogr. Chromatogr. Commun.*, 2 (1979) 599.
27 K. Grob and G. Grob, *J. Chromatogr.*, 125 (1976) 471.
28 V. Pretorius, J. W. du Toit and J. C. Davidtz, *J. High Resolut. Chromatogr. Chromatogr. Commun.*, 4 (1981) 79.
29 F. Janssen, unpublished results.

Journal of Chromatography, 235 (1982) 337–349
Elsevier Scientific Publishing Company, Amsterdam — Printed in The Netherlands

CHROM. 14,341

NUMERICAL TAXONOMY OF COMMON PHASES FOR GAS–LIQUID CHROMATOGRAPHY, USING CHLOROPHENOXY ALKYL ESTERS AS TEST SUBSTANCES

JACQUES O. DE BEER*
Instituut voor Hygiëne en Epidemiologie, J. Wytsmanstraat 14, B-1050 Brussels (Belgium)
and
AUBIN M. HEYNDRICKX
Laboratorium voor Toxicologie, Rijksuniversiteit te Gent, Hospitaalstraat 13, B-9000 Ghent (Belgium)
(Received August 7th, 1981)

SUMMARY

Numerical taxonomy of the retention indices of the methyl and pentafluorobenzyl esters of ten chlorophenoxy alkyl acids has been employed to determine the relationships between phases used for gas–liquid chromatography.

INTRODUCTION

In a previous paper[1] we described and compared the gas–liquid chromatographic (GLC) behaviour of the methyl and pentafluorobenzyl (PFB) ester of ten chlorophenoxy alkyl acids on different liquid phases with increasing McReynolds constants. On liquid phases with similar McReynolds constants, identical separation patterns and analogous retention indices were established. A plot of the retention indices against a specific polarity constant from the McReynolds system gave complete information about the GLC behaviour on the examined phases. On more polar phases the retention indices of the chlorophenoxyacetic acid derivatives showed larger increases in comparison with the other derivatives. This also explained the changes in the elution order with increasing phase polarity.

We now examine whether these selected GLC phases can be classified, using the retention indices of the methyl and PFB esters of the ten structurally related chlorophenoxy alkyl acids as test substances. The method employed is that of numerical taxonomy, previously applied by Massart and co-workers[2–7].

THEORETICAL

Taxonomy can be defined as the classification of individual species into groups with respect to their mutual resemblance. These groups can be linked to form more extensive groups, so generating a hierarchical system. In numerical taxonomy, a part of the "cluster" analysis developed by Sneath and Sokal[8], the object is to classify

0021-9673/82/0000–0000/$02.75

operational taxonomic units (OTUs) according to the values of a set of (taxonomic) characters. For example, solvents used for thin-layer chromatography (TLC) can be classified according to the resulting migration patterns for a mixture of compounds. The TLC solvents are the OTUs and the migration patterns the taxonomic characters, the values of which are given by the respective R_F values in the different solvent systems. The next step is to compare each OTU with the other OTUs and to evaluate their resemblance. The taxonomic similarity between pairs of OTUs is represented by means of one calculated value, the "similarity" coefficient. In chromatography, two important "similarity" coefficients are the distance coefficient and the correlation coefficient.

The distance coefficient

The greater the distance between the taxonomic characters of two OTUs, the greater is the mutual lack of similarity. Many mathematical formulae have been derived to express the distance between OTUs. A convenient formula was elaborated by Sneath and Sokal[8], which yields the taxonomic or Euclidean distance, D

$$D = \left[\sum_{i=1}^{n} (x_{ij} - x_{ik})^2 \right]^{1/2}$$

where j and k are the OTUs, in this case the selected GLC phases on which the separations are performed; x_{ij} is the numerical value of the (taxonomic) character i for OTU j, *i.e.*, the retention index of compound i on phase j; n is the number of (taxonomic) characters or the number of compounds that is injected on each examined GLC phase.

The correlation coefficient

The correlation coefficient must be regarded as a mathematical expression of the relationship and/or proportionality between pairs of OTUs. When two chromatographic systems show a high correlation, the first system yields practically no further information about the second. Moffat and co-workers[9,10] demonstrated that pairs of chromatographic systems, the retention parameters of which show the lowest correlation, yield the highest "discriminating power".

The dendrogram

After the similarity coefficients have been computed, a "similarity" matrix, $i_{max} \times i_{max}$ (i_{max} = number of OTUs), can be constructed, which is the basis of the actual classification step. The purpose of this is to form "clusters" of OTUs for which within-group distance or variance is minimized and between-group variance is maximized. To achieve this, a variety of linkage or clustering techniques can be applied. The main consideration is to select the smallest distance or the best correlation.

If the most similar GLC phases, *e.g.*, A and B, are assumed to belong to one group A', the distance between this group and the other liquid phases can be calculated:

$$D_{A'C} = \frac{1}{2}(D_{AC} + D_{BC})$$

So the two columns with two series of similarity coefficients for A and B can be eliminated from the matrix and replaced by one column with one series of similarity coefficients for A′. In this way a new matrix is constructed and the procedure is repeated until only one column with one series of coefficients remains. This method of matrix reduction, calculating the arithmetical mean, is called the "weighted pair group" method.

In the next step the dendrogram is constructed which illustrates graphically the resulting classification. From the dendrogram, appropriate chromatographic systems can be selected.

RESULTS

We have examined whether the retention indices (Tables I and II) of the methyl esters or the PFB esters of the ten chlorophenoxy acids are useful as taxonomic characters to demonstrate the similarities or differences between the ten GLC phases. Both the correlation and the distance coefficients were tested.

The correlation coefficients

The PFB esters. In Table III the correlation coefficients between the retention indices of the ten PFB esters on each GLC phase are compiled in a 10 × 10 matrix. It is clear that the GLC phases XE-60 (6) and OV-225 (7) exhibit the best relationship. In contrast, the correlation between phases DC-200 and OV-275 is very poor. So phases 6 and 7 may be considered as belonging to the same group, 6′, which is related to the other phases by the arithmetical mean values:

(6) + (7) → (6′): $r = 0.9999$

$$\left.\begin{matrix}1 \textit{ versus } 6\text{: } 0.9879\\ 1 \textit{ versus } 7\text{: } 0.9885\end{matrix}\right\} \rightarrow 1 \textit{ versus } 6' = 0.9882$$

$$\left.\begin{matrix}2 \textit{ versus } 6\text{: } 0.9795\\ 2 \textit{ versus } 7\text{: } 0.9802\end{matrix}\right\} \rightarrow 2 \textit{ versus } 6' = 0.9799$$

$$\left.\begin{matrix}3 \textit{ versus } 6\text{: } 0.9824\\ 3 \textit{ versus } 7\text{: } 0.9829\end{matrix}\right\} \rightarrow 3 \textit{ versus } 6' = 0.9827$$

$$\left.\begin{matrix}4 \textit{ versus } 6\text{: } 0.9950\\ 4 \textit{ versus } 7\text{: } 0.9955\end{matrix}\right\} \rightarrow 4 \textit{ versus } 6' = 0.9953$$

$$\left.\begin{matrix}5 \textit{ versus } 6\text{: } 0.9956\\ 5 \textit{ versus } 7\text{: } 0.9962\end{matrix}\right\} \rightarrow 5 \textit{ versus } 6' = 0.9959$$

$$\left.\begin{matrix}8 \textit{ versus } 6\text{: } 0.9981\\ 8 \textit{ versus } 7\text{: } 0.9981\end{matrix}\right\} \rightarrow 8 \textit{ versus } 6' = 0.9981$$

$$\left.\begin{matrix}9 \textit{ versus } 6\text{: } 0.9928\\ 9 \textit{ versus } 7\text{: } 0.9928\end{matrix}\right\} \rightarrow 9 \textit{ versus } 6' = 0.9928$$

$$\left.\begin{matrix}10 \textit{ versus } 6\text{: } 0.9832\\ 10 \textit{ versus } 7\text{: } 0.9832\end{matrix}\right\} \rightarrow 10 \textit{ versus } 6' = 0.9832$$

A new reduced 9 × 9 matrix can be obtained (Table IV). In this matrix the best relationship is shown for phases 4 (OV-17) and 5 (QF-1), belonging to a common group 4′. This matrix is also further reduced as follows:

TABLE I

RETENTION INDICES OF METHYL ESTERS

Abbreviations: CPIP = *p*-chlorophenoxyisobutyric acid; MCPP = methylchlorophenoxy-2-propionic acid; MCPA = methylchlorophenoxyacetic acid; 2,4-DP = 2,4-dichlorophenoxy-2-propionic acid; 2,4-D = 2,4-dichlorophenoxyacetic acid; 2,4,5-TP = 2,4,5-trichlorophenoxy-2-propionic acid; 2,4,5-T = 2,4,5-trichlorophenoxyacetic acid; MCPB = methylchlorophenoxybutyric acid; 2,4-DB = 2,4-dichlorophenoxybutyric acid; 2,4,5-TB = 2,4,5-trichlorophenoxybutyric acid (for formulae *cf.* ref. 1).

Ester	*Apolane* (C_{87})	*DC-200*	*DC-11*	*OV-17*	*QF-1*	*XE-60*	*OV-225*	*NPGA*	*FFAP*	*OV-275*
(1) CPIB-CH_3	1444	1475	1498	1703	1891	1907	1955	1950	2025	2156
(2) MCPP-CH_3	1497	1519	1546	1769	1947	1985	2035	2038	2115	2227
(3) MCPA-CH_3	1522	1524	1549	1812	1994	2059	2113	2144	2242	2362
(4) 2,4-DP-CH_3	1567	1576	1597	1847	2034	2089	2142	2144	2242	2347
(5) 2,4-D-CH_3	1594	1594	1615	1900	2099	2189	2241	2271	2395	2521
(6) 2,4,5-TP-CH_3	1705	1716	1738	1988	2170	2235	2288	2300	2371	2446
(7) 2,4,5-T-CH_3	1734	1736	1753	2049	2241	2349	2403	2453	2551	2644
(8) MCPB-CH_3	1734	1740	1756	2024	2236	2288	2337	2352	2420	2510
(9) 2,4-DB-CH_3	1796	1800	1813	2106	2316	2393	2444	2461	2551	2628
(10) 2,4,5-TB-CH_3	1968	1955	1962	2266	2479	2570	2619	2651	2719	2769

TABLE II

RETENTION INDICES OF PFB ESTERS

Ester	*Apolane* (C_{87})	*DC-200*	*DC-11*	*OV-17*	*QF-1*	*XE-60*	*OV-225*	*NPGA*	*FFAP*	*OV-275*
(1) CPIB-PFB	1848	1935	1953	2162	2574	2548	2563	2557	2521	2746
(2) MCPP-PFB	1902	1978	1998	2229	2635	2627	2647	2652	2620	2819
(3) MCPA-PFB	1964	2021	2037	2316	2733	2760	2771	2821	2820	3006
(4) 2,4-DP-PFB	1980	2044	2060	2316	2733	2760	2771	2778	2758	2952
(5) 2,4-D-PFB	2041	2090	2118	2408	2849	2912	2919	2966	2982	3182
(6) 2,4,5-TP-PFB	2118	2179	2191	2460	2882	2912	2919	2943	2904	3062
(7) 2,4,5-T-PFB	2187	2228	2240	2561	3012	3080	3085	3150	3147	3304
(8) MCPB-PFB	2205	2263	2272	2561	3012	3023	3034	3067	3047	3182
(9) 2,4-DB-PFB	2278	2329	2332	2646	3106	3135	3144	3184	3178	3304
(10) 2,4,5-TB-PFB	2444	2480	2492	2815	3291	3347	3343	3392	3363	3460

TABLE III

CORRELATION COEFFICIENTS BETWEEN THE RETENTION INDICES OF THE PFB ESTERS ON THE EXAMINED GLC PHASES

	1 *Apolane*	*2* *DC-200*	*3* *DC-11*	*4* *OV-17*	*5* *QF-1*	*6* *XE-60*	*7* *OV-225*	*8* *NPGA*	*9* *FFAP*	*10* *OV-275*
(1) Apolane	1.0000	0.9988	0.9991	0.9981	0.9969	0.9879	0.9885	0.9791	0.9648	0.9443
(2) DC-200		1.0000	0.9995	0.9942	0.9927	0.9795	0.9802	0.9683	0.9515	0.9281
(3) DC-11			1.0000	0.9951	0.9940	0.9824	0.9829	0.9714	0.9553	0.9333
(4) OV-17				1.0000	0.9995	0.9950	0.9955	0.9894	0.9790	0.9622
(5) QF-1					1.0000	0.9956	0.9962	0.9904	0.9811	0.9656
(6) XE-60						1.0000	0.9999	0.9981	0.9928	0.9832
(7) OV-225							1.0000	0.9981	0.9928	0.9832
(8) NPGA								1.0000	0.9978	0.9908
(9) FFAP									1.0000	0.9971
(10) OV-275										1.0000

TABLE IV

REDUCED 9 × 9 MATRIX

	1	*2*	*3*	*4*	*5*	*6′*	*8*	*9*	*10*
1	1.0000	0.9988	0.9991	0.9981	0.9969	0.9822	0.9791	0.9648	0.9443
2		1.0000	0.9995	0.9942	0.9927	0.9799	0.9683	0.9515	0.9281
3			1.0000	0.9951	0.9940	0.9827	0.9714	0.9553	0.9333
4				1.0000	0.9995	0.9953	0.9894	0.9790	0.9622
5					1.0000	0.9959	0.9904	0.9811	0.9656
6′						1.0000	0.9981	0.9928	0.9832
8							1.0000	0.9972	0.9908
9								1.0000	0.9971
10									1.0000

$$\left.\begin{matrix}1 \textit{ versus } 4\text{: } 0.9981\\ 1 \textit{ versus } 5\text{: } 0.9969\end{matrix}\right\} \rightarrow 1 \textit{ versus } 4' = 0.9975$$

$$\left.\begin{matrix}2 \textit{ versus } 4\text{: } 0.9942\\ 2 \textit{ versus } 5\text{: } 0.9927\end{matrix}\right\} \rightarrow 2 \textit{ versus } 4' = 0.9935$$

$$\left.\begin{matrix}3 \textit{ versus } 4\text{: } 0.9951\\ 3 \textit{ versus } 5\text{: } 0.9940\end{matrix}\right\} \rightarrow 3 \textit{ versus } 4' = 0.9946$$

$$\left.\begin{matrix}6' \textit{ versus } 4\text{: } 0.9953\\ 6' \textit{ versus } 5\text{: } 0.9959\end{matrix}\right\} \rightarrow 6' \textit{ versus } 4' = 0.9956$$

$$\left.\begin{matrix}8 \textit{ versus } 5\text{: } 0.9894\\ 8 \textit{ versus } 5\text{: } 0.9904\end{matrix}\right\} \rightarrow 8 \textit{ versus } 4' = 0.9899$$

$$\left.\begin{matrix}9 \textit{ versus } 4\text{: } 0.9790\\ 9 \textit{ versus } 5\text{: } 0.9811\end{matrix}\right\} \rightarrow 9 \textit{ versus } 4' = 0.9801$$

$$\left.\begin{matrix}10 \textit{ versus } 4\text{: } 0.9622\\ 10 \textit{ versus } 5\text{: } 0.9656\end{matrix}\right\} \rightarrow 10 \textit{ versus } 4' = 0.9639$$

In the same way, new matrixes (8 × 8, 7 × 7, ...) can be constructed which are reduced step by step.

The best correlation coefficients in each reduced matrix are:

6 + 7 → 6′	$r = 0.9999$	in 10 × 10 matrix
4 + 5 → 4′	$r = 0.9995$	9 × 9
2 + 3 → 2′	$r = 0.9995$	8 × 8
1 + 2′ → 1′	$r = 0.9990$	7 × 7
6′ + 8 → 8′	$r = 0.9981$	6 × 6
9 + 10 → 9′	$r = 0.9971$	5 × 5
1′ + 4′ → 1″	$r = 0.9958$	4 × 4
8′ + 9′ → 8″	$r = 0.9937$	3 × 3
8″ + 1″ → 1‴	$r = 0.9730$	2 × 2

Hence the dendrogram can be plotted as shown in Fig. 1. This illustrates the relationship of one individual phase with other grouped phases. So it seems that OV-17 and QF-1 are more similar to the apolar phases and the NPGA is more similar to XE-60 and OV-225 than to FFAP. On this dendrogram we can also distinguish two separate groups of liquid phases with different chromatographic properties.

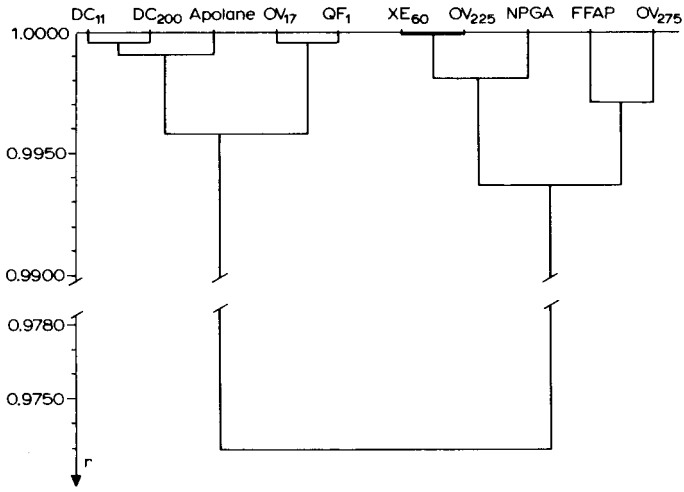

Fig. 1. Dendrogram plotted by means of the correlation coefficients of the PFB esters.

The methyl esters. The same methodology is followed for the methyl esters. The correlation coefficients between their retention indices on the ten GLC phases are given in Table V. This 10 × 10 matrix also can be reduced step by step. The highest correlation coefficients in each reduced matrix are:

6 + 7 → 6′	$r = 0.9999$	in 10 × 10 matrix
2 + 3 → 2′	$r = 0.9999$	9 × 9
4 + 5 → 4′	$r = 0.9989$	8 × 8
1 + 2′ → 1′	$r = 0.9986$	7 × 7
6′ + 8 → 8′	$r = 0.9979$	6 × 6
9 + 10 → 9′	$r = 0.9969$	5 × 5
1′ + 4′ → 4″	$r = 0.9945$	4 × 4
8′ + 9′ → 8″	$r = 0.9883$	3 × 3
1″ + 8″ → 1‴	$r = 0.9669$	2 × 2

The resulting dendrogram is plotted in Fig. 2. A similar pattern between the GLC phases is seen as for the PFB esters.

The distance coefficients

The PFB esters. In Table VI the distance coefficients between the retention indices of the ten PFB esters on each GLC phase are compiled in a 10 × 10 matrix. The smallest distance is found between phases XE-60 and OV-225. Stepwise reduction of each matrix using the "weighted pair group" method yields for each matrix the lowest "distance" coefficients:

6 + 7 → 6′	$D = 34.76$	in 10 × 10 matrix
2 + 3 → 2′	$D = 50.42$	9 × 9
8 + 9 → 8′	$D = 76.05$	8 × 8

TABLE V

CORRELATION COEFFICIENTS BETWEEN THE RETENTION INDICES OF THE METHYL ESTERS ON THE EXAMINED GLC PHASES

	1 *Apolane*	*2* *DC-200*	*3* *DC-11*	*4* *OV-17*	*5* *QF-1*	*6* *XE-60*	*7* *OV-225*	*8* *NPGA*	*9* *FFAP*	*10* *OV-275*
(1) Apolane	1.0000	0.9987	0.9985	0.9969	0.9958	0.9865	0.9853	0.9751	0.9548	0.9284
(2) DC-200		1.0000	0.9999	0.9932	0.9921	0.9794	0.9779	0.9656	0.9422	0.9156
(3) DC-11			1.0000	0.9930	0.9914	0.9789	0.9776	0.9654	0.9417	0.9147
(4) OV-17				1.0000	0.9989	0.9960	0.9954	0.9888	0.9742	0.9551
(5) QF-1					1.0000	0.9954	0.9945	0.9871	0.9728	0.9550
(6) XE-60						1.0000	0.9999	0.9976	0.9902	0.9777
(7) OV-225							1.0000	0.9981	0.9912	0.9789
(8) NPGA								1.0000	0.9964	0.9876
(9) FFAP									1.0000	0.9969
(10) OV-275										1.0000

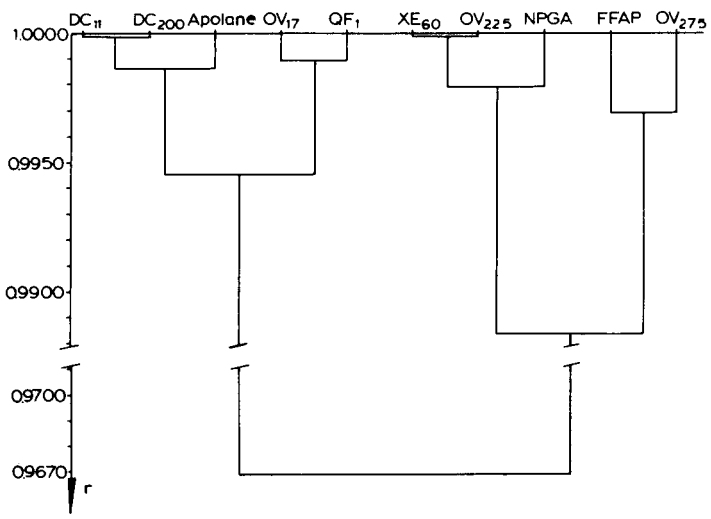

Fig. 2. Dendrogram plotted by means of the correlation coefficients of the methyl esters.

6′ + 8′ → 6″	D = 126.84	7 × 7
5 + 6″ → 5′	D = 191.19	6 × 6
1 + 2′ → 1′	D = 210.29	5 × 5
5′ + 10 → 10′	D = 638.86	4 × 4
1′ + 4 → 4′	D = 1009.97	3 × 3
4′ + 10′ → 10″	D = 2270.93	2 × 2

The resulting dendrogram is plotted in Fig. 3.

The methyl esters. In Table VII the 10 × 10 matrix is given for the distance coefficients between the retention indices of the ten methyl esters on each GLC phase. Here the smallest distance is found between DC-200 and apolane (C_{87}). After stepwise reduction of this matrix, the lowest distance coefficients for each matrix are:

1 + 2 → 2′	D = 43.31	in 10 × 10 matrix
7 + 8 → 8′	D = 77.98	9 × 9
2′ + 3 → 3′	D = 80.78	8 × 8
6 + 8′ → 6′	D = 195.15	7 × 7
5 + 6′ → 5′	D = 318.89	6 × 6
9 + 10 → 9′	D = 319.08	5 × 5
5′ + 9′ → 5″	D = 719.45	4 × 4
3′ + 4 → 4′	D = 874.31	3 × 3
4′ + 5″ → 4″	D = 1551.40	2 × 2

The resulting dendrogram is plotted in Fig. 4.

TABLE VI

DISTANCE COEFFICIENTS BETWEEN THE RETENTION INDICES OF THE PFB ESTERS ON THE EXAMINED GLC PHASES

	1 *Apolane*	*2* *DC-200*	*3* *DC-11*	*4* *OV-17*	*5* *QF-1*	*6* *XE-60*	*7* *OV-225*	*8* *NPGA*	*9* *FFAP*	*10* *OV-275*
(1) Apolane	0	189.09	236.11	1110.70	2488.81	2581.31	2609.11	2713.42	2663.62	3187.16
(2) DC-200		0	50.42	931.68	2308.47	2402.82	2430.16	2535.80	2486.92	3007.52
(3) DC-11			0	886.77	2263.11	2357.56	2384.82	2490.65	2441.78	2961.46
(4) OV-17				0	1378.37	1471.37	1498.82	1604.18	1555.85	2077.96
(5) QF-1					0	125.65	139.22	257.12	243.35	714.95
(6) XE-60						0	34.76	141.03	123.27	621.00
(7) OV-225							0	121.28	121.76	591.47
(8) NPGA								0	76.05	494.87
(9) FFAP									0	543.67
(10) OV-275										0

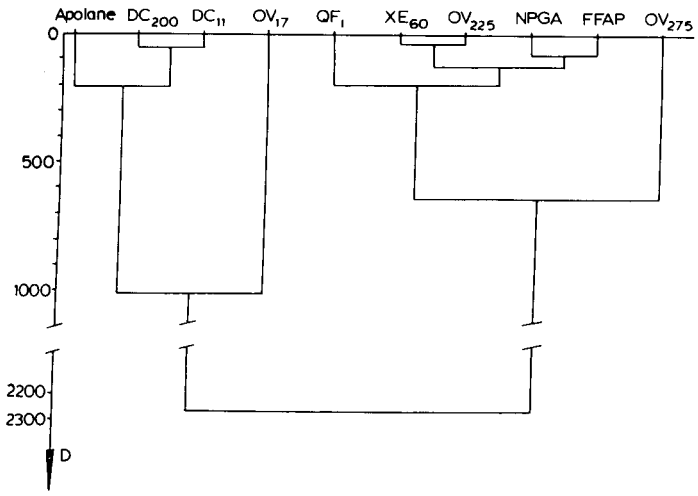

Fig. 3. Dendrogram plotted by means of the distance coefficients of the PFB esters.

DISCUSSION

Similar GLC phases can easily be recognized by observing the position of the chlorophenoxy acetic esters on the chromatograms with respect to the other chlorophenoxy esters. In contrast, the "2-propionic" and "butyric" esters cannot be employed to elucidate any relationship between GLC phases, based on their correlation coefficients.

The resulting dendrograms, plotted by means of either the correlation coefficients or the distance coefficients, divide the examined GLC phases into two main groups which can be designated as "apolar" and "polar", reflecting the strongly divergent separation patterns. The significance of the correlation coefficients is questionable since the number of examined solutes chromatographed on the different GLC phases is rather small and the correlation coefficients between their retention indices on these phases are rather high. However, when the two dendrograms are considered together, the resulting classification of the GLC phases is exactly as predicted by classical theories. In both dendrograms four groups of phases can clearly be distinguished:

(1) strictly apolar phases: Apolane (C_{87}), DC-11 and DC-200
(2) intermediate apolar phases including OV-17 and QF-1
(3) intermediate polar phases including XE-60, OV-225 and NPGA
(4) extremely polar phases including FFAP and OV-275

The dendrograms, obtained from the distance coefficients, exhibit a similar phase classification. It is noteworthy however that QF-1 and OV-17 in both dendrograms are classed in a different cluster and are considered as not related. OV-17 is in the same cluster as apolane (C_{87}), DC-11 and DC-200; QF-1 on the other hand is related to XE-60, OV-225 and NPGA. In these dendrograms there is also only one group of intermediate phases, without any distinction between intermediate apolar and intermediate polar phases.

TABLE VII

DISTANCE COEFFICIENTS BETWEEN THE RETENTION INDICES OF THE METHYL ESTERS ON THE EXAMINED GLC PHASES

	1 *Apolane*	*2* *DC-200*	*3* *DC-11*	*4* *OV-17*	*5* *QF-1*	*6* *XE-60*	*7* *OV-225*	*8* *NPGA*	*9* *FFAP*	*10* *OV-275*
(1) Apolane	0	43.31	98.21	919.52	1534.60	1747.07	1908.89	1971.92	2247.39	2554.67
(2) DC-200		0	63.34	898.59	1513.25	1726.99	1888.56	1952.27	2227.50	2533.67
(3) DC-11			0	839.56	1453.95	1668.22	1829.57	1893.57	2168.17	2473.90
(4) OV-17				0	615.73	828.77	990.10	1054.44	1329.70	1636.64
(5) QF-1					0	223.28	379.71	449.28	722.32	1027.23
(6) XE-60						0	162.36	227.93	504.03	815.36
(7) OV-225							0	77.98	344.66	655.00
(8) NPGA								0	279.52	594.95
(9) FFAP									0	319.08
(10) OV-275										0

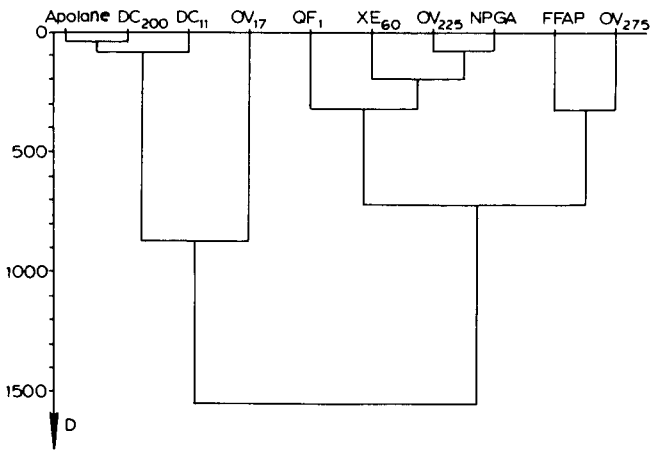

Fig. 4. Dendrogram plotted by means of the distance coefficients of the methyl esters.

The strong polar character of OV-275 is confirmed. In the dendrogram of the methyl esters, FFAP must be considered as a strong polar phase clustered with OV-27.5, but in that of the PFB-esters FFAP and NPGA are linked with XE-60 and OV-225. Here OV-275 appears as an isolated extremely polar phase.

The "distance" between polar and apolar phases is more clearly expressed by the retention indices of the PFB esters than those of the methyl esters. We believe, however, that the phase classification is more exactly reproduced by the correlation coefficients, perhaps because the whole separation patterns are compared. Nevertheless, the dendrograms plotted by means of the distance coefficients allow one to select those GLC phases, whose mutual distances, expressed by the respective difference between the retention indices of each test solute, differ most. Numerical taxonomy using both the correlation and distance similarity coefficients is an important mathematical tool, enabling the classification and combination of chromatographic systems.

The obtained results allow to consider two extreme points of view: the first believes in the use of a limited set of phases to solve all GLC problems; the second states that complicated separations cannot be achieved using a restricted set of GLC phases. We conclude that the selection of an optimal set of liquid phases and the chromatographic information they provide remains influenced by the studied series of chemically related compounds. It is not the aim of numerical taxonomy to develop a classification system for GLC phases, but to select those GLC phases which yield identical or divergent separations of a group of compounds.

REFERENCES

1 J. de Beer, C. van Peteghem and A. Heyndrickx, *J. Chromatogr.*, 157 (1978) 97.
2 D. L. Massart and H. de Clercq, *Anal. Chem.*, 46 (1974) 1988.
3 H. de Clercq and D. L. Massart, *J. Chromatogr.*, 115 (1975) 1.
4 A. Eskes, F. Dupuis, A. Dykstra, H. de Clercq and D. L. Massart, *Anal. Chem.*, 47 (1975) 2168.
5 H. de Clercq, D. van Oudheusden and D. L. Massart, *Analusis*, 3 (1975) 500.
6 D. L. Massart, M. Lauwereys and P. Lenders, *J. Chromatogr. Sci.*, 12 (1974) 617.
7 D. L. Massart and H. L. de Clercq, *Advan. Chromatogr.*, 16 (1978) 75.
8 P. H. A. Sneath and R. R. Sokal, *Numerical Taxonomy*, Freeman, San Francisco, CA, 1973.
9 A. C. Moffat, K. W. Smalldon and C. Brown, *J. Chromatogr.*, 90 (1974) 1.
10 A. C. Moffat and K. W. Smalldon, *J. Chromatogr.*, 90 (1974) 9.

Journal of Chromatography, 235 (1982) 351–363
Elsevier Scientific Publishing Company, Amsterdam — Printed in The Netherlands

CHROM. 14,363

PREPARATION AND PROPERTIES OF STATIONARY PHASES CONTAINING IMMOBILIZED, ELECTRICALLY NEUTRAL NON-MACROCYCLIC IONOPHORES FOR LIQUID–SOLID CHROMATOGRAPHY

P. GROSSMANN and W. SIMON*
Department of Organic Chemistry, ETH-Zentrum, CH-8092 Zurich (Switzerland)
(Received September 11th, 1981)

SUMMARY

Novel stationary phases for liquid–solid chromatography have been prepared by immobilizing electrically neutral, non-macrocyclic ionophores on porous glass, silica and styrene–divinylbenzene copolymers. The chromatographic behaviour of these sorbents is described. They show selectivity for alkali and alkaline earth metal cations and have been used to separate such ions.

INTRODUCTION

Stationary phases which provide new selectivity characteristics are of great interest in high-performance liquid chromatography (HPLC). By covalently binding organic complexing agents to insoluble supports it is hoped that the impressive selectivity behaviour of many of these compounds can be transferred to chromatographic systems.

Various approaches have recently been reported for the immobilization of metal-chelating functional groups on insoluble supports, either for the separation or for the preconcentration of different metal cations. Styrene–divinylbenzene copolymers have often been used as supports for the immobilization of various complexing molecules. Brozio[1] synthesized resins containing pyridine-2,6-dicarboxylic acids. Fritz and co-workers demonstrated the applicability of styrene–divinylbenzene copolymers containing immobilized thioglycolate[2,3], aromatic α-hydroxyoxime[4] and amide groups[5,6] for the separation of several transition metal ions. Insolubilized noncyclic poly(oxyethylene) derivatives were used by Yanagida and co-workers[7] to separate alkali and alkaline earth metal cations, with separation times of 1–4.5 h. Sugii and co-workers described the synthesis and applicability of styrene–divinylbenzene resins containing thiohydantoinyl groups[8], nitrosoresorcinol groups[9], β-diketones[10] and 8-hydroxyquinoline[11]. Blasius and co-workers[12–14] made extensive studies of organic resins containing macrocyclic crowns and cryptands.

A number of sorbents based on organic resins other than styrene–divinylbenzene copolymers have been described by Siggia[15], Bowen[16] and Smid[17,18] and their co-workers. The use of silica as a solid support has also received considerable atten-

0021-9673/82/0000-0000/$02.75

tion. For the preconcentration of trace metals, Leyden and co-workers[19–21] used silica with immobilized diamines. Cram and co-workers[22] reported on the separation of chiral amino ester salts using silica with covalently bound macrocyclic compounds, and Siggia and co-workers[23,24] described the synthesis of silica with pyrrolidone groups for the separation of shale oil and oestrogens.

In this paper we describe the synthesis and chromatographic behaviour of new stationary phases prepared by immobilizing electrically neutral, non-macrocyclic molecules (ionophores) on porous glass, silica and styrene–divinylbenzene copolymers. These ionophores induce substantial cation selectivity in solvent polymeric (liquid) membrane electrodes. Therefore, the new column packings described are expected to show selectivity for these cations (alkali and alkaline earth metal cations).

EXPERIMENTAL

Synthesis of stationary phases

Phase 1. The resin was first chloromethylated by adding 30 ml of freshly distilled chloromethyl methyl ether to 5 g Styragel (macroporous styrene–divinylbenzene copolymer, 20–40 μm spherical particles, 100-Å pores; Waters Assoc. No. 27123) in a flask immersed in a water thermostat. After stirring (overhead stirrer) for 1.5 h at room temperature, the temperature was raised to 66°C and 1.52 g (5.84 mmol) freshly distilled anhydrous stannic chloride in 15 ml chloromethyl methyl ether were added dropwise. Stirring was then continued under reflux for 1 h. The product was cooled, filtered off and washed successively with the following solvents: dioxan–water (3:1); dioxan with 10% concentrated hydrochloric acid; dioxan; dioxan with increasing amounts of methanol; methanol. The chloromethylated Styragel was dried for 4 days at 0.02 Torr and analysed for chlorine: 15.40 wt.-% chlorine (4.34 mmol chlorine per g dry resin).

In the coupling reaction, a solution of 258 mg (0.581 mmol) ionophore II[26] (Fig. 1) in water–ethanol (1:1) was neutralized to pH = 7 by adding aqueous caesium carbonate (0.02 *M*). The solvent was then evaporated and the residue dried over P_2O_5 for several days. A solution of this residue (caesium salt of ionophore II) in 7 ml dimethyl sulphoxide–dimethylformamide (5:7, v/v) was added to 1313 mg chloromethylated Styragel (see above). This slurry was then stirred for 8 h at 50°C and afterwards for 40 h at 80°C. After cooling, the product (stationary phase 1) was filtered off and washed successively with the following solvents: dimethyl sulphoxide; dimethyl sulphoxide–water; dimethylformamide; dimethylformamide–water; dimethylformamide; acetone, methanol. After drying at room temperature and 0.02 Torr, 1731 mg of stationary phase 1 were obtained.

Phase 2. The chloromethylated resin was aminated as follows. Chloromethyl-

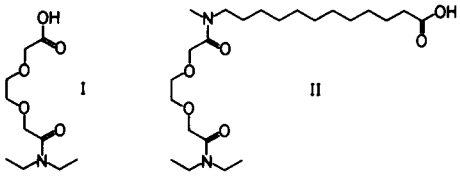

Fig. 1. Structures of ionophores I and II.

ated Styragel, 2.5 g containing 15.4 wt.-% Cl (see above), was swollen in chloroform for 2 h at room temperature and then heated at 60–80°C in dioxan for 3 h. The solvent was then sucked off and a solution of 11.4 g (190 mmol) freshly distilled ethylenediamine in 1.27 g water was added dropwise while stirring and cooling to 0°C. The mixture was then stirred at 0°C for 2 h and afterwards overnight at room temperature. The mixture was then allowed to stand for 6 days at room temperature, after which the beads were filtered off, washed thoroughly with water and dried for 4 days at 0.02 Torr. The aminated resin beads contained 1.19 wt.-% chlorine and 7.99 wt.-% nitrogen (5.71 mmol nitrogen per g resin).

In the coupling reaction, 1419 mg of the aminated Styragel were swollen on a glass frit for 1 h with dimethylformamide, filtered off and washed for 10 min with dimethylformamide–triethylamine (10:1). The resin was then washed three times each with dimethylformamide and methylene chloride, transferred to a flask and 945 mg (4.05 mmol) ionophore I[26], dissolved in 3 ml methylene chloride were added. After stirring for 20 min under a dry atmosphere, a solution containing 836 mg (4.05 mmol) N,N′-dicyclohexylcarbodiimide in 4 ml methylene chloride was added. The reaction mixture was stirred for 2 h at room temperature, for 30 min at 40–50°C and finally for 3 h at room temperature. The product was filtered off, washed with methylene chloride, ethanol, acetic acid, water and methanol and dried under vacuum (12 Torr) for 4 h at 40°C. Yield of phase 2: 1818 mg.

Phase 3. Porous glass was silanized as follows. Three grams of porous glass (Bio-Glass 200, 200–400 mesh irregular particles, 200-Å pores, pore volume 35%; Bio-Rad Labs.) were first cleaned by heating at 80–90°C in 10% nitric acid solution for 1 h. The glass beads were then filtered off, washed thoroughly with water and dried for 4 h at 60–70°C under vacuum (12 Torr). The beads were conditioned to a relative humidity of 15% by placing them over a saturated solution of lithium chloride in a desiccator for 2 days. N-(2-aminoethyl)-3-aminopropyltrimethoxysilane (Pierce Inorganics, No. P. 98008), 24.5 mmol dissolved in 50 ml toluene, was then added. After stirring (overhead stirrer) for 1 h at room temperature, the temperature was slowly raised to 110–120°C and the slurry was refluxed for 16 h. The product was then cooled, filtered over a glass frit and rinsed with toluene, ethanol and acetone. The silanized glass beads were then dried overnight at 100–110°C. Elemental analysis of the product: 5.24 wt.-% carbon; 0.98 wt.-% hydrogen; 1.71 wt.-% nitrogen.

In the coupling reaction, 1137 mg silanized glass beads were dried for 2 days over P_2O_5 at 0.02 Torr and then slurried in 4 g benzene and 4 g chloroform. To this mixture were added 2 g freshly distilled triethyleneamine. The acid chloride of ionophore I[26], 4.21 mmol dissolved in 5 ml benzene–chloroform (4:1, v,v), was then added dropwise under nitrogen. After shaking the mixture for 3 days at room temperature, the product was filtered off, washed with chloroform, ethanol, water and methanol and dried for several hours at 60–70°C. Yield: 1219 mg.

Phase 4. Silica (Lichrospher SI 100, 10-μm spherical particles, 100-Å pores, specific surface area 250 m^2/g; Merck No. 9312) was silanized with N-(2-aminoethyl)-3-aminopropyltrimethoxysilane by the procedure described above. To 1871 mg of this silanized silica, 4.03 mmol of the acid chloride of ionophore I[26] were coupled by the procedure described for stationary phase 3, to yield 2064 mg phase 4.

Characterization of stationary phases

Infrared spectra of the stationary phases were obtained on a Perkin-Elmer spectrophotometer (Model 283) from pellets consisting of 4 mg stationary phase in 300 mg KBr.

Two methods were used for the determination of the ionophore content of the stationary phases. In the first the change in weight of the stationary phase was measured before and after the reaction. In the second method, the changes in the elemental composition of the stationary phases were determined. For further details see ref. 26.

Column chromatography

An Altex pump (model 110A; Altex Scientific, Berkeley, CA, U.S.A.), a pulse dampener (Model 716583; Pye Unicam, Cambridge, Great Britain) and a sample injector, Type 70-10 (Rheodyne, Berkeley, CA, U.S.A.) were combined with a conductivity detector, consisting of a flow-through measuring cell constructed in this laboratory[27] and a conductivity meter PW 9501 (Philips, Eindhoven, The Netherlands). The stainless-steel columns 100–150 × 4.1–4.6 mm I.D.) were filled by the slurry packing technique (ethanol, with a pressure of about 1000 p.s.i. for stationary phases 1 and 2, 2000 p.s.i. for phases 3 and 4. A 1-ml volume of a 0.5 *M* solution of a potassium salt (with a specified anion) was then passed ten times through the column in order to convert the anion-exchange sites of the sorbents (primary and secondary amino groups) into the desired form. The columns were rinsed with pure solvents until the eluent was free of ionic impurities (conductivity detection). Before each injection, the anion-exchange sites of the packings had to be converted by use of the above procedure into the anion contained in the injected solution in order to avoid anion exchange between different anions and hence irreproducible retention volumes of the injected salts.

Sample volumes of 20 μl ($1 \cdot 10^{-3}$ to $5 \cdot 10^{-2}$ *M*) were injected at a mobile phase flow-rate of about 0.5–2 ml/min. Experiments at room temperature were conducted without thermostatting. For elevated temperatures, the columns were jacketed and the temperature was controlled by circulating water through the system from a thermostat. Retention volumes were calculated from the measured flow and retention times; plate numbers, N, were calculated from $N = (t_R/\sigma)^2$ where t_R is the retention time and σ is the peak width at 60.7% of the peak height.

RESULTS AND DISCUSSION

Preparation and characterization of the stationary phases

The stationary phases were prepared by binding one of the two ionophores shown in Fig. 1 to porous glass, silica or macroporous styrene–divinylbenzene copolymer. The expected structures of the prepared stationary phases are shown in Fig. 2. Some of the functional groups used to couple the ionophore to the supporting material will remain unsubstituted and thus necessitate conditioning of the stationary phase prior to use, as described in the Experimental.

The KBr-pellet IR spectra obtained after each step in the synthesis are in agreement with the expected structures. For example, in Fig. 3 the IR spectrum of the starting material (macroporous styrene–divinylbenzene copolymer) is compared with

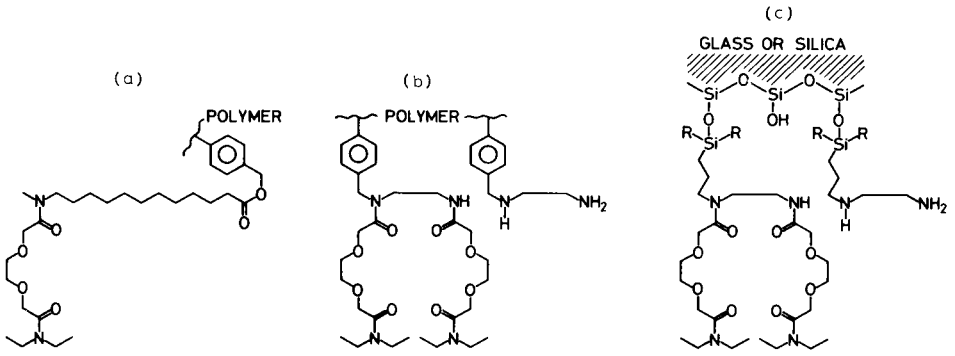

Fig. 2. Expected structures of stationary phases 1 (a), 2 (b), 3 (c) and 4 (c).

that of the final product (stationary phase 1), in which ionophore II is immobilized on the copolymer by an ester bond. This bond leads to characteristic absorption bands at 1730 cm^{-1} (C–0 stretching frequency) and 1260 cm^{-1} (C–O stretching frequency). In addition to the absorption bands of the starting material (Fig. 3A), prominent bands appear in the spectrum of the final product (Fig. 3B) at 1645 cm^{-1} and 1110 cm^{-1}. These are similar to the C–O stretching vibration of the disubstituted amide groups and to the C–O–C stretching vibration of the ether groups found in the IR spectrum of ionophore II.

The properties of the stationary phases, the results of elemental analyses and the calculated loadings with ionophore are summarized in Tables I and II. According to Table II, the prepared stationary phases are loaded with about 0.2–1.0 mmol ionophore per gram of product.

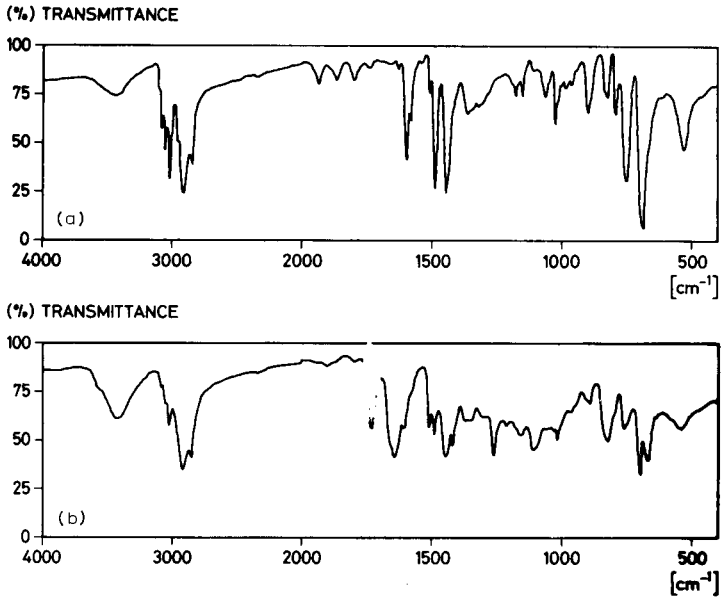

Fig. 3. Infrared spectra (in KBr pellets) of styrene–divinylbenzene copolymer (a) and stationary phase 1 (b).

TABLE I

PROPERTIES OF THE STATIONARY PHASES

S/DVB = Styrene–divinylbenzene copolymer.

Phase	*Support material*			*Immobilized ionophore*	*Bond type (ionophore/ support material)*
	Type	*Particle diameter (μm)*	*Pore diameter* (Å)		
1	S/DVB	20–40	100	II	Ester
2	S/DVB	20–40	100	I	Amide
3	Glass	40–80	200	I	Amide
4	Silica	10	100	I	Amide

TABLE II

ELEMENTAL ANALYSIS AND CAPACITY OF THE STATIONARY PHASES

Phase	*Elemental analysis (%)*				*Capacity* obtained by*			
	C	*H*	*N*	*O*	*Weight increase*	*Elemental analysis*		
						C	*N*	*O*
1	73.89	7.13	0.89	3.06	0.592	–	0.318	0.319
2	73.32	7.98	7.43	1.51	1.021	–		0.236
3	8.68	1.48	2.39		0.314	0.316	0.659	–
4	18.61	2.81	4.08		0.436	0.374	0.600	–

* Ionophore (mmol) per gram of dry stationary phase.

Chromatographic behaviour

Selectivity. After conditioning of the columns, the selectivities of the stationary phases were determined by injecting solutions of various salts and measuring their retention volumes. The results (Fig. 4) demonstrate that the stationary phases described lead to a different retention volume for each salt and thus induce cation selectivity. These differences in retention volume are mainly due to variations in the complex formation. From a comparison of Fig. 4C and 4D, the selectivity depends not only on the ionophore–cation interactions, but also on the type of support (resin, glass, silica) used. Except in the case of phase 4, all the stationary phases retain barium and calcium much more strongly than the alkali metals. This is in agreement with the selectivity sequence induced in solvent polymeric membranes by similar ionophores[25]. Ion-selective liquid membrane electrodes and chromatographic systems are basically different, so that utmost care should be taken when correlating experimentally determined selectivity factors[27].

Influence of the mobile phase. The complex formation constant for the ionophore–cation interaction is also influenced by the dielectric constant of the solvent: usually, the lower the dielectric constant the stronger is the interaction[28]. Thus, low selectivities for the present systems are expected when water is used as the mobile

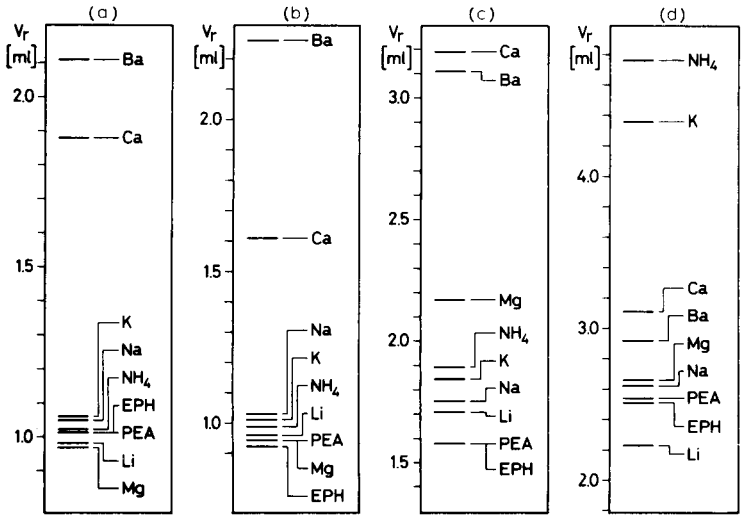

Fig. 4. Selectivities. a, Stationary phase 1. Column: 150 × 4.6 mm. Mobile phase: water–ethanol (2:8 v/v). b, Stationary phase 2. Column: 150 × 4.6 mm. Mobile phase: water–ethanol (3:7 v/v). c, Stationary phase 3. Column: 130 × 4.1 mm. Mobile phase: water–ethanol (1:1 v/v). d, Stationary phase 4. Column: 150 × 4.6 mm. Mobile phase: water. Injection in each case: 20 μl, $2 \cdot 10^{-2}$ *M*. PEA = (±)-α-Phenylethylammonium chloride; EPH = (±)-ephedronium chloride.

phase. If methanol or ethanol is added to the mobile phase to decrease the dielectric constant, the retention volumes should increase. The experimental results for stationary phases 1 and 2 shown in Fig. 5 confirm this.

Influence of anions on the retention of the cations. The retention of a salt depends on both the cation and the anion because electroneutrality requires the binding of a cation together with an anion. The influence of the type of anion for stationary phases 2 and 3 is shown in Table III: it is seen that the retention volume of a given cation increases with increasing polarizability and lipophilicity of the anion[14].

Column efficiency. In addition to the selectivity of the stationary phase, the

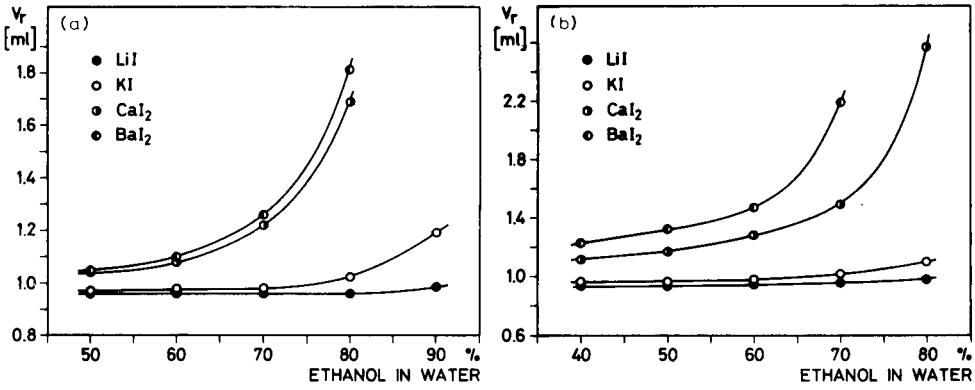

Fig. 5. Influence of the mobile phase on retention volumes on stationary phases 1 (a) and 2 (b). Column: 150 × 4.6 mm. Mobile phase flow-rate: 1.1–1.3 ml/min. Injection: 20 μl, $2 \cdot 10^{-2}$ *M*.

TABLE III

INFLUENCE OF ANIONS ON THE RETENTION OF CATIONS ON STATIONARY PHASES 2 AND 3

Anion	*Retention volumes on stationary phase 2* (ml)*			*Retention volumes on stationary phase 3** (ml)*	
	K^+	Ca^{2+}	Ba^{2+}	K^+	Ca^{2+}
Acetate	0.96	1.00	1.05	1.57	2.15
Chloride	0.98	1.14	1.35	1.61	2.26
Bromide	0.98	1.24		1.69	2.55
Nitrate	1.00	1.27	1.55	1.81	2.81
Iodide	1.04	1.73	2.54	1.87	3.23
Thiocyanate	1.12	2.68	4.49	1.93	3.55
Perchlorate	1.08	3.80	7.35	1.96	4.12

* Column: 150 × 4.6 mm. Mobile phase: water–ethanol (3:7 v/v); flow-rate 1.2 ml/min. Injection: 20 μl, $2 \cdot 10^{-2}$ *M*.

** Column: 130 × 4.1 mm. Mobile phase: water–ethanol (1:1 v/v); flow-rate 1.35 ml/min. Injection: 20 μl, $2 \cdot 10^{-2}$ *M*.

efficiency of the packed column is also important. The stationary phases described yield columns for which the plate number markedly decreases with increasing retention volume; a typical example is provided by phase 2 (see Fig. 6). This reduction in plate number cancels the advantage gained through increased selectivity. Methods of reducing this effect by variation of the major parameters (mobile phase flow, injected sample amount, temperature, additives to the mobile phase) were investigated.

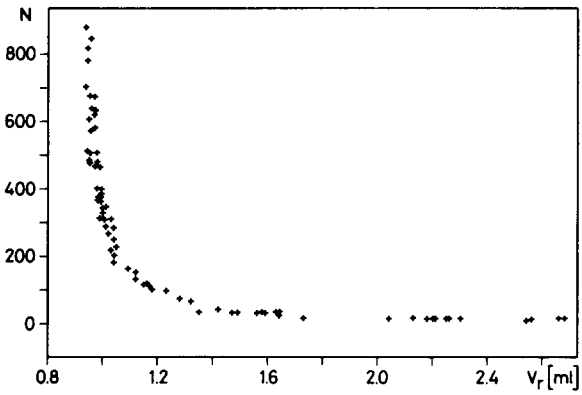

Fig. 6. Column efficiency for stationary phase 2. Column: 150 × 4.6 mm. Mobile phase flow-rate: 1–1.2 ml/min. Injection: 20 μl, $2 \cdot 10^{-2}$ *M*.

Influence of the mobile phase flow-rate. Using stationary phase 4 (Fig. 7), the influence of the flow speed on the retention volume and the plate number was studied. For lower velocities the retention volume slightly increases and the plate number decreases somewhat. This means that in the flow-rate range chosen (0.1–3 ml/min) plate number fall-off is always present with increasing retention and nothing is gained from flow reduction.

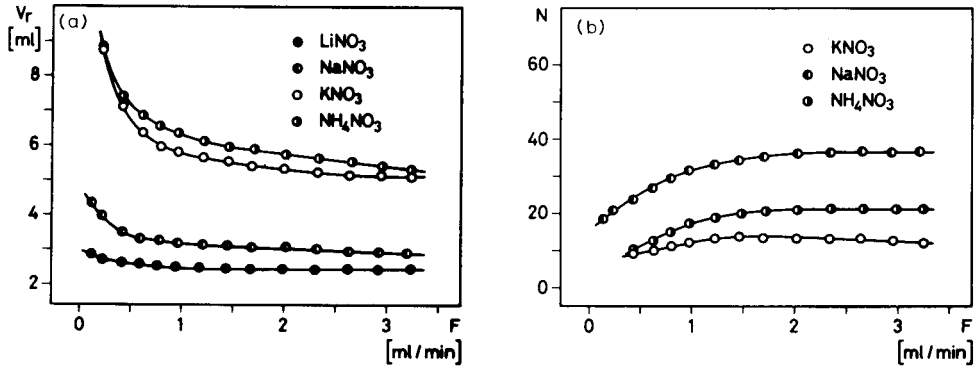

Fig. 7. Influence of mobile phase flow-rate on retention volumes and column efficiency for stationary phase 4. Column: 150 × 4.6 mm. Mobile phase: water doubly distilled. Injection: 20 μl, $2 \cdot 10^{-2}$ *M*.

Influence of the sample amount. The loading of a chromatographic system through injection of too large samples results in broad, asymmetric elution profiles because of operation in the non-linear portion of the distribution isotherm. The effect of the amount of sample injected was studied for phase 1 (see Fig. 8). The retention volume decreases with decreasing sample concentration. This is a strong indication of non-linearity of the adsorption isotherm. At the same time the plate number increases. However, even for very low sample concentrations, the plate number decreases with increasing retention.

Influence of the temperature. Increasing the temperature of a liquid chromatographic system generally leads to faster elution and an increase in plate number (a lowering of the viscosity of the mobile phase and an increase in the mobility of the sample molecules lead to faster mass transport). For the stationary phases described, heating should accelerate the kinetics of complexation and hence improve the plate number. This is illustrated for stationary phase 2 in Fig. 9. The change in plate number is decidedly less than expected; for barium and calcium the plate numbers are less than 50 at 60°C, as compared to 350 (20°C) and 450 (60°C) for potassium. From Table IV it is seen that, for stationary phase 3, an increase in temperature from 20 to

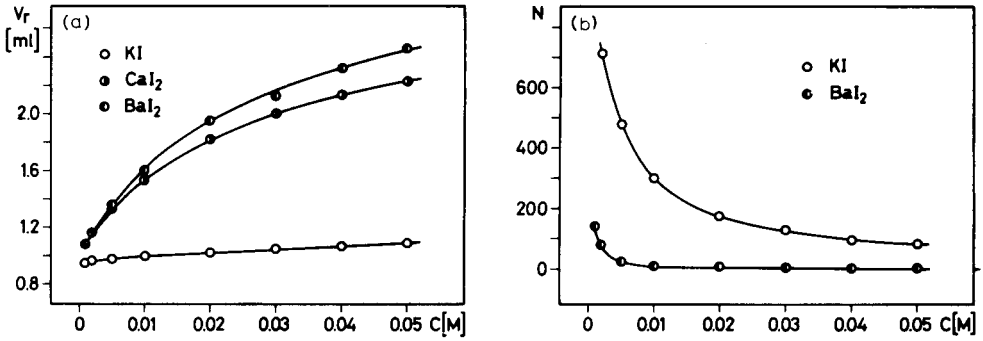

Fig. 8. Influence of sample concentration on retention volumes and column efficiency for stationary phase 1. Column: 150 × 4.6 mm. Mobile phase: water–ethanol (2:8 v/v); flow-rate 1.2 ml/min. Injection: 20 μl.

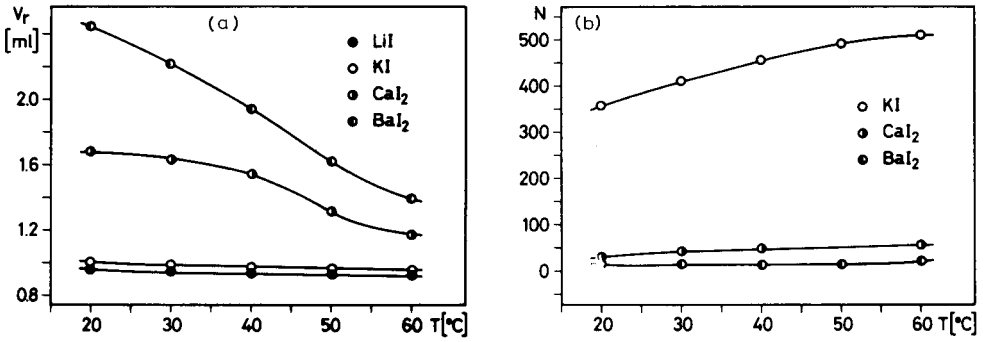

Fig. 9. Influence of temperature on retention volumes and column efficiency for stationary phase 2. Column: 150 × 4.6 mm. Mobile phase: water–ethanol (3:7 v/v); flow-rate 0.9-1.0 ml/min. Injection: 20 μl, $2 \cdot 10^{-2}$ *M*.

TABLE IV

RETENTION-DEPENDENT PLATE NUMBER FALL-OFF AT 20°C AND 50°C FOR STATIONARY PHASE 3

Column: 90 × 5 mm. Mobile phase: water–ethanol (1:1 v/v); flow-rate 1.5 ml/min. Injection: 20 μl, $2 \cdot 10^{-2}$ *M*.

20°C		*50°C*	
V_r *(ml)*	*N*	V_r *(ml)*	*N*
1.77	168	1.73	239
2.09	74	2.12	127
2.70	48	2.59	78
3.20	37	2.89	71

50°C somewhat increases the plate numbers, but the retention-dependent plate number fall-off is still observed.

Additives to the mobile phase. In analogy to the behaviour often observed for reversed-phase systems, an attempt was made to increase the plate numbers through addition of a buffer (phosphate at pH 7) or of salts (sodium nitrate or benzoate, tetramethylammonium nitrate). Fig. 10a and 10b depict the results for stationary phase 4 with $LiNO_3$ and KNO_3: increasing ionic strength leads to a somewhat faster elution of the sample. However, Fig. 10c shows that the plate number fall-off for this phase is not improved by addition of ionic species. This behaviour is typical of all of the investigated systems.

Chromatographic separations

Since the solvent largely determines the degree of interaction between cations and immobilized ionophores, the cation retention on the stationary phases described may be fixed through choice of the mobile phase. Therefore, by appropriate selection of mobile phases, the stationary phases described may be used for rapid separations of alkali and alkaline earth metal cations. Studies conducted with phase 2 using mobile phases of various ethanol to water ratios show clearly that the separation

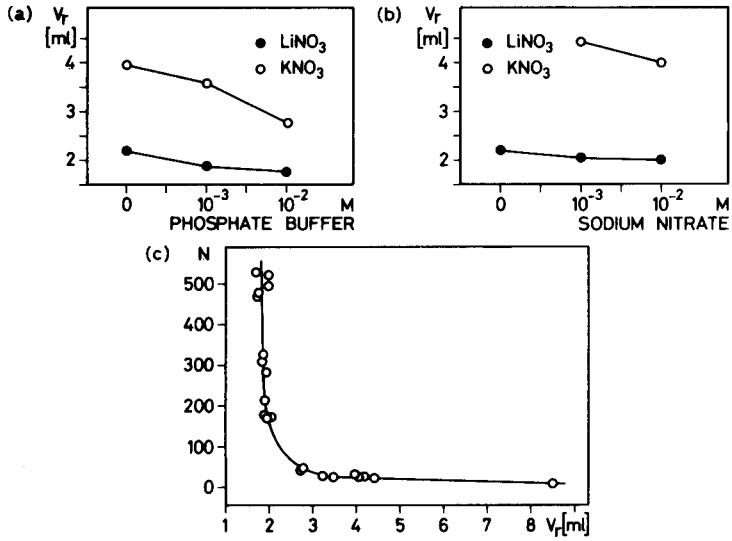

Fig. 10. Influence of additives to the mobile phase for stationary phase 4. a, Mobile phase with sodium phosphate buffer (pH = 7); b, mobile phase with sodium nitrate; c, column efficiency, resulting from experiments with additives to the mobile phase. Column: 150 × 4.6 mm. Mobile phase: water with additives; flow-rate 2 ml/min. Injection: 20 µl, $2 \cdot 10^{-2}$ *M*.

factor between, *e.g.*, magnesium and calcium, increases with increasing ethanol content, *i.e.*, with decreasing mobile phase polarity (Fig. 11). In spite of the increasing separation factor, the resolution between magnesium and calcium is not improved to the desired degree because the plate number of calcium decreases with increasing retention of calcium. For this reason, baseline separation of magnesium and calcium is not possible by isocratic elution. However, as illustrated in Fig. 12, baseline separation on stationary phase 2 between, *e.g.*, lithium and barium can be achieved by using a solvent gradient elution procedure.

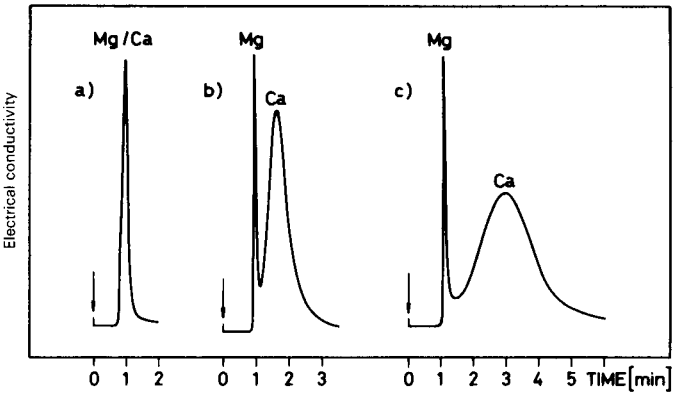

Fig. 11. Separation of magnesium and calcium iodide on stationary phase 2. Column: 150 × 4.6 mm. Mobile phase: water–ethanol [6:4 v/v (a), 3:7 v/v (b) and 2:8 v/v (c)]; flow-rate: 1.2 ml/min (a) and 1 ml/min (b and c). Injection: 20 µl of a mixture of magnesium and calcium; for a and c, $1.8 \cdot 10^{-3}$ *M*, MgI_2, $1.8 \cdot 10^{-2}$ *M* CaI_2; for b, $2.8 \cdot 10^{-3}$ *M* MgI_2, $1.7 \cdot 10^{-2}$ *M* CaI_2.

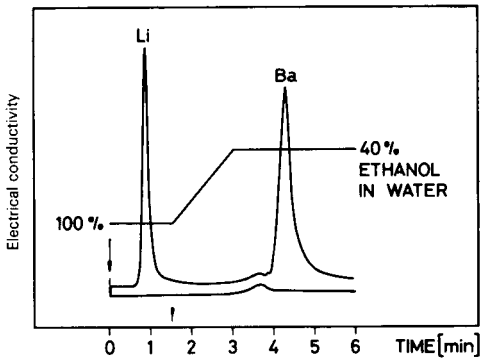

Fig. 12. Separation of lithium and barium on stationary phase 2. Column: 150 × 4.6 mm. Injection: 20 μl; $1.1 \cdot 10^{-2}$ *M* LiI, $9.2 \cdot 10^{-3}$ *M* BaI_2. Mobile phase: gradient, 100% ethanol for 1.5 min, then linear gradient to 40% (v/v) ethanol in water in 1.5 min; flow-rate 1.2 ml/min.

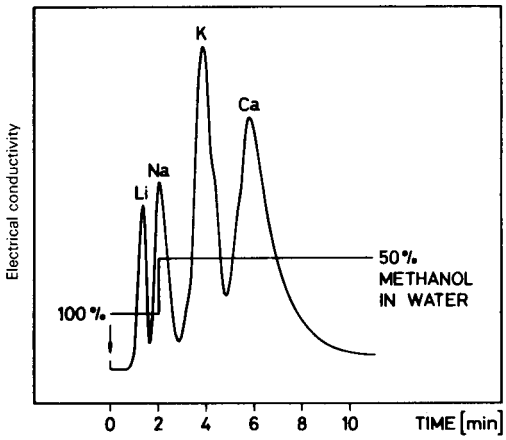

Fig. 13. Separation of lithium, sodium, potassium and calcium iodide on stationary phase 3. Column: 130 × 4.1 mm. Mobile phase: step gradient, methanol for 2 min, then methanol–water (1:1 v/v); flow-rate 1.4 ml/min. Injection: 20 μl; $4.1 \cdot 10^{-3}$ LiI, $4.6 \cdot 10^{-3}$ *M* NaI, $1.3 \cdot 10^{-2}$ *M* KI, $9.2 \cdot 10^{-3}$ *M* CaI_2.

Through judicious choice of the solvent gradient, rapid separations of cations having markedly different elution characteristics are possible with the stationary phases described. For example, Fig. 13 illustrates the quite rapid separation of lithium, sodium, potassium and calcium on stationary phase 3 using gradient elution.

CONCLUSIONS

The results demonstrate that the non-cyclic neutral carriers indeed induce a substantial cation selectivity when immobilized on porous glass, silica and styrene–divinylbenzene copolymer. The possibility of using these new stationary phases for separations of alkali and alkaline earth metal cations was investigated and it is shown that, through careful choice of the mobile phase, they are adequate for this purpose. However, in spite of the high selectivity, this use of these stationary phases was only partially successful, owing to the low efficiency of the packed columns, which resulted

in a substantial broadening and overlapping of bands. It should be noted that similar systems (complexing agents, immobilized on solid supports) show the same behaviour with respect to efficiency[7,14,29,30]. This low efficiency is probably due to two underlying mechanisms.

The first is of a thermodynamic nature. The ionophores used in this work are able to form 1:1 and 1:2 complexes with cations[31,32]. In liquid–liquid chromatography this may lead to non-linear distribution isotherms[27]. Immobilizing these ionophores may therefore provide sorbents with a non-linear adsorption isotherm. The second mechanism is of a kinetic nature. The complexation and decomplexation reaction between the immobilized ionophores and the cations could be so slow that equilibrium is not attained in chromatographic systems. Calculations of elution profiles based on a simple mathematical model indeed show that there should be not only elution profile broadening but also tailing if the sample's distribution equilibrium between the stationary and liquid phase is not attained[26].

REFERENCES

1 B. Brozio, *Thesis No. D 83*, Berlin, 1964.
2 E. M. Moyers and J. S. Fritz, *Anal. Chem.*, 48 (1976) 1117.
3 R. J. Phillips and J. S. Fritz, *Anal. Chem.*, 50 (1978) 1504.
4 J. N. King and J. S. Fritz, *J. Chromatogr.*, 153 (1978) 507.
5 G. M. Orf and J. S. Fritz, *Anal. Chem.*, 50 (1978) 1328.
6 C. Pohlandt and J. S. Fritz, *J. Chromatogr.*, 176 (1979) 189.
7 H. Fujita, S. Yanagida and M. Okahara, *Anal. Chem.*, 52 (1980) 869.
8 A. Sugii and N. Ogawa, *Chem. Pharm. Bull.*, 24 (1976) 1349.
9 A. Sugii and N. Ogawa, *Talanta*, 26 (1979) 970.
10 A. Sugii, N. Ogawa and T. Ochiai, *Chem. Pharm. Bull.*, 25 (1977) 1596.
11 A. Sugii, N. Ogawa and M. Hisamitsu, *Chem. Pharm. Bull.*, 26 (1978) 798.
12 E. Blasius, W. Adrian, K.-P. Janzen and G. Klautke, *J. Chromatogr.*, 96 (1974) 89.
13 E. Blasius and P.-G. Maurer, *Makromol. Chem.*, 178 (1977) 649.
14 E. Blasius, K.-P. Janzen, W. Adrian, G. Klautke, R. Lorscheider, P.-G. Maurer, V. B. Nguyen, T. Nguyen Tien, G. Scholten and J. Stockemer, *Z. Anal. Chem.*, 284 (1977) 337.
15 M. B. Colella, S. Siggia and R. M. Barnes, *Anal. Chem.*, 52 (1980) 967.
16 L. A. Fernando, M. L. Miles and L. H. Bowen, *Anal. Chem.*, 52 (1980) 1115.
17 S. Kopolow, T. E. Hogen Esch and J. Smid, *Macromolecules*, 6 (1973) 133.
18 J. Smid, S. C. Shah, R. Sinta, A. J. Varma and L. Wong, *Pure Appl. Chem.*, 51 (1979) 111.
19 D. E. Leyden, G. H. Luttrell and T. A. Patterson, *Anal. Lett.*, 8 (1975) 51.
20 D. E. Leyden and G. H. Luttrell, *Anal. Chem.*, 47 (1975) 1612.
21 D. E. Leyden, G. H. Luttrell, A. E. Sloan and N. J. DeAngelis, *Anal. Chim. Acta*, 84 (1976) 97.
22 G. Dotsevi, Y. Sogah and D. J. Cram, *J. Amer. Chem. Soc.*, 97 (1975) 1259.
23 T. H. Mourey and S. Siggia, *Anal. Chem.*, 52 (1980) 881.
24 T. H. Mourey, S. Siggia, P. C. Uden and R. J. Crowley, *Anal. Chem.*, 52 (1980) 885.
25 W. E. Morf, D. Ammann, R. Bissig, E. Pretsch and W. Simon, in R. M. Izatt and J. J. Christensen (Editors), *Progress in Macrocyclic Chemistry*, Band 1, Wiley, New York, Chichester, Brisbane, Toronto, 1979, p. 1.
26 P. Grossmann, *Thesis No. 6734*, ETH Zurich, 1980.
27 K. H. Schellenberg, *Thesis No. 6475*, ETH Zurich, 1979.
28 N. N. L. Kirsch, *Thesis No. 5842*, ETH Zurich, 1976.
29 B. Brozio, *Thesis No. D83*, Berlin, 1974, p. 70.
30 V. A. Davankov and A. V. Semechkin, *J. Chromatogr.*, 141 (1977) 313.
31 W. Simon, W. E. Morf and D. Ammann, in R. H. Wasserman, R. A. Corradino, E. Carafoli, R. H. Kretsinger, D. H. MacLennan and F. L. Siegel (Editors), *Calcium-Binding Proteins and Calcium Function*, North-Holland, New York, Amsterdam, Oxford, 1977, p. 50.
32 K. Neupert-Laves and M. Dobler, *Helv. Chim. Acta*, 60 (1977) 1861.

Journal of Chromatography, 235 (1982) 365–376
Elsevier Scientific Publishing Company, Amsterdam — Printed in The Netherlands

CHROM. 14,295

GEL PERMEATION CHROMATOGRAPHY OF A POLYAMIDE–EPICHLOROHYDRIN RESIN AND SOME OTHER CATIONIC POLYMERS

G. BRUCE GUISE* and GEOFFREY C. SMITH
CSIRO Division of Textile Industry, Belmont, Geelong (Australia)
(Received August 17th, 1981)

SUMMARY

The gel permeation chromatography of cationic polymers, a polyamide–epichlorohydrin resin (Hercosett 125), poly(2-vinylpyridine) and polyethyleneimine, was compared on a selection of silica gel columns with neutral and cationic surface modifications.

The elution volumes of the polymer peaks were very dependent on the pH, ionic strength and the column, but were also influenced by the type of salts in the eluent and the polymer concentration. In some cases it was possible to elute the cationic polymer anywhere between the high-molecular-weight exclusion limit and the low-molecular-weight total permeation limit.

The polymer peak in Hercosett 125 split into two under certain conditions. This appears to be related to the presence in Hercosett 125 of polymers of different structures.

Universal calibration methods and viscosity measurements have been used to indicate conditions where interaction between the cationic polymers and the columns and/or solvent was minimal and these conditions have been used to estimate the molecular weight of Hercosett 125.

INTRODUCTION

Cationic polyamide–epichlorohydrin (PAE) resins prepared by reaction of epichlorohydrin with polyamide derived from adipic acid and diethylenetriamine (Fig. 1) are widely used as paper wet-strength additives[1] and to shrink-resist wool[2,3]. Several chemical studies[4,5] have investigated the cross-linking reactions and reactive groups in PAE resins but little is known about the molecular weight or molecular weight distribution of PAE resins, apart from a recent gel filtration study[6].

This paper reports an investigation of the wool shrink-resist resin Hercosett 125 (Hercules, Australia) by gel permeation chromatography (GPC). The objective of this work was to develop analytical methods to follow chemical changes during the application of Hercosett 125 to wool.

Most GPC studies have been on neutral polymers rather than polyelectrolytes. One reason for this is that suitable columns for high-pressure aqueous GPC have only

0021-9673/82/0000–0000/$02.75

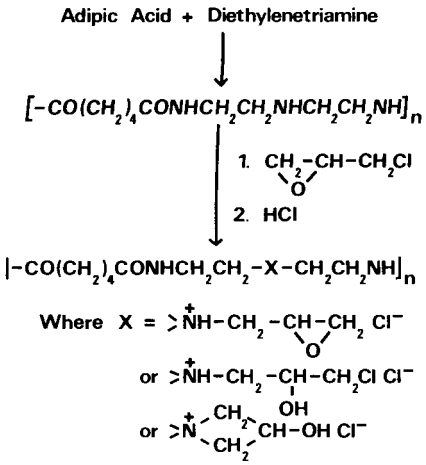

Fig. 1. Preparation and structure of the PAE resins.

become available recently, but even with these columns there are difficulties in molecular weight calibration with polyelectrolytes[7–12]. There are a number of GPC effects peculiar to polyelectrolytes due to ionic interactions between the polymer and column (*e.g.*, ion exclusion, Donnan equilibrium ion inclusion) and due to changes (*e.g.*, with pH or ionic strength) of the apparent dimensions of polyelectrolyte molecules in solution. These effects and ways to minimise them (*e.g.*, by choice of columns and eluents) have been discussed in detail elsewhere[7–12].

In the present study Hercosett 125 and some cationic polymers of known structure, poly(2-vinylpyridine) (PVP) and polyethyleneimine (PEI), were examined on two classes of surface-modified silica gel columns; A, with a neutral surface modification and B, with a cationic surface modification. Surface modification is necessary to prevent the strong adsorption of polyelectrolytes onto unmodified silica[7–9]. The second class was examined in the hope of preventing adsorption effects caused by the slight negative surface charge in the first class. Such cationic columns have recently been used by Talley and Bowman[13,14] for the GPC of certain cationic polymers.

EXPERIMENTAL

Materials

The Hercosett 125 sample was provided by Hercules. All the chromatograms of Hercosett 125 in this paper were run within a week approximately 3 months after the date of manufacture. This approach avoided the changes that occur due to cross-linking during storage.

The other polymers were commercial samples, used without further purification, and their sources and molecular weights are indicated in Table I. Other chemicals were analytical grade.

Quaternary ammonium salt solutions were prepared by diluting 25 % solutions of the quaternary ammonium hydroxides (BDH) with water and then adjusting to the desired pH with either nitric or phosphoric acid.

TABLE I

POLYMERS

Name	*Source*	$\bar{M}_n$*
Dextran T10	Pharmacia	10,000
T40		40,000
T500		500,000
Poly(2-vinylpyridine) Batch 2	Pressure Chemical	30,000
Batch 3		90,000
Batch 5		230,000
Batch 7		600,000
Poly(ethyleneimine) PEI 6	Dow Chemical	600
PEI 12		1200
PEI 18		1800

* Manufacturer's data.

Chromatography

A Varian 4100 syringe pumping system, a Rheodyne loop injector using a 100-μl loop, a Varian refractive index detector and a Varian Vari-chrom variable-wavelength ultraviolet detector set at 230 nm were used. The supports prepared in this laboratory were packed into 250 × 4.6 mm I.D. stainless-steel columns. All chromatograms were run at room temperature (about 22°C) with a flow-rate of 1.3 ml/min for column II and 1 ml/min for the other columns. Table II gives details of the columns used in this study.

Unless otherwise stated, the GPC results have been presented as apparent molecular weights in order to make comparisons between columns. The molecular weights quoted in Table III are for peak maxima and were determined by direct comparison with dextran standards. They are hence referred to as apparent molecular weights.

Viscometry

Viscosities were determined with a Ubbelohde viscometer at 25°C.

RESULTS AND DISCUSSION

The most pronounced features (Table III) in the present aqueous GPC study were the shifts of the cationic polymer peaks, on all five columns, to longer elution volumes (*i.e.*, reduced apparent molecular weight) when the pH and/or the ionic strength was increased. Such shifts have been noted before in polyelectrolyte GPC[7–10], but the magnitude of the shifts on columns I and II appeared to be greater with the cationic polymers than reported previously[10,11] with anionic polymers. The reasons for these shifts have been discussed previously[7–11] and involve ion exclusion and conformational changes. However, adsorption (which appeared to increase as both the pH and the ionic strength was raised) must be significant. At very high ionic strengths (*e.g.*, Fig. 2) adsorption became so pronounced that the intensity of the cationic peaks decreased markedly and the peak tailed considerably.

TABLE II

COLUMNS

No.	*Type/Source*	*Source*	*Modification*	*Silica*	*Pore size* (nm)*
I	μBondagel E-Linear	Waters Assoc.	Hydrophilic ether*		12.5–100
II	TSK-G-3000SW	Toyo Soda	Glyceryl ether*		Unknown
III	Zorbax SAX	DuPont	Quaternary ammonium* ions		6
IV	Cationic modified**	Method from ref. 13**	$-(CH_2)_3NH-CH_2CH(OH)-CH_2NMe_3^+$	LiChrosorb Si 500 (E. Merck)	50
V	Cationic modified	Method from ref. 13**	$-(CH_2)_3NH-CH_2CH(OH)-CH_2NMe_3^+$	LiChrosorb Si 100 (E. Merck)	10

* Manufacturers' literature.

** Packed in these laboratories.

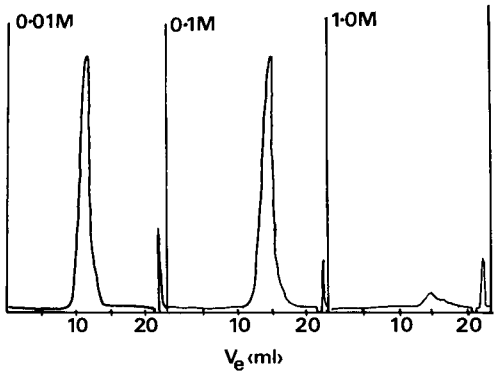

Fig. 2. GPC of mol.wt. 30,000 poly(2-vinylpyridine) in $NaNO_3$ solutions of various ionic strengths (pH 3) on column II (refractive index detector). V_e = Elution volume.

In addition to the above effects, Hercosett 125 (but not the other cationic polymers) showed two polymer peaks under certain conditions. This is illustrated in Figs. 3 and 4 (which show series on columns II and I at different pH values) and in Fig. 5 (which shows a series on column II of increasing ionic strength at constant pH).

There were also minor effects (which have not been illustrated) related to the polymer concentration (distortion and fusion of peaks which was avoided by the use of dilute solutions) and to the nature of the salts in the eluent. Only solutions of sodium or alkylammonium nitrate and phosphate were examined. Alkylammonium salts gave slightly sharper peaks than when sodium salts were used. Nitrates avoided the possibility of ion binding of HPO_4^{2-} to cationic molecules but phosphate had a greater buffering capacity.

In view of these various effects, before Hercosett 125 was studied, experiments

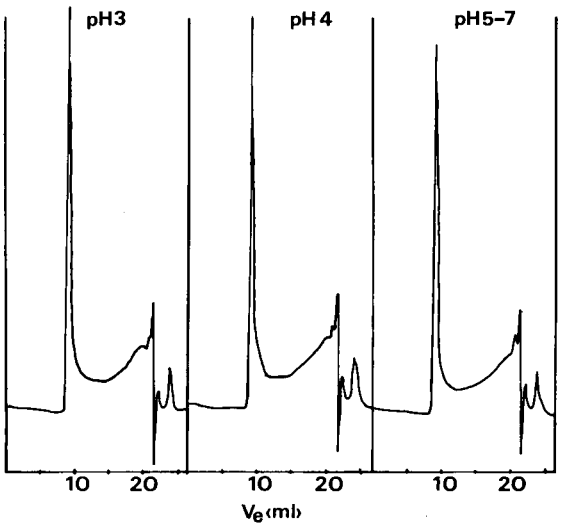

Fig. 3. GPC of Hercosett 125 in 0.1 *M* $NaNO_3$ solutions at various pH values on column II (refractive index detector).

TABLE III

APPARENT MOLECULAR WEIGHTS OF CATIONIC POLYELECTROLYTES AS DETERMINED BY GPC ON VARIOUS COLUMNS

Values are based on direct comparison with dextran standards. NE = not eluted; NT = not tested.

Column	*Salt*	*Conc. (M)*	*pH*	*PVP*				*PEI*			*Hercosett 125*
				30,000	*90,000*	*230,000*	*600,000*	*6*	*12*	*18*	
I	$NaNO_3$	0.05	3	NE	NE	NE	NE	6000	10,000	14,000	>500,000 tailing to TPL*
		0.1	3	NE	NE	NE	NE	3500	5000	6000	TPL peak only
	$NEt_4H_2PO_4$	0.2	3	NT	NT	NT	NT	900	2000	500	>500,000 + 5000
		0.2	6	NT	NT	NT	NT	NT	NT	NT	TPL only
		0.1									
	$NEt_4H_2PO_4$ + NaH_2PO_4	0.1 + 0.2	3	NE				2000	Insol.	Insol.	>500,000 + 4000
II	$NaNO_3$	0.01	3	55,000	200,000	>300,000	>300,000	700	1400	2200	>300,000 + 7000
		0.1	3	35,000	110,000	>300,000	>300,000	600	1200	2200	>300,000 + 3000
		1.0	3	6000	25,000	NT	NT	600	1200	2200	>300,000 + 3000
	$NEt_4H_2PO_4$ + NaH_2PO_4	0.1 + 0.2	3	30,000	90,000	NT	NT	600	Insol.	Insol.	>300,000 + 3000
III	$NaNO_3$	0.1	3	>25,000	>25,000			8000	9000	11,000	>25,000 + 14,000
IV	HNO_3	0.001	3	>800,000	>800,000			NT	NT	NT	800,000 + 80,000
	NaH_2PO_4	0.001	4.8	NE	NE	>800,000	>800,000	NT	NT	NT	800,000 + 80,000
	$NaNO_3$	0.1	3	60,000	300,000	>800,000	>800,000	NT	NT	NT	500,000 + 20,000
	NEt_4NO_3	0.1	3	30,000	120,000	500,000	>800,000	NT	NT	NT	350,000 + 10,000
V	$NaNO_3$	0.1	2	>50,000		NT	NT	10,500	15,000	19,000	50,000 + 20,000
		0.1	3	>50,000		NT	NT	7500	10,500	12,500	50,000 + 20,000
		0.2	3	40,000	>50,000	NT	NT	4800	7800	10,000	50,000 + 20,000

* TPL = Total permeation limit.

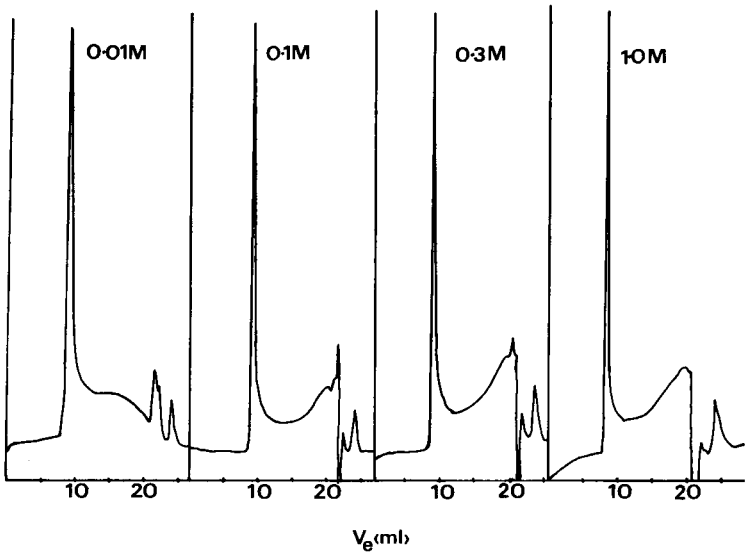

Fig. 4. GPC of Hercosett 125 in $NaNO_3$ solutions of various ionic strengths (pH 3) on column II (refractive index detector).

were performed with poly(2-vinylpyridine) and polyethyleneimine samples of known molecular weight.

Comparison of columns

If the two neutral modified columns I and II were compared, column II gave slightly better resolution, was less sensitive to changes in pH or ionic strength, but took a longer time for each analysis. PVP adsorbed strongly on column I at all ionic strengths examined, and the PEI peaks on this column tailed indicating some adsorption. With column I, the changes caused by increased ionic strength were more pro-

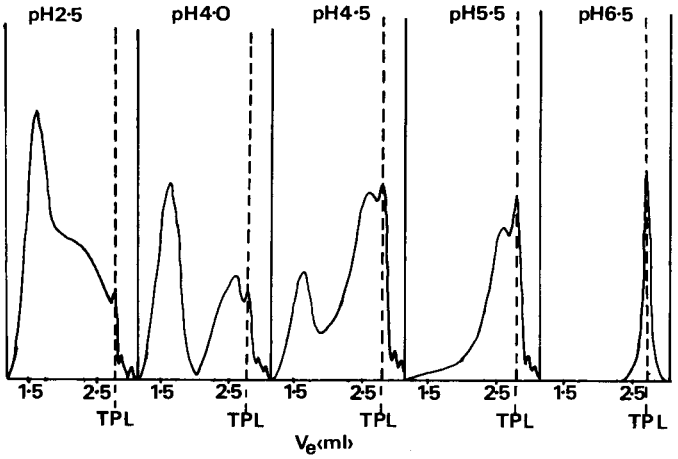

Fig. 5. GPC of Hercosett 125 in 0.05 *M* $NEt_4H_2PO_4$ on column I at various pH (refractive index detector). TPL = Total permeation limit.

nounced with Na^+ and Me_4N^+ than with Et_3NH^+, Et_4N^+ or Bu_4N^+ (where Me = methyl, Et = ethyl and Bu = butyl). In contrast, with column II, the various cations behaved similarly.

Column III which was designed for ion exchange chromatography was limited to molecular weights below about 25,000. Column IV prepared by Talley and Bowman's method[13] with silica (pore size 50 nm) deteriorated during use but column V (pore size 10 nm) was stable. With column IV the back pressure increased gradually until it was unusable, and this was faster at pH 2–3 than at pH 6 and replicate preparations deteriorated at different rates. Consequently, the cationic modified columns were limited to molecular weights around 40,000, although some results of higher molecular weights were obtained from column IV before deterioration became excessive. All the cationic columns showed significantly higher molecular weights (except at very high ionic strength) than expected for the PVP and PEI standards when calibrated directly against dextran standards, indicating ion exclusion effects.

If the cationic and neutral modified columns were compared for a given ionic strength, the cationic columns gave higher apparent molecular weights, presumably due to ion exclusion. As far as sensitivity to pH and ionic strength and adsorption effects were concerned, the cationic columns were generally similar in behaviour to column II and less sensitive than column I.

Determination of molecular weight

The approach used in the present study to obtain molecular weights for Hercosett 125 from the GPC data involved the use of established "universal" calibration methods[15,16] with dextran standards to find conditions where the correct molecular weights were obtained for PVP and PEI samples of known molecular weight. Hercosett 125 was then run under the same conditions and also the intrinsic viscosity was measured with the GPC eluent as solvent. The universal calibration method then gave a molecular weight for Hercosett 125.

The "universal" calibration line was drawn from the GPC data of a series of dextran standards which were eluted from a particular column at essentially the same position, independent of pH or ionic strength. The solvent composition was then varied until the points for the cationic polymer standards fell on the dextran calibration line. When this happens, it is an indication that interactions between the polymer and the column and/or solvent are minimal, but it may not apply to other cationic polymers, *e.g.*, Hercosett 125. This coincidence may be a fortuitous balance of opposing interactions, but viscosity measurements can be used to give an indication whether polyelectrolyte conformational changes are likely to be significant.

This universal calibration approach could only be used with column II since (i) on column IV the PVP calibration line did not coincide with the dextran line (Fig. 7) as observed before[13], and (ii) on the other columns the PVP standards were either strongly adsorbed or totally excluded. Universal calibration was performed, firstly by Benoit's method[15] (Figs. 6 and 7) and secondly by the "Southern" method[16] (Fig. 8), using published Mark–Houwink constants[17] for dextran and intrinsic viscosities, determined in this work, for PVP and PEI. With both methods the calibration lines for dextran, PVP and PEI coincided in 0.1 *M* $NaNO_3$ (adjusted to pH 3 with nitric acid) or 0.1 *M* $NEt_4H_2PO_4$ + 0.2 *M* NaH_2PO_4 (pH 3). From intrinsic viscosity measurements at different ionic strengths (Fig. 9) it can be seen that the eluent where

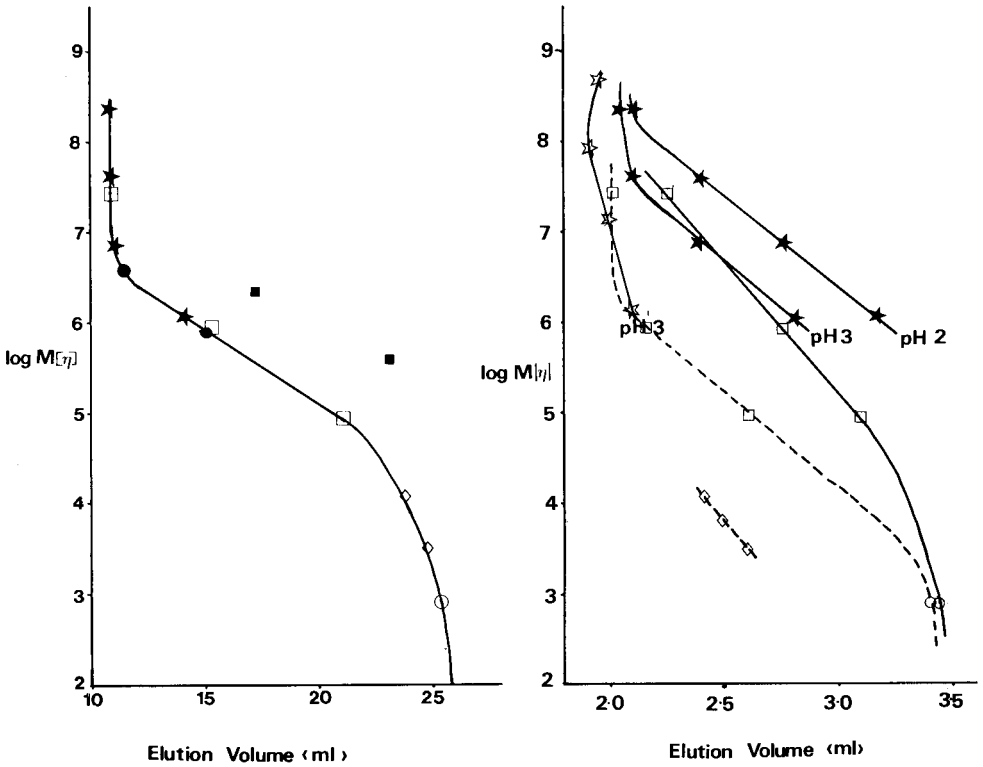

Fig. 6. Universal calibration {log ([η] × mol.wt.) *vs.* elution volume} of column II with dextran in water and PVP in aqueous salt solutions. □ = Dextran in water; ○ = sucrose in water; ✳ = PVP in 0.1 *M* $NaNO_3$ (pH 3); ■ = PVP in 1.0 *M* $NaNO_3$ (pH 3); ● = PVP in 0.1 *M* $NEt_4H_2PO_4$ + 0.2 *M* NaH_2PO_4 (pH 3); ◇ = PEI in 0.1 *M* $NaNO_3$.

Fig. 7. Universal calibration of column IV with dextran in water and PVP in aqueous salt solutions. ◇ = PVP in 0.01 *M* $NaNO_3$; other symbols as in Fig. 6.

the universal calibration lines coincided corresponded (for most polymer samples) to where the intrinsic viscosity had dropped nearly to its limiting value. Barth[7] has recommended that in polyelectrolyte GPC the ionic strength should be chosen such that the intrinsic viscosity has reached the limiting value in order to minimize effects from rod–coil conformational changes. In the present case Barth's recommendation could not be strictly followed as, in the region of the minimum intrinsic viscosity, adsorption started to occur.

Hercosett 125, under the "optimum" GPC conditions noted above (0.1 *M* $NEt_4H_2PO_4$ + 0.2 *M* NaH_2PO_4, pH 3 on column II) appeared as a broad peak with $\bar{M}_n$ = 2100 and $\bar{M}_w$ = 11,000 which merged into a peak of smaller area with molecular weight >300,000. The value assigned to the broad peak agrees closely with that obtained from gel filtration[6]. In addition to the errors inherent in the calibration method used, it should be noted that branching is possible and this would make the actual molecular weight slightly higher.

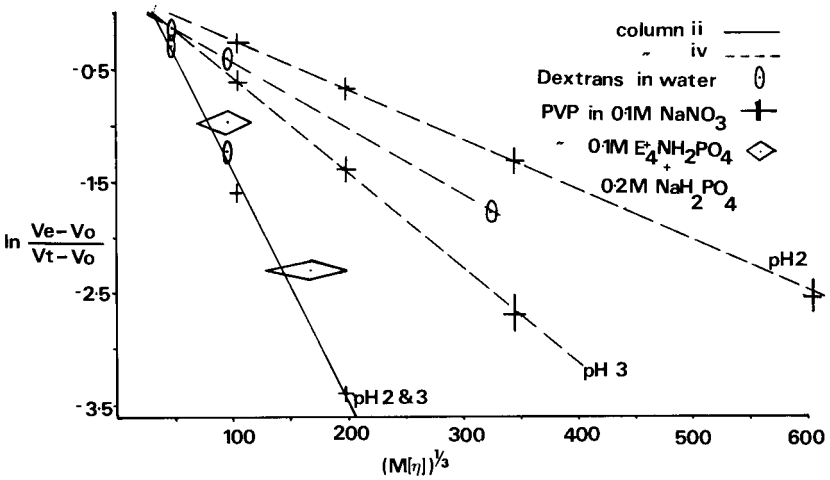

Fig. 8. "Southern" calibration method $\{\ln (V_e - V_0)/(V_t - V_0)$ *vs.* (mol.wt. $\times$ $[\eta])^{\frac{1}{3}}\}$ of columns II and IV with dextran in water and PVP in aqueous salt solutions. V_e = Elution volume; V_t = total permeation volume; V_0 = total interstitial volume; —— = Column II; - - - = column IV; ○ = dextrans in water; + = PVP in 0.1 *M* $NaNO_3$; ◇ = PVP in 0.1 *M* $NEt_4H_2PO_4$ + 0.2 *M* NaH_2PO_4.

GPC of Hercosett 125

In the GPC of Hercosett 125 there were two peaks eluted after the total permeation limit which appeared to be low-molecular-weight species, since they were not present after dialysis or acetone precipitation. One of the peaks had a strong UV absorption maximum at 315 nm and adsorbed strongly onto columns above pH 4. This peak was also observed in the GPC on Sephadex G-20[6].

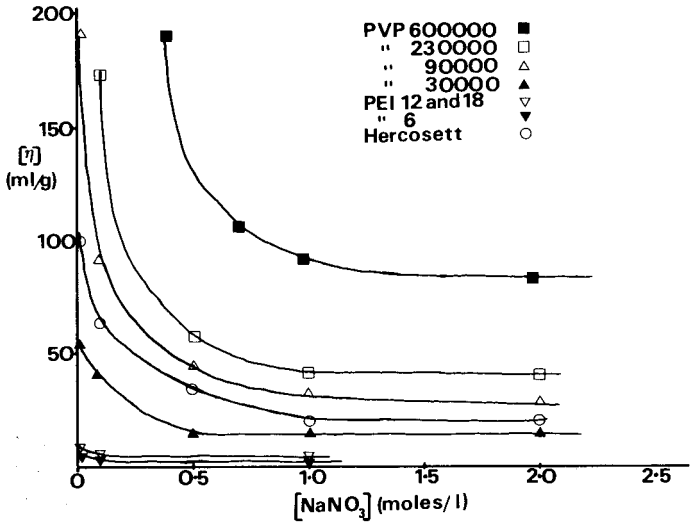

Fig. 9. Intrinsic viscosity, $[\eta]$, *vs.* ionic strength, ($NaNO_3$ solutions, pH 3) for cationic polymers used in this study.

The polymeric material in Hercosett 125 showed as two peaks which shifted position and/or intensity when the pH, ionic strength or column was changed (*cf.*, Figs. 3–5). As the pH and/or ionic strength increased, the intensity of the high-molecular-weight peak decreased, the low-molecular-weight peak shifted to lower apparent molecular weight (as observed before with PVP and PEI), and eventually there was only a peak at the total permeation limit. Peak area measurements indicated that when the high-molecular-weight peak decreased the low-molecular-weight peak increased. The high-molecular-weight limit of column I was higher than column II, and the high-molecular-weight peak on column II tailed from the exclusion limit. On column I the high-molecular-weight peak was eluted after the exclusion limit of the column, but did not shift its position with changes in pH or ionic strength.

It was demonstrated that the changes with increasing pH were reversible and were not due to cross-linking, by collecting fractions from chromatograms using one pH and rechromatographing at other pH values.

The explanation we advance for the peak splitting in Hercosett 125 involves changes in the extent of adsorption onto the column and the well known conformational changes[18] found in polyelectrolytes whereby extended rod-like molecules are converted to much more compact coiled conformations by reduction of the charge or increase in ionic strength.

The structure of Hercosett 125 in Fig. 1 is an oversimplification. In the first reaction, the excess of amino groups over carbonyl groups and the different reactivity of the amino groups result in a low-molecular-weight polyamide containing diethylenetriamine units, in which various combinations of from one to three of the amino groups have reacted. In the second reaction with epichlorohydrin, each amino group can be converted into several possible structures. Thus, in Hercosett 125, molecules of any molecular weight will have a number of different structures. Titration curves of Hercosett 125 with dilute NaOH and HCl indicate that there is a range of base strengths including some weakly basic groups which are not protonated at pH 4. This distribution of base strengths is consistent with the mixtures of different structures.

Our explanation for the two peaks is that some of the species present occur as an apparently high-molecular-weight peak due to either (i) ion exclusion from the column or (ii) by adopting a rod-like conformation with a large hydrodynamic volume. This peak is reduced when the ionic strength increases or the pH is raised (which reduces the number of positive charges), due to one or more of the following: (a) elimination of ion exclusion, (b) increased adsorption onto the column, and (c) collapse of a rod conformation to a more compact coiled conformation. The changes of viscosity with ionic strength (Fig. 9) are consistent with conformational changes; however, this could occur in both peaks.

CONCLUSIONS

The present study suggests that the commercial neutral modified silica columns I and II are more useful for the aqueous GPC of cationic polymers than the three cationic modified columns examined. Column II also can be used for a greater range of cationic polymers than column I. The commercial aqueous GPC columns I and II appear to be generally less suitable for cationic than for neutral or anionic polymers. Cationic polymers show greater changes than anionic ones in the elution position

when the pH or ionic strength is changed. This is probably a reflection that silica (even at pH 2–3) has a negative surface charge which increases as the pH becomes more alkaline. This problem was not overcome by modification of the silica surface with cationic groups, as this resulted in anomalously high apparent molecular weights due to ion exclusion effects (*i.e.*, electrostatic repulsion). In addition, satisfactory cationic modified columns for molecular weights above about 40,000 could not be prepared.

Universal calibration methods have been used to indicate the conditions with column II where polymer–column interactions appear to be minimal, and these conditions have been used to assign to Hercosett 125 a $\bar{M}_n = 2100$ and $\bar{M}_w = 11{,}000$. The errors in this operation are probably greater than in the molecular weights assigned by GPC for neutral and anionic polymers.

In summary, of the GPC systems examined, the one which was applicable to a wider range of cationic polymers used column II, pH 3–4, and 0.1–0.5 *M* ionic strength. These eluents are not unexpected as this pH range is where the negative surface charge on the silica is least, and the ionic strength is sufficient to suppress ion exclusion. The use of higher ionic strengths (*e.g.*, in order to overcome conformational changes) resulted in increased adsorption onto the column, which does not appear to have been noted before in polyelectrolyte GPC.

ACKNOWLEDGEMENT

The assistance of Dr. Ian M. Russell of these laboratories is gratefully acknowledged for helpful advice, discussions and for packing columns.

REFERENCES

1 Hercules Inc., *U.S. Pat.*, 2,926,154 (1960).
2 R. H. Earle, Jr., R. H. Saunders and L. R. Kangas, *Appl. Polym. Symp.*, 18 (1971) 707.
3 P. Smith and J. H. Mills, *Chem. Tech.*, 3 (1973) 749.
4 M. E. Carr, W. M. Doane, G. E. Hamerstrand and B. T. Hofreiter, *J. Appl. Polym. Sci.*, 17 (1973) 721.
5 N. A. Bates, *Tappi*, 52 (1969) 1161.
6 W. de Fries, *D. Rev. Nat. Thesis*, Rheinisch-Westfälischen Technischen Hochschule, Aachen, 1979.
7 H. G. Barth, *J. Chromatogr. Sci.*, 18 (1980) 409.
8 B. Stenlund, *Advan. Chromatogr.*, 14 (1976) 37.
9 A. R. Cooper and D. S. Van Derveer, *J. Liquid Chromatogr.*, 1 (1978) 693.
10 H. G. Barth and F. E. Regnier, *J. Chromatogr.*, 192 (1980) 275.
11 Y. Kato, K. Komiya, H. Sasaki and T. Hashimoto, *J. Chromatogr.*, 193 (1980) 311.
12 A. C. M. Wu, W. A. Bough, E. C. Conrad and K. E. Alden, Jr., *J. Chromatogr.*, 128 (1976) 87.
13 C. P. Talley and L. M. Bowman, *Anal. Chem.*, 51 (1979) 2239.
14 Calgon Corporation, *U.S. Pat.*, 4,118,316 (1973).
15 Z. Grubisic, P. Rempo and H. Benoit, *J. Polym. Sci., Polym. Lett. Ed.*, 5 (1967) 753.
16 R. D. Hester and P. H. Mitchell, *J. Polym. Sci., Polym. Chem. Ed.*, 18 (1980) 1727.
17 J. Brandrup and E. H. Immergut (Editors), *Polymer Handbook*, Wiley, New York, 2nd ed., 1975, p. IV-33.
18 C. Tanford, *Physical Chemistry of Macromolecules*, Wiley, New York, 1963, p. 306.

Journal of Chromatography, 235 (1982) 377–387
Elsevier Scientific Publishing Company, Amsterdam — Printed in The Netherlands

CHROM. 14,338

GEL PERMEATION CHROMATOGRAPHY OF CATIONIC POLYMERS ON PW GEL COLUMNS

PAUL L. DUBIN*,* and IRVIN J. LEVY
Clairol Research Laboratories, 2 Blachley Road, Stamford, CT 06922 (U.S.A.)
(Received August 25th, 1981)

SUMMARY

Universal calibration studies show that several cationic polyelectrolytes can be characterized by aqueous exclusion chromatography, without adsorption effects, using PW (Toyo Soda) hydrophilic gel columns. No other commercially available, high-performance packings are suitable for polycations, primarily because of charge-induced adsorption. In the case of the present columns, such interactions are minimized by 0.2 *M* NaCl in the mobile phase, which also provides an ionic strength sufficient to suppress Donnan equilibrium salt peaks.

INTRODUCTION

Until rather recently, aqueous exclusion chromatography was associated primarily with biopolymer separations, namely "gel filtration" of proteins on cross-linked polyacrylamide and dextran gels. Because these supports are not mechanically strong, aqueous exclusion chromatography did not at first share in the rapid progress in high-pressure liquid chromatography towards high resolution and short analysis time. With the advent of commercially available hydrophilic stationary phases for high-pressure exclusion chromatography, aqueous gel permeation chromatography (GPC) currently represents a field of expanding applications which may now fully benefit from the technology and theories developed for non-aqueous systems.

Substrates for aqueous GPC are of three general types: porous silica or glass, derivatized siliceous supports, and "semi-rigid" cross-linked polymer gels. The characteristics of these packings have been thoroughly reviewed[1], and the burgeoning literature on aqueous GPC contains numerous references to their applications to dextran, acidic polysaccharides, non-ionic synthetic polymers such as poly(ethylene oxide) and poly(vinyl alcohol), acrylic polyanions, and proteins. In contrast, only two references describe the exclusion chromatography of cationic polymers. The first report presents fragmentary data for a quaternized Styragel-type column with very limited resolution[2]. The second describes the chromatography of (uncharacterized) quaternized poly(4-vinylpyridine) and poly(N,N-diallyldimethylammonium

* Present address: Department of Chemistry, Purdue University, Indianapolis, IN 46205, U.S.A.

0021-9673/82/0000–0000/$02.75

chloride) on column packings made by coupling porous glass or silica to a quaternized aminopropylsilane[3]. Among the difficulties encountered in the latter work were (1) the necessity for strong acid (0.1 N HNO_3) in the mobile phase to ionize unquaternized bonded phase amine, and (2) low column efficiencies (*ca.* 500 plates ft.$^{-1}$) and correspondingly long run times (2–3 h). In any event, neither of these two quaternized substrates is commercially available. Since the principal applications of cationic polymers —as flocculants in water treatment, paper making and sewage processing— are ones in which the polymers' molecular weight distribution (MWD) plays a central role, the lack of readily available high efficiency aqueous GPC columns has major consequences for these technologies.

Siliceous packings may be presumed to always contain some level of acidic silanol groups capable of dissociation and consequent electrostatic binding to polycations. Thus, a non-ionic semi-rigid gel would appear less prone to adsorption. PW packings (Toyo Soda) are hydrophilic cross-linked polyether gels containing $-CH_2-CH(OH)CH_2O-$ repeat units[4] whose application to non-ionic linear polymers, dextrans, acidic polysaccharides and proteins have been well documented[4–7]. In this report we discuss the characterization of cationic synthetic polymers with PW columns[8].

EXPERIMENTAL

Apparatus

The GPC system consisted of a Milton Roy Minipump, a Rheodyne Model 7010 injector equipped with a 200-μl loop, and a Waters Associates R401 differential refractometer. The columns employed, Toyo Soda G3000 PW and G5000 PW, both 30 cm long, were preceded by an in-line stainless steel fritted filter (Rheodyne). At a flow-rate of 30 ml h^{-1} the back pressure was 100–200 p.s.i. per column.

Materials

Narrow MWD poly(ethylene oxide) (PEO) samples with MWs $< 2 \cdot 10^4$, as determined by end group analysis, were supplied by Union Carbide or Dow Chem. High-molecular-weight broad distribution PEO samples characterized by light-scattering were from Aldrich. Dextrans were supplied by Pharmacia with intrinsic viscosities, and with MWs from light-scattering. Poly(dimethyldiallylammonium chloride) (PDMDAAC) was a commercial product "Merquat 100" or low MW homologs, all from Calgon. Their MWs were determined from intrinsic viscosities in 0.1 M NaCl at 30°C, using the relationship $[\eta] = 3.5 \cdot 10^{-4} \cdot \bar{M}_w^{0.62}$, which was developed on the basis of viscosity and light-scattering data supplied by the manufacturer along with similar data from the literature[9]. Narrow MWD fractions of polyethyleneimine (PEI) were kindly provided by Professor R. Stratton, Institute of Paper Chemistry, along with viscosity data and MWs from ultracentrifugation[10]. Poly(N-vinylacetamide) (PVAc) fractions were gifts from Dynapol, with MWs obtained by osmometry and GPC[11] and intrinsic viscosities calculated from the relationship[12] $[\eta]_{H_2O,30°C} = 1.6 \cdot 10^{-3} \cdot \bar{M}_n^{0.52}$. A sample of polyvinylamine (PVA) was from the same source, its MW determined from that of the PVAc precursor. Globular proteins were from Sigma. A high-molecular-weight cationic polymer for water treatment, poly(methacrylamidopropyltrimethylammonium chloride) (PMAPTAC) was a gift from Texaco. An ionene polymer of unknown MW was kindly provided by Professor

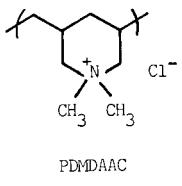

PDMDAAC

Poly(dimethyldiallylammonium chloride)

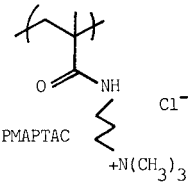

Poly(methacrylamidopropyltrimethylammonium chloride)

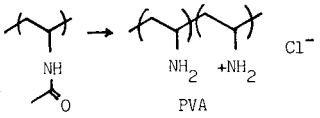

PVAc ⟶ poly(vinylamine)

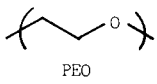

Poly(ethyleneoxide)

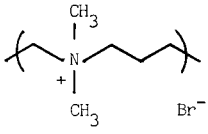

4,4 Ionene

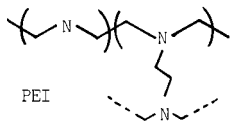

Polyethylenimine

Fig. 1. Structures of synthetic polymers used in this study.

P. Ander, Seton Hall University. Structures of the synthetic polymers mentioned above are shown in Fig. 1.

Methods

Polymers were dissolved in the mobile phase and clarified with 0.45-μm HAWP filters (Millipore). The concentration of polymer injected onto the column ranged from 0.1 to 1.0 wt. % corresponding roughly to RI detector attenuations of $\frac{1}{2}\times$ to $4\times$. The lowest concentrations were necessary for the higher-molecular-weight polymers in order to avoid signal noise due to viscosity-related pressure pulses in the refractometer cell as the sample eluted from the column.

PEI and PVA samples were typically applied to the columns as the free base, at pH = 10. Since the pH of the sample eluents were more than 9, it could be assumed that these polymers were largely un-ionized during chromatography.

Intrinsic viscosities of PDMDAAC were measured in 0.1 *M* NaCl at 30°C using a Schott AVS/N semi-automatic elution viscometer.

RESULTS AND DISCUSSION

Mobile phase supporting electrolyte

In the absence of simple salt, polyion molecular dimension —and hence retention volume— would be extremely sensitive to intra-molecular electrostatic repulsion. This effect would result in strong divergence of the elution behavior of non-ionic and ionic polymers and an excessive influence of salt impurities for the latter. Supporting electrolyte is thus a prerequisite for interpretable chromatograms. In the presence of 0.1 *M* citrate (selected for its buffering capacity and indifference to stainless steel) chromatograms of PDMDAAC were obscured by large and erratic negative peaks as shown in Fig. 2. Since these peaks were eliminated if the polymer solution was first brought to dialysis equilibrium with the mobile phase, they may be ascribed to Donnan equilibrium effects. When the polyion shares a common co-ion with the simple salt, the activity of the latter in the domain of the polymer is increased. The volume within the small pores, which may be regarded as analogous to an external dialysis solution from which polymer is excluded, then acquires a concentration of simple salt in excess of the bulk mobile phase. This salt is subsequently eluted as a so-called "ion-inclusion" peak[1]. In the present case, the Donnan equilibrium results in a depression in citrate ion activity and a consequent increase in citrate concentration in the immediate vicinity of the polymer. The concomitant depletion of citrate from the bordering volumes results in large negative peaks, since the refractive index increment of citrate is large. Such Donnan effects could be eliminated by choosing a salt of lower refractive index and valency, and maintaining a large salt:polymer ratio. Thus with 0.1–0.2 *M* NaCl in the mobile phase, and sample loads of less than 1 mg, no such interfering peaks were encountered.

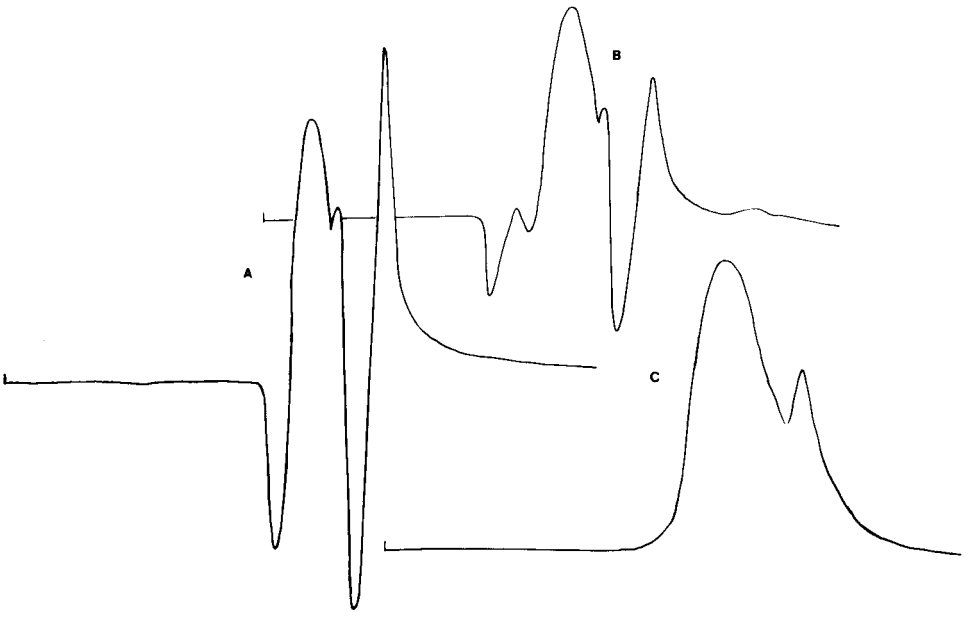

Fig. 2. Chromatograms of $5.2 \cdot 10^3$ MW PDMDAAC in: A, 0.1 *M* sodium citrate, direct solution; B, 0.1 *M* sodium citrate, partial dialysis; C, 0.2 *M* NaCl direct solution. G3000 PW column.

Calibration and efficiency

Fig. 3 shows calibration curves obtained in 0.1 *M* and 0.2 *M* NaCl using PEO standards. In order to employ the light-scattering MW reported for the broad distribution $1 \cdot 10^5$ MW PEO standard, the elution volume corresponding to $\bar{M}_w$ was calculated from the chromatogram in conjunction with a trial calibration curve based on a linear extrapolation from the other PEO data points. This procedure was extended to the $9 \cdot 10^5$ MW PEO sample with a somewhat lesser degree or certainty, reflected in the large error bar for V_e for this datum. The columns exhibited plate counts of 25,000–30,000 plates meter^{-1}, obtained using ethylene glycol or ^2H_2O. These efficiencies were maintained over several months of application.

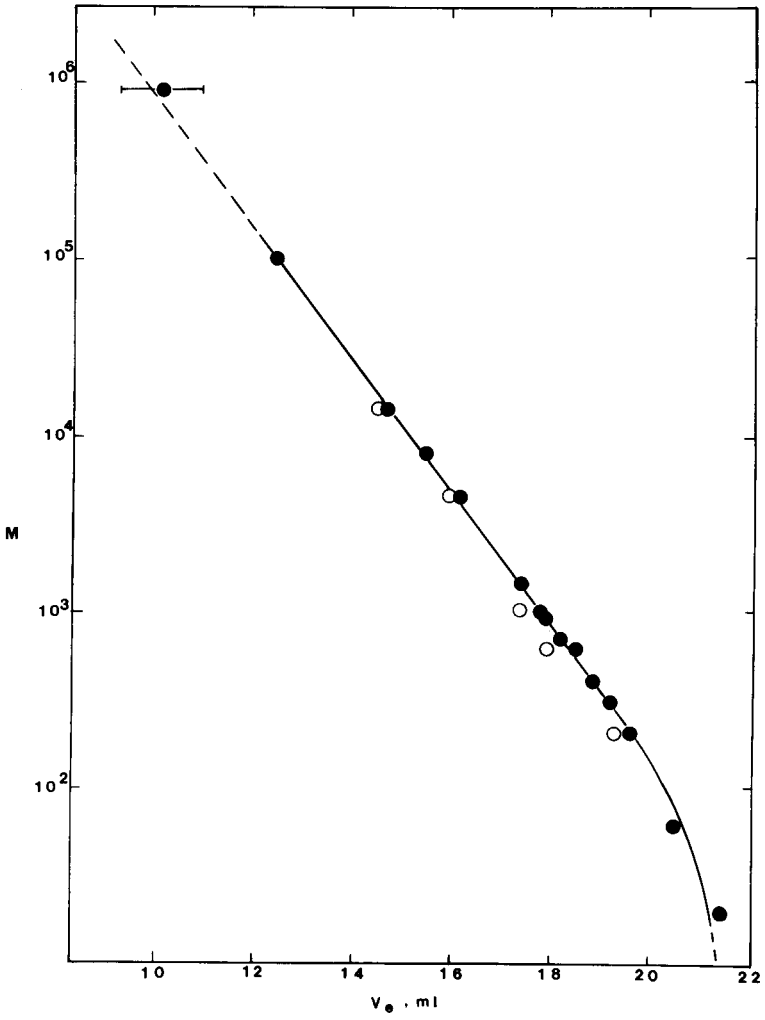

Fig. 3. PEO calibration curves for G5000 PW + G3000 PW columns, in 0.2 *M* NaCl (●) and 0.1 *M* NaCl (○).

Application to cationic polymers

Fig. 4–6 show chromatograms of several strongly cationic polyelectrolytes. All elute with no evidence of adsorption, *i.e.*, with no tailing and peak areas consistent with the sample mass. Table I compares apparent GPC MW values, based on PEO calibration curves, with MWs from other methods for the characterized polymers. With the exception of the result for PVA in 0.2 *M* NaCl, apparent peak MW values are lower than expected MWs by a factor of 2–4 in this solvent, and by a factor of 4–

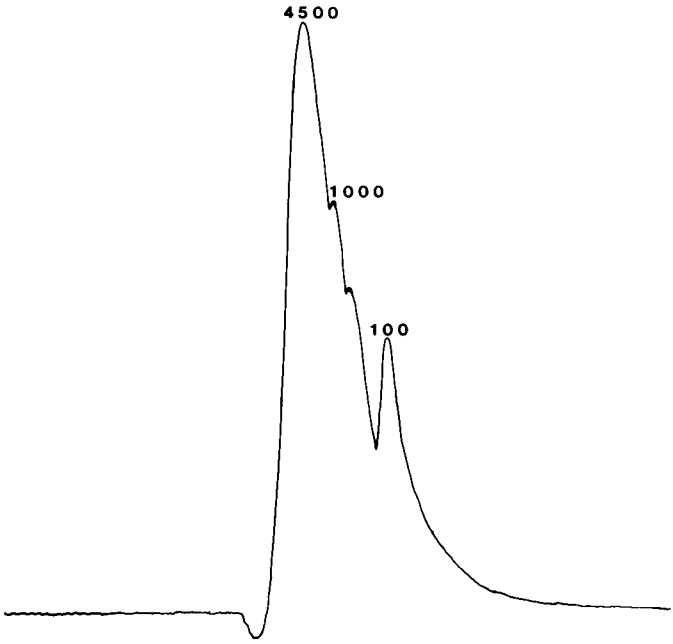

Fig. 4. Chromatogram of 4,4-ionene. Values shown are MWs based on PEO calibration. G3000 PW, 0.1 *M* NaCl.

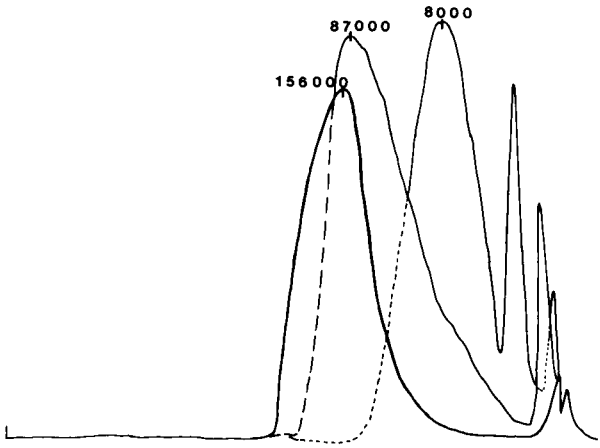

Fig. 5. Chromatograms of PMAPTAC samples of varying MWs. Values shown are peak MWs based on PEO calibration. G5000 PW + G3000 PW, 0.2 *M* NaCl.

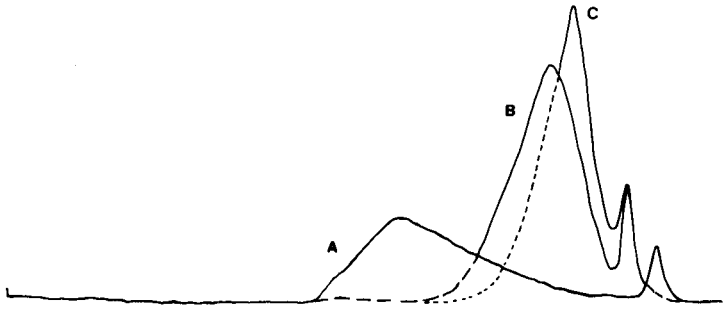

Fig. 6. Chromatograms of PDMDAAC samples. $\bar{M}_w = 4.5 \cdot 10^5$ (A); $5.4 \cdot 10^4$ (B); $5.2 \cdot 10^3$ (C). G5000 PW + G3000 PW, 0.2 *M* NaCl.

10 in 0.1 *M* NaCl. GPC retention times correlate with molecular volumes, as measured for example by $[\eta]M$, rather than molecular weights. Apparent MWs based on PEO elution may be low simply because PEO, primarily by virtue of its large contour length per unit mass, has a small ratio of molecular weight to molecular volume. Comparisons of MWs in Table I are also obscured by the difference between the measured MW, typically close to $\bar{M}_w$ or $\bar{M}_v$, and that of the species eluting at the chromatographic peak, usually intermediate between $\bar{M}_w$ and $\bar{M}_n$. Hence, low apparent GPC MW values do not of themselves provide evidence for adsorption. On the other hand, we observe increased retention relative to PEO (*i.e.*, lower M_p^{PEO}) at the lower ionic strength. This effect, contrary to that expected from changes in polymer dimensions due to electrostatic screening, is suggestive of polymer–substrate interactions. Separation of the effects of molecular dimensions from those of adsorption may best be accomplished by universal calibration methods.

TABLE I

EXPECTED MWs OF CATIONIC POLYMERS AND APPARENT GPC MOLECULAR WEIGHTS (RELATIVE TO POLYETHYLENE)

Sample	*Reported MW (method)*	*Apparent MW, M_p^{PEO}**	
		0.1 M NaCl	*0.2 M NaCl*
PDMDAAC	$4.5 \cdot 10^5$ (viscosity, light-scattering)	$5.0 \cdot 10^4$	$2.0 \cdot 10^5$
PDMDAAC	$1.2 \cdot 10^4$ (viscosity, light-scattering)	$1.2 \cdot 10^3$	$3.0 \cdot 10^3$
PDMDAAC	$5.2 \cdot 10^3$ (viscosity, light-scattering)	$8.0 \cdot 10^2$	$1.6 \cdot 10^3$
PEI	$1.4 \cdot 10^4$ (ultracentrifugation)[9]	$2.0 \cdot 10^3$	$4.5 \cdot 10^3$
PEI	$4.4 \cdot 10^3$ (ultracentrifugation)	$6.5 \cdot 10^2$	$2.0 \cdot 10^3$
PVA	$6.5 \cdot 10^4$ (osmometry and GPC of PVAc)[11]	**	$7.7 \cdot 10^4$

* From peak elution volume and PEO calibration curve.
** No elution.

Universal calibration

It has been amply demonstrated on both theoretical and experimental grounds that the product of intrinsic viscosity and MW determines, for all polymers in a given column–solvent system, the GPC distribution coefficient and hence the elution

volume. Thus, the congruence of $[\eta]M$ *vs.* V_e data for a variety of polymers with differing functional groups is strong evidence for the absence of non-steric effects. MW and viscosity data used for universal calibration plots in 0.1 *M* and 0.2 *M* NaCl are assembled in Table II. For non-ionic polymers such as PEO, PVAc and dextran, we may neglect the influence of salt on viscosity and employ the values of $[\eta]$ found in pure water. This approximation is supported by findings for PEO[17] and amylose[18]. For PEI, viscosity data obtained in 0.1 *M* NaCl were used[10]; in the pH range of the chromatography, 9–10, the change in viscosity with a two-fold increase in ionic strength is negligible[10]. Viscosities of PDMDAAC were measured only in 0.1 *M* NaCl; a small (*ca.* −10%) correction was made for 0.2 *M* NaCl, according to previously established relationships[9]. The intrinsic viscosity of β-lactoglobulin was obtained from a viscosity–MW relationship constructed from data for globular proteins[19].

TABLE II

MW AND VISCOSITY DATA FOR POLYMERS OF THIS STUDY

Polymer	*MW*	$[\eta]$ (dl g^{-1})	$[\eta]M$
PEO	$1.0 \cdot 10^5$*	0.93	$9.3 \cdot 10^4$
	$1.4 \cdot 10^4$**	0.25	$3.5 \cdot 10^3$
	$8.0 \cdot 10^3$**	0.18	$1.4 \cdot 10^3$
	$4.5 \cdot 10^3$**	0.13	$5.7 \cdot 10^2$
	$1.4 \cdot 10^3$**	0.070	$1.0 \cdot 10^2$
PVAc	$2.9 \cdot 10^5$	1.11**	$3.2 \cdot 10^5$
	$1.5 \cdot 10^5$	0.79	$1.2 \cdot 10^5$
	$1.7 \cdot 10^4$	0.25	$4.1 \cdot 10^3$
	$3.0 \cdot 10^3$	0.10	$3.0 \cdot 10^2$
Dextran	$7.3 \cdot 10^4$	0.28***	$2.0 \cdot 10^4$
	$4.0 \cdot 10^4$	0.21	$8.4 \cdot 10^3$
	$9.7 \cdot 10^3$	0.10	$9.7 \cdot 10^2$
PEI	$1.4 \cdot 10^4$	0.14§	$2.0 \cdot 10^3$
	$7.2 \cdot 10^3$	0.10[6]	$7.6 \cdot 10^3$
	$4.4 \cdot 10^3$	0.077	$3.4 \cdot 10^2$
β-Lactoglobulin	$1.8 \cdot 10^4$	0.034	$6.2 \cdot 10^2$
PDMDAAC	$4.5 \cdot 10^5$	0.80§§	$3.6 \cdot 10^5$
	$5.4 \cdot 10^4$	0.30	$1.6 \cdot 10^4$
	$1.6 \cdot 10^4$	0.14	$2.2 \cdot 10^3$
	$1.2 \cdot 10^4$	0.12	$1.4 \cdot 10^3$
	$5.2 \cdot 10^3$	0.070	$3.6 \cdot 10^2$

* From literature viscosity–MW data in pure water[13–16]. We neglect the influence of NaCl on the viscosity–MW relationship of PEO since 0.1 *M* KCl depresses the viscosity of high-molecular-weight PEO by less than 5% (see ref. 17).

** From viscosity–MW relationship in pure water[12] (see text).

*** Viscosity data in pure water supplied by manufacturer (see text).

§ Measured in 0.1 *M* NaCl at pH 10[10].

§§ Measured in 0.1 *M* NaCl (see text).

The samples of PVAc, PEI, dextran, and all but the high-molecular-weight PEO were fractions of narrow distribution and it was possible to plot $[\eta]M$ *vs.* peak elution volume without regard for the differences between the viscosity- or weight-average MW, and that corresponding to the chromatographic peak. On the other hand, this procedure could not be applied to the PDMAAC samples which were polydisperse with $\bar{M}_w/\bar{M}_n$ ranging from 2 to 10. (Many workers disregard this point and incorrectly identify the measured value of $J = [\eta]M$ —closest to the value of J for the hypothetical species having the viscosity average MW— with the peak elution volume.). An iterative procedure[20] was employed to calculate the elution volumes corresponding to $\bar{M}_w$ from the chromatograms of the PDMDAAC samples; this value, V_{M_w}, is better aligned with $[\eta]M$ than is the peak elution volume.

Universal calibration plots in 0.1 *M* and 0.2 *M* NaCl are shown in Fig. 7A and 7B, respectively. In the latter solvent, the data for PDMDAAC, PEO, dextran, PVAc and the globular protein β-lactoglobulin coincide with a single line, while the data for PEI show progressive deviations towards greater retention with increasing MW. In 0.1 *M* NaCl, the data for PDMDAAC are uniformly displaced to higher elution volumes, while those of the other cationic polymer, PEI, show clear evidence of adsorption with increasing MW.

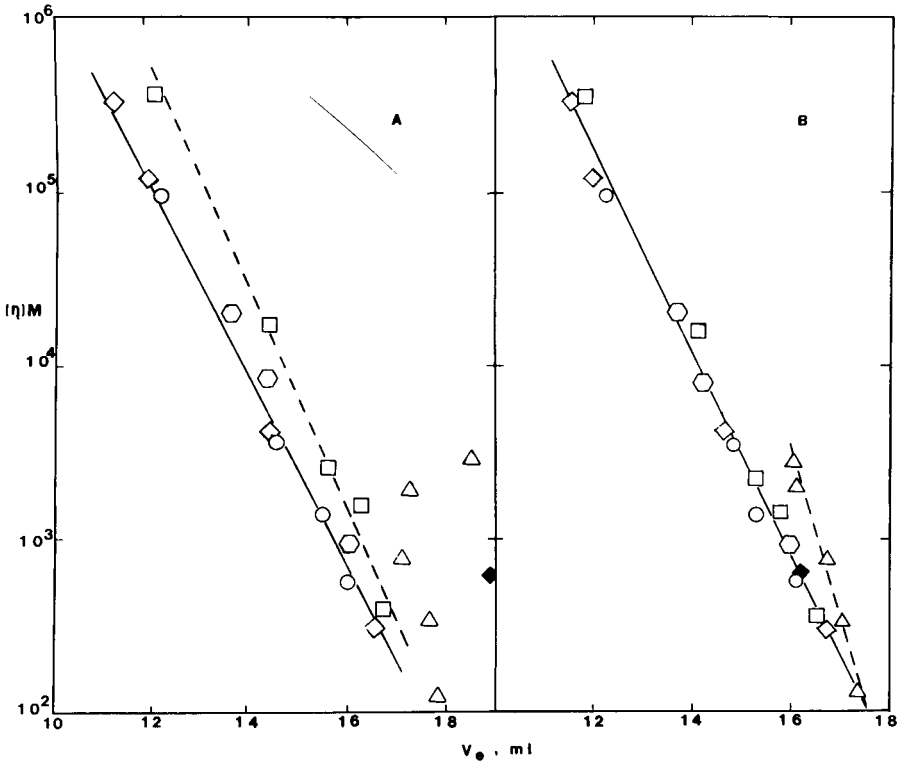

Fig. 7. Universal calibration plots for G5000 PW + G3000 PW in 0.1 *M* NaCl (A), 0.2 *M* NaCl (B). ○, PEO; ○, dextran; ◇, PVAc; □, PDMDAAC; △, PEI; ◆, β-lactoglobulin. V_e for PDMDAAC corresponds to M_w (see text).

The influence of ionic strength on the elution of PDMDAAC samples is illustrated further by the superimposed chromatograms of Fig. 8. As noted above, the shift to larger retention volumes with lower ionic strength cannot be explained by an alteration in molecular dimensions which should yield the opposite result. We may hypothesize that the presence of some anionic functional groups on the gel result in favorable interactions with the cationic polymers which in turn are screened by increased electrolyte concentration. Such an argument, however, is not in accord with the more dramatic retention of PEI, since that polymer should exhibit a positive charge density substantially lower than PDMDAAC. The unusual retention behavior of both PEI and PVA in their nearly un-ionized forms may indicate that hydrophobic interactions are also factors in gel chromatography with PW columns.

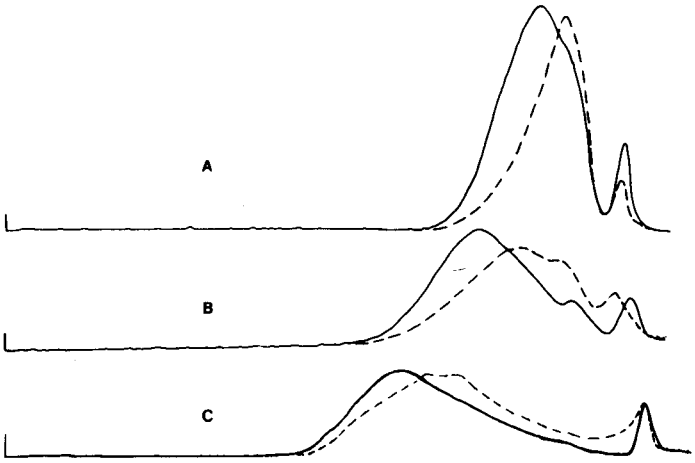

Fig. 8. Chromatograms of PDMDAAC samples in 0.1 *M* NaCl (– – –) and 0.2 *M* NaCl (—). $\bar{M}_w = 1.2 \cdot 10^4$ (A); $5.4 \cdot 10^4$ (B); $4.5 \cdot 10^5$ (C).

CONCLUSIONS

PW columns may be used for GPC analysis of polycations. Under appropriate ionic strength conditions, universal calibration data reveal no adsorptive effects for strongly cationic polymers. Weak polybases, namely polyethyleneimine and polyvinylamine, display more complex behavior and exhibit retarded elution, particularly at lower ionic strength. While evidence exists for both electrostatic and hydrophobic solute–gel interactions, these factors have yet to be resolved.

REFERENCES

1 H. G. Barth, *J. Chromatogr. Sci.*, 18 (1980) 409.
2 G. B. Butler, *U.S. Pat.*, 3,962,206, June 8, 1976.
3 C. P. Tally and L. M. Bowman, *Anal. Chem.*, 51 (1979) 2239.
4 T. Hashimoto, J. Sasaki, M. Aiura and Y. Kato, *J. Polym. Sci., Polym. Phys. Ed.*, 16 (1978) 1789.
5 Y. Kato, H. Sasaki, M. Aiura and T. Hashimoto, *J. Chromatogr.*, 153 (1978) 546.
6 T. Hashimoto, H. Sasaki, M. Aiura and Y. Kato, *J. Chromatogr.*, 160 (1978) 301.
7 Y. Kato, K. Komiya, H. Sasaki and T. Hashimoto, *J. Chromatogr.*, 193 (1980) 311.

8 P. L. Dubin and I. Levy, *Polym. Preprints*, 22, No. 1 (1981) 132.
9 S. Maxim, S. Ioan and A. Carpov, *Eur. Polymer. J.*, 13 (1977) 105.
10 G. M. Lindquist and R. Stratton, *J. Colloid Interface Sci.*, 55 (1975) 45.
11 P. L. Dubin, *J. Liquid Chromatogr.*, 3 (1980) 623.
12 A. R. Read and P. L. Dubin, unpublished results.
13 F. E. Baily, Jr. and R. W. Callard, *J. Appl. Polym. Sci.*, 1 (1959) 56.
14 C. Rossi and C. Cuniberti, *J. Polym. Sci., Polym. Lett., Ed.*, 2 (1964) 681.
15 D. K. Thomas and A. Charlesby, *J. Polym. Sci.*, 42 (1960) 195.
16 C. Sadron and P. Rempp, *J. Polym. Sci.*, 29 (1958) 127.
17 F. W. Stone and J. J. Stratta, in *Encyclopedia of Polymer Science and Technology*, Vol. 6, Wiley, New York, 1967, p. 131.
18 W. Banks, C. T. Greenwood, D. J. Houston and A. R. Proctor, *Polymer*, 12 (1971) 452.
19 C. Tanford, *Physical Chemistry of Macromolecules*, Wiley, New York, 1963, p. 394.
20 P. L. Dubin, S. L. Koontz and K. L. Wright, *J. Polym. Sci. Polym. Chem. Ed.*, 15 (1977) 2047.

Journal of Chromatography, 235 (1982) 389–399
Elsevier Scientific Publishing Company, Amsterdam — Printed in The Netherlands

CHROM. 14,323

"CHARGE-TRANSFER THIN-LAYER CHROMATOGRAPHY" OF VARIOUS BIOCHEMICALS

M. A. SLIFKIN*, W. A. AMARASIRI, C. SCHANDORFF and R. BELL
Department of Biochemistry, The University of Salford, Salford M5 4WT (Great Britain)
(First received August 6th, 1981; revised manuscript received September 5th, 1981)

SUMMARY

Thin-layer chromatographic studies have been made of purines, pyrimidines, nucleotides, nucleosides and amino acids with different charge acceptors either mixed together or with the acceptor as part of the stationary phase. These have been complemented with infrared spectrophotometry and fluorescence quenching studies.

INTRODUCTION

"Charge-transfer thin-layer chromatography" has been studied by several authors[1–4] either as a means of obtaining better separation of related compounds or as a technique to detect the formation of charge-transfer complexes. Previous studies have concentrated on organic donors and acceptors in the main. In this work studies on biochemical systems are reported.

Charge-transfer complexes are weak complexes involving electron donors and acceptors. In the ground state of the complex, there is a small amount of charge donated from the donor to the acceptor. On the absorption of light of suitable energy there is a much large donation of charge giving rise to the characteristic charge transfer absorption band and hence colour of the complex. Full discussion of this topic is given in the books of Mulliken and Person[5], Foster[6,7] and Slifkin[8]. The latter author specifically deals with charge-transfer complexes of biomolecules. The role of charge-transfer complexing in biochemical systems is the subject of much discussion and controversy[7,8], and hence analytical methods for proving or confirming the presence (or indeed otherwise) of charge-transfer forces in these systems are of some interest.

Three kinds of experiment have been carried out previously; those in which ready made thin-layer chromatography (TLC) plates are soaked in solutions of the acceptor in order to load them into the stationary phase; those in which plates are made using a slurry of silica gel and acceptor; and chromatography of mixtures of donor and acceptor on standard silica gel plates.

In our own experiments presented here we have utilised the latter two methods plus a more novel technique of covalently binding suitable acceptors to silica gel or cellulose and hence making up to plates.

0021-9673/82/0000–0000/$02.75

It is the difference between the R_F values of the donors with and without acceptor which is a measure of the interaction. Harvey and Halonen[1] have proposed the concept of a binding constant B, defined as

$$B = \frac{R_F - R_F'}{R_F} \times 100$$

where R_F is the value obtained in the absence of acceptor and R_F' in the presence of the acceptor. Harvey and Halonen[1] suggest that B is a direct measure of charge transfer interaction. In fact there are difficulties with this B parameter. Literature values are frequently negative owing to the increase of R_F with electron acceptor. Furthermore the B parameter is asymmetric, taking values from $-\infty$ to 100. It is not clear what the relationship is between B and the interaction forces or even whether two identical B values imply forces of the same magnitude if the R_F values are widely different.

EXPERIMENTAL

Chemicals were the purest commercially available and used as supplied, except quinone purified by sublimation and chloranil by recrystallisation. Silica gel used was Kieselgel GF_{254} from E. Merck (Darmstadt, G.F.R.). This contains a fluorescent indicator and was useful for the detection of the nucleic acid bases which showed up as a dark spot against a fluorescent background. The cellulose was MN300 for TLC from Machery, Nagel & Co. (Düren, G.F.R.). TLC plates were made using the Shandon Unoplan apparatus. All plates used were 20 × 20 cm squares of glass which were first thoroughly cleaned using Decon 75 surfactant. Two different kinds of slurry were made from which TLC plates were obtained. The first consisted of 40 g of silica gel mixed with 80 ml of benzene–95% ethanol (92:8). The second consisted of 40 g of silica gel mixed with 92 ml of distilled water and 8 ml of methanol. The silica gel thickness was set to 25 mm.

When impregnants were used, they were added to the slurry solvent to make up a $5 \cdot 10^{-5}$ M solution. After the slurry was spread on the plates, they were dried and then stored in an oven overnight. Plates containing riboflavin were stored in the dark to prevent photooxidation.

Cellulose plates were made using a slurry of 7 g of cellulose and 30 ml of water with 4 ml of ethanol, and otherwise as for silica gel.

Riboflavin covalently bound to cellulose was made according to the method of Arsenis and McCormick[9].

The silica gel riboflavon covalent compound was prepared using a method due to Mikeš *et al.*[10] for linking silica gel to 2-{(2,4,5,7-tetranitro-9-fluorenylidene)amino}oxy}proprionic acid. The steps in the procedure are shown in Fig. 1. The implementation can be found in ref. 10.

After chromatography amino acids were spotted using ninhydrin solution (2% in acetone) and the purines and pyrimidines were detected by ultraviolet (UV) light (254 nm).

All quoted R_F values are the mean of six readings.

Infrared (IR) spectra were obtained using a Unicam SP200G spectrophotome-

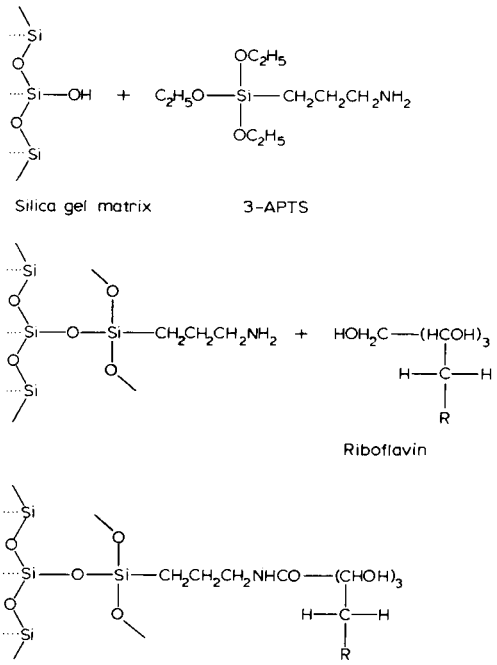

Fig. 1. The coupling of riboflavin to silica gel.

ter. Samples of complexes were evaporated from mixed ethanol–water solution in a rotary evaporator and made into KBr discs using standard sampling techniques. A Perkin-Elmer 2000 fluorescence spectrophotometer with constant temperature cell holder was used. All fluorescence quenching studies were carried out in pH 7 phosphate buffer.

RESULTS AND DISCUSSION

TLC of mixed solutions of pyrimidines with different electron acceptors, chloranil, bromanil, trinitrobenzene and tetracyanoethylene on silica gel yielded R_F values no different from those of the pyrimidines alone. IR spectroscopy of evaporates of mixed solutions appear to be the superposition of the IR spectra of the individual components. It can be assumed that in these systems any interaction is very weak.

With purines and the same acceptors there are obvious colour changes which are greatly intensified on freezing down to liquid nitrogen temperatures (colours of evaporates are shown in Table I). This is usually taken to be due to charge-transfer complexing[5–8]. Some of these systems when evaporated display electron spin resonance (ESR) signals as listed in Table II, which is an indication of electron decoupling. Table III lists R_F values of both individual compounds and mixtures with charge acceptors. In almost all cases the R_F values of the mixtures show retardation compared with the individual components, together with streaking between the two spots of the mixture. The streaking would seem to imply that there is some weak interaction in these systems leading to continual formation and dissociation of complexes between the purines and acceptors. The retardation of the spots has been interpreted by

TABLE I

COLOURS OF THE PURINE–ACCEPTOR COMPLEXES

TCNE = Tetracyanoethylene; TNB = 1,3,5-trinitrobenzene.

	TCNE	*Chloranil*	*Bromanil*	*p-Benzo-quinone*	*TNB*
Uric acid	Yellow	Pale yellow	Light brown	Dirty yellow	Cream
Caffeine	Yellow	Light green	Reddish brown	Brown	Cream
2,6-Diamino-purine	Yellow	Light green	Reddish brown	Brown	Cream
6-Methylamino-purine	Bright yellow	Yellow	Chocolate brown	Chocolate brown	Cream
Adenine	Bright yellow	Dirty green	Light brown	Light brown	Pale yellow
Hypoxanthine	Bright yellow	Dirty green	Chocolate brown	Brown	Buff
Purine	Bright yellow	Pale yellow	Brown	Brown	Pink

Schenk *et al.*[4], who observed similar effects in organic systems, as arising from weak complexing. TLC does appear to give an indication of weak interactions between molecules by comparing the difference between systems and individual components. The pyrimidines, which show no interaction under these conditions, have rather higher ionisation potentials than the purines[11] and are expected consequently to form weaker complexes.

Details of the IR spectra of the evaporates of these systems are given in the Appendix, and they indicate the presence of charge transfer forces between the purines and acceptors.

An alternative method of examining weak interactions is to have one of the interacting components incorporated into the stationary phase of the TLC plate. The method of soaking a silica gel TLC plate in a solution of the impregnant is, we feel, unsatisfactory as one has little control over the amount of impregnant or its distri-

TABLE II

COMPLEXES THAT GAVE ESR SIGNALS

	TCNE	*Chloranil*	*Bromanil*	*p-Benzo-quinone*	*TNB*
Uric acid	Yes	No	No	Yes	No
Caffeine	Yes	Yes	No	No	No
2.6-Diaminopurine	Yes	No	No	No	No
Hypoxanthine	Yes	No	No	No	No
6-Methylaminopurine	Yes	No	No	Yes	Yes
Adenine	Yes	Yes	Yes	No	No
Purine	Yes	No	No	No	No

TABLE III

R_F VALUES OF PURINES, ACCEPTORS AND THEIR MIXTURES ON SILICA GEL

S = Streaky; BQ = *p*-benzoquinone. Solvent, chloroform–methanol (4:1).

	TCNE (0.85)	*Chloranil (0.82)*	*Bromanil (0.88)*	*TNB (0.84)*	*BQ (0.86)*
Uric acid (0.31)	0.28,0.84	0.21,0.74 S	0.26,0.75 S	0.25,0.89	0.29,0.90
Caffeine (0.82)	0.71,0.85	0.82,0.87 S	0.77,0.84	0.69,0.81	0.80,0.85
2,6-Diaminopurine (0.20)	0.16,0.85	0.18,0.83	0.13,0.84	0.14,0.87 S	0.14,0.85
Hypoxanthine (0.20)	0.17,0.85 S	0.17,0.85 S	0.16,0.85 S	0.15,0.85 S	0.18,0.85
6-Methylamino-purine (0.51)	0.40,0.84	0.35,0.83 S	0.36,0.82 S	0.38,0.82 S	0.50,0.84
Adenine (0.30)	0.22,0.85 S	0.24,0.86 S	0.23,0.88 S	0.30,0.84 S	0.26,0.84 S
Purine (0.32)	0.29,0.85 S	0.28,0.82	0.25,0.88	0.26,0.79 S	0.30,0.85

bution through the stationary phase. The method of making up plates with the silica gel mixed with the impregnant is more satisfactory as one can at least have better control over the amount of impregnant and its distribution. Two different sets of experiment are reported, the first in which benzene was used as a binder and the second in which methanol was used. Our original intention was to use only benzene. This gives a very good quality plate with no flaking of the silica gel from the edges.

TABLE IV

R_F VALUES IN IMPREGNATED TLC PLATES; BENZENE BINDER

A = Plain; B = *p*-benzoquinone; C = trinitrobenzene; D = chloranil; solvent, chloroform–ethanol (4:1). E = *p*-Benzoquinone; F = trinitrobenzene; G = chloranil; H = plain; I = riboflavin; solvent, butanol–acetic acid–water (12:3:5).

	A	*B*	*C*	*D*	*E*	*F*	*G*	*H*	*I*
Caffeine	0.64	0.72	0.67	0.66	0.48	0.58	0.60	0.53	0.50
Uric acid	0.00	0.00	0.00	0.00	0.50	0.00	0.15	0.53	0.00
Adenine	0.24	0.36	0.26	0.35	0.40	0.49	0.53	0.33	0.47
2,6-Diamino-purine	0.14	0.20	0.15	0.00	0.27	0.47	0.49	0.17	0.41
Purine	0.30	0.39	0.32	0.21	0.41	0.51	0.50	0.37	0.00
Uracil	0.26	0.24	0.30	0.35	0.50	0.20	0.54	0.40	0.00
Adenosine	0.00	0.00	0.00	0.00	0.00	0.54	0.11	0.30	0.12
Thymine	0.31	0.34	0.40	0.28	0.58	0.42	0.56	0.50	0.58
Thymidine	0.24	0.21	0.30	0.34	0.40	0.31	0.55	0.44	0.52
Hypoxanthine	0.16	0.15	0.19	0.10	0.46	0.00	0.46	0.31	0.17
Gly					0.12	0.12	0.20	0.19	0.26
Ala					0.15	0.22	0.20	0.21	0.27
Pro					0.11	0.18	0.19	0.20	0.25
Phe					0.22	0.42	0.39	0.15	0.50
Try					0.25	0.52	0.45	0.27	0.56

However, the introduction of new safety rules in the University during the course of these experiments forbade the further use of benzene; the experiments were then continued using methanol.

The next set of experiments to be reported used benzene as a binder. R_F values for a variety of purines, pyrimidines and amino acids are given in Table IV. The corresponding B values are given in Table V.

TABLE V

B VALUES FOR IMPREGNATED TLC PLATES; BENZENE BINDER

Columns as in Table IV.

	B	*C*	*D*	*E*	*F*	*G*	*I*
Caffeine	−13	− 5	− 3	9	− 9	− 13	6
Uric acid	0	0	0	6	100	72	100
Adenine	−50	− 8	− 46	− 21	− 48	− 61	− 47
2,6-Diaminopurine	−43	− 7	100	− 58	−176	−188	−141
Purine	−30	− 6	30	− 11	− 80	− 35	100
Uracil	8	− 5	− 35	− 25	50	− 35	100
Adenosine	0	0	0	100	− 80	63	60
Thymine	−10	−29	10	− 16	16	− 12	− 16
Thymidine	13	−25	− 42	9	29	− 25	− 18
Hypoxanthine	6	−19	38	− 48	100	− 48	45
Gly				37	58	− 5	− 37
Ala				27	− 5	5	− 28
Pro				45	10	5	− 19
Phe				− 46	−180	−160	−233
Try				7	− 93	− 67	−107

Of the purines, 2,6-diaminopurine gives the biggest changes in R_F, *i.e.* the biggest B values. This compound, with its two amino groups, is expected to be the strongest charge donor among this group. However, this is not true for all the acceptors used. Similarly, in general the B values for the acceptors go in the order chloranil > trinitrobenzene > quinone in chloroform–methanol, and in exactly the reverse order in butanol–acetic acid–water. Chloranil forms stronger charge transfer complexes than trinitrobenzene, which in its turn is stronger than quinone[6]. The polarity of the solvent is clearly a determining factor in the interaction. Those purines that do not move during TLC are the very insoluble ones. In these experiments the pyrimidines do exhibit some interaction with the acceptors, thus showing this to be a more sensitive technique.

There is an interesting phenomenon among the amino acids in that the B values for the aromatic amino acids are much greater than those of the aliphatic amino acids for most acceptors, indicating the involvement of the pi-electrons in these interactions. There is no sign of new chemical compounds found with the acceptors, as suggested by Foster[7]. B values take both positive and negative values. Negative values have been explained by Schenk *et al.*[4] as being due to masking of active hydroxyl sites of silica gel by the acceptor. This is not a wholly satisfactory explanation, particularly as it can be easily demonstrated that in many of the systems studied, some of the impregnated acceptor itself moves up the plate with the solvent.

This is particularly noticeable when riboflavin is used, as the distribution of fluorescence after chromatography is changed even with no donor. These negative *B* values can arise by the impregnant actually dragging the donor with it up the plate and hence the largest negative values imply greatest interaction.

Although these experiments point to there being some correlation between charge transfer parameters and changes in R_F, the matter is by no means clear cut. The solvent used and even the binder, as will be subsequently shown, are as important if not more so in determining the interaction. However, one can clearly detect that these are weak interactions rather than strong chemical ones.

In view of the unsatisfactory nature of just mixing the acceptor with the silica gel, another technique has been tried in which roboflavin was covalently bound to silica gel or to cellulose. All these experiments were carried out using methanol as a stationary phase binder.

The results are shown in Table VI with corresponding *B* values in Table VII. The results with cellulose gave in all cases extremely small R_F values, which would suggest that there is very strong binding between these amino acids and riboflavin in this system. In these experiments, unlike the previous, there are no differences between aliphatic and aromatic amino acids indicating that in these systems it is the lone-pair electrons on the amino group of the amino acids which are primarily participating in the interaction. It will seem that in this system the π-electron system of the aromatic amino acids is unable to orient itself favourably with the acceptor. In view of the experimental difficulties of preparing cellulose-bound riboflavin and making good quality plates, it was decided to concentrate on riboflavin-bound silica gel, the results of which are also shown in Tables VI and VII.

TABLE VI

R_F VALUES IN IMPREGNATED PLATES; METHANOL BINDER

A = Plain; B = impregnated riboflavin; C = cellulose; D = riboflavin bound cellulose; E = 5% (w/w) bound riboflavin; F = 0.05% (w/w) bound riboflavin; G = 0.0125% (w/w) bound riboflavin; all with butanol–acetic acid–water (12:3:5) and silica gel, except for C and D.

	A	*B*	*C*	*D*	*E*	*F*	*G*
Phe	0.47	0.53	0.73	0.10	0.35	0.39	
Ile	0.44	0.50	0.80	0.11	0.36	0.35	
Tyr	0.43	0.50	0.54		0.36		
Ser	0.22	0.26	0.22	0.04	0.15	0.15	
Pro	0.22	0.22	0.45	0.04			
Glu	0.29	0.31	0.25	0.02	0.19	0.19	
Asp	0.25	0.27			0.12	0.12	
Ala	0.30	0.30			0.19	0.20	
Trp	0.43				0.33		
Adenosine	0.44				0.45	0.40	0.42
AMP	0.16				0.08	0.08	0.10
ADP	0.05				0	0.03	0.02
ATP	0.02				0	0.02	0
c-AMP	0.20				0.15	0.12	0.17
Cytosine	0.29				0.27	0.26	0.24
Thymine	0.61				0.57	0.51	0.54
Uracil	0.54				0.53	0.47	0.52
Adenine	0.45				0.45	0.38	0.43

TABLE VII

B VALUES FOR TLC PLATES USING METHANOL AS BINDER

Columns as in Table VI.

	B	*D*	*E*	*F*	*G*
Phe	−13	86	26	17	
Ile	−14	86	18	20	
Tyr	−16		16		
Ser	−18	82	32	32	
Pro	0	91			
Glu	− 7	92	35	35	
Asp	− 8		32	52	
Ala	0		37	33	
Trp	0		23		
Adenosine			−2	9	5
AMP			50	50	38
ADP			100	40	60
ATP			100	0	100
cAMP			25	40	15
Cytosine			7	10	17
Thymine			7	16	11
Uracil			2	13	4
Adenine			0	16	4

A novel set of experiments has been to use different ratios of bound silica gel to unbound silica gel, to see whether masking effects can be detected. In fact there are no significant differences between different amounts of acceptor, so that in these systems at least masking does not occur. Furthermore, with bound acceptors there are no negative *B* values, reinforcing the view that negative *B* values arise from the impregnant itself moving through the stationary phase dragging the donor with it.

Among the results shown in Tables VI and VII, are those for a group of nucleotides and nucleic acid bases. Adenosine, uracil, cytosine and adenine show little sign of interaction, unlike AMP, ADP, ATP and cAMP. It can be seen with this group of compounds that the presence of additional phosphate groups lowers the R_F value on plain silica gel according to the number of phosphate groups available. Interestingly cAMP, in which the phosphate group is less available for interaction, has a smaller R_F value than AMP on plain silica gel and also appears to be slightly less inhibited on the riboflavin bound silica gel. From these observations, it can be concluded that the major interaction with the riboflavin occurs through the phosphate group and that therefore there is competition between the riboflavin and silica gel for interaction with phosphate group.

Tsibris *et al.*[12] have suggested that the addition of a phosphate group to the adenosine molecule inhibits complex formation with riboflavin as indicated by fluorescence quenching studies. This is exactly the reverse of what is reported here. We have also carried out some fluorescence quenching experiments on these systems. Stern–Volmer plots are shown in Fig. 2 and dissociation constants therefrom in Table VIII. The values for AMP and adenosine agree with those of Tsibris *et al.*[12]. Those for ATP and cAMP are new. The dissociation constant for cAMP with its less readily available phosphate group is identical with that of the unphosphorylated adenosine

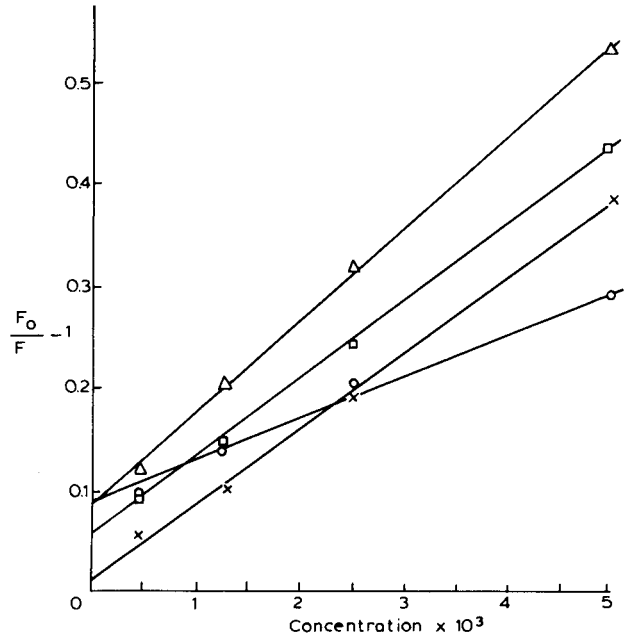

Fig. 2. Stern–Volmer plot showing the quenching of riboflavin fluorescence by adenosine (×), AMP (○), c-AMP (△) and ATP (□) at pH 7, and room temperature. Riboflavin concentration, $5 \cdot 10^{-3}$ *M*.

whereas that for AMP with its free phosphate group is higher and that for ATP lower. Thus there is no correlation between R_F or *B* values and fluorescence quenching, and the suggestion of Tsibris *et al.*[12] appears to be incorrect. The interaction involved in fluorescence quenching is not the same as that involved in TLC with riboflavin.

TABLE VIII

DISSOCIATION CONSTANTS OBTAINED FROM STERN–VOLMER PLOTS FOR THE QUENCHING OF RIBOFLAVIN BY NUCLEIC ACID BASES AND NUCLEOTIDES IN pH 7 PHOSPHATE BUFFER

r is the correlation coefficient in the linear regression analysis for the Stern–Volmer plots.

	Adenosine	*AMP*	*ATP*	*cAMP*
K_{diss} (× 10^3)	13.6	25.6	11.0	13.7
r	0.995	0.998	0.9995	0.999

An alternative form of charge-transfer chromatography is column chromatography using either molecular-sieving gels (Sephadex)[13–17] or silica gel matrices[18]. Thus Porath and Larsson[13] have looked at the chromatography of amino acids on Sephadex gels cross-linked to a variety of electron acceptors and shown that weak interactions including charge transfer occur between the amino acids and the acceptors. Similar results have been found from the chromatography of nucleotides on Sephadex linked to the acceptor acriflavin. In particular, it is shown that the purines

interact more strongly than pyrimidines[14], paralleling our results with TLC. Column chromatography on silica gel mixed with riboflavin has been found to give separation of enantiomeric forms of carbohelicenes by what is presumed to be charge-transfer interaction[18].

These different forms of column chromatography are more complex, expensive and time-consuming than TLC but probably give better resolution. These methods are complementary, in giving similar results, with the TLC method being useful for rapid and inexpensive screening of systems.

In conclusion, weak interactions in biochemical systems can be detected by different forms of "charge-transfer TLC". There is some correlation between parameters associated with charge transfer complexes and B values. Other factors, such as the method of preparation of the plate and solvent polarity, are also important in determining the interaction. The method of covalently binding the acceptor to the stationary phase is, we feel, a better method for these studies than just mixing the acceptor with the silica gel as it guards against migration of the acceptor.

APPENDIX

This is a very brief survey of the IR spectra obtained from evaporates of equimolar solutions.

(A) The purine chloranil evaporates exhibit the following common features:

(1) Shift of C–O stretch of chloranil from *ca.* 1690 to *ca.* 1670 cm^{-1}.

(2) Weakening of C–Cl stretch of chloranil at 725 cm^{-1}.

(3) Decrease of N–H stretching frequencies at 3300 cm^{-1}.

(4) Decrease of N–H deformation at 1610 cm^{-1}.

(5) Decrease of C–N stretching frequencies at 1310 cm^{-1}.

(6) Suppression of C–C (aromatic) stretches at 1580 cm^{-1}.

Purine bromanil evaporates are similar to the above showing features 1,3,6 and in addition,

(7) Weakening of C–Br stretch at 730 cm^{-1}.

Purine quinone evaporates are similar to the above with features 1 and 6, together with decrease of intensity of many stretching frequencies.

(B) Purine trinitrobenzene evaporates exhibit the following common features:

(1) Decrease and shift of C–C (aromatic) stretching frequencies to *ca.* 1540 cm^{-1}.

(2) Shift and decrease in intensities of trinitrobenzene stretches
(i) shift of stretch due to trinitro substitution (aromatic) from 1100 to 1180 cm^{-1};
(ii) shift of symmetric nitro stretches from 1380 to 1340 cm^{-1}.

(C) Purine TCNE spectra obtained from well-ground equimolar mixtures exhibit the following common features:

(1) New slight band at *ca.* 1530 cm^{-1}.

(2) Decrease in C–C (aromatic) stretch frequencies.

(3) Decrease in N–H deformation at 1620 cm^{-1}.

(4) Decrease in C–N stretching frequencies at 1280 and 1350 cm^{-1}.

All the above are consistent with the formation of charge-transfer complexes[19,20].

Evaporates of purine TCNE solutions give off a greenish blue vapour leaving a

bright yellow residue, except for caffeine and uric acid which leave behind a tarry substance. From IR and UV-visible spectroscopy it would appear that the yellow substance contains the 1,1,2,3,3,-pentacyanopropenide anion and the black residue is a tricyanoethanol.

REFERENCES

1 R. G. Harvey and M. Halonen, *J. Chromatogr.*, 25 (1966) 294.
2 A. Berg and J. Lam, *J. Chromatogr.*, 16 (1964) 157.
3 M. Franck-Neumann and P. Jössang, *J. Chromatogr.*, 14 (1964) 280.
4 G. H. Schenk, G. L. Sullivan and P. A. Fryer, *J. Chromatogr.*, 89 (1974) 49.
5 R. S. Mulliken and W. B. Person, *Molecular Complexes*, Wiley Interscience, New York, 1969.
6 R. Foster, *Organic Charge-Transfer Complexes*, Academic Press, London, 1969, p. 121.
7 R. Foster, in R. Foster (Editor), *Molecular Complexes* Vol. 2, Elek Science, London, 1974.
8 M. A. Slifkin, *Charge Transfer Interactions of Biomolecules*, Academic Press, London, 1971.
9 C. Arsenis and D. B. McCormick, *J. Biol. Chem.*, 241 (1966) 330.
10 F. Mikeš, G. Boshart and E. Gil-Av, *J. Chromatogr.*, 122 (1976) 205.
11 B. Pullman and A. Pullman, *Quantum Biochemistry*, Wiley-Interscience, New York, 1963.
12 J. C. M. Tsibris, D. B. McCormick and L. D. Wright, *Biochemistry*, 4 (1965) 2612.
13 J. Porath and B. Larsson, *J. Chromatogr.*, 155 (1978) 47.
14 J.-M. Egly and J. Porath, *J. Chromatogr.*, 168 (1979) 35.
15 J. L. Ochoa, J. Porath, J. Kempf and J.-M. Egly, *J. Chromatogr.*, 188 (1980) 257.
16 M. A. Vijayalakshmi and J. Porath, *J. Chromatogr.*, 177 (1979) 201.
17 J. Porath, *J. Chromatogr.*, 159 (1978) 13.
18 Y. H. Kim, A. Tishbee and E. Gil-Av, *J. Amer. Chem. Soc.*, 102 (1980) 5915.
19 M. A. Slifkin, *Chem. Phys. Lett.*, 7 (1970) 195.
20 M. A. Slifkin and R. H. Walmsley, *Spectrochim. Acta*, 26A (1970) 1237.

Journal of Chromatography, 235 (1982) 401–409
Elsevier Scientific Publishing Company, Amsterdam — Printed in The Netherlands

CHROM. 14,311

SEPARATION OF AMINO ACIDS ON REVERSED-PHASE COLUMNS AS THEIR COPPER(II) COMPLEXES*

ELI GRUSHKA* and SHULAMIT LEVIN
Department of Inorganic and Analytical Chemistry, The Hebrew University, Jerusalem (Israel)
and
C. GILON
Department of Organic Chemistry, The Hebrew University, Jerusalem (Israel)
(First received May 15th, 1981; revised manuscript received September 25th, 1981)

SUMMARY

We report the separation of amino acids on reversed-phase columns using aqueous mobile phases containing copper ions. Cu(II) forms complexes with the amino acids and therefore influences their retention times. More importantly the Cu–amino acid complex absorbs UV radiation with λ_{max} around 230 nm. Thus the solutes can be detected at relatively long wavelengths. The linearity of the detector signal and the detection limits were studied. Ssamples as small as 10 ng per 10 μl can be detected and the useful range of detection is over four orders of magnitude. The effects of the pH of the mobile phase were also studied: retention increases with pH, at least over the range investigated.

INTRODUCTION

The separation of amino acids is of great importance in many research areas. The number of publications dealing with this topic is voluminous. Chromatographic methods of separation have been used extensively for amino acid analysis. Perhaps foremost of all chromatographic techniques is that of ion exchange, coupled with post-column derivatization for detection purposes. In recent years other liquid chromatographic methods, in conjunction with either post- or pre-column derivatization steps with chromophores or fluorophores, have been utilized. Very little work has been reported in which amino acids derivatives have not been formed. For example, Molnár and Horváth[1] have used a reversed-phase system with extremely acidic mobile phases. Hancock *et al.*[2] have also used a reversed-phase system for the separation of amino acids. Schuster[3] has described the separation of these compounds using an amine column in the reversed-phase mode. The purpose of the present work is to describe a method which allows the separation of amino acids, as their Cu(II) complexes, on conventional reversed-phase columns, and a UV detector at *ca.* 230 nm. The amino acids are injected into the mobile phase which contains copper ions. The

* Presented at the *5th International Symposium on Column Liquid Chromatography, Avignon, May 11–15, 1981*. The majority of the papers presented at this symposium has been published in *J. Chromatogr.*, Vol. 218 (1981).

0021-9673/82/0000–0000/$02.75

presence of Cu(II) in the mobile phase affects the retention and facilitates the detection of the solutes.

Spies[4] has discussed the complex formed between an amino acid and Cu(II) and, most significantly, has studied the UV absorbance of such a complex. He found that the maximum of the absorbance is between 230 and 240 nm, depending on the amino acids, with molar absorptivities above 6000 l mol^{-1} cm^{-1}. Thus with a 1-cm absorption cell, micromolar concentrations of amino acids could be detected with conventional high-performance liquic chromatography (HPLC) UV detectors. While not as sensitive as fluoresence detectors, Cu(II)-aided detection can find use in many applications, such as in the synthesis of peptides. It is surprising, therefore, that the use of Cu(II) in amino acid analysis did not draw much attention, either in chromatography, or otherwise. Walton[5] has mentioned in his review on ligand-exchange chromatography that Cu(II), in addition to being the binding site, can be used for the detection of amino acids. Masters and Leyden[6] have described the use of copper-loaded silylated controlled-pore glass for the ligand exchange of amino sugars and amino acids. They have indicated that the presence of Cu(II) in the mobile phase can be utilized for the detection of the solutes analysed. More recently our group has been involved in the separation of amino acid enantiomers using chiral mobile phases in conjunction with reversed-phase columns[7]. The chiral reagent is a Cu(II) complex of L-aspartylalkylamide. We have noted that the presence of Cu(II) is essential not only for the enantiomeric resolution but also for the detection. A similar approach was described by Caude and Foucault[8]. None of the above-mentioned studies has investigated in detail the potential use of Cu(II) for the separation, detection and quantitative determination of amino acids.

It is of interest to mention here that the formation of amino-acid complexes with Cu(II) has been utilized to determine the amounts of amino acids indirectly. Kahn and Van Loon[9], as well as Slavin and Schmidt[10], have used atomic absorption spectrophotometers as LC detector in order to quantitate Cu(II) and hence the amino acids. A different approach was advanced by Loscombe *et al.*[11] who used a copper-selective electrode to detect the presence of amino acid–Cu(II) complex.

We describe here some initial experiments aimed at characterizing the chromatographic behaviour of amino acids in the presence of Cu(II) ions.

EXPERIMENTAL

Apparatus

All chromatographic runs were made with a Spectra-Physics SP8000 unit equipped with a variable-wavelength UV detector. The columns were 250 × 4.1 mm O.D. reversed-phase (ODS Partisil 10). The mobile phase consisted of triply distilled water containing $3 \cdot 10^{-4}$ *M* copper (II) chloride. In the pH study, the pH was controlled with an acetate buffer.

Reagents

All amino acids studied were obtained from Sigma (St. Louis, MO, U.S.A.). The water for the mobile phase and sample preparation was distilled in our laboratory.

Procedure

Chromatographic conditions: the column temperature was maintained at

34°C, except for the pH study (40°C). The flow-rate of the mobile phase was 1 ml/min. The calibration and detection study and the pH study were performed on different reversed-phase columns. Stock solutions of the amino acids were prepared and diluted as needed. Volumes of 10 μl of each sample were introduced onto the column with an injection valve.

Synthesis of a peptide

To study the utility of the method, the peptide TRF was synthesized as follows. pGlu-His-$NHNH_2$ was coupled by the "azide method" to proline amide. The peptide obtained (TRF) was purified on Sephadex G-25 using *n*-butanol–pyridine and 0.1 % acetic acid as eluent. The resulting peptide was desalted by ion-exchange chromatography. Elemental analysis of the peptide (general formula $C_{16}H_{22}O_4N_5$) showed the following composition: C 51.54, H 6.18, N 22.81 %. The calculated values are C 51.74, H 6.24 and N 22.63 %. The specific rotation was $[\alpha]_0^{25} = 63.2$ (C-1, water). The purity of the peptide was checked using a reversed-phase HPLC system[12].

Peptide hydrolysis

TRF (2 mg) was hydrolysed in boiling 6 *N* hydrochloric acid solution (1 ml) in an evacuated sealed tube for 24 h. The sample was desiccated to dryness. Amino acid analysis: Glu:His:Pro:NH_3 = 1:1:1:1.

RESULTS AND DISCUSSION

Cu(II) ions absorb strongly in the UV region below 240 nm. Thus when Cu(II) is added to the mobile phase there is an initial time period when the detector baseline is not stable. Once the system is equilibrated (after about 1 h) the baseline remains steady and the retention times are reproducible. At this point the solutes can be introduced to the column.

The first aim of the study was to establish the retention orders of the amino acids. Table I shows the capacity ratios of 19 amino acids with different functional groups. Of the 21 so-called "common amino acids" only cystine, isoleucine and glutamine are missing from Table I. Their absence is due to the lack of immediate

TABLE I

CAPACITY RATIOS OF SOME AMINO ACIDS

Mobile phase: $3 \cdot 10^{-4}$ *M* Cu(II) in water. Detection: UV at 230 nm.

Amino acids	*k'*	*Amino acids*	*k'*
Asp	0.24	nVl	3.5
Glu	0.29	lys	3.9
Gly	0.88	Met	4.2
Ser	0.97	Dopa	4.7
Asn	1.09	Arg	7.0
Ala	1.12	Leu	7.5
Thr	1.24	Tyr	9.6
His	1.86	Phe	28.0
Val	2.47	Trp	67.0
Pro	2.95		

availability in our laboratory. Table I shows that the acidic amino acids elute first while the basic ones elute with the hydrophobic amino acids.

The amino acids, it should be noted, were injected as received without pre- or post-column derivative formation. The solutes injected formed a complex with the Cu(II) in the mobile phase. The complex when eluted was detected at 230 nm.

The linearity of the detection system as well as the detection limit are, of course, of major importance. Fig. 1 shows typical calibration graphs for some amino acids. Table II gives the slopes of the lines and the correlation coefficients for the least-squares fit. The high values of the correlation coefficients should be noted. The data in Table II are given in the order of elution. The slopes, it is seen, are not only a function of the retention time.

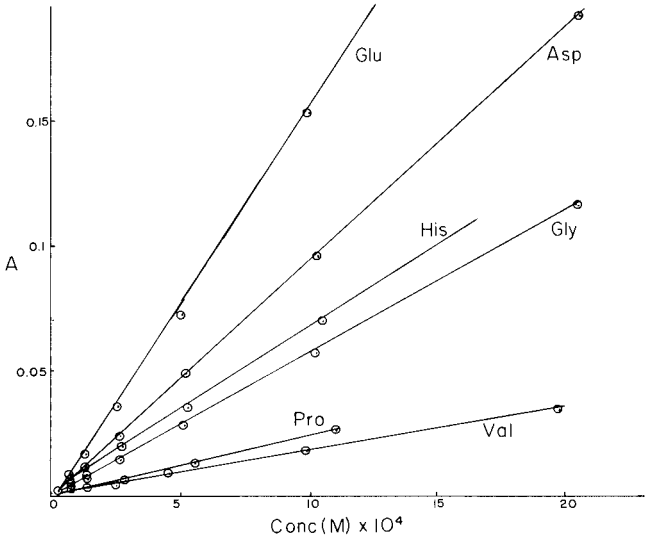

Fig. 1. Typical calibration graphs for amino acids using Cu(II)-aided detection.

TABLE II

SLOPES OF THE CALIBRATION GRAPHS FOR SEVERAL AMINO ACIDS

Amino acid	*Slope*	*Correlation coefficient*	*Response index*
Asp	93.25	0.9999	1.02
Glu	158.85	0.9994	1.10
Gly	56.51	0.9999	1.03
His	61.2	0.998	0.92
Val	17.28	0.9998	0.94
Pro	23.87	0.9999	1.10

The slopes should be related to the molar absorptivities (ε) of the amino acids. These can be obtained using Beer's law and the estimate of the solute concentration at peak maximum as described by Scott[13]:

$$\varepsilon = \frac{SWF}{VC_s b} \tag{1}$$

where S is the slope, W is the peak width (cm), F is the flow-rate (l/min), V is the volume injected (litres) C_s is the chart speed (cm/min) and b is the path length (cm). Table III shows the molar absorptivities of some solutes as calculated from eqn. 1. The variation in ε should be noted. Apparently the retention order does not seem to affect the ε values. Perhaps the different ε are indicative of the nature of the amino acid–Cu(II) complexes; *e.g.* the polar amino acids show higher molar absorptivities. Spies[4] has also found that the absorbance of the complex varies from one amino acid to another. Additional work is now being carried out in our laboratory to explain the differences in ε values. It must be stressed here the the ε values obtained from eqn. 1 are only approximations due to the assumptions made in developing that equation.

TABLE III

ESTIMATES OF MOLAR ABSORPTIVITIES (ε) OF SOME AMINO ACID–Cu COMPLEXES

Amino acid	ε ($l\,mol^{-1}\,cm^{-1}$)
Asp	3172
Glu	4449
Gly	1921
His	3550
Val	1106
Pro	2390

The values of ε reported here are, to the best of our knowledge, the only ones available in the literature for the amino acids concerned. Phan *et al.*[14] have reported molar absorptivities for Cu–arginine complexes. They found that $Cu(Arg)_2$ has a maximum absorbence at 237 nm with $\varepsilon = 7000$ l mol^{-1} cm^{-1}. They calculated that Cu(Arg) should have a maximum absorbence at $\lambda = 232$ nm with $\varepsilon = 3500$ l mol^{-1} cm^{-1}. In the present study the predominating complex is most probably. Cu–amino acid, and indeed we see from Table III that the molar absorptivities are, in general, close to the calculated value mentioned above. At a higher concentration of the amino acids studied here, the possibility of having the complex $Cu(amino\ acid)_2$ exists. The possible effect of such a species will be discussed shortly.

The utility of a method can be checked by its limit of detections and the linearity of the signal. Fig. 1 suggests that the method is linear over three orders of magnitude in the concentration of the amino acids.

To examine more closely the linearity, we employed the following equation, suggested by Scott[13]:

$$y = AC^r \tag{2}$$

where y is the detector signal, A is a constant, C is the concentration and r is the response index of the system. For truly linear detection r should be unity. Table II shows the response indices found in the present study. They vary from 0.92 for His to 1.10 for Glu and Pro. No correlation between the slope or the retention order and r was found. Note that although the response index exceeds the recommended limits of $\pm$ 0.02[13] the calibration graph is still valid as long as r is known.

A possible explanation for the deviation of r from unity might lie in the fact that as the concentration of the amino acids increases more of the tris-complex Cu(amino acid)$_2$ is formed. The concentration of Cu(II) in the mobile phase was $3 \cdot 10^{-4}$ M, while that of the amino acids varied from 10^{-6} to 10^{-3} M. At such low concentrations the predominating species is, very likely, Cu(amino acid). However, at amino acid concentrations of 10^{-3} M the possibility of forming some Cu(amino acid)$_2$ exists. If ε of Cu(amino acid) is different from that of Cu(amino acid)$_2$, then the calibration graph will show a curvature.

The detection limits were found from extrapolating the calibration graphs to signals twice the magnitude of the noise. Table IV gives these limits in units of ng per 10 μl (10 μl being the volume injected) as well as molar concentration. These limits are sufficiently low to make the method attractive in peptide synthesis. An example of how the method can be utilized will now be given.

TABLE IV

DETECTION LIMITS OF SOME AMINO ACIDS

Values in parentheses are molar concentrations.

Amino acid	*Detection limit (ng per 10 µl)*
Asp	6.65 ($5 \cdot 10^{-6}$ M)
Glu	11.8 ($8 \cdot 10^{-6}$ M)
Gly	0.413 ($5.5 \cdot 10^{-6}$ M)
His	3.1 ($2 \cdot 10^{-6}$ M)
Val	9.36 ($8 \cdot 10^{-6}$ M)
Pro	19.6 ($1.7 \cdot 10^{-5}$ M)

The tripeptide TRF was synthesized in our laboratory. Upon hydrolysis TRF yields Pro, His, Glu and NH_3 in a 1:1:1:1 ratio. Fig. 2a shows a chromatogram of a 1:1:1 synthetic mixture of the three amino acids. Fig. 2b shows the chromatogram of the above amino acids plus ammonium chloride. Fig. 2c shows the chromatogram of the hydrolysis products. Quantitation, using peak heights, showed that the ratio of the amino acids in the hydrolysate is indeed 1:1:1. The absolute purity of TRF was difficult to ascertain since the exact weight of the peptide in the sample hydrolysate was not known. It should be pointed out, perhaps, that the analysis was performed using *ca.* 2 mg of crude material.

NH_4^+ in the sample causes a negative deflection of the detector baseline. The complex $Cu(NH_3)_4^{2+}$ does absorb at 230 nm. However, the chromatographic run was carried out with an acidic mobile phase, and the equilibrium concentration of NH_3 is very small. Hence the elution of the NH_4^+ ion is characterized by a negative peak due to the dilution of the Cu(II) in the mobile phase.

Effect of the pH of the mobile phase

Amino acids can be in the form of AH_2^+, AH and A^- depending on the pH of the solution. There is evidence that the nature of the amino acid–Cu(II) complex is also pH dependent[15]. Moreover, the various species AH_2^+, AH and A^- have different retention times[16]. Consequently, it is expected that the pH of the mobile phase, in the present system, will have a large effect on the elution behaviour of the amino acids.

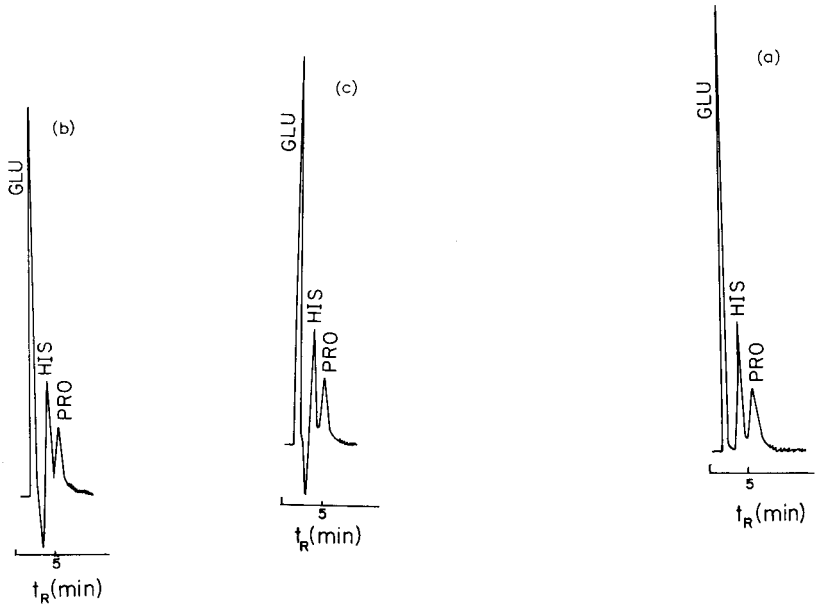

Fig. 2. (a) Chromatogram of synthetic mixtures of Glu, His and Pro. Mobile phase: $3 \cdot 10^{-4}$ M Cu(II) in water. Flow-rate: 1 ml/min. Detection: 230 nm. (b) Chromatogram of synthetic mixture of Glu, NH_4^+, His and Pro. Same conditions as in (a). (c) Chromatogram of the hydrolysis products of the tripeptide TRF. Same conditions as in (a). t_R = Retention time.

Table V shows capacity factors (k') of some amino acids, using mobile phases at different pH values. The trend is clear: lower pH values mean shorter retention times. The trend is more apparent from a plot of k' values *versus* pH. Fig. 3 shows such a plot for several amino acids. In general the change in k' values is higher at the high pH

TABLE V

EFFECT OF pH OF MOBILE PHASE ON THE k' VALUES

Amino acid	*pH*					
	6.7	*6*	*5.6*	*4.6*	*3.7*	*3.3*
Asp	0.46	0.03	0	0	0	0
Glu	0.5	0.054	0.027	0.014	0	0
Gly	0.18	0.07	0	0	0	0
Ala	0.22	0.095	0	0	0	0
His	–	–	–	0.18	0.17	0.15
Val	1.45	1.0	0.77	0.43	0.26	0.15
Pro	1.07	0.67	0.49	0.20	0.12	0.11
Lys	0.91	–	–	0.096	0.12	0.096
Nva	1.6	1	0.76	0.40	0.28	0.14
Met	2.01	1.44	1.14	0.75	0.54	0.48
Leu	4.08	3.06	2.5	1.39	1.07	1.1
DOPA	–	–	1.02	0.88	0.59	0.65
Tyr	–	–	2.17	1.47	1.03	1.18
Arg	1.82	0.95	0.38	0.20	0.12	0.14

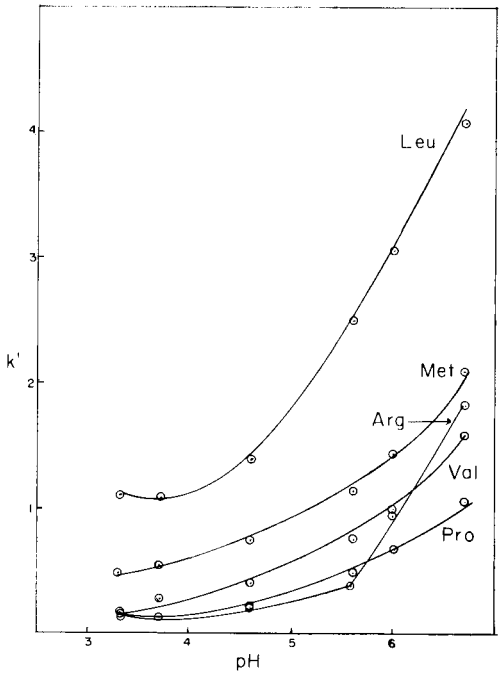

Fig. 3. Dependence of k' of some amino acids on the pH of the mobile phase.

values. This is understood in terms of the higher stability of the amino acid–Cu(II) complex in more basic solutions. The change in k' values is particularly noticeable with the basic amino acids, *e.g.* Arg. For some of the amino acids the capacity ratios are higher at pH 3.3 than at 3.7. We do not know yet whether the increase in k' is real or an artifact of measuring very low numbers. We are currently studying this behaviour.

Mobile phases of relatively high pH are advantageous not only because they retard the amino acids to a greater extent, but also because they allow better detection sensitivities. Initial work in our laboratory shows that the molar absorptivities of the amino acid–Cu(II) complexes are much higher at basic pH values. Thus better detection limits than reported here are feasible.

In summary, it is shown that separation of amino acids on reversed-phase columns is feasible with the aid of Cu ions in the mobile phase. The sensitivities achieved indicate that the approach reported here can find use in many cases such as peptide synthesis. Presently we are studying the effect of the Cu(II) concentration on the separation. In addition we are attempting to obtain the formation constant of the complex, much in the same way as we have done with nucleotides–Mg[17]. The use of metal cations to affect the resolution, to improve detection limits, and to obtain physico-chemical information further demonstrates the great versatility of chromatographic separations. Metal-aided chromatography allows the scientist to employ the full range of chemical reactions to achieve the separation.

REFERENCES

1 I. Molnár and Cs. Horváth, *J. Chromatogr.*, 142 (1977) 623.
2 W. S. Hancock, C. A. Bishop and M. T. W. Hearn, *Anal. Biochem.* 92 (1979) 170.
3 R. Schuster, *Anal. Chem.*, 52 (1980) 617.
4 J. R. Spies, *J. Biol. Chem.*, 195 (1952) 65.
5 H. F. Walton, *Separ. Purif. Methods*, 4 (1975) 189.
6 R. G. Masters and D. E. Leyden, *Anal. Chim. Acta*, 98 (1978) 9.
7 C. Gilon, R. Leshem and E. Grushka, *Anal. Chem.*, 52 (1980) 1206.
8 M. Caude and A. Foucault, *Anal. Chem.*, 51 (1979) 459.
9 N. Kahn and J. C. van Loon, *J. Liquid Chromatogr.*, 2 (1979) 23.
10 W. Slavin and G. J. Schmidt, *J. Chromatogr. Sci.*, 17 (1979) 610.
11 C. R. Loscombe, G. B. Cox and J. A. W. Dalziel, *J. Chromatogr.*, 166 (1978) 403.
12 R. Burgens and J. Rivier in A. Loffett (Editor), *Peptides 1976*, University of Brussels, Brussels, 1976, p. 85.
13 R. P. W. Scott, *Liquid Chromatography Detectors*, Elsevier, Amsterdam, 1977.
14 C. V. Phan, L. Tosi and A. Gardnier, *J. Inorg. Nucl. Chem.*, 37 (1975) 2385.
15 M. Itabashi and K. Itoh, *Bull. Chem. Soc. Jap.*, 53 (1980) 3131.
16 Cs. Horvath, W. Melander and I. Molnar, *Anal. Chem.*, 49 (1977) 142.
17 E. Grushka and F. K. Chow, *J. Chromatogr.*, 199 (1980) 283.

Journal of Chromatography, 235 (1982) 411–416
Elsevier Scientific Publishing Company, Amsterdam — Printed in The Netherlands

CHROM. 14,353

HIGH-PERFORMANCE THIN-LAYER CHROMATOGRAPHY OF 2,4-DINITROPHENYL-AMINO ACIDS ON LAYERS OF RP-8, RP-18 AND AMMONIUM TUNGSTOPHOSPHATE

LUCIANO LEPRI*, PIER GIORGIO DESIDERI and DANIELA HEIMLER
Institute of Analytical Chemistry of the University of Florence, Florence (Italy)
(Received September 12th, 1981)

SUMMARY

The chromatographic characteristics of eighteen DNP-amino acids, of dinitrophenol and dinitroaniline were studied on RP-8 and RP-18 plates eluted with aqueous–organic solutions and with mixtures of organic solvents. The optimum conditions for the separation of the highest number of compounds were studied and a two-dimensional chromatogram is reported. On home-made layers of ammonium tungstophosphate, water, aqueous solutions of ammonium nitrate and nitric acid and water–methanol mixtures were used as eluents to separate the pairs of DNP-amino acids which exhibit the same chromatographic behaviour on RP-8 and RP-18 plates.

INTRODUCTION

In the separation of 2,4-dinitrophenyl (DNP)-amino acids, chromatographic techniques have extensively been employed[1] for the identification of N-terminal amino acids and, therefore, for the determination of protein and peptide structure. Thin-layer chromatography of DNP-amino acids has been carried out on layers of cellulose[2,3], polyamide[4–6], silica gel[7,8] and wool cortical cells[9]. Recently, plates of silanized silica gel alone or impregnated with anionic and cationic detergents, and also layers of ammonium tungstophosphate, were successfully used in the separation of amino acids[10,11], peptides[12,13] and aromatic amines[14]. It was therefore of interest to investigate the behaviour of DNP-amino acids and to complete the studies carried out by the other researchers.

On layers of silanized silica gel, the two-dimensional technique can be used, eluting in the two directions with aqueous and non-aqueous mobile phases, so that the adsorption properties of the layer are changed and better separations can be achieved[15]. Besides water-soluble and ether-soluble DNP-amino acids, we examined also 2,4-dinitrophenol and 2,4-dinitroaniline, which are formed by photolysis or in the dinitrophenylation of the N-terminal amino acids.

0021-9673/82/0000–0000/$02.75

EXPERIMENTAL

Standard solutions were prepared by dissolving the DNP-amino acids (Serva, Heidelberg, G.F.R.) in water–methanol (1:2). The sample volume used was 0.2–0.3 μl in the case of RP-8 and RP-18 plates (E. Merck, Darmstadt, G.F.R.) and 0.5 μl for the ammonium tungstophosphate layers. The compounds were visualized by exposure of the silanized silica gel layers to UV light (360 nm with dried plates or 254 nm with wett ones). On ammonium tungstophosphate the spots were identified by their yellow colour which deepens on exposure to ammonia vapours. The preparation of the last layers was carried out as described previously[14].

The migration distance was 6 cm in the case of RP-8 and RP-18 plates and 10 cm in the case of ammonium tungstophosphate, unless otherwise stated. All the measurements were carried out at 25°C using a Desaga thermostatic chamber.

The following abbreviations are used: DNP = dinitrophenyl; Gly = glycine; Ala = alanine; Ser = serine; Thr = threonine; Val = valine; Leu = leucine; Ile = isoleucine; Pro = proline; Met-O_2 = methionine sulphone; Trp = tryptophan; Phe = phenylalanine; Tyr = tyrosine; Asp = aspartic acid; Glu = glutamic acid; $CuSO_3Na$ = sodium cysteate; Lys = lysine; Arg = arginine; His = histidine; DNP-OH = dinitrophenol; DNP-NH_2 = dinitroaniline.

RESULTS AND DISCUSSION

Silanized silica gel layers (RP-8 and RP-18)

Table I lists the chromatographic characteristics of eighteen DNP-amino acids, dinitrophenol and dinitroaniline on RP-8 and RP-18 plates eluted with 1 *M* acetic acid in 60% methanol. The elution time in both cases is 90 min. Similar results are obtained on the two layers; in the case of RP-18 plates, however, more compact spots and a better resolution of the compounds are achieved. Subsequent experiments were therefore performed on RP-18 layers.

Since the DNP-amino acids contain a very weak[19] basic group, the use of more acidic eluents than those of column 2 (such as 1 *M* acetic acid + 1 *M* hydrochloric acid in 60% methanol) does not result in large differences in the chromatographic behaviour of most compounds, since the species in solution remain practically the same. In contrast, an increase of the apparent pH of the eluent, involving the deprotonation of the carboxyl group, results in different retentions of the compounds, with the exception of dinitroaniline.

The most remarkable differences in the chromatographic behaviour of the DNP-amino acids with respect to the acid medium are observed for elution with 1 *M* ammonia in 60% methanol. Under such conditions most compounds run with the solvent front or are less strongly retained than with acidic solutions owing to the presence in their molecules of one or more negative charges. The only exception is α-N-DNP-Arg, which is more strongly retained than in acidic solution and, as the behaviour of DNP-NH_2 shows, also with decreasing percentage of the organic solvent in the eluent, owing to the replacement of acetic acid with ammonia. With the alkaline eluent, the elution time increases from 90 to 100 min.

The chromatographic behaviour of the DNP-amino acids on RP-18 plates eluted with aqueous–organic solutions seems to be controlled by a reversed-phase

partition mechanism since their affinity towards the stationary phase decreases the higher is the polarity of the compound (see the R_F sequence of the series Ser, Thr, Gly, Ala, Val, Leu). The lower retention of a given compound having positive or negative charges compared to the neutral form supports this assumption.

The influence of the ionic strength on the chromatographic characteristics of the DNP-amino acids is shown by the data of columns 4 and 5; these data were obtained by adding 3% potassium chloride to the eluents of columns 2 and 3. The presence of this salt in the eluent does not result in large differences in R_F values in acidic media, where the compounds are predominantly in the non-ionic form. In alkaline solution, a remarkable increase of the affinity towards the stationary phase for most DNP-amino acids and, particularly, for those with more marked hydrophobic characteristics, is observed. This can probably be ascribed to increasing hydrophobic interactions between the compounds having a negative charge and the stationary phase, and is similar to the behaviour of phenols on layers of silanized silica gel (C_2) alone or impregnated with anionic detergents[16], and on layers of Dowex 40-X4 (Na^+)[17].

The dependence of the R_F values of DNP-amino acids on the ionic strength of the eluent in alkaline media can be used to obtain or to improve separations among the different compounds. The importance of this ionic strength effect had already been pointed out by us[18] in the separations of polypeptides on RP-2 plates.

With non-aqueous eluents, such as hexane–ethyl acetate–acetic acid (see columns 6 and 7 of Table I), interesting results are achieved, since the elution time decreases to 15 min and the affinity sequence of the DNP-amino acids is completely different from that observed with aqueous–organic eluents. The content of acetic acid is the same (2%) in both eluents employed and accounts for the compact spots observed. As the percentage of the non-polar compound, hexane is increased the R_F values is generally decreased without a change in the affinity sequence of the DNP-amino acids.

With both eluents, the compounds with marked polar characteristics, such as DNP-$CySO_3Na$ and α-N-DNP-Arg, remain at the application point, while those with marked hydrophobic characteristics, such as DNP-OH, DNP-Leu and DNP-Ile, run practically with the solvent front. Furthermore, the sequence of R_F values for members of homologous series (*e.g.*, Ser, Thr, Gly, Ala, Val and Leu) is opposite to that found with aqueous–organic eluents.

In order to explain the behaviour of DNP-amino acids in non-aqueous solvents we can assume that the free –OH groups of the silanized silica gel participate in an adsorption mechanism involving a stationary phase with polar characteristics[15]. Even the different solubilities of the DNP-amino acids in the mobile phase may affect the retention of those compounds such as $CySO_3Na$ and α-N-DNP-Arg, which are soluble only in polar solvents and which remain at the starting point when eluting with non-aqueous solutions containing high percentages of non-polar hydrocarbons.

Since the separation of all or most of the DNP-amino acids cannot be achieved with only one elution, either with aqueous–organic or non-aqueous eluents, we used the two-dimensional technique. The data of Table I show that the optimum conditions for the separation of the highest number of compounds can be achieved by eluting in the first direction with hexane–ethyl acetate–acetic acid (80:18:2) (see column 7) and in the second direction with 1 *M* ammonia + 3% potassium chloride in 60% methanol (see column 4).

TABLE I

R_F VALUES OF DNP-AMINO ACIDS ON RP-8 AND RP-18 PLATES WITH DIFERENT ELUENTS

Compound	*1 M Acetic acid in 60% methanol*		*1 M NH_3 in 60% methanol RP-18*	*3% KCl + 1 M acetic acid in 60% methanol RP-18*	*3% KCl + 1 M NH_3 in 60% methanol RP-18*	*Hexane–ethyl acetate–acetic acid (75:23:2) RP-18*	*Hexane–ethyl acetate–acetic acid (80:18:2) RP-18*
	RP-8	*RP-18*					
1 DNP-Gly	0.62	0.57	0.86	0.58	0.68	0.71	0.56
2 DNP-Ala	0.49	0.43	0.85	0.47	0.60	0.86	0.73
3 DNP-Ser	0.74	0.70	0.89	0.71	0.78	0.37	0.25
4 DNP-Thr	0.64	0.62	0.87	0.63	0.69	0.48	0.35
5 DNP-Val	0.32	0.27	0.78	0.27	0.40	0.96	0.87
6 DNP-Leu	0.22	0.17	0.68	0.18	0.26	0.99	0.94
7 DNP-Ile	0.22	0.17	0.69	0.19	0.27	0.99	0.94
8 DNP-Pro	0.52	0.53	0.87	0.52	0.62	0.83	0.72
9 DNP-Met-O_2	0.74	0.69	0.91	0.72	0.79	0.15	0.08
10 DNP-Trp	0.33	0.30	0.83	0.30	0.43	0.85	0.71
11 DNP-Phe	0.27	0.22	0.72	0.22	0.32	0.92	0.86
12 Di-DNP-Tyr	0.16	0.10	0.48	0.10	0.12	0.66	0.51
13 DNP-Asp	0.70	0.68	0.91	0.71	0.88	0.41	0.29
14 DNP-Glu	0.65	0.62	0.91	0.64	0.88	0.49	0.36
15 DNP-CySO_3Na	0.94	0.91	0.92	0.85	0.93	0.00	0.00
16 Di-DNP-Lys	0.24	0.18	0.64	0.20	0.26	0.57	0.38
17 α-N-DNP-Arg	0.70	0.68	0.59	0.80	0.71	0.00	0.00
18 Di-DNP-His	0.48	0.43	0.85	0.35	0.54	0.00	0.00
19 DNP-OH	0.53	0.51	0.91	0.52	0.75	0.99	0.96
20 DNP-NH_2	0.48	0.48	0.35	0.51	0.41	0.92	0.75

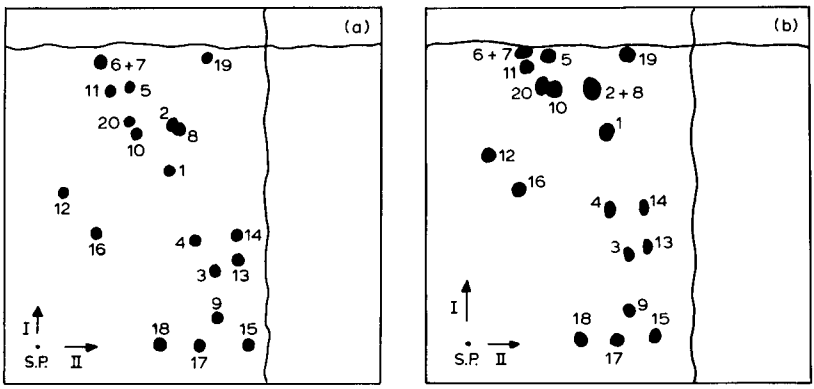

Fig. 1. Theoretical (a) and experimental (b) two-dimensional chromatograms on RP-18 plates. Eluents: in the first direction, hexane–ethyl acetate–acetic acid (80:18:2); in the second direction, 1 *M* ammonia + 3% potassium chloride in 60% methanol. DNP-amino acids as in Table I. S.P. = Starting point.

Fig. 1a indicates the theoretical separation and Fig. 1b shows the experimental one obtained with a mixture of all twenty compounds. This separation is on the whole better than those previously reported[2–9].

Ammonium tungstophosphate (AWP) layers

The data obtained on layers of AWP–$CaSO_4 \cdot \frac{1}{2}H_2O$ (0.5:2, 2:2, 4:2 and 8:2) eluted with aqueous and aqueous–organic solutions showed that, as in the case of amino acids[11] and primary aromatic amines[12,13], the DNP-amino acids are more strongly retained with increasing concentration of AWP on the layer. Compact spots, however, are observed only with AWP–$CaSO_4 \cdot \frac{1}{2}H_2O$ (4:2 and 8:2).

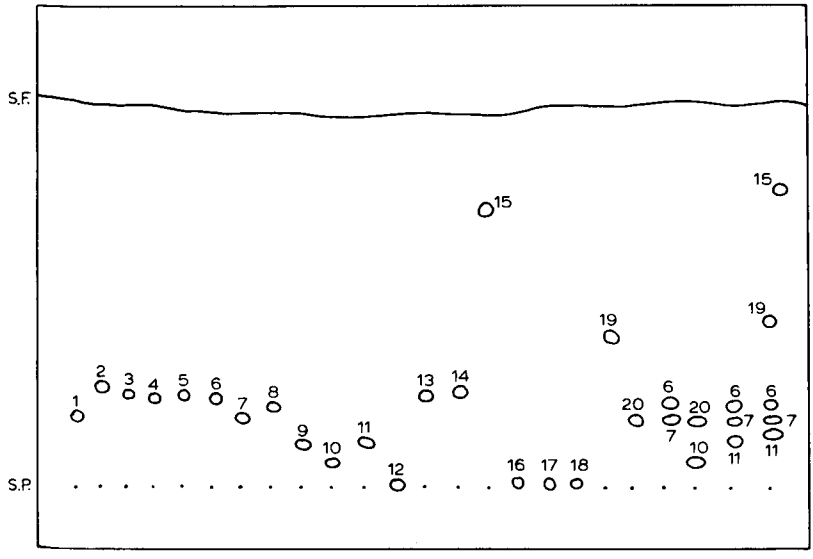

Fig. 2. Thin-layer chromatogram on AWP–$CaSO_4 \cdot \frac{1}{2}H_2O$ (4:2). Eluent: water–methanol (80:20). Elution time; 150 min. DNP-amino acids as in Table I. S.P. = Starting point; S.F. = solvent front.

Fig. 2 shows the chromatogram obtained on AWP–$CaSO_4 \cdot \frac{1}{2}H_2O$ (4:2) eluted with water–methanol (80:20 v/v). On replacing this eluent with water, solutions of ammonium nitrate and nitric acid, the sequence of the DNP-amino acids does not change. The compounds are strongly retained with the above eluents, with the exception of DNP-$CySO_3Na$ which is weakly retained when eluting with water or with water–methanol (80:20), whereas it exhibits a higher affinity towards the stationary phase in the presence of nitric acid or ammonium nitrate (*e.g.*, 1 *M*). The solubility of the compounds affects their chromatographic behavior; all three di-DNP-amino acids remain at the starting point when eluting with water and with water–methanol (80:20), owing to their low solubility.

Fig. 2 also shows some separations which are important from an analytical point of view, such as those concerning pairs of DNP-amino acids which are difficult to separate (Ala/Pro and Leu/Phe) or exhibit the same chromatographic behaviour on RP-18 plates under all experimental conditions (Leu/Ile).

REFERENCES

1 J. Rosmus and Z. Deyl, *J. Chromatogr.*, 70 (1972) 221.
2 R. L. Munier and G. Sarrazin, *Bull. Soc. Chim. Fr.*, (1965) 2959.
3 R. C. Munier and G. Sarrazin, *J. Chromatogr.*, 22 (1966) 347.
4 K.-T. Wang, J. M. K. Huang and I. S. Y. Wang, *J. Chromatogr.*, 22 (1966) 362.
5 K.-T. Wang, J. M. K. Huang and I. S. Y. Wang, *J. Chromatogr.*, 22 (1966) 362.
5 K.-T. Wang and I. S. Y. Wang, *J. Chromatogr.*, 24 (1966) 460.
6 K.-T. Wang and I. S. Y. Wang, *J. Chromatogr.*, 27 (1967) 318.
7 D. Wolz, A. R. Fahmy, G. Pataki, A. Niederwieser and H. Brenner, *Experientia*, 19 (1963) 213.
8 M. Brenner, A. Niederwieser and G. Pataki, in E. Stahl (Editor), *Dünnschicht Chromatographie*, Springer, Berlin, 2nd ed., 1967, p. 696.
9 P. R. Brady and R. M. Hoskinson, *J. Chromatogr.*, 54 (1971) 65.
10 L. Lepri, P. G. Desideri and D. Heimler, *J. Chromatogr.*, 195 (1980) 65.
11 L. Lepri, P. G. Desideri and D. Heimler, *Ann. Chim. (Rome)*, 71 (1981) 89.
12 L. Lepri, P. G. Desideri and D. Heimler, *J. Chromatogr.*, 195 (1980) 187.
13 L. Lepri, P. G. Desideri and D. Heimler, *J. Chromatogr.*, 207 (1981) 412.
14 L. Lepri, P. G. Desideri and D. Heimler, *J. Chromatogr.*, 207 (1981) 29.
15 K. Macek, Z. Deyl and M. Smrž, *J. Chromatogr.*, 193 (1980) 421.
16 L. Lepri, P. G. Desideri and D. Heimler, *J. Chromatogr.*, 195 (1980) 339.
17 L. Lepri, P. G. Desideri, M. Landini and G. Tanturli, *J. Chromatogr.*, 109 (1975) 365.
18 L. Lepri, P. G. Desideri and D. Heimler, *J. Chromatogr.*, 211 (1981) 29.

Journal of Chromatography, 235 (1982) 417–426
Elsevier Scientific Publishing Company, Amsterdam — Printed in The Netherlands

CHROM. 14,330

AMINO ACID ANALYSIS USING STANDARD HIGH-PERFORMANCE LIQUID CHROMATOGRAPHY EQUIPMENT

GRAHAM J. HUGHES* and KASPAR H. WINTERHALTER
Laboratorium für Biochemie der Eidgenössischen Technischen Hochschule, ETH-Zürich, CH-8092 Zürich (Switzerland)
and
ERNST BOLLER and KENNETH J. WILSON
Biochemisches Institut der Universität Zürich, CH-8028 Zürich (Switzerland)
(Received July 21st, 1981)

SUMMARY

The components normally employed for high-performance liquid chromatography, with the addition of an interface, have been used to construct an amino acid analyser. Detection was effected with either ninhydrin or *o*-phthalaldehyde. The separation of amino acids normally found in protein hydrolysates was performed within 45 min. Reproducibility of the time for peak elution enabled peak-height or -area measurements to be used for quantitation in the range 10 pmol to 25 nmol. The compositions of the buffers that achieve these fast analysis times and permit quantitation at the low pmol level using *o*-phthalaldehyde detection are given.

INTRODUCTION

In any study of the primary structure of proteins the most frequently required analysis is that of amino acids. The successful application of high-performance liquid chromatography (HPLC) techniques to this analysis has been demonstrated by the performance of modern amino acid analysers such as the Durrum D-500. To date, HPLC of amino acids or derivatives thereof has been performed on either sulphonated polystyrene or silica-based supports[1,2].

Commercially available instruments basically utilize the method of analysis originally described by Spackman *et al.*[3]. Essentially, amino acids are separated by cation exchange on cross-linked sulphonated polystyrene using citrate buffers, and detection is effected by post-column derivatization utilising ninhydrin[4] or the more recently introduced fluorogenic reagent *o*-phthalaldehyde (OPA)[5]. The use of a "micro-bead" resin with a uniform diameter of about 10 μm or less, improved buffer composition and high-pressure chromatographic techniques have led to a decrease in the analysis time from the original 24 h to approximately 1 h. Moreover, a 100-fold increase in sensitivity makes it possible to analyse samples containing less than 1 nmol of each amino acid, utilising ninhydrin. This is a consequence of the use of microbore

0021-9673/82/0000–0000/$02.75

columns and improved spectrophotometer design. Analysis at the level of a few picomoles is possible when OPA is used[6].

Silica-based chromatographic supports are less compressible than polystyrene and therefore flow-rates can be increased, allowing, in some instances, a shorter analysis time. Numerous reports on the HPLC of a variety of amino acid derivatives have appeared, *e.g.*, PTH-[7,8], DABTH-[9] and dansyl-[10,11]. The derivatization step, however, is tedious if numerous samples have to be processed and may introduce errors. Separation of all the free amino acids found in normal protein hydrolysates within 30 min has been achieved by normal-phase chromatography on NH_2-silica[1]. Detection is effected by absorption at 200 nm. Interference with the analysis by contaminants should always be considered, especially at high sensitivity. Reversed-phase ion-pair chromatography of amino acids, utilizing OPA post-column derivatization, has been reported[2]; however, Glu and Gly are not separated and Thr is poorly resolved from the latter. The speed of analysis (30 min) combined with the sensitivity of OPA detection make this a promising alternative to analysis on polystyrene supports.

We describe here how an HPLC apparatus normally employed for peptide or protein separation[12–15] can be used for amino acid analysis. The reproducibility, speed of analysis and sensitivity are equal to or better than those of most commercially purpose-built analysers.

EXPERIMENTAL

Buffers and reagents

Unless stated otherwise, the chemicals used were of the best available grade from either Merck (Darmstadt, G.F.R.) or Fluka (Buchs, Switzerland). The cation-exchange resins used were DC-4A, DC-6A (Durrum, Sunnyvale, CA, U.S.A.) and Aminex A-9 (BioRad Labs, Richmond, CA, U.S.A.). Stainless-steel columns (250 × 4.6 or 3.2 mm I.D.) were slurry packed (reservoir volume, 10 ml) in buffer C, at 70°C, with a flow-rate of 2 ml/min (4.6 min I.D. column) or 1 ml/min (3.2 mm I.D. column).

The compositions (per litre) of the buffers used for detection with OPA were as follows:

Buffer A 0.2 *N* Na^+; pH 3.25: 3 g of NaOH, 8.9 g of Na_2SO_4, *ca.* 8.2 ml of formic acid, 10 ml of 1-propanol.

Buffer B (0.2 *N* Na^+; pH 4.25); 8 g of NaOH, *ca.* 10 ml of formic acid.

Buffer C (1.1 *N* Na^+; pH 7.9) 28 g NaOH, 40 g of trisodium citrate, *ca.* 26.4 ml of formic acid.

Sample application buffer: 14.2 g of Na_2SO_4, 20 ml of formic acid.

Detection buffer (pH 10.3): 43 g of KOH, 62 g of boric acid, 1 ml of 2-mercaptoethanol, 2 ml of 30% (w/w) Brij (Pierce, Rockford, IL, U.S.A.), 200 mg of OPA (in 2 ml of methanol).

Formic acid was distilled from ninhydrin. Ammonia contamination in buffers A and B can be reduced by filtration through DC-3A resin (Na^+ form) (Durrum, Palo Alto, CA, U.S.A.). The detection buffer was stored in amber-glass bottles under nitrogen.

When ninhydrin detection was utilized, the buffers for column elution were Pico buffer systems II A, B and C (Pierce, Rotterdam, The Netherlands) and in later work Hi-Phi eluents Na-A, B and C (Dionex, Sunnyvale, CA, U.S.A.). The solution

for ninhydrin detection was prepared as follows: 20 g of ninhydrin and 2 g of hydrindantin (Pierce) were dissolved in 750 ml of dimethylsulphoxide (Merck), 250 ml of 4 *M* sodium acetate pHix-buffer (Pierce) was added and the solution was kept under nitrogen.

For both detection systems, sodium hydroxide (0.2 *N*) was used for column regeneration.

Apparatus

The system used for OPA detection is shown in Fig. 1. Buffers A, B and C and 0.2 *N* sodium hydroxide solution were connected to a Model 110A buffer pump (Altex, Berkeley, CA, U.S.A.) via an eight-port motorized valve (Kontron, Zürich, Switzerland). For analysis of peptide hydrolysates, buffers A, B and C and regeneration were connected to positions 1, 2, 3 and 4 respectively. Sample application was effected via a Kontron Model 100 automatic sample injector fitted with a 100-μl loop. The column was fixed in a stainless-steel water-jacket and the temperature was controlled via a Haake Proportional water-bath (Haake, Karlsruhe, G.F.R.). A pressure gauge (0–4000 p.s.i.) was connected via a Swagelok $\frac{1}{16}$-in. T-piece between the sample injector and the buffer pump. Detection solution was pumped (Altex Model 110A) and mixed with the eluate from the column via a Swagelok $\frac{1}{16}$-in. T-piece. For OPA

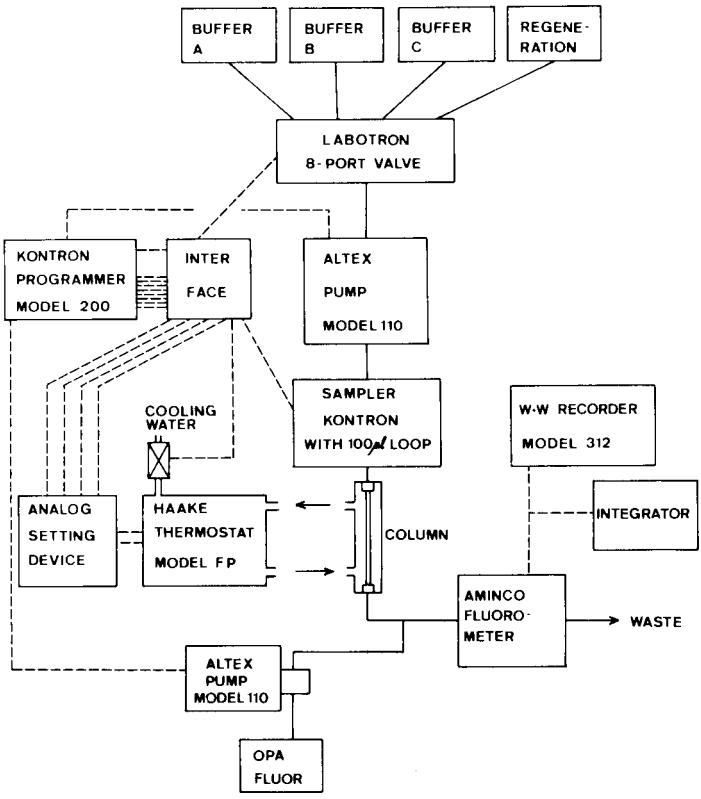

Fig. 1. Apparatus for amino acid analysis.

the reactants were mixed in 3 m of PTFE tubing (0.3 mm I.D.) and detection was carried out with an Aminco Fluoro Monitor (American Instrument Co., Silverspring, MD, U.S.A.) set at the least sensitive range, and equipped with a 70-μl flow cell; filters were as supplied for fluram detection. For detection with ninhydrin, the solutions were mixed through 10 m of PTFE tubing (0.3 mm I.D.) maintained at 120°C by submersion in a Haake Model SK58 oil-bath, and absorption at 440 and 570 nm was measured with a Kontron spectrophotometer.

Located after the derivatization pump and connected in series were a stainless-steel column (250 × 4.6 mm I.D.) containing a 10-cm high bed of DC-6A (to reduce pulsation noise), 2 m of PTFE tubing (0.3 mm I.D.) and a pressure gauge (0-200 p.s.i.). PTFE back-pressure coils 3 m × 0.3 mm I.D.) were connected to the outlet of each detector. Chromatograms were plotted by a two-channel recorder (W + W Model 312, Kontron) and integrated by a Supergrator 3 (Columbia Scientific Industries, Austin, TX, U.S.A.).

A microprocessor (Altex Model 420, modified for eight external flags, or a Kontron Model 200, normally employed to control the flow-rate of two pumps for grandient elution) was used to control all functions of the analyser. The buffer pump was controlled as A and the derivatizing pump as B. Flow-rates were as follws: 3.2 mm I.D. column, column eluant and OPA solution 0.4 ml/min, ninhydrin 0.2 ml/min; 4.6 mm column, column eluent and OPA solution 0.62 ml/min, ninhydrin 0.32 ml/min. The recorder chart speed could be controlled by the microprocessor. Flag 7 controls the buffer selection; one contact closure (duration 0.01 min) caused the valve to rotate by one port. Flag 8 (duration 0.05 min), activated after column regeneration, returned the buffer valve to the start position (buffer A). The sample injector and integrator were started by a contact closure, duration 10 sec, of flag 5. Five flags were used for temperature control of the column. Flags 1–4, by switchin a 10-turn potentiometer in series with the programming input of the Haake thermostat, enabled up to four temperatures to be used. Rapid cooling was achieved by circulation, via a magnetic valve (controlled by flag 6), of mains water through a coil in the Haake bath. Details of the interface between microprocessor and rotary valve are given in Fig. 2.

RESULTS AND DISCUSSION

HPLC is useful for the analysis and preparative isolation of peptides and proteins[12–17]. An apparatus of this kind, which can be used for both isolation and amino acid analysis, has the advantages of lower cost than analysers built for exclusive use in amino acid analysis and of greater versatility. This, in turn, allows more readily the most effective use of equipment.

The equipment commonly employed for HPLC (Altex or Kontron) consists of a microprocessor which controls the flow-rates of two pumps; gradient elution from two solvents is achieved by adjustment of these rates. Detection of peptides is carried out either by post-column derivatization, via a sampling valve, with the fluorogenic reagents fluorescamine[12,13,18] or OPA[13,19], or directly by absorption in the UV region[14,15,20]. We have used these elements, with a small number of additions, to construct an amino acid analyser.

In Fig. 3A the elution profile of standard mixture of amino acids using ninhyd-

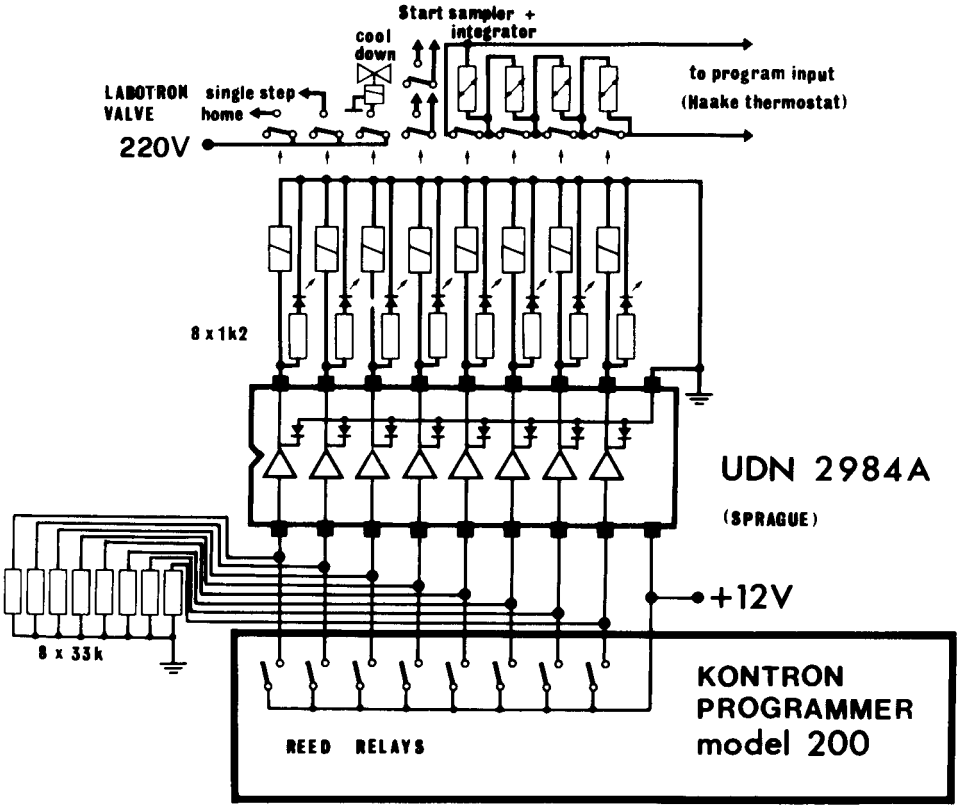

Fig. 2. Circuit diagram for the interface between the microprocessor and the rotary valve. The cost of the components was approximately half that of a standard analytical HPLC column, and the time for construction was 12 h. k = kΩ.

rin is shown. DC-4A resin packed in a stainless-steel column (250 × 4.6 mm I.D.) was eluted with the Pico system II buffers. Stainless-steel columns permit the use of higher pressure than the more commonly used glass columns and thus higher flow-rates are possible. The analysis time, including regeneration and equilibration, for a standard hydrolysate (not including tryptophan) is 60 min, the buffer is pumped at a flow-rate of 0.62 ml/min and the back-pressure is 1500–2500 p.s.i. Similar chromatograms were obtained using DC-6A resin, but, Thr and Ser were not as well resolved. Aminex A9 resin gave unsatisfactory resolution under these conditions. Commercially available buffers were used for elution because of convenience and their constant chemical composition. Initial work was carried out with Pico system II buffers, and although the elution times remained fairly constant, recent stocks of buffer A produced an increase of the ammonia plateau, equivalent to approximately 5 nmol of amino acid. The contamination may be largely removed by filtration through Dowex 50 (Na^+). Hi-Phi eluent buffers give equivalent resolution under the same conditions, with no appreciable interference with the baseline, but the analysis time is 6 min longer than with Pico buffers.

Reproducibility of the chromatography is evident from a comparison of stan-

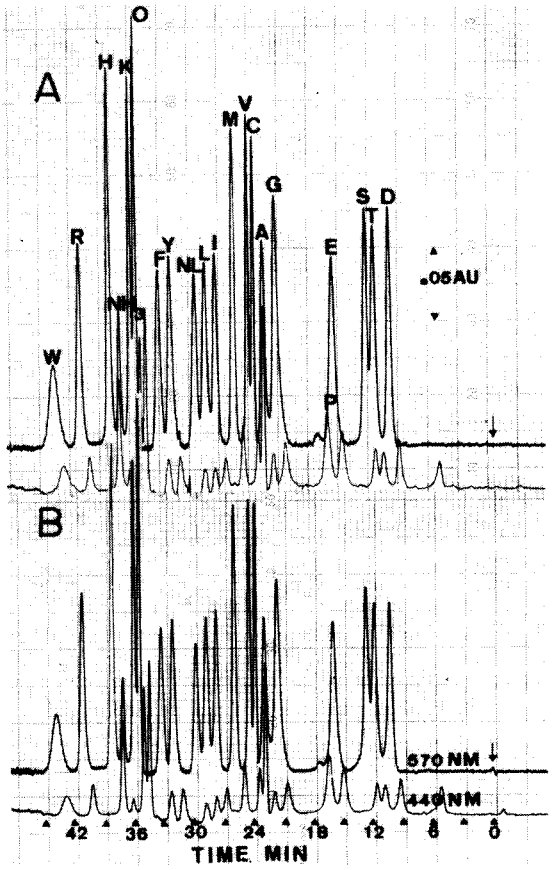

Fig. 3. Chromatograms of a standard mixture of amino acids (10 nmol) using ninhydrin for detection. B was obtained 50 analyses after A. The column (250 × 4.6 mm I.D.) of DC-4A was eluted with Pico system II buffers A, B and C for 17, 15 and 14 min, respectively. Buffers A and C contain 1 and 5% of propan-1-ol, respectively. The equilibration temperature was 40°C and changes to 60, 69 and 75°C were at 6, 28 and 32 min, respectively. Regeneration and re-equilibration were for 6 and 18 min, respectively. Mains water cooling for 6 min was initiated immediately after regeneration. The column back-pressure was 2200 p.s.i. at 40°C and 1500 p.s.i. at 75°C. Abbreviations are standard one-letter codes with the exceptions of NL = norleucine and O = ornithine.

dard runs, 50 analyses apart, shown in Fig. 3A and B. The time of elution for each amino acid is constant to within 20 sec and the peak width is constant. To achieve this reproducible separation, ammonia filtration columns and other sources of large dead volumes must be excluded. A gradual accumulation of air from the buffers in such devices causes alteration of the dead volume, which consequently produces a difference in eluent composition at any buffer change. A constant time of peak elution has two advantages: (1) interpretation of an analysis in which only one or few amino acids are present is easier; (2) peak heights can be used for quantitation.

The use of ninhydrin for detection limits the sensitivity to the high picomole level. When a higher sensitivity is required, fluorescence detection using OPA is available. Below the 1 nmol level, impurities present in commercial buffers make the

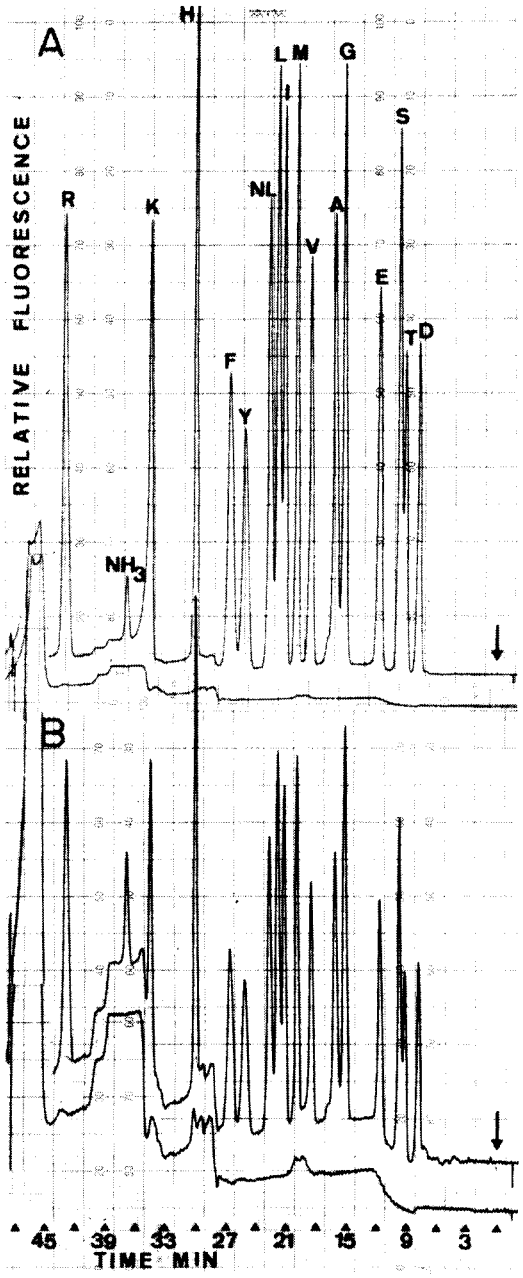

Fig. 4. Elution profile of a standard mixture of amino acids using OPA for detection. A, 1 nmol per component; B, 100 pmol per component. The column (250 × 3.2 mm I.D.) of DC-4A was eluted with formate buffers (see Experimental). Elution with buffers A, B and C for 13, 11 and 16 min, respectively. The equilibration temperature was 38°C and changes to 59 and 75°C were at 8 and 26 min, respectively. Regeneration and re-equilibration were for 4 and 14 min, respectively. The column back-pressure was 2500 p.s.i. at 38°C and 1600 p.s.i. at 75°C. Injection to injection time was 60 min.

TABLE I

ANALYSIS OF STANDARD AMINO ACID MIXTURES WITH CALIBRATION AT 1.0 nmol USING OPA FOR DETECTION

Amino acid	*Elution time (min)**		*Standard deviation (nmol) for 1.0 nmol***		*10 pmol*§§	*100 pmol*§§			*200 pmol*§§		*10 nmol*§§		*25 nmol*§§
	Mean	*Maximum deviation*			*c*§§§	*a****	*b*§	*c*§§§	*a****	*b*§	*a****	*b*§	*a****
			*a****	*b*§									
Asp	7.98	± 0.03	0.013	0.015	11.0	99	97	98	206	202	10.02	10.00	25.9
Thr	9.35	± 0.01	0.012	0.013	10.8	99	101	95	193	195	10.02	9.95	26.5
Ser	9.92	± 0.02	0.010	0.008	12.5	101	103	100	197	200	10.31	10.53	20.5†
Glu	11.90	± 0.03	0.017	0.014	9.5	110	105	102	217	204	9.84	10.30	24.6
Gly	15.37	± 0.02	0.011	0.011	11.8	101	99	101	195	193	10.56	10.63	18.7†
Ala	16.32	± 0.02	0.008	0.010	11.5	102	99	100	198	197	10.21	10.24	23.0†
Val	18.70	−0.03, + 0.08	0.020	0.024	11.1	116	103	99	212	202	10.01	10.16	23.8
Met	20.11	−0.05, + 0.13	0.012	0.023	9.6	103	96	95	194	185	10.74	10.90	19.2†
Ile	21.33	−0.05, + 0.14	0.010	0.010	11.1	102	102	98	198	195	10.40	10.54	19.9†
Leu	22.01	−0.05, + 0.13	0.005	0.013	11.0	100	102	100	194	196	10.51	10.71	18.9†
NorLeu	22.85	−0.06, + 0.12	0.008	0.005	10.4	102	100	98	198	195	10.40	10.50	22.4†
Tyr	25.32	−0.06, + 0.12	0.009	0.005	11.1	101	99	98	191	193	10.30	10.33	25.5
Phe	26.78	−0.05, + 0.13	0.012	0.013	10.6	100	100	98	191	194	10.34	10.50	26.0
His	30.22	−0.06, + 0.13	0.028	0.023	11.0	141	93	98	223	204	9.88	11.00	15.6†
Lys	34.69	−0.08, + 0.11	0.024	0.026	10.6	62	89	100	228	185	9.33	10.18	18.8†
Arg	42.99	−0.16, + 0.21	0.013	0.020	11.2	114	106	99	197	196	10.27	10.53	23.0

* Average for 30 samples.

** 7 standard runs.

*** Determined from peak area measured by automatic integration.

§ Determined from peak height measured automatically.

§§ Average for 2 samples.

§§§ Determined from manual measurement of peak height; the constant baseline was taken into consideration.

† Saturation of photomultiplier.

preparation of buffers essential. We have found that the formate buffers described under Experimental permit short analyses times and quantitation at the low picomole level. Fig. 4 shows the elution profiles of standard mixtures of amino acids at the 1 nmol and 100 pmol levels. It should be noted that the column had been through a minimum of 50 analyses (resolution frequently diminishes with column age) and that the buffers were not freshly prepared. The elution times and peak widths are similar, again indicating that peak heights may be used for quantitation. Results from the analyses of standard amino acid mixtures, containing 10 pmol to 25 nmol per component, eluted with formate buffers and detected with OPA, are given in Table I. The results clearly show the linearity of response for both peak area and peak height over a range of three orders of magnitude. Analysis on as little as 10 pmol per amino acid component is readily possible, but here quantitation is restricted to manual measurement of the peak height.

In contrast to ninhydrin, OPA does not react with proline and cysteine produces a relative fluorescence that is too low for practical use. Methods for the detection of proline, albeit with a low relative response, by post-column oxidation with chloramine-T[21] or sodium hypochlorite[22], prior to reaction with OPA, have been reported. Either two analyses are performed, one with and one without an oxidizing agent, or during one analysis valve switching is arranged in such a way that the oxidant is added only during elution of proline. In this work no attempt was made to measure proline using OPA; when such measurements were obligatory, ninhydrin detection was utilized. Insensitivity to cysteine has not presented problems as the response to the far more commonly analysed alkylated derivatives is equal to that of the other amino acids.

Our work on post-translational modification of proteins made the analysis of amino acids specifically modified by radioactively labelled ^{14}C and ^{3}H reagents necessary. A convenience of OPA detection is that fractions may be used directly for scintillation counting, without the need for split-stream valves.

Further work[13–15] has confirmed that the application of HPLC technology to peptide/protein analysis and preparative isolation has become a powerful tool. In this paper we have shown that this instrumentation can be used with equal success for the analysis of amino acids, thus substantially decreasing the cost of the equipment while simultaneously increasing its versatility.

ACKNOWLEDGEMENTS

This research was supported by grant 0.330.077.98-3 from the Eidgenössische Technische Hochschule, Zurich. Kontron International and the Sandoz-Stiftung, Sandoz AG, are thanked for their additional support.

REFERENCES

1 R. Schuster, *Anal. Chem.*, 52 (1980) 617–620.
2 M. K. Radjai and R. T. Hatch, *J. Chromatogr.*, 196 (1980) 319–322.
3 D. H. Spackman, W. H. Stein and S. Moore, *Anal. Chem.*, 30 (1958) 1190–1206.
4 S. Moore, W. H. Stein, *J. Biol. Chem.*, 211 (1954) 907–913.
5 M. Roth, *Anal. Chem.*, 43 (1971) 880–882.
6 J. R. Benson and P. E. Hare, *Proc. Nat. Acad. Sci. U.S.*, 72 (1975) 619–622.

7 C. L. Zimmermann, E. Appella and J. J. Pisano, *Anal. Biochem.*, 77 (1977) 569–573.
8 N. D. Johnson, M. W. Hunkapiller and L. E. Hood, *Anal. Biochem.*, 100 (1979) 335–338.
9 K. J. Wilson, K. Rodger and G. J. Hughes, *FEBS Lett.*, 108 (1979) 87–91.
10 H. Engelhardt, J. Asshauer, U. Neve and N. Weigland, *Anal. Chem.*, 46 (1974) 336–340.
11 E. Bayer, E. Grom, B. Kaltenegger and R. Uhmann, *Anal. Chem.*, 48 (1976) 1106–1109.
12 G. J. Hughes, K. H. Winterhalter and K. J. Wilson, *FEBS Lett.*, 108 (1979) 81–86.
13 G. J. Hughes, C. De Jong, R. Fischer, K. H. Winterhalter and K. J. Wilson, *Biochem. J.*, 199 (1981) 61–67.
14 A. Honegger, G. J. Hughes and K. J. Wilson, *Biochem. J.*, 199 (1981) 53–59.
15 K. J. Wilson, A. Honegger and G. J. Hughes, *Biochem. J.*, 199 (1981) 43–51.
16 M. Rubinstein, S. Stein and S. Udenfriend, *Proc. Nat. Acad. Sci. U.S.*, 75 (1978) 669–671.
17 P. E. Petrides, R. T. Jones and P. Böhlen, *Anal. Biochem.*, 105 (1980) 383–388.
18 P. Böhlen, S. Stein, J. Stone and S. Udenfriend, *Anal. Biochem.*, 67 (1975) 438–445.
19 E. H. Creaser and G. J. Hughes, *J. Chromatogr.*, 144 (1977) 69–75.
20 W. S. Hancock, C. A. Bishop, R. L. Prestidge and M. T. W. Hearn, *Anal. Biochem.*, 89 (1978) 203–212.
21 E. G. Drescher and K. S. Lee, *Anal. Biochem.*, 84 (1978) 559–569.
22 P. Böhlen and M. Mellet, *Anal. Biochem.*, 94 (1979) 313–321.

Journal of Chromatography, 235 (1982) 427–433
Elsevier Scientific Publishing Company, Amsterdam — Printed in The Netherlands

CHROM. 14,351

SYSTEMATIC USE OF AFFINITY DIFFERENCES BETWEEN IMMOBILIZED LECTIN GELS FOR DEMONSTRATION OF GLYCOPROTEIN MOLECULAR VARIANTS

THE EXAMPLE OF RADISH β-FRUCTOSIDASE

L. FAYE*
Laboratoire de Photobiologie, Centre de Biochimie et Physiologie Cellulaires, Faculté des Sciences de Rouen, 76130 Mont-Saint-Aignan (France)
J. P. SALIER
INSERM U-78, 76230 Bois-Guillaume (France)
and
A. GHORBEL
Laboratoire de Photobiologie, Centre de Biochimie et Physiologie Cellulaires, Faculté des Sciences de Rouen, 76130 Mont-Saint-Aignan (France)
(First received May 18th, 1981; revised manuscript received September 7th, 1981)

SUMMARY

The glycoprotein β-fructosidase from radish seedlings was used as an example. The extended charge heterogeneity of this enzyme does not allow analytical investigations on the microheterogeneity of the carbohydrate moiety by lectin crossed affinity immunoelectrophoresis. This microheterogeneity was investigated by a new approach of affinity chromatography on to columns of immobilized concanavalin A and *Lens culinaris* agglutinin displaying different affinities. This series of gels allowed a new approach for the detection and control of the microheterogeneity of the glycoprotein sugar moiety. The general chromatographic procedure requires (1) flat gradient elution to observe the heterogeneous forms, (2) re-chromatography and/or crossed chromatography for monitoring the biological significance of the heterogeneous elutions observed and (3) systematic "crossed chromatography" for the detection of further heterogeneous forms.

INTRODUCTION

Molecular heterogeneity in the carbohydrate moeity of glycoproteins has often been investigated by lectin affinity experiments. Crossed affinity immunoelectrophoresis (CAIE) with lectin has been shown to be a powerful technique[1–3] and a recent improvement, carbohydrate electroendosmotic elution, increased its sensitivity[4]. However, this CAIE technique cannot always be used without purified preparations as a control[4] and also it requires either monospecific antisera or biological charac-

0021-9673/82/0000–0000/$02.75

terization for molecular variant detection. Another limitation to CAIE analysis is charge heterogeneity: commonly observed with particular glycoproteins and even suspected for some lectins in CAIE conditions, this phenomenon can produce heterogeneous immunoprecipitation patterns without any relation to lectin binding heterogeneity. Hence chromatography on immobilized lectin columns may, in some instances, be the only method for the study of carbohydrate variants. The wellknown drawbacks of this technique, as generally observed for affinity chromatography, are primarily non-biospecific interactions with the ligand or gel matrix (for a review, see ref. 5), but precautions to avoid non-sugar-specific binding on immobilized lectin columns have also been described[6,7].

In this paper, a new application of column affinity chromatography is described for the characterization and isolation of glycoprotein molecular variants; it takes advantage of (1) affinity differences between two immobilized concanavalin A (Con A) gels, (2) crossed chromatography and (3) the flat gradient elution technique. Extensive studies of sugar-specific interactions have shown that elution profiles obtained from high- or low-affinity columns are not linked to enzyme charge or mass heterogeneity or to carbohydrate degradation, so that good evidence is provided for the microheterogeneity of the glycoprotein sugar moiety.

In our hands, radish β-fructosidase (β-FFase) has proved to give a good example of the technique: this enzyme is a glycoprotein[8] containing 7.7% of carbohydrates[9] and displaying largely heterogeneous behaviour on agarose gel electrophoresis[10], which hindered its study using lectin CAIE. The method reported here allowed us to observe and isolate three carbohydrate variants of β-FFase.

EXPERIMENTAL

Chemicals

The two different immobilized lectins used in this study, Con A and *Lens culinaris* agglutinin (LCA), were purchased either from Pharmacia (Con A-Sepharose, batch 18812; LCA-Sepharose, batch 7767) or from Reactifs IBF, Pharmindustrie (Con A-Ultrogel, batch L.593; LCA-Ultrogel, batch L.127). Methyl α-mannoside (Me-α-Man) was obtained from IBF and all other chemicals from Merck.

Enzyme source and assay

β-FFase was isolated from light-grown radish seedlings irradiated for 72 h with a standard far-red light source[11]. The crude enzyme preparation used here was obtained after Sephadex G-25 (Pharmacia) chromatography of radish seedling extract as described elsewhere[9]. β-FFase activity was measured as described elsewhere[9].

Affinity chromatography on to immobilized lectin columns

All affinity chromatography was performed at room temperature. The lectin columns (22 × 1.6 cm I.D.) were equilibrated with 85 mM citrate phosphate buffer (pH 6.5) containing 1 *M* sodium chloride, 1 m*M* magnesium chloride, 1 m*M* manganese chloride and 1 m*M* calcium chloride. Enzyme samples (0.5 ml) were made from freeze-dried powder dissolved in the same equilibration buffer and were applied on to the columns after centrifugation (3100 *g*, 15 min). After washing the gel with the same buffer, the bound glycoproteins were first eluted with a linear Me-α-Man

gradient (0 to 2.5 m*M*, total volume 100 ml). After an equilibration step with at least 25 ml of 2.5 m*M* Me-α-Man, a second 100-ml gradient from 2.5 to 100 m*M* Me-α-Man was sometimes applied. For the standard procedures presented here, a stepwise 100 m*M* Me-α-Man elution was prefered. The columns were eluted at 46 ml/h, the eluate was monitored with an ultraviolet densitometer at 280 nm, collected in 3.6-ml fractions and measured for β-FFase activity. Prior to re-chromatography, if any, the fractions in a given peak of β-FFase activity were pooled, concentrated on an Amicon PM 30 ultrafiltration membrane and finally dialysed against the equilibration buffer. The retardation coefficient (R_c) is expressed here as V_e/V_i, where V_e is the elution volume of β-FFase activity on lectin columns in the presence of equilibration buffer and V_i is the enzyme elution volume when β-FFase was chromatographed on the same column in the presence of 100 m*M* Me-α-Man.

RESULTS

Elution profiles on Con A columns

When chromatographed on Con A-Sepharose, β-FFase was first completely retained on this column and then partly (90%* of the recovered enzyme activity) eluted as a sharp peak (I_s) in the first volumes of a gentle linear Me-α-Man gradient (0–2.5 m*M*) as shown in Fig. 1. A second enzyme form (II_s = 10%) was eluted homogeneously with approximately 25 m*M* of this competing glycoside, as calculated from a second linear gradient (2.5–100 m*M* me-α-Man) (not shown). Finally, more than 90% of the enzyme activity in the originally applied material was recovered; the residual activity could not be eluted from the column with higher Me-α-Man concentrations.

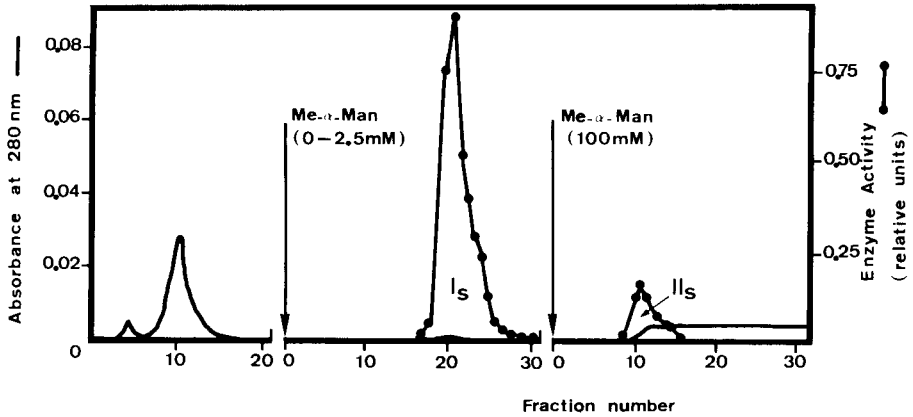

Fig. 1. Con A-Sepharose elution profile of β-FFase (crude enzyme preparation). Fraction size, 3.6 ml. Starting buffer, 85 m*M* citrate phosphate buffer (pH 6.5) containing 1 *M* NaCl, 1 m*M* $MgCl_2$, 1 m*M* $MnCl_2$ and 1 m*M* $CaCl_2$. First arrow indicates start of elution with linear Me-α-Man gradient (50 ml × 2 from 0 to 2.5 m*M*). Second arrow indicates start of elution with buffer containing 100 m*M* Me-α-Man. The first enzyme peak (I_s) represents 90% and the second peak (II_s) 10% of the recovered enzyme activity.

* All values are the means of at least three experiments performed on the same column.

This result was strengthened by Con A-Ultrogel chromatography (Fig. 2A). β-FFase elution profiles on this lower affinity column[12] allowed one to distinguish (a) an unbound form (I_u) representing 57% of the recovered enzyme activity and eluted as a highly retarded trailing peak with equilibration buffer lacking Me-α-Man; the heterogeneity in the elution profile of this first enzyme form was highly reproducible and reflected different affinity levels (R_c 1.4, 1.7, 2.0); (b) a loosely bound form (II_u; 43%) which was eluted in the first volumes of the Me-α-Man gradient (0–2.5 m*M*) as a sharp peak (Fig. 2A). No more activity was eluted with 100 m*M* of this competing glycoside.

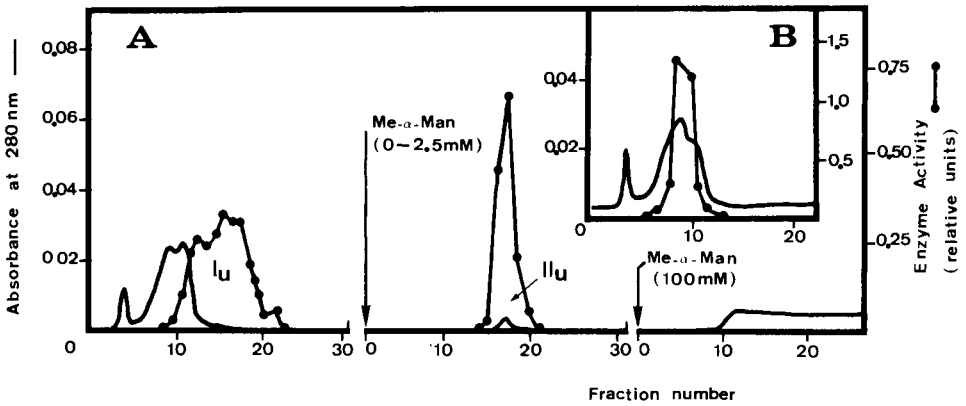

Fig. 2. Con A-Ultrogel elution profile of β-FFase (crude enzyme preparation). (A) Fraction size and elution conditions as in Fig. 1. The first peak (I_u showing retarded elution) represents 57% and the second peak (II_u) 43% of the recovered enzyme activity. Starting buffer, sample and column contained 100 m*M* Me-α-Man. The whole enzyme activity was unbound and eluted without any retardation when compared with elution of other extract proteins.

Establishment of biological significance of heterogeneous elution profiles

The two fractions isolated from either Con A column were eluted in their original position when re-chromatographed separately on the same column. Further, the whole of the enzyme activity was recovered with the unretained proteins when the sample, column and equilibration buffer were supplemented with 100 m*M* Me-α-Man, whatever the gel in use; in particular, the heterogeneity and retardation of the first peak on Con A-Ultrogel completely disappeared under the last experimental conditions (see Fig. 2B, insert). Hence the heterogeneity observed in elution profiles on Con A columns did not result from (1) column overloading, (2) non-sugar-specific interactions with the immobilized lectin or (3) sieving effects.

Elsewhere, the Con A-Ultrogel-retarded fraction (I_u) was completely bound on Con A-Sepharose and subsequently eluted as a sharp peak with a 0–2.5 m*M* Me-α-Man gradient, indicating that degradation in the β-FFase carbohydrate moiety occurring before or during Con A-Ultrogel chromatography could not account for the weak affinity observed on this last gel.

Finally, all chromatographic runs were performed in the presence of a high sodium chloride concentration (1 *M*) to prevent enzyme electrostatic interactions with Con A or the gel matrix, as the latter case has already been described for β-FFase from different origins[9,13].

When β-FFase was chromatographed on immobilized LCA, it was unretained on LCA-Ultrogel and not adsorbed but specifically retarded on the LCA-Sepharose column (R_c 1.13) (not shown). The very different elution profiles obtained from Con A and LCA immobilized on the same matrix give new evidence to exclude non-specific interactions with the matrix and/or sieving effects as an explanation of heterogeneous profiles.

Crossed chromatography for detection of microheterogeneity

The different ratios observed for low- and high-affinity forms on each column (see Table I) were indicative of greater complexity than was inferred from a single elution profile exhibiting two molecular variants. To obtain more precisely the relationships between the molecular variants isolated from each column chromatography, the first and second forms obtained from Con A-Sepharose (I_s and II_s, respectively) were re-chromatographed separately on Con A-Ultrogel. The fraction showing the highest affinity for Con A-Sepharose (II_s) was completely retained on Con A-Ultrogel and was eluted as a single peak with Me-α-Man; however, as shown in Fig. 3, a β-FFase form of lower affinity on Con A-Sepharose (I_s) could be further divided

TABLE I

SUMMARY OF THE VARIOUS FRACTIONS ISOLATED FROM CON A-SEPHAROSE OR CON A-ULTROGEL CHROMATOGRAPHY, RE-CHROMATOGRAPHY AND CROSSED-CHROMATOGRAPHY

Results expressed as percentage of total enzyme activity recovered from the column.

Sample	*Immobilized lectin*	*Fraction*			
		Unretained, unretarded	*Unretained but retarded*	*Retained and eluted with 0–2.5 mM Me-α-Man*	*Retained and eluted with 100 mM Me-α-Man*
		Single chromatography:			
CEP*	Con A-Sepharose	–	–	(I_s) 90	(II_s) 10
CEP + sugar**	Con A-Sepharose	100	–	–	–
CEP	Con A-Ultrogel	–	(I_u) 57 (R_c 1.4, 1.7, 2.0)	(II_u) 43	–
CEP + sugar	Con A-Ultrogel	100	–	–	–
CEP	LCA-Sepharose	–	100 (R_c 1.13)	–	–
CEP + sugar	LCA-Sepharose	100	–	–	–
CEP	LCA-Ultrogel	100	–	–	–
		Re-chromatography on the same column:			
I_s***	Con A-Sepharose	–	–	100	–
II_s	Con A-Sepharose	–	–	–	100
I_u	Con A-Ultrogel	–	100	–	–
II_u	Con A-Ultrogel	–	–	100	–
		Crossed chromatography:			
I_u***	Con A-Sepharose	–	–	100	–
I_s	Con A-Ultrogel	–	45	55	–
II_s	Con A-Ultrogel	–	–	100	–

* CEP = crude enzyme preparation.

** CEP + sugar: chromatography performed in 100 m*M* competiting glycoside (Me-α-Man).

*** I_s, II_s, I_u, II_u: fractions used separately for re-chromatography or crossed chromatography.

into a non-adsorbed, retarded fraction (45%) and a bound fraction (55%) when re-chromatographed on to Con A-Ultrogel. Further studies of these last elution patterns showed them to be linked to sugar-specific interactions with the immobilized lectin. This result, obtained from crossed chromatography, is indicative of at least three molecular variants of β-FFase.

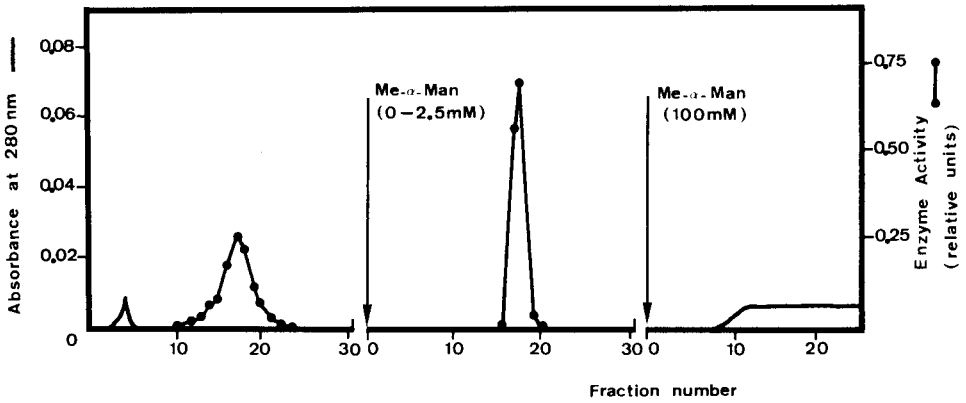

Fig. 3. Re-chromatography on to Con A-Ultrogel of β-FFase made of the first major peak (I_s) obtained from Con A-Sepharose chromatography (see Fig. 1). Fraction size and elution conditions as in Fig. 1. The first peak (showing retarded elution) represents 45% and the second peak 55% of the recovered enzyme activity.

DISCUSSION

Preliminary observations obtained from immunochemical analysis[14] and affinity precipitation techniques showed that β-FFase charge heterogeneity may arise from microheterogeneity in the sugar moiety of this enzyme; in contrast with the complete specific enzyme precipitation obtained when using glutaraldehyde cross-linked Con A as affinity adsorbent, only partial precipitation of β-FFase activity was observed when the largest amount of soluble Con A was used[8]. In order to obtain a better understanding of β-FFase microheterogeneity, we developed a new application of lectin affinity chromatography for the detection and isolation of molecular variants that differ only slightly in their affinity for lectins.

It is not our purpose here to investigate the origin of affinity differences between Ultrogel- and Sepharose-bound lectins. First reported by Kerckaert and Bayard[12] with Con A-reactive rat α-fetoprotein, in the present study these differences were confirmed for Con A, and also for LCA in the case of radish β-FFase interactions. Differences in the binding techniques used for lectin immobilization either on cyanogen bromide-activated Sepharose or on glutaraldehyde-activated Ultrogel probably induced changes in lectin affinity by slight conformational alterations of the interacting site. We report here that these changes in the affinity of immobilized Con A make available an immobilized Con A (Con A-Ultrogel) whose binding affinity is intermediate between those of Con A-Sepharose and LCA-Sepharose ones. Consequently, our chromatographic method is based on the use of this series of gels: systematic chromatography of the sample on to each of these gels, completed by crossed chromatography of given fractions from one gel on to another allowed us to

observe and isolate further microheterogeneous forms of β-FFase, not detectable from a single affinity chromatography.

Few results have been reported on the use of gradient elution on lectin columns[15–17]. Preliminary investigations with this technique allowed us to use the lowest concentrations of eluting glycoside to obtain the highest purification factor for β-FFase from Con A-Sepharose chromatographic steps[9]. Here, a flat gradient is shown to be extremely helpful in investigating affinity differences and in distinguishing among molecular variants of glycoproteins.

The literature provides many examples of non-specific adsorption to immobilized lectins[18]. In our study care was taken to avoid such artefacts; in particular, the use of 1 *M* sodium chloride in the buffer prevented ionic interactions. Further, extensive studies including re-chromatography and crossed chromatography allowed us to exclude enzyme degradation, binding capacity saturation, gel sieving effects and non-sugar-specific interactions as explanations for elution profile heterogeneity. Hence our experimental conditions provide good evidences for β-FFase molecular microheterogeneity in oligosaccharide side-chains, with at least three molecular variants of this enzyme. Further analysis of radish β-FFase lectin-binding heterogeneity is now in progress in relation to the structure, localization and charge variations of the enzyme.

In summary, we have developed a new approach for the detection and control of the microheterogeneity of the glycoprotein sugar moiety. This approach takes advantage of presently available immobilized lectin gels displaying different affinities for a given glycoprotein and requires (1) flat gradient elutions to observe the heterogeneous forms, (2) re-chromatography and/or crossed chromatography for study of the biological significance of the heterogeneous elutions observed and (3) systematic crossed chromatography for the detection of further heterogeneous forms.

ACKNOWLEDGEMENTS

This work was supported by the Centre National de la Recherche Scientifique (LA 203).

REFERENCES

1 T. C. Bøg-Hansen and C. H. Brogren, *Scand. J. Immunol.*, 4 Suppl. 2 (1975) 135.
2 T. C. Bøg-Hansen, O. J. Bjerrum and J. Ramlau, *Scand. J. Immunol.*, 4 Suppl. 2 (1975) 141.
3 T. C. Bøg-Hansen, in J. M. Egly (Editor), *Affinity Chromatography and Molecular Interactions*, Les Colloques de l'INSERM, INSERM, Paris, 1979, Vol. 86, p. 399.
4 J. P. Salier, L. Faye, D. Vercaigne and J. P. Martin, *Electrophoresis*, 1 (1980) 193.
5 P. O'Carra, S. Barry and T. Griffin, *Methods Enzymol.*, 34 (1974) 108.
6 T. Mega and Y. Matsushima, *J. Biochem.*, 81 (1977) 571.
7 J. T. Dulaney, *Mol. Cell. Biochem.*, 21 (1979) 43.
8 L. Faye and C. Berjonneau, *Biochimie*, 61 (1979) 51.
9 L. Faye, C. Berjonneau and P. Rollin, *Plant Sci. Lett.*, 22 (1981) 77.
10 L. Faye, *Anal. Biochem.*, 112 (1981) 90.
11 R. Malcoste, C. Huault, G. Larcher and P. Rollin, *Physiol. Veg.*, 10 (1972) 575.
12 J. P. Kerckaert and B. Bayard, *Biochem. Biophys. Res. Commun.*, 92 (1980) 95.
13 D. W. A. Roberts, *J. Chromatogr.*, 153 (1978) 532.
14 L. Faye, C. Berjonneau and A. Ghorbel, *Arch. Biochem. Biophys.*, in press.
15 S. R. Harvey and T. M. Chu, *Cancer Res.*, 35 (1975) 3001.
16 A. A. Farooqui and A. B. Roy, *Biochem. Biophys. Acta*, 452 (1976) 431.
17 M. G. Brattain, P. M. Kimball, T. G. Pretlow and M. E. Marks, *Biochem. J.*, 163 (1977) 247.
18 M. W. Davey, E. Sulkowski and W. A. Carter, *Biochemistry*, 15 (1976) 704.

Journal of Chromatography, 235 (1982) 435–443
Elsevier Scientific Publishing Company, Amsterdam — Printed in The Netherlands

CHROM. 14,331

STUDIES BY AFFINITY CHROMATOGRAPHY ON THE NAD(P)H AND FAD SITES OF NITRATE REDUCTASE FROM *ANKISTRODESMUS BRAUNII**

ANTONIO J. MÁRQUEZ, MIGUEL A. DE LA ROSA and JOSÉ M. VEGA*,**
Departamento de Bioquímica, Facultad de Biología y C.S.I.C., Universidad de Sevilla, Sevilla (Spain)
(Received August 4th, 1981)

SUMMARY

Both native NAD(P)H-nitrate reductase (E.C. 1.6.6.2.) from *Ankistrodesmus braunii* and the FAD-depleted enzyme are adsorbed on blue dextran–Sepharose at two different sites. The binding of the native enzyme involves the NAD(P)H active site, while that of the deflavoenzyme uses the FAD site. The holoenzyme can be specifically eluted by 0.5 m*M* NAD(P)H, but the elution of the deflavoenzyme was achieved only by the simultaneous addition of 1 m*M* FAD and 0.5 *M* KCl to the washing buffer.

Incubation of native or flavin-free nitrate reductases with *p*-hydroxymercuribenzoate prevents adsorption of both types of enzyme on blue dextran–Sepharose, which indicates the presence of sulphydryl groups in the sites for NAD(P)H and FAD.

Binding studies of the holoenzyme on three different kinds of NAD-Agarose indicate that the NAD(P)H-domain is acting as a crevice in which the nicotinamide ring of the nucleotide should be placed at the bottom. In addition, the structure of the binding site for FAD seems to be similar to that for NAD(P)H.

INTRODUCTION

NAD(P)H-nitrate reductase (E.C. 1.6.6.2.) from the green alga *Ankistrodesmus braunii* catalyzes the assimilatory reduction of nitrate to nitrite using reduced pyridine nucleotides as electron donors. In addition, two enzymatic activities which participate sequentially in the transfer of electrons from NAD(P)H to nitrate are present in the enzyme complex; the first is an FAD-dependent NAD(P)H-diaphorase and the sec-

* Abbreviations: FAD = flavin–adenine dinucleotide; FMN = riboflavin 5′-phosphate; NAD = nicotinamide–adenine dinucleotide, oxidized; NADH = nicotinamide–adenine dinucleotide, reduced; NADP = nicotinamide–adenine dinucleotide phosphate, oxidized; NADPH = nicotinamide–adenine dinucleotide phosphate, reduced.

** Permanent address: Departamento de Bioquímica, Facultad de Químicas, Universidad de Sevilla, Sevilla, Spain.

0021-9673/82/0000–0000/$02.75

ond is the molybdoprotein terminal nitrate reductase[1]. FAD-depleted nitrate reductase lacks all the NAD(P)H-dependent activities.[2]

Thompson *et al.*[3] have proposed that blue dextran forms complexes with a wide range of proteins because it is specific for a super-secondary structure called the "dinucleotide fold". This structure involves about 120 amino acids arranged in a β-sheet core composed of five or six parallel strands which are connected by α-helical intrastrand loops located above and below the β-sheet[4,5]. The dinucleotide fold is known to form the NAD- and ATP-binding sites of several enzymes, and to be present in the structure of others. Thus, blue dextran–Sepharose columns have been used in the final purification stages of several enzymes, which were displaced from the affinity columns by addition of low concentrations of their nucleotide substrates to the elution solvents[3].

Recently, affinity chromatography on blue dextran–Sepharose was used successfully in the purification of nitrate reductase from several organisms[6]. In particular, nitrate reductase from *A. braunii* has been purified to homogeneity by a simple method which includes affinity chromatography on blue dextran–Sepharose as the main step, the enzyme being specifically eluted from the column by addition of NADH to the washing buffer[7,8]. From these results, it was suggested that NAD(P)H-nitrate reductase from *A. braunii* also contains the dinucleotide fold in its NAD(P)H-domain[9].

Affinity chromatography on FAD-Sepharose has been employed for the purification of fungal nitrate reductase[10,11], since assimilatory nitrate reductase from eukaryotic organisms is an FAD-containing enzyme[6].

In this paper, we describe a study of the interaction of *A. braunii* nitrate reductase with blue dextran–Sepharose and with three different NAD-Agaroses, in order to obtain information about the nature of the NAD(P)H-binding site of the enzyme. We have found that the FAD-free enzyme is specifically adsorbed on blue dextran–Sepharose by the flavin-binding site, which may mean that the enzyme possesses a local FAD-domain structure similar to the dinucleotide fold.

MATERIALS AND METHODS

Materials

Tris, EDTA, FAD, *p*-hydroxymercuribenzoate, reactive blue dextran 2–Sepharose CL-6B and β-nicotinamide adenine dinucleotide–Agaroses (N-1008, N-6130 and N-9505) were purchased from Sigma (St. Louis, MO, U.S.A.). NADH and NADPH were obtained from Boehringer (Mannheim, G.F.R.), methyl viologen and dithioerythritol from Serva (Heidelberg, G.F.R.), alumina for disrupting cells from Alcoa (Arkansas, U.S.A.) and streptomycin sulphate was from Cía. Española de Penicilina (Spain).

Preparation of native and flavin-depleted nitrate reductases

Ankistrodesmus braunii strain 202-7c from Göttingen University's culture collection was grown as previously described[12]. The cells were harvested by low speed centrifugation and ground at 0°C with alumina in a mortar. The broken material was extracted with 10 m*M* potassium phosphate buffer, pH 7.0, containing 0.15 m*M* dithioerythritol, 0.10 m*M* EDTA and 20 μM FAD (buffer A) for native nitrate

reductase, and the same buffer without FAD (buffer B) for the flavin-free enzyme; 7 ml buffer per g, wet weight, of cells were added. The homogenate was centrifuged at 27,000 *g* for 15 min, and the supernatant was used as the crude extract.

A solution of 0.1 *M* streptomycin sulphate, pH 7.0, was added dropwise to the crude extract (1 ml per 10 ml extract). After 10 min at 0°C with continuous stirring, the suspension was centrifuged at 27,000 g for 15 min, and the resulting supernatant was used for affinity chromatography.

Affinity chromatography

Blue dextran–Sepharose and NAD-Agaroses were packed in columns of 65 × 7.5 mm and 40 × 5 mm, respectively. Before use, the column beds were washed with ten volumes of 2 *M* KCl and then equilibrated with twenty volumes of the starting buffer. A constant flow-rate of 12 ml/h was used for the blue dextran–Sepharose column, and 6 ml/h for the NAD-Agarose ones.

Enzyme activity

NADH- and reduced methyl viologen-nitrate reductase activities were determined colorimetrically by measuring the nitrite formation. The reaction mixture contained (in a final volume of 1 ml) 0.1 *M* Tris–HCl buffer, pH 7.5, 10 m*M* potassium nitrate, a donor of electrons and an adequate amount of enzyme. The donors were present at the following concentrations: NADH, 0.3 m*M*; or sodium dithionite, 4.6 m*M*, plus methyl viologen, 0.15 m*M*. The reaction was started by addition of the enzyme and stopped after 5 min by rapid oxidation of the electron donor system in a Vortex mixer.

Analytical methods

Protein was estimated by the method of Bailey[13], with bovine serum albumin as standard. The absorbance of standards at 279 nm was measured to determine their concentration ($\varepsilon^{1\%}_{279\,nm}$ = 0.067 g^{-1} ml cm^{-1}). Nitrite was estimated as described by Snell and Snell[14].

RESULTS AND DISCUSSION

Behaviour of native nitrate reductase and flavin-free enzyme on blue dextran–Sepharose

A phosphate buffer of low ionic strength and pH 7.0, supplemented with 0.15 m*M* dithioerythritol, 0.10 m*M* EDTA and 20 μM FAD (buffer A), was used for optimum adsorption of native nitrate reductase on blue dextran–Sepharose[9]. The enzyme retained in the column was eluted by addition of NADH to the eluting buffer (Fig. 1A). NADPH was also able to promote the elution of nitrate reductase from the affinity column, although it was less efficient than NADH. FAD-free nitrate reductase in buffer B (without FAD) was also adsorbed on blue dextran–Sepharose, but in this case NADH alone (Fig. 1B) or in the presence of FAD (Fig. 1C) was unable to elute the enzyme. In all cases, 3 *M* KCl promoted the elution of both holoenzyme and deflavoenzyme.

It can be deduced, therefore, that native nitrate reductase from *A. braunii* is adsorbed on blue dextran–Sepharose via its NAD(P)H-domain. Because the Michaelis constant (K_M) of the enzyme for NADH and NADPH are 13 and 23 μM respectively[1], it is logical that NADH has a higher efficiency than NADPH as eluent.

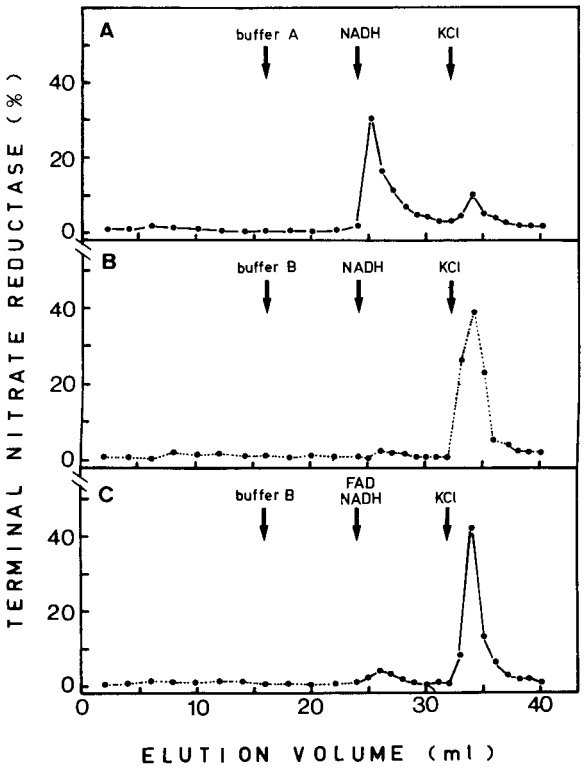

Fig. 1. Elution profiles of nitrate reductase adsorbed on blue dextran–Sepharose in the absence or presence of FAD. Three nitrate reductase preparations were obtained, as described in Materials and methods, from 2 g of cells. The native enzyme was in buffer A (———), while the flavin-depleted nitrate reductase was prepared with buffer B (– – –). The enzyme solutions were separately applied to a blue dextran-Sepharose column previously equilibrated with the corresponding buffer. After adsorption, the column bed was washed with the same buffer, which was supplemented as indicated with 0.5 m*M* NADH, 1 m*M* FAD or 3 *M* KCl. 1-ml Fractions were collected, and reduced methyl viologen-nitrate reductase activity was measured by adding 0.1-ml aliquots of each fraction to the reagents of the standard assay. 100% activity corresponds to the sum of activities of the pool of fractions collected in each case.

On the other hand, the adsorption of FAD-free nitrate reductase on blue dextran–Sepharose seems proceed through its FAD-binding site, probably due to the higher affinity of the enzyme for FAD (K_M = 4 n*M*)[2] than that for NADH.

Both types of interaction of nitrate reductase with blue dextran–Sepharose possess ionic character, because the elution from the affinity column can be carried out in both cases by increasing the ionic strength of the buffer. Moreover, the results shown in Fig. 2 indicate that FAD-depleted nitrate reductase is more strongly bound to blue dextran–Sepharose than the holoprotein, since a lower ionic strength was necessary to elute the latter.

Similar results have recently been reported for NADH-cytochrome b_5 reductase, which is an FAD-requiring enzyme[15]. Holoenzyme is adsorbed on blue dextran–Sepharose at low ionic strength and is eluted by NADH, while the flavin-free enzyme is more strongly bound and is eluted by the simultaneous addition of FAD and NADH

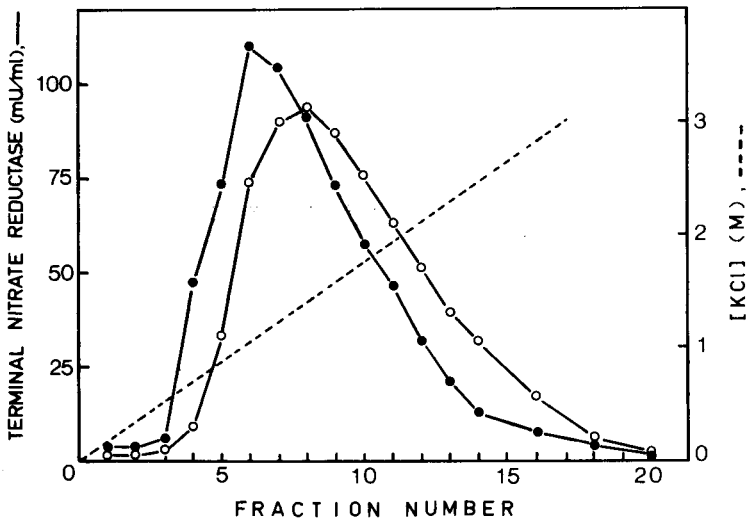

Fig. 2. Elution with a linear gradient of KCl of native nitrate reductase and FAD-free enzyme from a blue dextran–Sepharose column. A nitrate reductase preparation obtained from 2 g of cells with buffer A was applied to a blue dextran–Sepharose column. After a brief washing with buffer A, the elution was carried out with a linear gradient of 0–3 *M* KCl in the same buffer. 1-ml Fractions were collected, and reduced methyl viologen-nitrate reductase activity (●) was determined by adding 0.1 ml of each fraction to the reagents of the standard assay. A similar experiment was repeated under identical conditions, but using buffer B throughout the procedure. In this case, the terminal nitrate reductase activity is represented by open circles (○).

to the eluting buffer. Separately, the cofactors have no effect. It has been also reported that Cibacron blue and blue dextran–Sepharose bind to the FMN-binding site of flavocytochrome b_2, and the authors[16] suggested that the enzyme possesses a local flavin-binding structure similar to the dinucleotide fold.

Elution by FAD of flavin-depleted nitrate reductase adsorbed on blue dextran–Sepharose

When a preparation of nitrate reductase free from FAD was adsorbed on a blue dextran–Sepharose column, the enzyme could be eluted by the simultaneous addition of 1 m*M* FAD and 0.5 *M* KCl to the washing buffer (Fig. 3). Separately, FAD or KCl was unable to elute the enzyme. These results are compatible with the idea that flavin-depleted nitrate reductase is specifically retained by blue dextran–Sepharose through its flavin-domain, forming a tight complex with the dye ligand. Apparently, it is necessary to weaken the bond between deflavoenzyme and blue dextran–Sepharose by increasing the ionic strength so that FAD can elute the apoenzyme. It is of interest that FAD by itself did not elute flavin-free cytochrome b_5 reductase from a blue dextran–Sepharose column[15], while an FMN gradient displaced the FMN-depleted flavocytochrome b_2 (ref. 16).

Effect of NADH and p-hydroxymercuribenzoate on adsorption of nitrate reductase on blue dextran–Sepharose

When native nitrate reductase was incubated with 1 m*M* NADH for 10 min at

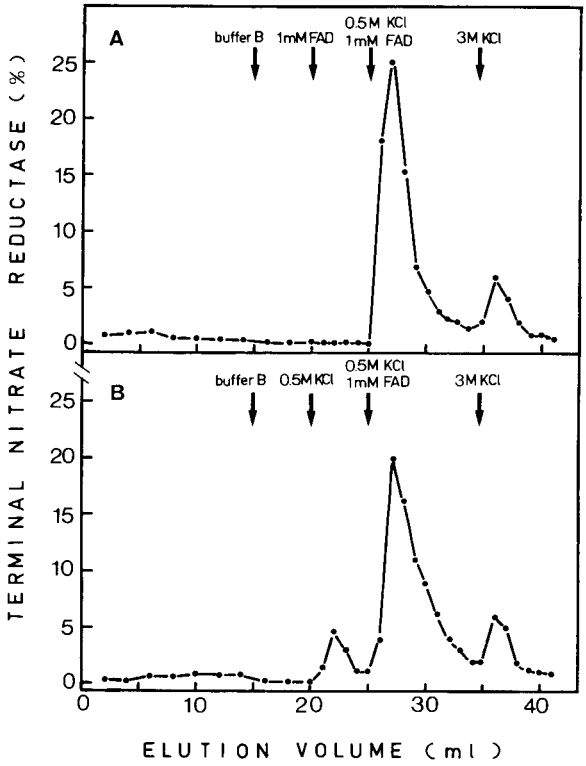

Fig. 3. Elution profile with FAD plus KCl of flavin-depleted nitrate reductase adsorbed on blue dextran–Sepharose. Two nitrate reductase preparations, each from 2 g of cells, were obtained with buffer B as described in Materials and methods. After adsorption on blue dextran–Sepharose, the column bed was washed with buffer B, and then 1 m*M* FAD, 0.5 *M* KCl or 3 *M* KCl was added to the washing buffer as indicated by arrows. 1-ml Fractions were collected and the reduced methyl viologen-nitrate reductase activity was measured by adding 0.1 ml of each fraction to the reagents of the standard assay. 100% activity corresponds to the sum of activities of pooled fractions collected in each case.

0°C, before application to a blue dextran–Sepharose column, the enzyme was not retained by the affinity column (not shown). This may be explained by the fact that reduced pyridine nucleotide binds to the enzyme through its active site for NAD(P)H and, therefore, the complex NADH–holoenzyme cannot be adsorbed on blue dextran–Sepharose. Similar results were obtained when FAD-free nitrate reductase was incubated with 1 m*M* NADH before chromatography. This behaviour can be understood if the structure of the flavin-domain in nitrate reductase is similar to that of the NAD(P)H, *i.e.*, both sites fit the dinucleotide fold, and NADH is also able to bind to the enzyme through the flavin-binding site. Support for this idea is provided by the fact that FAD may be substituted by NADH in the protection of the NADH-diaphorase activity of nitrate reductase against inactivation in dilute solutions[2].

When nitrate reductase in buffer A without dithioerythritol was incubated at 0°C for 10 min with 5 μM *p*-hydroxymercuribenzoate, a typical sulphydryl groups reagent, before application of the enzyme solution to a blue dextran–Sepharose column, only 37% of nitrate reductase was adsorbed on the column (Table I). Like-

wise, if FAD-depleted enzyme was first incubated in buffer B under the same conditions, only 40% of the apoenzyme applied to the column was retained (Table I). These results confirm the similarity of the two dinucleotide-binding sites of nitrate reductase, and indicate that the presence of –SH groups is essential for the binding of NAD(P)H and FAD to the enzyme.

TABLE I

EFFECT OF *p*-HYDROXYMERCURIBENZOATE ON THE ADSORPTION OF NITRATE REDUCTASE ON BLUE DEXTRAN–SEPHAROSE

Native and flavin-depleted nitrate reductases were prepared from 1 g, wet weight, of cells, as described in Materials and methods, except that the phosphate buffers did not contain dithioerythritol. The enzyme preparations were incubated alone or with 5 μM *p*-hydroxymercuribenzoate (*p*HMB) at 0°C for 10 min. They were separately applied to a blue dextran–Sepharose column, and the amount of enzyme retained in the column was determined after elution with 3 *M* KCl.

Preincubation system	*Nitrate reductase adsorbed (%)*	
	Native	*Flavin-depleted*
Enzyme	95	93
Enzyme + *p*HMB	37	40

It has previously been suggested that free sulphydryl groups of nitrate reductase from eukaryotic organisms participate in the binding of NAD(P)H to the enzyme[17,18]. Similar results have been reported for the enzyme from *A. braunii*[1,7]. In addition, an active participation of –SH groups in the electron flow from NAD(P)H to FAD has been reported for nitrate reductase from *Neurospora crassa*[19].

From the above data it can be deduced that sulphydryl groups are also required for the binding of FAD. It is obvious that multiple interactions between flavin and protein are involved in the binding. Thus, Choi and McCormick[20] suggest that the interaction of flavin with hen egg white riboflavin-binding protein is mainly due to hydrophobic interaction of the flavin ring system with non-polar groups of the protein, and hydrogen bonding of the hydroxyl groups of the flavin. Yubisui and Takeshita[21] have reported that tryptophan and tyrosine seem to participate in the binding of FAD to NADH-cytochrome b_5 reductase. In all cases, the isoalloxazine ring seems to be placed in the crevice of the flavin-domain of flavoproteins[15,20,22,23].

Adsorption of nitrate reductase on three different NAD-Agaroses

Three different NAD-Agaroses were used to study the geometrical orientation of reduced pyridine nucleotides when bound to nitrate reductase. The Agaroses contained β-nicotinamide adenine dinucleotide covalently bound through: (1) C-8 of adenine, with a carbon chain of six carbons between the NAD and the Agarose matrix (N-1008); (2) ribose hydroxyls, with a carbon chain of six carbons between the NAD and the Agarose matrix (N-6130) and (3) N^6 of adenine, with a spacer of eight carbons (N-9505). The code numbers for the NAD-Agarose are those of Sigma.

The results shown in Fig. 4 indicate that nitrate reductase is adsorbed on NAD-Agarose only when pyridine nucleotide is attached through adenine (N-1008 and N-9505). When NAD is bound through ribose hydroxyls to Agarose (N-6130), no adsorption of nitrate reductase is observed (Fig. 4, centre). It seems that the

NAD(P)H-binding site is acting as a crevice in the bottom of which the nicotinamide ring of the pyridine nucleotide would be placed. Therefore, when pyridine nucleotide is bound to Agarose through adenine, the other end of the molecule, *i.e.*, nicotinamide, may enter to the bottom of the NAD(P)H-domain. When the NAD-Agarose bond is formed through ribose hydroxyls, the molecule of pyridine nucleotide lies across the crevice and cannot bind to the enzyme.

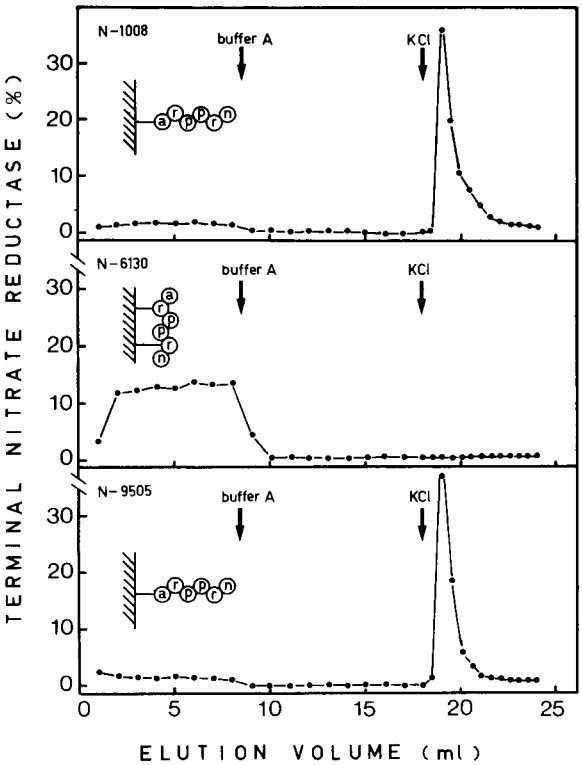

Fig. 4. Elution profile of native nitrate reductase adsorbed on three different NAD-Agaroses. Three nitrate reductase preparations, each from 1 g of cells, were obtained with buffer A as described in Materials and methods. Each enzyme solution was applied to the NAD-Agarose columns, which differed in the bonding between pyridine nucleotide and Agarose (see text). The columns were then washed with buffer A and eluted with 2 *M* KCl in the same buffer. 0.5-ml Fractions were collected, and the reduced methyl viologen-nitrate reductase activity was measured by adding 0.1 ml of each fraction to the reagents of the standard assay. 100% activity corresponds to the sum of activities of the pooled fractions collected in each case. The type of NAD-Agarose used is indicated by its code number. Note that N-1008 and N-9505 differ by the spacer (6 and 8 carbons, respectively). a = Adenine; r = D-ribose; P = phosphate and n = nicotinamide.

In conclusion, when NAD(P)H and FAD are accommodated in their respective domains in nitrate reductase, nicotinamide and isoalloxazine would be placed at the bottom of the crevices. Then, rotation of the molecule would allow the nicotinamide to take up a position where it makes contact with the isoalloxazine ring of flavin, and the electron transfer takes place between both nucleotides.

Schulz *et al.*[23] have elucidated the three-dimensional structure of the flavoenzyme glutathione reductase, which binds two dinucleotides: FAD and NADPH. They

observed that the NADPH- and FAD-domains are very similar and resemble other nucleotide-binding proteins with respect to chain fold and binding mode. Thus, the same general dinucleotide-domain pattern has been observed in the structurally known nucleotide-binding proteins[5,24]. This evolutionary relationship between the two domains indicates that a primordial gene duplication accompanied or followed by gene splicing is likely[23].

ACKNOWLEDGEMENTS

The authors wish to thank Professor Losada for his help. This work was supported by grants from the Comisión Asesora de Investigación Científica y Técnica (Spain), the Centro de Estudios de la Energía (Spain) and the Philips Research Laboratories (The Netherlands).

REFERENCES

1 A. Herrero, M. A. De la Rosa, J. Diez and J. M. Vega, *Plant Sci. Lett.*, 17 (1980) 409.
2 M. A. De la Rosa, A. J. Márquez and J. M. Vega, *Z. Naturforsch.*, (1981) in press.
3 S. T. Thompson, K. V. Cass and E. Stellwagen, *Proc. Nat. Acad. Sci. U.S.*, 72 (1975) 669.
4 M. G. Rossmann, D. Moras and K. W. Olsen, *Nature (London)*, 250 (1974) 194.
5 G. E. Schulz and R. H. Schirmer, *Nature (London)*, 250 (1974) 142.
6 M. Losada, M. G. Guerrero and J. M. Vega, in A. Trebst and H. Bothe (Editors), *Biochemistry and Physiology of Nitrogen and Sulfur Metabolism*, Springer, Berlin, 1981, p. 30.
7 M. A. De la Rosa, J. Diez, J. M. Vega and M. Losada, *Eur. J. Biochem.*, 106 (1980) 249.
8 M. A. De la Rosa, J. M. Vega and W. G. Zumft, *J. Biol. Chem.*, 256 (1981) 5814.
9 M. A. De la Rosa, J. Diez and J. M. Vega, *Rev. Esp. Fisiol.*, 36 (1980) 177.
10 M. G. Guerrero, K. Jetschmann and W. Völker, *Biochim. Biophys. Acta*, 482 (1977) 19.
11 S. S. Pan and A. Nason, *Biochim. Biophys. Acta*, 523 (1978) 297.
12 E. Kessler, W. Längner, I. Ludewig and H. Weichmann, *Studies on Microalgae and Photosynthetic Bacteria*, Japan. Soc. Plant Physiol., Tokyo, 1963, p. 7.
13 J. L. Bailey, *Techniques in Protein Chemistry*, Elsevier, Amsterdam, 2nd ed., 1967, p. 340.
14 F. D. Snell and C. T. Snell, *Colorimetric Methods of Analysis*, Van Nostrand, New York, 1949, p. 804.
15 D. Pompon, B. Guiard and F. Lederer, *Eur. J. Biochem.*, 110 (1980) 565.
16 D. Pompon and F. Lederer, *Eur. J. Biochem.*, 90 (1978) 563.
17 A. Relimpio, P. J. Aparicio, A. Paneque and M. Losada, *FEBS Lett.*, 17 (1971) 226.
18 J. L. Barea, J. M. Maldonado and J. Cárdenas, *Physiol. Plant.*, 36 (1976) 325.
19 N. K. Amy, R. H. Garrett and B. M. Anderson, *Biochim. Biophys. Acta*, 480 (1977) 83.
20 J. D. Choi and D. B. McCormick, *Arch. Biochem. Biophys.*, 204 (1980) 41.
21 T. Yubisui and M. Takeshita, *J. Biol. Chem.*, 255 (1980) 2454.
22 M. Gervais, F. Labeyrie, Y. Risler and O. Vergnes, *Eur. J. Biochem.*, 111 (1980) 17.
23 G. E. Schulz, R. H. Schirmer, W. Sachsenheimer and E. F. Pai, *Nature (London)*, 273 (1978) 120.
24 M. G. Rossmann, A. Liljas, C. I. Bränden and L. J. Banaszak, in P. D. Boyer (Editor), *The Enzymes*, Vol. 11, Academic Press, New York, 3rd ed., 1975, p. 62.

Journal of Chromatography, 235 (1982) 445–452
Elsevier Scientific Publishing Company, Amsterdam — Printed in The Netherlands

CHROM. 14,321

DETERMINATION OF PENTAZOCINE AND TRIPELENNAMINE IN BLOOD OF T'S AND BLUES ADDICTS BY GAS–LIQUID CHROMATOGRAPHY WITH A NITROGEN DETECTOR

MARY ANN MACKELL and ALPHONSE POKLIS*
Departments of Pathology and Pharmacology, St. Louis University School of Medicine, 1402 South Grand Blvd, St. Louis, MO 63104 (U.S.A.)
(Received August 26th, 1981)

SUMMARY

A procedure for the quantitative determination of pentazocine (T's) and tripelennamine (Blues) in blood obtained from T's and Blues addicts is described. The underivatized drugs were analyzed by gas–liquid chromatography with a nitrogen detector. The retention times relative to mepivicaine (internal standard) on OV-17 at 220°C were: tripelennamine 0.69 and pentazocine 1.77. The linear ranges of blood standards were: tripelennamine, 0.10–1.00 μg/ml; pentazocine, 0.50–5.0 μg/ml. For simultaneous analysis, the within-run and between-run CVs of tripelennamine were 5.6% ($n = 23$) and 13% ($n = 12$); and for pentazocine 5.2% ($n = 23$) and 9.9% ($n = 12$). Mean recoveries over the range of standards were: tripelennamine, 103% ± 2.5% ($n = 12$); pentazocine 77.8% ± 3.6% ($n = 12$).

INTRODUCTION

During the past four years, the abuse of pentazocine and tripelennamine, known as "T's and Blues", has become epidemic among intravenous drug addicts in many of the major cities of the midwest United States[1–3]. Several procedures applicable to the detection of the drugs in urine have been reported[3–5]; however, to date, no method had addressed the simultaneous detection of the drug combination in blood. Methods described for the specific determination of pentazocine have utilized spectrofluorometry[6,7], gas–liquid chromatography (GLC)[8–11], mass spectrometry[12] and radioimmunoassay[13].

The spectrofluorometric method lacks specificity due to presence of pentazocine metabolites. The radioimmunoassay is not commercially available and the preparation of pentazocine antibodies is beyond the capabilities of most toxicology laboratories. The GLC procedures usually involve derivatization for electron-capture detection[8–10] and are designed to determine pentazocine in blood or plasma at normal therapeutic concentrations of 10–50 ng/ml. T's and Blues addicts routinely inject from 4–10 times the therapeutic dose of pentazocine, and obtain blood concentrations well above the therapeutic range. Methods for the specific detection of tripe-

0021-9673/82/0000–0000/$02.75

lennamine have included GLC–mass spectrometry for metabolite studies[14] or GLC and ultraviolet spectrophometry for a massive overdose[15].

This communication presents a GLC procedure using a nitrogen detector which has suitable sensitivity for simultaneous detection of tripelennamine and pentazocine in blood obtained from T's and Blues addicts. The method may be applied to clinical or post mortem blood specimens. The drugs are chromatographed underivatized.

EXPERIMENTAL

Reagents

Benzene was found satisfactory from a commercial source, distilled in glass (Burdick & Jackson Labs., Muskegon, MI, U.S.A.). Isopropanol (2-propanol) was redistilled. Carbonate buffer, pH 11, was prepared by dissolving 21.0 g of sodium carbonate and 420.0 mg of sodium bicarbonate in sufficient distilled water to make 1 l. The pH was checked and adjusted by the addition of solid carbonate or bicarbonate as necessary. All other reagents were analytical (AR) grade. All glassware was acid-washed with hydrochloric acid (1 mol/l), and then silanized with 2% dimethyldichlorosilane (Sigma, St. Louis, MO, U.S.A.) in benzene.

Standards

Stock standards, 1.00 g/l, were prepared by separately dissolving 11.42 mg of tripelennamine hydrochloride (TP) (Ciba-Geigy, Ardsley, NY, U.S.A.) and 11.29 mg of pentazocine hydrochloride (PZ) (Winthrop, New York, NY, U.S.A.) in 10.0 ml of methanol. Intermediate standards, 0.100 g/l, were prepared by dilution of 1.00 ml of each stock standard with 10.0 ml of methanol. Mixed standards in blood were prepared daily by adding the following combinations of intermediate standards to 10-ml volumetric flasks and diluting to volume with drug-free blood: 10 μl of TP and 50 μl of PZ; 20 μl of TP and 100 μl of PZ; 50 μl of TP and 250 μl of PZ; and 100 μl of TP and 500 μl of PZ. The resultant blood standards contained the following concentrations (μg/ml of blood): 0.10 of TP and 0.50 of PZ; 0.20 of TP and 1.0 of PZ; 0.5 of TP and 2.5 of PZ; and 1.0 of TP and 5.0 of PZ.

Stock internal standard, 10.0 g/l, of the internal standard was prepared by dissolving 115.0 mg of mepivicaine hydrochloride (Breon, New York, NY, U.S.A.) in 10.0 ml of methanol. An intermediate standard, 0.025 g/l, was prepared by dilution of 50 μl of the stock standard with 10.0 ml of methanol. The extracting solvent containing the internal standard was prepared by diluting 1.00 ml of the intermediate standard with 500 ml of benzene–2-propanol (9:1).

Gas chromatography

All analyses were performed on a Perkin-Elmer Sigma 2 Gas Chromatograph equipped with a nitrogen detector (Perkin-Elmer, Norwalk, CT, U.S.A.). The detector response was recorded and integrated with a Perkin-Elmer Sigma 10 Data Station. The detector bead adjustment was 5.0 (2.26 A). Chromatography was performed on a glass column (1.8 m × 4 mm I.D.) packed with 3% OV-17 on Chromosorb W HP, 80–100 mesh (Alltech Assoc., Arlington Heights, IL, U.S.A.). The column was conditioned by temperature programming from 50°C at 2°C/min to 350°C,

which was held for 12 h before being connected to the detector. The temperatures were: injection port, 250°C; column, 220°C; and detector, 275°C. Gas flow-rates and/or pressures were: nitrogen carrier gas, 30 ml/min, 100 p.s.i.g.; air, 26 p.s.i.g.; and hydrogen, 12 p.s.i.g.

Under these conditions, the retention times were: tripelennamine, 2.7 min; mepivicaine (internal standard), 3.9 min; and pentazocine, 6.9 min. The relative retention times (RRT) of tripelennamine and pentazocine to the internal standards were 0.69 and 1.77, respectively.

Procedure

Pipet 2.0 ml of blood (samples, bood standards, and drug-free blood as a blank) into 15-ml glass culture tubes with PTFE-lined screw caps. Adjust the pH to *ca.* 11 by addition of 2.0 ml of carbonate buffer. Add 10 ml of benzene–2-propanol (9:1) *containing the internal standard*, and extract for 5 min. Centrifuge (1000 *g* for 3 min) and transfer the solvent (upper) layer to a second set of 15-ml screw-capped tubes. Add 5.0 ml of HCl (0.5 *N*), extract for 5 min, and after centrifugation, aspirate and discard the solvent (upper) phase. Add 0.5 ml of NaOH (5.0 *N*) to the acid extract to adjust the pH to 10–11 (check pH, and add extra NaOH dropwise if necessary), then add 5.0 ml of benzene–2-propanol (9:1) *without internal standard, extract* for 5 min and centrifuge. Transfer the solvent (upper) layer to a 10-ml test tube and dehydrate over anhydrous Na_2SO_4. Transfer the dried solvent to a 10-ml centrifuge tube add one drop of 1% ethanolic HCl and evaporate under dry nitrogen at 60°C to *ca.* 1.0-ml volume. Remove heat, and allow the remaining solvent to evaporate at room temperature under dry nitrogen. Dissolve the residue in 50 μl of methanol and inject 2–4 μl into the gas chromatograph. Rinse the syringe thoroughly between injections with HCl (1 *N*) mol/l followed by methanol to prevent carry-over. Routinely chromatograph methanol between every fourth analysis to check for carry-over or "ghosting".

Calculate the peak-area ratio (peak area of tripelennamine and/or pentazocine to that of mepivicaine internal standard) for each sample and determine the blood concentration by comparison to the peak-area ratios (relative peak areas) of the extracted standards.

RESULTS

Standard curves constructed from analyses of blood containing known concentrations of tripelennamine and pentazocine are presented in Fig. 1. The least-squares linear regression equations for tripelennamine and pentazocine were: y (peak area ratio, tripelennamine/mepivicaine) = $5.870x$ (tripelennamine, μg/ml) + 0.10, (r = 0.998); and y (peak area ratio, pentazocine/mepivicaine) = $0.9135x$ (pentazocine, μg/ml) − 0.22, (r = 0.999). The within-run coefficient of variation (c.v.) for tripelennamine (target concentration, 0.20 μg/ml) was 5.6% (n = 23) and that for pentazocine (target concentration, 1.0 μg/ml) was 5.2% (n = 23). Chromatograms of an extracted blood standard and blood obtained from a T's and Blues addict are presented in Figs. 2 and 3, respectively. The between-run C.V. calculated by three determinations on a single day for four successive weeks were: tripelennamine (target concentration, 0.20 μg/ml) 13% (n = 12); and pentazocine (target concentration,

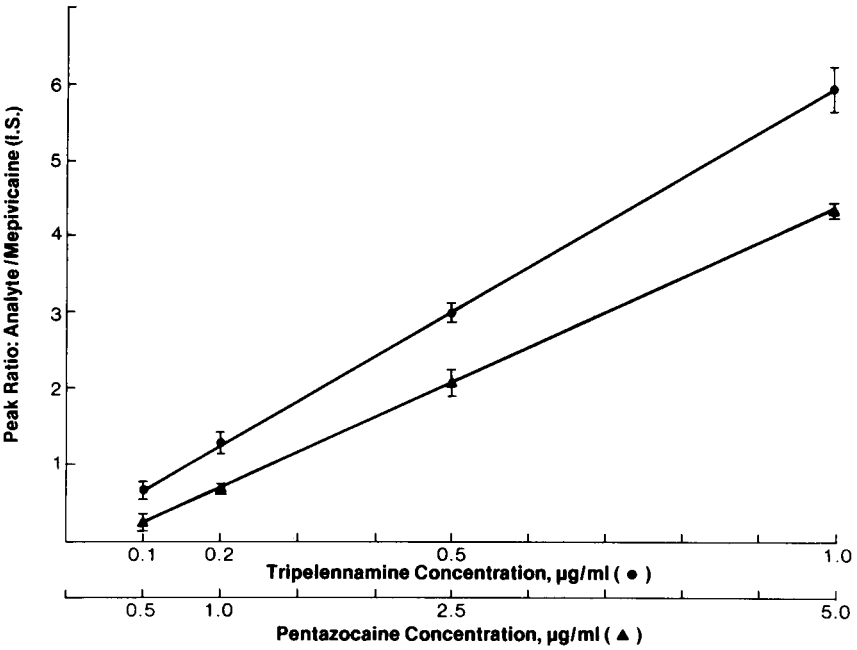

Fig. 1. Calibration curve for blood extracted standards of tripelennamine (●) and pentazocine (▲). Points represent the mean of three determinations, 2 S.D. in brackets.

0.50 µg/ml) 9.9% (n = 12). The absolute, uncorrected analytical recovery both for tripelennamine and pentazocine, calculated by comparison of peak areas obtained from supplemented blood samples with those of non-extracted standards, is pre-

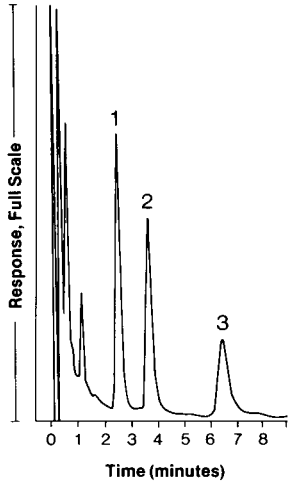

Fig. 2. Chromatogram of an extracted blood standard. Peaks: 1 = tripelennamine, 0.02 µg/ml; 2 = mepivicaine (I.S.); 3 = pentazocine, 0.50 µg/ml.

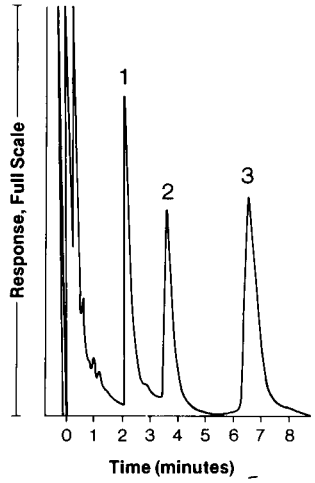

Fig. 3. Chromatogram of an extract of post mortem blood obtained from a T's and Blues addict. Peaks: 1 = tripelennamine, 0.20 µg/ml; 2 = mepivicaine (I.S.); 3 = pentazocine, 3.3 µg/ml.

sented in Table I. The mean recoveries over the concentration range of the standards for tripelennamine and pentazocine were: 103 % + 2.5 % and 77.8 % + 3.6 %, respectively. This incomplete recovery of pentazocine, as well as variations in aliquoting, were corrected by use of extracted blood standards and internal standard (mepivicaine).

TABLE I

RECOVERY OF TRIPELENNAMINE AND PENTAZOCINE ADDED TO BLOOD

Tripelennamine (μg/ml)			*Pentazocine (μg/ml)*		
Added	*Recovered**	*Recovery (%)*	*Added*	*Recovered**	*Recovery (%)*
0.10	0.105 ± 0.006	105 %	0.50	0.405 ± 0.01	81 %
0.20	0.21 ± 0.011	105 %	1.0	0.780 ± 0.03	78 %
0.50	0.50 ± 0.030	100 %	2.0	1.59 ± 0.07	79.5 %
1.0	1.02 ± 0.041	102 %	5.0	3.64 ± 0.17	72.8 %

* Mean ± S.D. (n = 3).

Thirty-two basic drugs which are commonly encountered in clinical or post mortem blood analyses (Table II) were screened for interference in the proposed assay by comparing the retention times of their non-extracted methanol solutions with that of tripelennamine, pentazocine and mepivicaine. Acidic drugs, as well as morphine and hydromorphone, were not screened because they would not be extracted under the alkaline conditions of the assay.

TABLE II

RELATIVE RETENTION TIMES (RRT) TO MEPIVICAINE OF 32 COMMON BASIC DRUGS SCREENED FOR INTERFERENCE

Drug	*RRT*	*Drug*	*RRT*
Amitriptyline	1.31	Medazepam	1.60
Cholordiazepoxide	4.48	Meperidine	0.30
Chlorpromazine	2.48	Methadone**	1.03
Cocaine*	1.70	Methaqualone*	1.69
Codeine	1.32	Nordiazepam	4.25
Chlorpheniramine***	0.70	Normeperidine	0.46
Desalkyl flurzazepam	3.50	Nortriptyline	1.55
Desipramine*	1.79	Oxazepam	2.24
Diazepam	3.06	Phencyclidine	0.44
Doxepin	1.56	Phendimetrazine	0.18
Flurazepam	6.30	Phenmetrazine	0.19
Haloperidol	> 6.00	Propoxyphene	1.15
Imipramine	1.48	Procaine	0.90
Ketamine	0.53	Quinine	> 6.00
Lidocaine	0.47	Thioridazine	> 6.00
Methapyrilene***	0.68	Tranylcypromine	0.18

* Chromatographs as pentazocine.
** Chromatographs as mepivicaine.
*** Chromatographs as tripelennamine.

Cocaine, desipramine and methaqualone, when injected simultaneously with pentazocine, produced a single peak. While these compounds are not resolved under the conditions of the assay, in our experience they have not represented a significant problem. Under the conditions of the assay cocaine is seldom detected in blood except in rare instances of drug overdose and methaqualone is not co-administered with T's and Blues by local addicts. To date, no case of T's and Blues abuse has also involved these drugs. Methadone elutes with mepivicaine internal standard. While methadone is commonly used in the treatment of heroin addiction, its use in the treatment of pentazocine dependency is controversial, since methadone's addiction potential is greater than that of pentazocine[16]. While performing post mortem toxicological analyses in over 40 T's and Blues cases we have not encountered methadone in any case. Chlorpheniramine and methapyrilene elute as tripelennamine. However, chlorpheniramine is seldom present in blood in detectable concentrations, and methapyrilene has been removed from the pharmaceutical market in the U.S.A. by the Food and Drug Administration due to its potential as a carcinogen. The other basic drugs in Table I did not interfere with the assay.

DISCUSSION

When 2 μl of the extracted standards are injected, this method gives a linear response for tripelennamine and pentazocine over the range of concentrations presented, 0.10–1.0 mg/ml and 0.5–5.0 mg/ml, respectively. If the concentration of either drug in a test sample fell below the standards the chromatogram was repeated using 4 μl of extract.

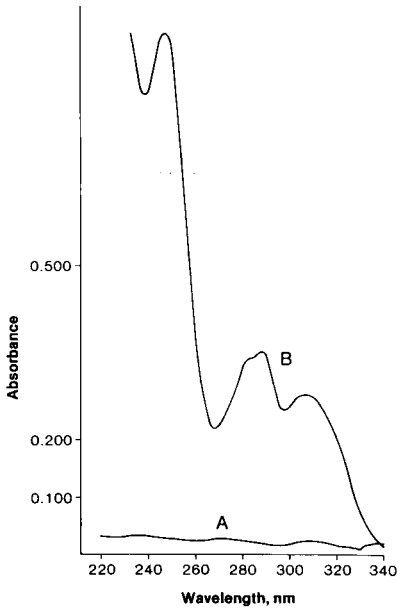

Fig. 4. Ultraviolet absorption spectrum of an extract (0.5 *N* H_2SO_4) of liver obtained from T's and Blues addict. (A) Blank of 0.5 *N* H_2SO_4 extract of drug-free liver; (B) characteristic mixed spectra of tripelennamine, 308 nm and 243 nm, and pentazocine, 288 nm.

T's and Blues addicts dissolve various ratios of tripelennamine and pentazocine tablets in water to produce an injectable solution[3]. Therefore there is a wide variation in the amount of each drug administered and the resultant blood concentrations. Concentrations of tripelennamine and pentazocine in blood obtained from T's and Blues addicts generally range from 0.1–0.5 μg/ml and 0.25–3.5 μg/ml, respectively. No constant ratio of tripelennamine to pentazocine has been observed in blood samples analyzed in our laboratory. In a few instances, extraction of a second blood sample with appropriate adjustment of the internal standard and concentration into 25 μl of methanol has been necessary to determine low blood concentrations of either drug. While the method is less sensitive than previous GLC pentazocine methods, it does permit simultaneous quantitative determination of both drugs at blood concentrations observed in T,s and Blues addicts.

The method is not presented as a general blood drug screening procedure. When available, urine should be analyzed prior to the blood analysis in order to determine the presence of other drugs[3–5]. For post mortem analysis when urine is not available, we recommend that drug screening be performed on liver specimens. Both tripelennamine and pentazocine may be readily determined in liver by direct extraction into diethylether[17]. Tripelennamine and pentazocine produce a characteristic mixed ultraviolet absorption spectrum in 0.5 *N* H_2SO_4 extract of liver (Fig. 4). The maxima at 306–310 nm and 238–243 nm are typical of tripelennamine, and the maximum at 286–289 nm is a slightly distorted pentazocine spectrum. The acid extract is back-extracted into organic solvent and subjected to thin-layer chromatographic analysis to resolve the mixture and/or confirm the presence of other basic drugs. If blood is the only specimen available, we routinely perform temperature-programmed GLC drug screening analysis on SE-30 liquid phase as described by Peel and Perrigo[18,19]. Those drugs which may interfere with the presented T,s and Blues procedure (chlorpheniramine, cocaine, desipramine, methadone, methapyrilene and methaqualone), if present, are readily detected and resolved from tripelennamine and pentazocine by any one of these screening methods.

REFERENCES

1 C. V. Showalter and L. Moore, *J. Amer. Med. Ass.*, 239 (1978) 1610.
2 *Proceedings, Community Correspondents Group, 8th Meeting, Washington, DC, June 4–6, 1980*, National Institute of Drug Abuse, Rockville, MD, 1980.
3 A. Poklis and P. L. Whyatt, *J. Forensic Sci.*, 25 (1980) 72.
4 K. K. Kaistha and R. Tadrus, *J. Chromatogr.*, 155 (1978) 214.
5 R. W. Reid and C. M. Gerbeck, *Clin. Chem.*, 27 (1981) 10.
6 B. A. Berkowitz, J. H. Asling, S. M. Shnider and E. L. Way, *Clin. Pharmacol. Therap.*, 10 (1969) 320.
7 K. O. Borg and A. Mikaelsson, *Acta Pharm. Suecica*, 7 (1970) 673.
8 K. A. Pittman and C. Davison, *J. Pharm. Sci.*, 62 (1973) 765.
9 H. Brötell, H. Ehrsson and O. Gyllenhaal, *J. Chromatogr.*, 78 (1973) 293.
10 S. E. Swezey and T. F. Blaschke, *J. Chromatogr.*, 154 (1978) 256.
11 S. P. James and R. H. Waring, *J. Chromatogr.*, 78 (1973) 417.
12 S. Agurell, L. O. Boreus, E. Gordon, J. E. Lindgren, M. Ehrnebo and U. Lonroth, *J. Pharm. Pharmacol.*, 26 (1974) 1.
13 T. A. Williams and K. A. Pittman, *Res. Commun. Chem. Pathol. Pharmacol.*, 7 (1974) 119.
14 N. K. Chaudhuri, O. A. Sevando, M. J. Manniello, R. C. Luders, D. K. Chao and M. F. Bartlett, *Drug Metabol. Disposition*, 4 (1976) 372.
15 M. Bayley, F. M. Walsh and M. J. Valaske, *J. Forensic Sci.*, 20 (1975) 539.

16 C. V. Showalter, *J. Amer. Med. Ass.*, 244 (1980) 1224.
17 L. R. Goldbaum and T. J. Domanski, in A. Stolman (Editor), *Progress in Chemical Toxicology*, Vol. 2, Academic Press, New York, 1965, p. 221.
18 H. W. Peel and B. Perrigo, *Canad. Soc. Forensic Sci. J.*, 9 (1975) 69.
19 B. Perrigo and H. W. Peel, *J. Chromatogr. Sci.*, 19 (1981) 219.

Journal of Chromatography, 235 (1982) 453–459
Elsevier Scientific Publishing Company, Amsterdam - Printed in The Netherlands

CHROM. 14,334

HIGH-PERFORMANCE LIQUID CHROMATOGRAPHIC PROCEDURE FOR SEPARATION AND QUANTIFICATION OF ZEATIN AND ZEATIN RIBOSIDE FROM PEARS, PEACHES AND APPLES

E. A. STAHLY* and D. A. BUCHANAN
USDA-ARS, Tree Fruit Research Laboratory, 1104 N. Western Avenue, Wenatchee, WA 98801 (U.S.A.)
(Received September 7th, 1981)

SUMMARY

A method for purification of zeatin and zeatin riboside from plant extracts for quantification by high-performance liquid chromatography (HPLC) is described. Initial separation is by chromatography on insoluble polyvinylpyrrolidone (PVP) and C_{18} Porasil B columns, followed by thin-layer chromatography on silica gel H. The final separations and quantification are done with methanol–water (pH 7) and then acetonitrile–water (pH 3) on μBondapak C_{18} analytical HPLC columns.

INTRODUCTION

To measure the zeatin content of developing fruit of pear, peach, and apple, we have developed a purification procedure adaptable to final quantification of zeatin (Z) and zeatin riboside (ZR) by high-performance liquid chromatography (HPLC). HPLC has been frequently used in the separation of cytokinins from plant extracts[1–11], but only Arteca *et al.*[1] and Dekhuijzen[4] used HPLC for final quantification. Hahn[5], Kannangara *et al.*[8] and Morris *et al.*[10] showed chromatograms of cytokinin separation, but the peaks were difficult to quantify, and bioassay was generally relied upon. Buban *et al.*[2] and Monselise *et al.*[9] used silica columns, but peaks were not satisfactory for quantification.

The disadvantage of bioassays and some of the problems associated with derivatization of cytokinins for determination by gas chromatography (GC) have been pointed out by others[5,11,12]. There are a number of advantages associated with the use of HPLC for quantifying Z and ZR: relatively large sample volumes can be injected; derivatization is not necessary; peaks with elution times similar to known cytokinins can be recovered and bioassayed; and HPLC is faster and more precise than bioassay.

The non-specificity of the HPLC UV-detector is a disadvantage. While as little as 5 ng Z can be easily detected, numerous UV absorbing coextractives of Z generally occur in plant extracts and mask the presence of Z. The problem is to remove those impurities that strongly absorb in the UV and interfere with the detection of Z and ZR.

A major class of UV interferants, phenols, can be at least partially excluded

0021-9673/82/0000–0000/$02.75

from plant extracts by chromatography on insoluble polyvinylpyrrolidone (PVP)[1,2,8,9,12–14] and the dry weight of the extract reduced as well[8,14]. PVP chromatography is an attractive first step[8], since the extract is generally aqueous. The buffered aqueous fraction from PVP containing cytokinins can be passed over a column of C_{18} Porasil B*[,10] and the cytokinins concentrated on the column while other impurities such as sugars are not retained. This step is more rapid and more nearly quantitative than partitioning with *n*-butanol and does not require handling large volumes of organic solvents.

This report describes the use of columns of PVP and C_{18} Porasil B to initially separate and concentrate the cytokinins Z and ZR from plant extracts and the subsequent steps necessary to allow final quantification by HPLC.

MATERIALS AND METHODS

Initial purification

Five to 10 ml of the filtered aqueous fraction from an alcoholic extract of small pear fruit, equivalent to 33 g fresh weight (f.w.) were adjusted to pH 3.5 and loaded on top of a 1.9 × 20 cm column of PVP (Polyclar AT, GAF Corp.). PVP was prepared by suspending it in distilled water several times and decanting the fines. After the column was prepared, it was washed with several column volumes of the developing buffer, 0.013 *M* KH_2PO_4, pH 3.5[15], prior to use. The column had a flow-rate of about 3 ml min^{-1}. The extract was washed slowly onto the column with the developing solvent. The first 40 ml of eluent, including the extract volume, were discarded and the next 80 ml, which contained Z and ZR, collected and the pH adjusted to 7.

The entire 80 ml were then passed through a 0.8 × 4.0 cm column of C_{18} Porasil B (Waters Assoc.) which retained and concentrated the Z and ZR[10]. This column was prepared by slurrying 1 g of C_{18} Porasil B in acetonitrile, pouring the slurry into the column, and allowing it to settle by gravity. Several more column volumes of acetonitrile were pumped through the column with sufficient pressure to generate a flow-rate of about 3 ml min^{-1}, before changing over to distilled water prior to the introduction of the eluent from the PVP column. After the eluent had passed through the column, the column was washed with about 5 ml of distilled water to remove the initial buffer; 10 ml of 5% acetonitrile buffered at pH 7 with 0.01 *M* $(NH_4)_2HPO_4$ to remove the most polar compounds; and finally with 5 ml distilled water to remove the acetonitrile and buffer. Zeatin and ZR were eluted with 4 ml of ethanol and the ethanol removed under reduced pressure. The residue was dissolved in 3 × 100 μl methanol and stripped on a 500-μm silica gel H (silica gel 60H, EM Reagents) thin-layer plate that was previously washed in methanol–acetone (1:1) and then activated at 110°C for 30 min. The plate was developed in water saturated *n*-butanol in an ammonia atmosphere with appropriate standards. After development the standards were located with a 254-nm UV lamp while the plate was still moist. Zones comparable to the Z and ZR standards were scraped from the plate after it was dried. The silica gel was eluted four times with 2 ml of 90% methanol and the

* Trade names and the names of commercial companies are used in this publication solely to provide specific information. Mention of a trade name or manufacturer does not constitute a guarantee or warranty of the product by the U.S. Department of Agriculture, nor an endorsement by the Department over other products not mentioned.

methanol taken to dryness under reduced pressure. The residue was redissolved in 200 μl of the mobile phase for the first HPLC separation.

HPLC analysis

We used a Waters Associates Model 244 liquid chromatograph equipped with a 6000 p.s.i. pump and Model 440 ultraviolet fixed wavelength detector (254 or 280 nm) and a Valco injector with a 100-μl loop. The columns used were Waters Associates μBondapak C_{18}, 300 × 3.9 mm I.D. All separations were done isocratically. Peak areas were measured with a single-channel computing integrator (Spectra-Physics Minigrator).

The mobile phase for the initial separation was methanol–water (20:80) buffered at pH 7 with triethylammonium bicarbonate (TEAB)[7] with a flow-rate of 1.0 ml min^{-1}.

Zones with the same elution time as Z and ZR were collected and taken to dryness under reduced pressure. Even though the peaks were not readily apparent during separation on the first HPLC column, zones corresponding to those of Z and ZR standards could be collected and Z and ZR recovered reproducibly. The residue was dissolved in 200 μl of the second mobile phase and 100 μl chromatographed on the second column with a mobile phase of acetonitrile–water (8.5:91.5) buffered at pH 3 with 0.02 *M* ammonium acetate, with a flow-rate of 1.0 ml min^{-1}. The alcoholic extract from small pear fruits (33 g f.w.) treated as described yielded a chromatogram with easily quantifiable peaks of Z and ZR (Fig. 2). When the procedure described was found to yield a relatively clear chromatogram with quantifiable peaks of Z and ZR, each step was examined for recovery and reproducibility using Z and ZR standards of 50, 100, 200, 400, and 800 ng. Finally, Z and ZR standards were taken through the entire procedure and the results examined by linear regression.

RESULTS AND DISCUSSION

PVP

The advantages and usefulness of PVP for purifying and initially separating plant extracts are well documented[1,2,8,9,13,14]. We agree with Kannangara *et al.*[8] that PVP is ideal for the initial purification of plant extracts. However, the columns must be carefully prepared and the pH carefully controlled to keep Z and ZR in the expected elution volume. Properly used, little loss of Z or ZR is anticipated for this step[9].

C_{18} Porasil B

There are a number of advantages in using a small open column of C_{18} Porasil B. The column used did not conform to the general rule that relates column height to column width because the shorter column allowed a flow-rate of about 3 ml min^{-1} without the necessity of high pressure. Concentration and recovery of Z and ZR from this column is preferable to exhaustive solvent extraction, which, by its nature, leads to some losses and requires handling and removal of large volumes of solvent. Thus, the C_{18} Porasil B column saves time, energy, and solvent, and elution of Z and ZR from it is essentially quantitative. The column can be manipulated to be more selective than solvent extraction since many substances which interfere with Z determi-

nation are coextracted with Z into *n*-butanol. Sugars and very polar compounds are not retained by the C_{18} Porasil B column. By using a column with the same functionality as the analytical columns, those compounds irreversibly bound in the C_{18} phase can be removed and prolong the analytical column life.

Recoveries with the standard deviations of Z and ZR standards passed through PVP and C_{18} Porasil B were 90.3 ± 5.1% and 96.7 ± 4.7%, respectively.

Thin-layer chromatography

Adsorption chromatography on silica gel was a technique with another mechanism to separate Z and ZR from interfering coextractives. The first problem we encountered was finding a solvent that would completely remove Z and ZR from the origin and then separate them as much as possible from other UV absorbing compounds. Chromatography on silica gel H with water saturated *n*-butanol in an ammonia atmosphere was effective for this purpose. Z and ZR were compact spots or zones at R_F 0.70 and 0.45, respectively, with these conditions. A more difficult problem was recovery of Z and ZR from silica gel. Best results were achieved by preparing our own plates from silica gel H as described and eluting with 90% methanol. Recoveries and standard deviations for Z and ZR under these conditions were 80.4 ± 4.4% and 78.5 ± 6.1%, respectively.

This step was slow, but effective for separating Z and ZR from other materials that interfered with final separation and quantification by HPLC. We found no substitute for it.

HPLC

The isocratic mobile phase compositions chosen for the two separations provided different, but easily reproducible conditions to isolate finally and quantify Z and ZR[8]. The dedicated columns can be easily and quickly cleaned by increasing the solvent strength prior to equilibration for another sample. The use of TEAB[7] to adjust the pH of the first mobile phase was important because no solvent residue was left after evaporation. The sample residue was easily dissolved in the second mobile phase for injection on the second column. The usefulness of two columns with the same functionality but with different mobile phases[8] provided the selectivity necessary for separating Z and ZR from interfering substances on the first column and then quantifying them in a relatively clear area of the chromatogram from the second column. This procedure is effective as well as quicker and simpler than the commonly used Sephadex separations[2–4,6–9]. Recoveries and standard deviations of Z and ZR standards through these two columns were 82.2 ± 8.9% for Z and 88.6 ± 10.2% for ZR.

A series of standards of Z and ZR were analyzed by the procedure described and the recovery data related to the initial amounts by linear regression. Ninety-five percent confidence bands were then calculated for each line (Fig. 1a and 1b). This information suggests that the amount of plant material chosen for this type of analysis should contain at least 100 ng of Z or ZR. More accurate determinations of Z or ZR could be made near the midpoint of their recovery curves, which in this case was 400 ng. The regression lines for both Z and ZR standards accounted for 98% of the variability in recovery of Z and ZR attributable to a change in the initial amount of each.

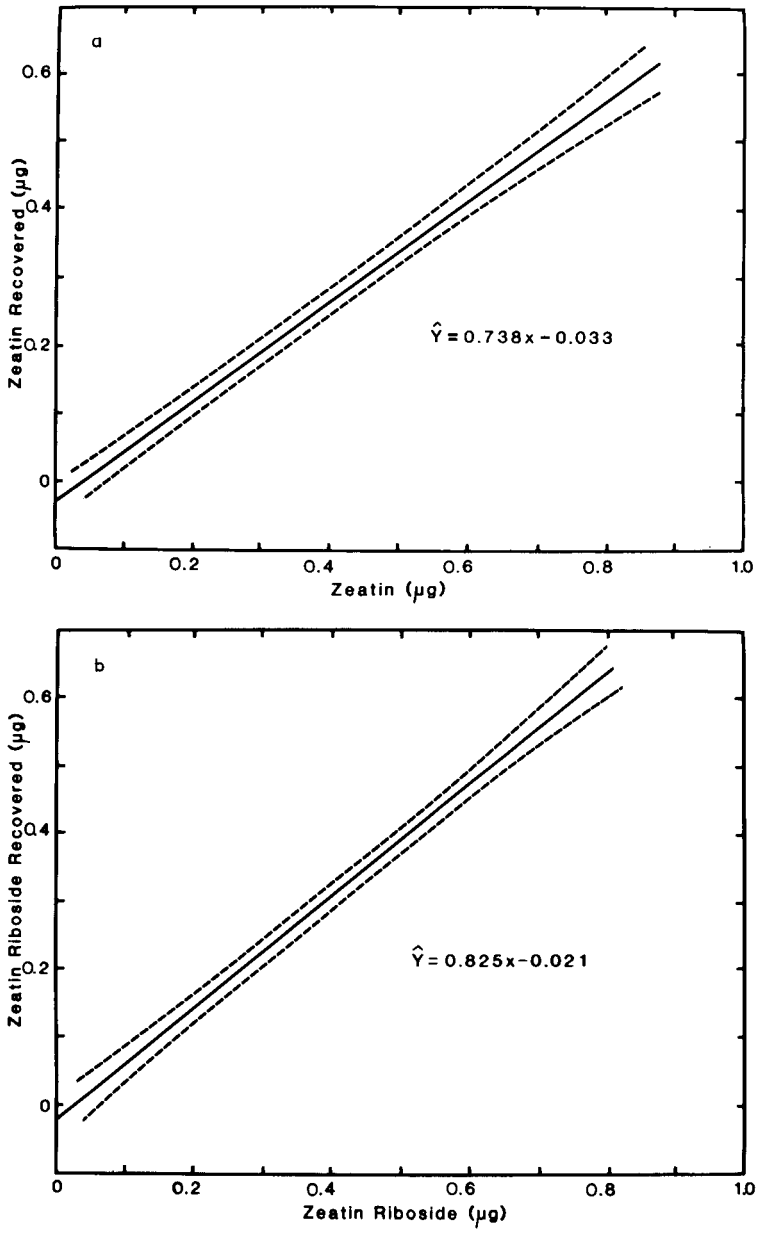

Fig. 1. Regression lines for recovery with 95% confidence bands for zeatin (a) and zeatin riboside (b) standards through purification procedure described in text.

The regression lines with their 95% confidence bands, once constructed, can be used to calculate sample unknowns. Preferably a minimum of two or three determinations can be done for each experimental sample. Then the amount of Z or ZR with its confidence interval can be taken from the appropriate regression line.

A pear fruit extract carried through the procedure described yielded a chroma-

togram with two peaks with retention times corresponding to authentic *trans*-zeatin and *trans*-zeatin riboside (Fig. 2b). When a similar extract was "spiked" with Z and ZR, and carried through the same procedure, peaks in the Z and ZR zone were enhanced (Fig. 2c). Quantification of the two peaks at 254 nm and 280 nm gave the same values for zeatin, indicating the presence of only one UV absorbing compound in that peak. There was a slight discrepancy between values for ZR suggesting there may have been another peak associated with ZR in the pear extract. The peaks were active in an *Amaranthus caudatus* bioassay[16].

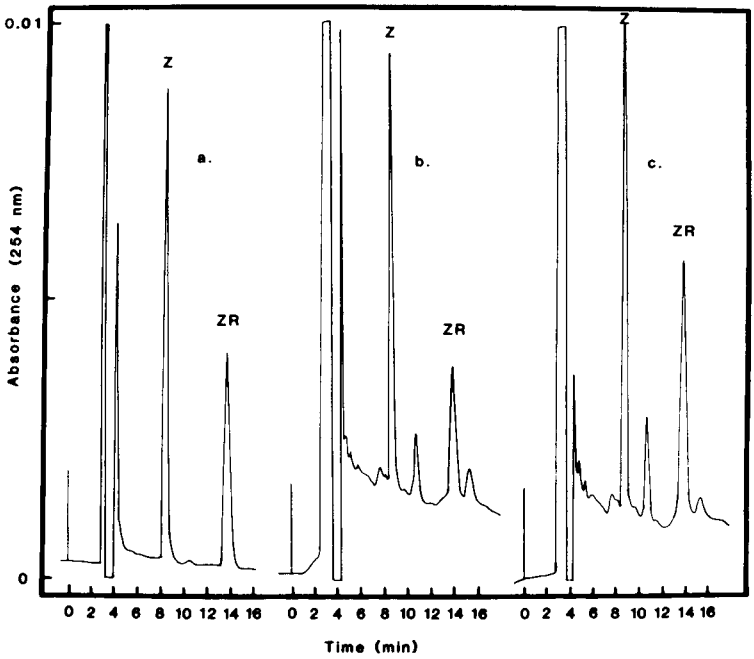

Fig. 2. Separation of zeatin and zeatin riboside standards (a), from pear fruit extract (b), and pear fruit extract spiked with zeatin and zeatin riboside (c) by reversed-phase HPLC. Column: μBondapak C_{18} (300 × 3.9 mm I.D.). Flow-rate: 1 ml min^{-1}. Mobile phase: acetonitrile–water (8.5:91.5) buffered at pH 3 with 0.01 *M* ammonium acetate.

After the procedure was developed, it was further evaluated by making duplicate ethanolic extracts of 127-g f.w. samples of small apple fruits from about 50 days after bloom. One extract was separated into three equal subsamples and the other into two subsamples for analysis. Zeatin estimates for the triplicate samples were 3.3, 2.9, and 2.9 ng/g f.w. and for the duplicate samples 2.8 and 2.7 ng/g f.w. The ZR peak was not adequately separated from a strongly absorbing impurity for the integrator to make an accurate estimate. However, peak heights from the duplicate samples were measured to be about one and one-half times those from the triplicate samples.

This procedure was useful for separating Z and ZR in extracts of small pear and apple fruits. Interfering constituents of extracts change with plant tissue chosen as well as the stage of development or physiological state of the plant material, so

adjustments may be necessary to maintain Z and ZR in relatively clear areas of the final chromatogram. The changes necessary can usually be made in the TLC step by changes in the developing solvent. Some manipulation of the composition of the mobile phases for the HPLC columns can also be made to shift Z and ZR into clear areas of the final chromatogram.

The procedure described avoids extremes of pH and has a minimum number of steps. Recovery through the entire system was reproducible. Any step could be omitted if the extract warranted. Each step has sufficient latitude for modification, so the method could be adapted to other plant extracts. By adjusting conditions, starting with PVP separation, abscisic acid (ABA), indoleacetic acid (IAA), and gibberellins may also be isolated. For instance, we found ABA had an elution volume of 100 ml from PVP as we used it, and could easily be included with the cytokinins fraction.

The number of steps could probably be reduced further through the use of a preparative HPLC column[11] in place of TLC and the first HPLC analytical column. Another option that may be promising for reducing the number of steps is the use of an analytical column with some residual hydroxyl sites, perhaps 10–20%, in place of TLC and the first HPLC column.

ACKNOWLEDGEMENTS

The authors thank the Washington State Tree Fruit Research Commission for their financial support; Dr. G. Richardson, Statistician, USDA/AR-W, Fort Collins, CO, for statistical advice; and Dr. R. Kammereck, Washington State University, Tree Fruit Research Center, Wenatchee, WA, for helpful suggestions.

REFERENCES*

1 R. N. Arteca, B. W. Poovaiah and O. E. Smith, *Plant Physiol.*, 65 (1980) 1216.
2 T. Buban, A. Varga, J. Tromp, E. Knegt and J. Bruinsma, *Z. Pflanzenphysiol.*, 89 (1978) 289.
3 M. G. Carnes, M. L. Brenner and C. R. Anderson, *J. Chromatogr.*, 108 (1975) 95.
4 H. M. Dekhuijzen, *Physiol. Plant.*, 49 (1980) 169.
5 H. Hahn, *Plant Cell Physiol.*, 17 (1976) 1053.
6 J. A. Holland, E. H. McKerrell, K. J. Fuell and W. J. Borrows, *J. Chromatogr.*, 166 (1978) 545.
7 R. Horgan and M. R. Kramers, *J. Chromatogr.*, 173 (1979) 263.
8 T. Kannangara, R. C. Durley and G. M. Simpson, *Physiol. Plant*, 44 (1978) 295.
9 S. P. Monselise, A. Varga, E. Knegt and J. Bruinsma, *Z. Pflanzenphysiol.*, 90 (1978) 451.
10 R. O. Morris, J. B. Zaerr and R. W. Chapman, *Planta*, 131 (1976) 271.
11 M. L. Brenner in N. B. Mandava (Editor), *Plant Growth Substances*, A.C.S. Symposium Series 111, 1979, Ch. 8, p. 221.
12 A. Zelleke, G. C. Martin and J. M. Labavitch, *J. Amer. Soc. Hort. Sci.*, 105 (1980) 50.
13 N. L. Biddington and T. H. Thomas, *J. Chromatogr.*, 75 (1973) 122.
14 J. L. Glenn, C. C. Kuo, R. C. Durley and R. P. Pharis, *Phytochemistry*, 11 (1972) 345.
15 N. L. Biddington and T. H. Thomas, *J. Chromatogr.*, 121 (1976) 107.
16 N. L. Biddington and T. H. Thomas, *Planta*, 111 (1973) 183.

* *Editor's note:* See also E. M. S. MacDonald, D. E. Akiyoshi and R. O. Morris, *J. Chromatogr.*, 214 (1981) 101, and G. C. Martin, R. Morgan and I. M. Scott, *J. Chromatogr.*, 219 (1981) 167.

Journal of Chromatography, 235 (1982) 461–470
Elsevier Scientific Publishing Company, Amsterdam — Printed in The Netherlands

CHROM. 14,333

RAPID, SPECIFIC METHOD FOR DIETHYLSTILBESTROL ANALYSIS USING AN IN-LINE PHOTOCHEMICAL REACTOR WITH HIGH-PERFORMANCE LIQUID CHROMATOGRAPHY AND FLUORESCENCE DETECTION

A. T. RHYS WILLIAMS* and S. A. WINFIELD
Perkin-Elmer Limited, Post Office Lane, Beaconsfield, Buckinghamshire, HP9 1QA (Great Britain)
and
R. C. BELLOLI
Department of Chemistry, California State University, Fullerton, CA 92634 (U.S.A.)
(Received September 7th, 1981)

SUMMARY

Low ppb* levels of diethylstilbestrol in biological samples of human and animal origin can be determined using a unique in-line separation–photoreaction–fluorescence detection analytical system. After a very simple extraction procedure, the diethylstilbestrol is separated from interfering substances by high-performance liquid chromatography, photoconverted to a fluorescent product, and detected by fluorescence spectroscopy at optimised excitation–emission wavelengths. A sample can be extracted and analysed in less than 1 h.

INTRODUCTION

Despite the fact that it is a known carcinogen, diethylstilbestrol (DES, I), 4,4′-(1,2-diethyl-1,2-ethenediyl)-bis-(*E*)-phenol, is used for both human and animal applications because of its estrogenic activity[1]. It is one of the cheapest of the synthetic estrogens to produce and is probably the most controversial. It has been banned from use in animal feeds in the U.S.A. and in many European countries[2]. However, its efficiency in promoting weight-gain is so high that illegal uses persist and the detection of DES continues to be a major concern[2].

Residues of DES expected in animal tissues and fluids from its use as a growth promoting agent can be as low as the ng/g (ppb) range[3]. Two analytical methods that have been found to be sufficiently sensitive to determine such amounts are radioimmunoassay[4] and gas chromatography (GC) with an electron-capture detector (ECD)[5,6] or with mass spectrometric (MS) detection[7]. Nanogram levels of DES have also been detected by thin-layer chromatography (TLC) using sulphuric acid-induced fluorescence[8] or the fluorescence of the dansyl derivative[9–12].

* Throughout this article, the American billion (10^9) is meant.

0021-9673/82/0000–0000/$02.75

The BP[13] and USP[14] methods for determining large quantities of DES, such as in DES tablets, rely on the well known transformation of DES, I, into a fluorescent tricyclic compound, 3,4,4a,4b,5,6-hexahydro-3,6-dioxo-9,10-diethylphenanthrene, II (eqn. 1)[15,16]:

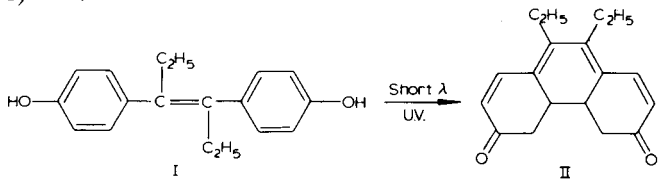

I II (1)

Using this specific photochemical transformation, improved analytical methods have been published for the determination of large[17] as well as very small[18,19] (ppb) levels of DES. The ppb level determinations involve, in one case[18], a very lengthy procedure for biological samples, and, in the other case[19], two-dimensional TLC with visual detection.

The currently available, sensitive methods for determining lower levels of DES suffer from a number of disadvantages. Radioimmunoassay is a complicated and time consuming procedure. The GC–EC and GC–MS methods[6] involve the preparation of derivatives and lengthy extraction and clean-up procedures. Similar disadvantages apply to the TLC procedures[8,12].

In this paper is presented a method for DES analysis which represents a great improvement in speed and simplicity while still being able to detect ppb levels. In our system, the output from an high-performance liquid chromatographic (HPLC) column is fed directly into an in-line photochemical reactor where the reaction in eqn. 1 takes place. The continuously flowing stream is then allowed to pass through the LC flow cell of a fluorescence spectrometer whose excitation and emission monochromators have been set to give a maximum response for the DES photoproduct, II. Extensive sample preparation is not necessary and the entire chromatography is complete, including a column flush cycle, in less than 40 min.

EXPERIMENTAL

Solvents and reagents

Water was distilled, deionized, and pH-adjusted to 3.5 with phosphoric acid. Diethyl ether (Aristar, 99.7%) was distilled through a 30-cm Vigreux column. Acetonitrile (BDH, "for liquid chromatography") was used without further purification. Phosphate buffer solution was 0.1 *N*, pH 7.4 and made from BDH phosphate buffer, 0.1 *M*. Ethanol was BDH (AnalaR, 99.7–100%) and was used without further purification. The acetonitrile–water mixture and the acetonitrile itself were thoroughly degassed under vacuum.

A DES (donated by S. Dixon, Agricultural Research Council, Great Britain) solution was made by dissolving 1.0 mg in 20 ml of ethanol. This solution was diluted 1/100 to give a solution containing 0.5 ng/μl of DES. This diluted solution was used for the experiments described in this paper.

A hexestrol (HES, II) (donated by S. Dixon, Agricultural Research Council, Great Britain) solution was made up in a similar manner with 1.1 mg in 20 ml of ethanol and diluted accordingly.

Apparatus

The liquid chromatograph was a Perkin-Elmer Series 3B model which contained an acetonitrile–water (50:50) mixture in one pump module and pure acetonitrile in the second pump module. Sample injection was made via a 20-μl loop injector (Rheodyne). The column used was a 25 × 0.45 cm RP-8 (reversed phase octylsilyl) column (Perkin-Elmer Serial Number P 798). The design of the in-line photoreactor has been described by Twitchet *et al.*[20].

The stream, including the DES photoproduct, was passed into an LC flow cell incorporated into a Perkin-Elmer Model 3000 fluorescence spectrometer. Excitation and emission monochromators were set at 280 and 390 nm, respectively, with both slits set at 10 nm. Chromatograms were recorded on a Parker-Elmer Model 56 recorder (Fig. 1).

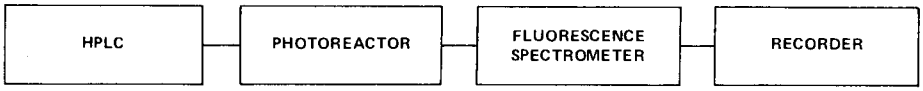

Fig. 1. Diagram of analytical system.

Sample preparation

DES extraction from human urine. To 10 ml of human urine (several sources used) in a separating funnel was added the appropriate amount of DES in ethanol. This mixture was extracted with 10 ml of diethylether. (Note: the initial addition of 6 *N* HCl to the urine, as specified in ref. 21 upon which this procedure is based, gave difficult emulsions.) The ether layer was then washed with 10 ml of the phosphate buffer solution. The ether solution was filtered through a cone (spatula tip amount) of anhydrous sodium sulphate into a 5-ml test-tube. The separating funnel was washed with 3 ml of diethyl ether and this was added, through filtration, to the original ether extract. The ether extract was evaporated to dryness with a warm water-bath. A 100-μl volume of ethanol was added to the tightly stoppered test-tube and this solution was used for the analyses described later.

DES addition to cow urine, plasma, and sera extracts. Ethanol and DES in ethanol were added to test-tubes containing extracts from cow urine, plasma, or sera to give a total volume of 100 μl. The extracts were supplied to us by S. Dixon, Agricultural Research Council, Great Britain and were prepared in the following manner. To 0.5 ml of urine, plasma, or sera (pretreated with Sigma β-glucuronidase) are added 2.5 ml of double distilled water. This solution is extracted with 5 ml of diethylether. After homogenization, the layers are separated and the ether layer is frozen in a dry ice–acetone bath. The ether extract is decanted from the frozen layer and evaporated to dryness.

Chromatography procedure

A sample is injected into the liquid chromatograph via a 20-μl loop injector. Isocratic elution is then performed with an acetonitrile–water (50:50) (pH 3.5) mixture (pump A) at a flow-rate of 1.5 ml/min. When the DES photoproduct II has completely eluted (about 10 min), the chromatograph is switched to pump B which is set to flush pure acetonitrile at a flow-rate of 2.0 ml/min through the column. After 20 min of flushing, pump A is re-activated and the 50:50 mixture is allowed to flow

through the column for 10 min. After this equilibration period, the recorder baseline has become re-established at its original setting and a subsequent analysis can be performed. Total chromatography time is about 40 min.

The extraction procedures given above do not completely clean-up the biological samples. Therefore, with continuous heavy use, it is recommended that the column be flushed overnight with a small flow (0.1 ml/min) of acetonitrile and the column frits be cleaned periodically to prevent excessive pressure build-up in the system.

Determination of excitation–emission wavelengths for DES

A solution of DES was placed in a fluorescence spectrometer (Perkin-Elmer Model 3000) and irradiated at 280 nm for 5 min (15-nm slit). Using 280 nm (2.5-nm slit) as the excitation wavelength, the emission spectrum (5.0-nm slit) of the irradiated DES solution was recorded between 300–500 nm. The emission spectrum (300–500 nm), excitation 280 nm, of the same DES solution before irradiation was also recorded.

RESULTS AND DISCUSSION

Excitation–emission wavelengths

The selection of optimum excitation and emission wavelengths will give the greatest sensitivity for the fluorescence detection of the desired photoproduct II, while minimizing or eliminating altogether interfering peaks. Therefore, the emission spectrum from 300–500 nm, using excitation at 280 nm, was recorded for DES solutions before and after irradiation at 280 nm. Fig. 2a and 2b clearly show that DES is converted to a fluorescence photoproduct, presumably II, which has a maximum emission at 390 nm. DES itself has only a small absorption under these conditions. The fluorescence detection in the experiments to be described were, therefore, all done at excitation and emission wavelengths of 280 and 390 nm, respectively.

Calibration curve for pure DES solutions

The standard DES solution (0.5 ng/μl) was diluted to 0.75, 0.50 and 0.25 of its original concentration. Each diluted sample and the original were subjected to liquid chromatography, photoreaction and fluorescence detection. The peak heights were graphed versus the dilution factor to give the graph in Fig. 3. These 20-μl injections place from 10 to 2.5 ng of DES onto the column and the analytical system responds in a linear fashion to this successful attempt to construct a calibration curve for low ng amounts of pure DES in ethanol solution. The single peak (other than a short retention peak ethanol) for the DES photoproduct appears in 9.5 min but is completely absent if the experiment is repeated with the lamp in the photoreactor turned off. This "lamp on–lamp off" effect[20] is demonstrated in later figures in this paper.

Human urine experiments

Fig. 4 shows the chromatogram (a) resulting from the extraction (according to the scheme described in the Experimental section) of 12.5 ng of DES added to 10 ml of human urine and (b), a blank, resulting from the extraction of 10 ml of the same

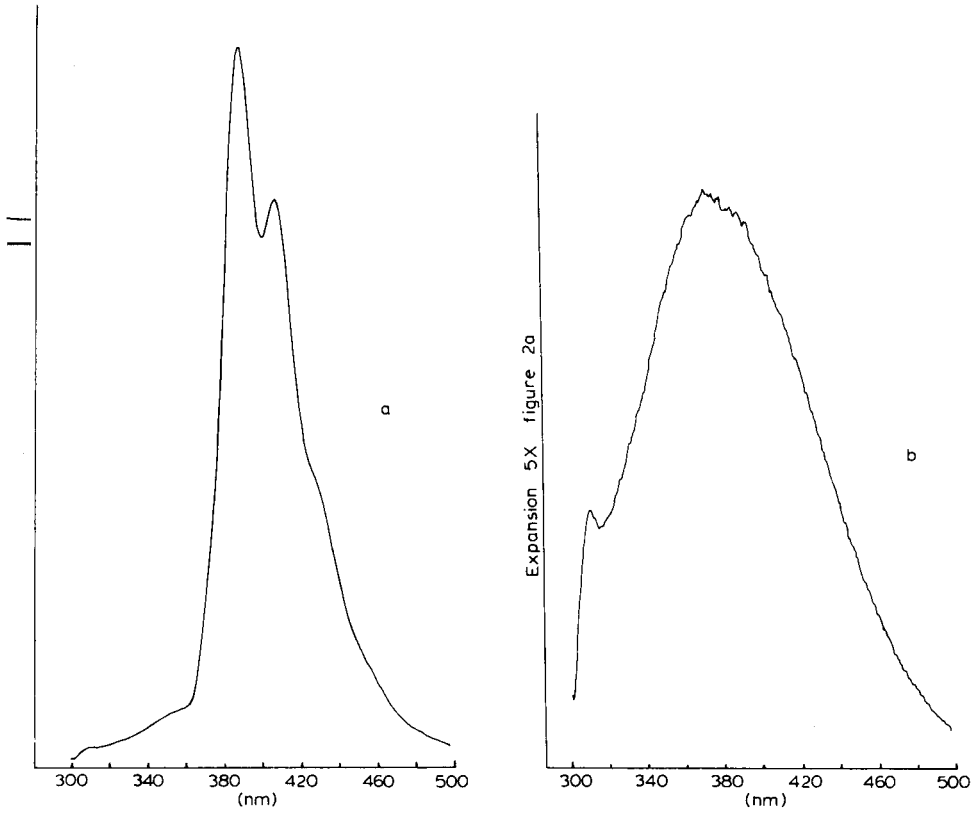

Fig. 2. a, Emission spectrum (excitation 280 nm) of DES photoproduct (II) after irradiation of DES solution at 280 nm for 5 min. b, Emission spectrum of DES before irradiation (expansion 5 × that of a).

urine with no DES added. The extra peak at 9.5 min has the same retention time as in the pure DES experiments and exhibits the same "lamp on–lamp off" behaviour.

Separate experiments established that about 60–70% of the DES was recovered by the very simple extraction procedure. Furthermore, these extractions of low ng levels of DES could be duplicated to within 10% or less. Therefore, the 12.5 ng of DES originally added, as described above, should have been reduced to less than 10 ng by the extraction procedure. This DES and the urine residues are dissolved in 100 μl of ethanol and 20 μl of this solution is injected. Therefore, the peak for the DES photoproduct in Fig. 4a represents less than 2 ng of DES on the column. Also, because there was originally 12.5 ng in 10 ml of urine, Fig. 4a demonstrates that our system can detect levels of DES of 1 ng/g (1 ppb) or less in human urine.

The calibration curve of Fig. 5 was the result of separate extractions in which 37.5, 25, and 12.5 ng, respectively, of DES were added to urine samples before extraction. Fig. 5 shows that very low ppb levels of DES can be quantitatively extracted and determined by this method. Furthermore, once the reagents are prepared and the instrumental system is established, the entire extraction and chromatography of DES in human urine can be accomplished in less than 1 h. Daily calibration of the system is desirable.

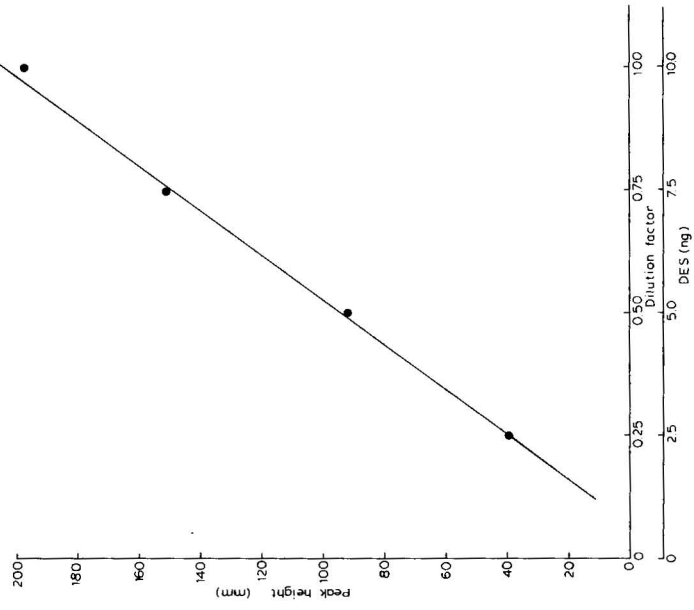

Fig. 3. Calibration curve for low ng levels of pure DES in ethanol solution.

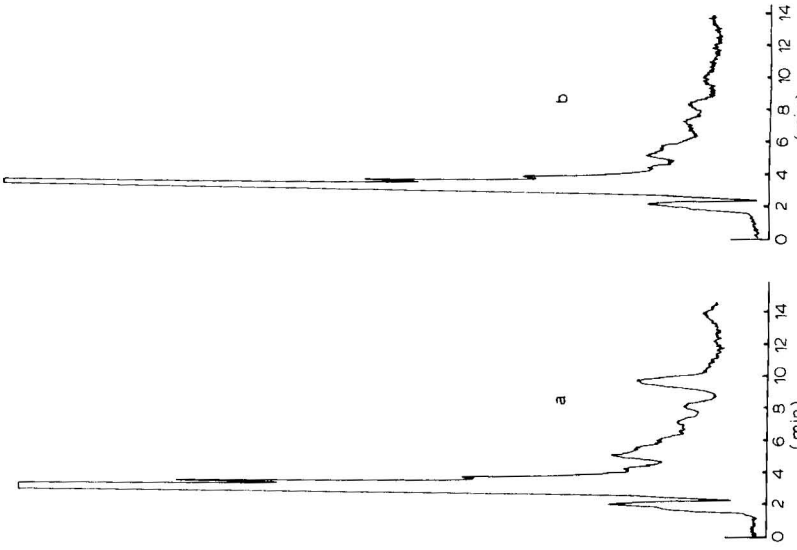

Fig. 4. Chromatograms of human urine extracts: a, 12.5 ng DES added before extraction; b, blank.

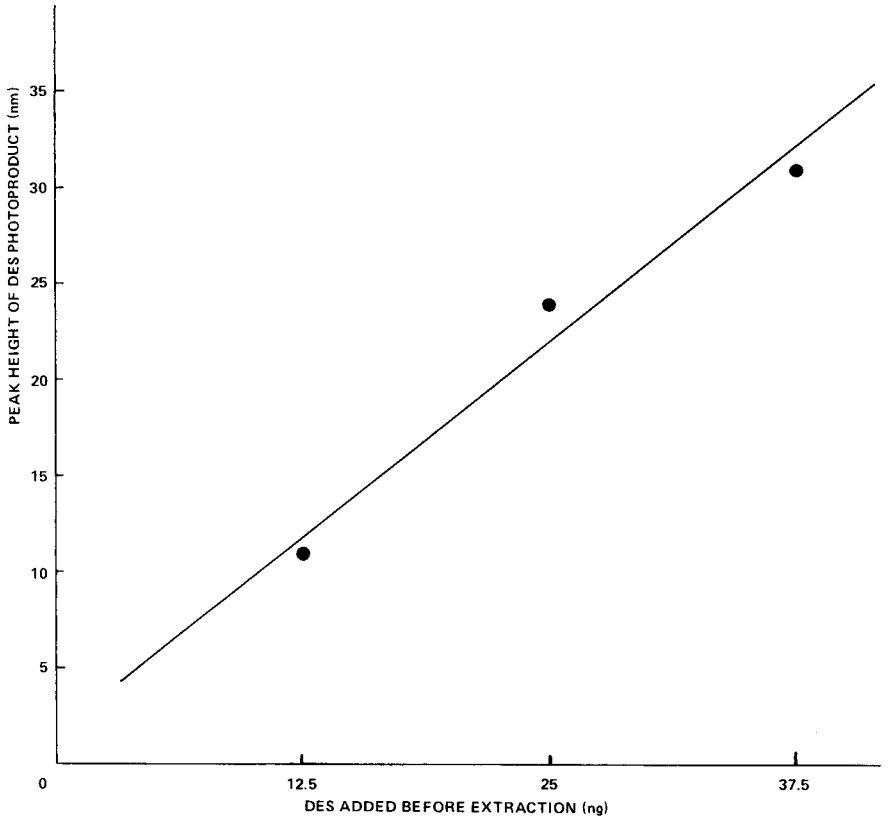

Fig. 5. Calibration curve for DES extracted from human urine.

Cow urine, plasma, and sera experiments

A limited number of blanks made up by the ether extraction of cow urine, plasma, and sera as described in the Experimental section were available to us[21]. To each of these were added 50 μl of the 0.5 ng/μl DES solution, *i.e.*, 25 ng of DES, and 50 μl of ethanol. These samples were chromatographed according to the conditions previously described with the following results.

Fig. 6a shows the expected peak for the DES photoproduct at about 9.5 min in the cow urine samples. Fig. 6b is a repeat injection of the same sample as that in 6a except that the lamp is turned off off and no photoconversion of DES into II takes place. Fig. 6c represents a different cow urine sample with no DES added, *i.e.*, simply dissolved in 100 μl of ethanol, with the lamp on.

The "lamp on–lamp off" effect is shown again in the chromatograms of Fig. 7. Fig. 7a and b are from the same solution of cow plasma in ethanol to which DES (25 ng) had been added. Some differences in the chromatograms when the lamp is turned off, other than the disappearance of the peak for II, are to be expected. The UV lamp undoubtedly causes other photochemical transformations which destroy or create fluorescent substances in these biological materials.

CONCLUSIONS

The analytical method described in this paper allows for the highly specific, quantitative determination of DES at levels comparable to existing methods.

However, compared to the lengthy extraction, work up, and derivatisation procedures characteristic of other methods, our method is unrivalled for speed and simplicity. It is also free of the subjectivity that is inherent in the visual spot identification of most of the TLC methods.

ACKNOWLEDGEMENTS

We wish to gratefully acknowledge the loan of the photoreactor by P. J. Twitchett, Home Office Forensic Science Laboratory, Priory House, Gooch Street North, Birmingham, Great Britain, who was responsible for its design.

R. C. Belloli wishes to thank Perkin-Elmer Ltd., Great Britain, for the opportunity to participate in this project and for the laboratory support provided. Direct financial support was provided to him by a National Science Foundation Science Faculty Professional Development Grant, NSF-SPI-8013093, which is also hereby acknowledged.

We also acknowledge the donation of DES, HES, and animal extract samples by Dr. S. Dixon of the Agricultural Research Council, Great Britain.

REFERENCES

1 A. Burger, *Medical Chemistry*, Part I, Wiley-Interscience, New York, 3rd ed., 1970, pp. 746–747.
2 J. Becker, *Nature (London)*, 289 (1981) 215.
3 B. Hoffmann, *J. Steroid Biochem.*, 11 (1979) 919.
4 W. Stoeckl, F. Bamberg, H. S. Choi and N. Goetzinger, *Wien. Tieraerztl Monatsschr.*, 65 (1978) 329; *C.A.*, (1978) 85364C.
5 M. C. Bowman, *J. Ass. Offic. Anal. Chem.*, 61 (1978) 1253.
6 L. Laitem, P. Gaspar and I. Bello, *J. Chromatogr.*, 156 (1978) 267.
7 J. J. Ryan and W. F. Miles, *Int. J. Environ. Anal. Chem.*, 5 (1978) 133.
8 R. Verbeke, *J. Chromatogr.*, 177 (1979) 69.
9 H. J. Stan and F. W. Hohls, *Z. Lebensm.-Unters.-Forsch.*, 166 (1978) 287.
10 K. Vogt, *Arch. Lebensmittelhyg.*, 29 (1978) 178.
11 K. Vogt and K. L. Oehrle, *Arch. Lebensmittelhyg.*, 28 (1977) 44.
12 K. Vogt, *Arch. Lebensmittelhyg.*, 30 (1979) 168.
13 *British Pharmacopoeia*, 1973, H.M.S.O., London, 1973, p. 443.
14 *The United States Pharmacopoeia*, Mack Publishing Co., Easton, PA, 19th Revision, 1975, pp. 142–143.
15 J. M. Goodyear, L. S. Hatfield and M. M. Marsh, *J. Amer. Pharm. Ass., Sci. Ed.*, 43 (1954) 605.
16 D. Banes, *J. Ass. Offic. Agr. Chem.*, 44 (1961) 323.
17 A. R. Lea, W. J. Kayaba and D. M. Hailey, *J. Chromatogr.*, 177 (1979) 61.
18 E. J. Lumberger, D. Banes, F. M. Kunze and S. H. Colson, *J. Ass. Offic. Agr. Chem.*, 46 (1963) 471.
19 P. L. Schuller, *J. Chromatogr.*, 31 (1967) 237.
20 P. J. Twitchett, P. L. Williams and A. C. Moffat, *J. Chromatogr.*, 149 (1978) 683.
21 J. A. F. de Silva and L. D'Arconte, *J. Forensic Sci.*, 14 (1969) 184.

Journal of Chromatography, 235 (1982) 471–480
Elsevier Scientific Publishing Company, Amsterdam — Printed in The Netherlands

CHROM. 14,327

USE OF C_{18} REVERSED-PHASE LIQUID CHROMATOGRAPHY FOR THE ISOLATION OF MONOTERPENE GLYCOSIDES AND NOR-ISOPRENOID PRECURSORS FROM GRAPE JUICE AND WINES

P. J. WILLIAMS*, C. R. STRAUSS and B. WILSON
The Australian Wine Research Institute, Private Bag, P.O. Glen Osmond, South Australia 5064 (Australia)
and
R. A. MASSY-WESTROPP
Department of Organic Chemistry, University of Adelaide, P.O. Box 498, Adelaide, South Australia 5001 (Australia)
(Received August 31st, 1981)

SUMMARY

Glycosidic derivatives of monoterpene flavourants of grapes and wines can be preparatively isolated by selective retention on a C_{18}-bonded reversed-phase adsorbent. These components can thus be concentrated by a factor of 20,000 in a single chromatographic step. Class separation of monoterpene glycosides at different oxidation levels can also be achieved on the reversed-phase adsorbent.

The process has also led to the discovery of precursors of 2-phenylethanol, benzyl alcohol, damascenone, vitispirane and 1,1,6-trimethyl-1,2-dihydronaphthalene. Additionally, many other related nor-isoprenoid compounds not previously known in grapes have been observed.

INTRODUCTION

It is now understood that terpene flavourants of grapes are derived from a pool of non-volatile precursor compounds in the fruit[1]. Indirect evidence suggested that these compounds are glycosidic derivatives of monoterpenes, although not simply β-D-glucosides[2]. Recent investigations in this laboratory have confirmed this proposal[3]. During the course of research on this topic techniques for the isolation of terpene glycosides in amounts sufficient for structural elucidation have been required.

Glycosides of non-iridoid monoterpenes have been recognised relatively recently as plant constituents and a variety of techniques have been used to isolate these hydrophilic compounds. Croteau and Martinkus[4], after lyophilizing aqueous leaf extracts, used thin-layer chromatography (TLC), ion-exchange chromatography and gel permeation chromatography to purify neomethyl-β-D-glucoside. Francis and Allcock[5] isolated β-D-glucosides of geraniol, nerol and citronellol from aqueous extracts of rose petals by solvent extraction followed by silica gel chromatography and

0021-9673/82/0000–0000/$02.75

preparative thin-layer electrophoresis. Subsequently, Banthorpe and Mann[6] applied the same techniques to petals of *Tanacetum vulgare*. Similarly, Sakata and Mitsui[7], Bohlmann and Grenz[8], and Tschesche *et al.*[9] extracted plant material directly with organic solvents and, after clean-up of the extracts on silica gel, conventional chromatographic procedures were used to isolate β-D-glucosides and derivatives of several monoterpenoids.

Unfortunately these techniques were either inappropriate or found to be unsuitable for the isolation of monoterpene glycosides from grape juice and wines. In the case of grape juice, the presence in aqueous solution of large amounts of glucose and fructose, together with other free sugars, makes the problem of separation of small amounts of glycosides extremely difficult. On the other hand, the isolation from wines in which most of the sugars have been removed by fermentation, is also complicated by the presence of glycerol and the isomeric butane-2,3-diols. Several techniques were tried unsuccessfully, including solvent extraction and subsequent TLC, gel filtration of both juice and wines and ion-exchange chromatography of juice on a column of cation exchanger in the calcium form[10] and on an anion exchanger in the bisulphite form[11,12].

Eventually it was found that chromatography of juice or dealcoholised wine on a C_{18}-bonded reversed-phase adsorbent allowed separation of monoterpene glycosides free from other polar components, *i.e.* sugars, organic acids, glycerol, etc. The latter components were totally eluted from the column with water. This technique has also facilitated the separation of grape glycosidic precursors of monoterpenes at the linalool oxidation level from those at the higher linalool oxide oxidation state. Furthermore, precursors of the grape and wine volatile constituents, vitispirane[13], 1,1,6-trimethyl-1,2-dihydronaphthalene (TDN)[14] and damascenone[15,16] have also been isolated by C_{18} reversed-phase chromatography. It is now recognised that these last components co-occur with a number of other thirteen-carbon constituents not previously identified in grapes.

EXPERIMENTAL

Isolation of isoprenoid precursors on reversed phase

Juice or dealcoholised wine was peristaltically pumped down a glass column (470 × 15 mm I.D.) containing C_{18} reversed-phase adsorbent (Applied Science Labs., State College, PA, U.S.A.; Hi-flosil, 80–100 mesh) (40 g) at rates up to 400 ml/h, depending on the viscosity of the solution. After loading, the column was flushed with a volume of water equal to three times the volume of the applied sample. Retained material was then eluted with methanol (250 ml), and this fraction concentrated to dryness *in vacuo* and stored in an evacuated desiccator over KOH pellets. In a typical experiment 100 mg of concentrate was obtained from 2 l of grape juice.

Separation of isoprenoid precursors on reversed phase

A concentrate (*ca.* 50 mg), prepared as described above, was dissolved in water (*ca.* 10 ml) and peristaltically pumped, at 50 ml/h, down a glass column (80 × 5 mm I.D.) containing C_{18} reversed-phase adsorbent (3.5 g). The column was flushed with water (25 ml), 20% aqueous acetic acid (15 ml), water (25 ml), 30% aqueous acetic acid (15 ml), water (25 ml) and methanol (25 ml). The 30% aqueous acetic acid

fraction and subsequent water wash were pooled, concentrated *in vacuo* and stored as above. The methanol eluate was similarly concentrated and stored.

Preparative isolation

For the isolation of linalool oxidation state glycoside precursors used in structural elucidation studies[3], the above processes were combined.

Muscat of Alexandria grape juice was centrifuged (16,500 *g*, 15 min) and the clear supernatant (15.75 l) passed down the larger C_{18} reversed-phase column. The methanol eluate, after evaporation, was then rechromatographed on the small column of the bonded phase. Acetic acid fractions from the second column, after removal of solvent, were set aside for future study. The residue, eluted from the small column with methanol, was concentrated to give highly active material (100 mg) which yielded predominantly linalool oxidation state monoterpenoids on hydrolysis.

Hydrolysis of fractions

Dried samples (*ca.* 1 mg) of 30% acetic acid fraction or methanol fraction from the reversed-phase columns, were taken up in water (2 ml). Each sample was adjusted to either pH 1 or pH 3 (glass electrode) with 1% aqueous perchloric acid. The solutions were washed with cold Freon F11 (2 × 15 ml) to ensure removal of any volatiles prior to hydrolysis. Then each acidified solution was heated on a steam bath at 100°C for 20 min, cooled, and re-extracted with cold Freon (2 × 15 ml). The organic extracts of the hydrolysates were made up to 30 ml and one half of this taken and concentrated as previously described[17] for analysis by gas chromatography (GC) or GC–mass spectrometry (MS).

GC and GC–MS

Analytical GC was performed on a Perkin-Elmer Sigma 2 instrument using a glass support-coated open tubular (SCOT) column (96 m × 0.5 mm I.D.) of SP-1000 liquid phase on Chromosorb R support. The column was operated isothermally at 50°C for 10 min and then programmed at 1°C/min to 180°C and held at the upper temperature for 20 min. Nitrogen carrier gas was used at a linear velocity of 19 cm/sec.

GC–MS analyses were made on a Finnigan 4021 GC–MS data system. The chromatograph was equipped with a SP-1000, glass SCOT column (105 m × 0.5 mm I.D.) with helium as carrier gas at a linear velocity of 39 cm/sec. Injections were made with a 10:1 split at an injector temperature of 250°C. The column was held at 60°C for 10 min, programmed at 1°C/min to 180°C and held at this temperature for 20 min. Electron impact mass spectra were taken at 70 eV, scanning upwards from *m/z* 35 to *m/z* 350 each second, with a 0.1-sec delay between each scan.

RESULTS AND DISCUSSION

Clarified juice from Muscat of Alexandria grapes was passed through a column packed with C_{18} reversed phase. Hydrolysis of the eluent did not produce volatile monoterpenes thus confirming the absence of monoterpene precursors[1] in the column effluent. Water washing of the bonded phase did not elute any of the precursors, indicating efficient retention of these compounds by the C_{18} reversed phase. However,

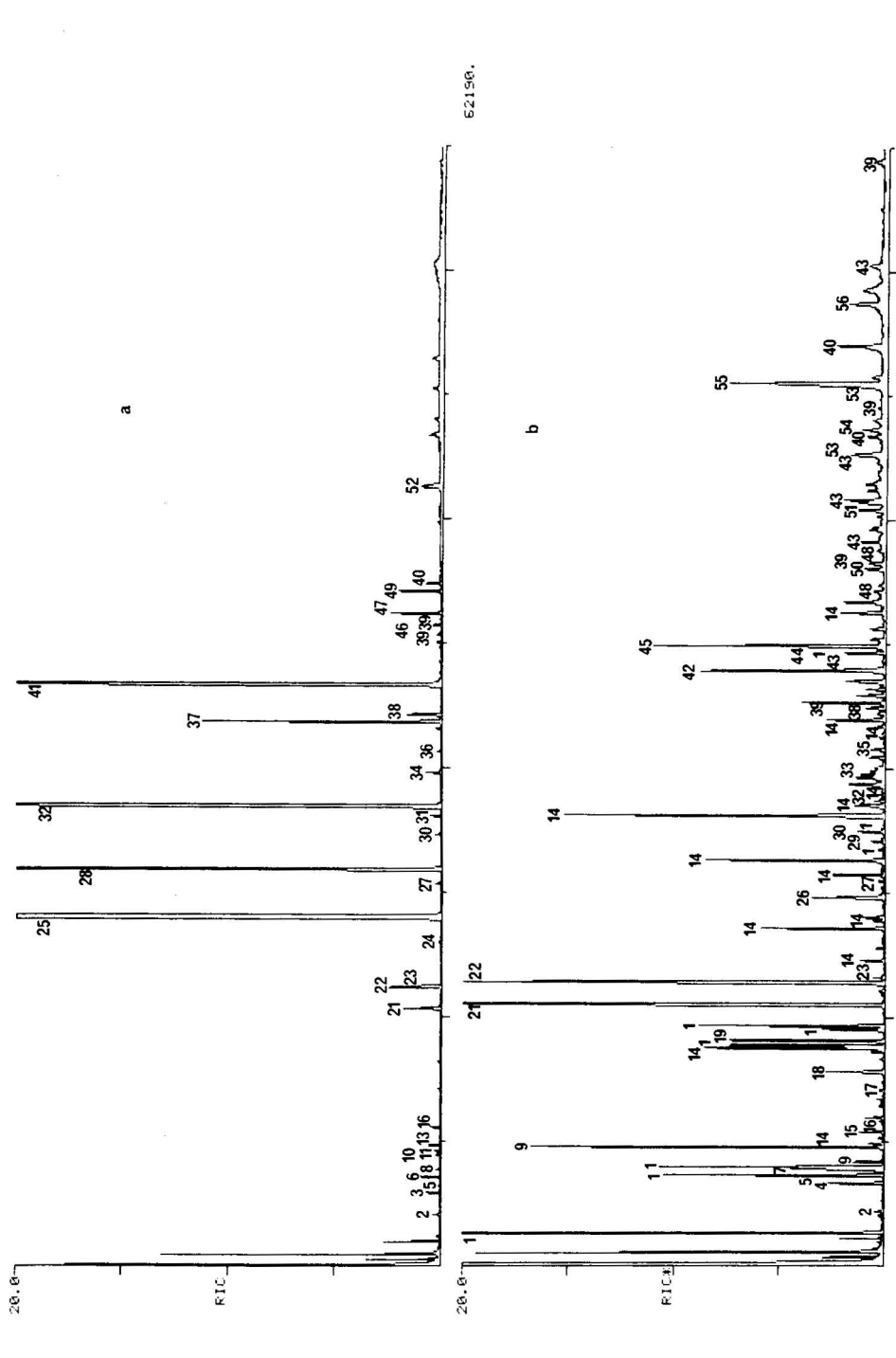

Fig. 1. Reconstructed ion chromatogram from the GC–MS data system of Freon extracts of the total material selectively retained by C_{18} reversed phase from Muscat of Alexandria grape juice, after eluton with methanol, and (a) hydrolysis at pH 3, (b) hydrolysis at pH 1. Peak identities are in Table I and GC–MS conditions in the Experimental section.

TABLE I

COMPOUNDS IDENTIFIED IN CHROMATOGRAMS SHOWN IN FIGS. 1 AND 2

Peak No.	*Assignment**	*Evidence for assignment***	*Refs.*
1	A monoterpenoid at the linalool oxidation state		
2	2,6,6-Trimethyl-2-vinyltetrahydropyran	A	17
3	Myrcene	B,C	18,19
4	1,4-Cineole	B,C	20,21
5	α-Terpinene	B,C	18,19
6	Limonene	B,C	18,19
7	1,8-Cineole	B,C	20,21
8	*trans*-5-Isopropenyl-2-methyl-2-vinyltetrahydrofuran	A	17
9	An isomeric 2,2-dimethyl-5-(1-methylpropenyl) tetrahydrofuran	A	17
10	*Z*-Ocimene	B,C	18,21
11	*cis*-5-Isopropenyl-2-methyl-2-vinyltetrahydrofuran	A	17
12	γ-Terpinene	B,C	18,19
13	*E*-Ocimene	B,C	18,21
14	A monoterpenoid at the linalool oxide oxidation state		
15	*p*-Cymene	B,C	18,21
16	Terpinolene	B,C	18,19
17	A trimethylbenzene	D	
18	*n*-Hexanol	A	14
19	3,5,5- or 2,6,6-Trimethylcyclohex-2-enone	B	21,22
20	4-Isopropenyltoluene	D	
21	*trans*-Furan linalool oxide	A	17
22	*cis*-Furan linalool oxice	A	17
23	Nerol oxide	A	17
24	Isomeric vitispiranes	A	13
25	Linalool	A	17
26	Terpinen-1-ol	B	21
27	Terpinen-4-ol	A,B	21
28	Hotrienol	A	17
29	A trimethyltetrahydronaphthalene	B,D	23
30	*Z*-Ocimenol	A	17
31	*E*-Ocimenol	A	17
32	α-Terpineol	A	17
33	1,1,6-Trimethyl-1,2-dihydronaphthalene	A	14
34	*trans*-Pyran linalool oxide	A	17
35	2,2,6-Trimethylcyclohexane-1,4-dione	B	21
36	*cis*-Pyran linalool oxide	A	17
37	Nerol	A	17
38	Damascenone	A	24
39	A C_{13} nor-isoprenoid compound at the damascenone oxidation level		
40	An unknown nor-isorpenoid		
41	Geraniol	A	17
42	Benzyl alcohol	A	21
43	A C_{13} nor-isorpenoid compound at the vitispirane oxidation level		
44	An unknown C_{14} nor-isoprenoid hydrocarbon		
45	2-Phenylethanol	A	14
46	*Z*-2,6-Dimethylocta-3,7-diene-2,6-diol	B,D	25

(Continued on p. 476)

TABLE I *(continued)*

Peak No.	*Assignment**	*Evidence for assignment***	*Refs.*
47	*E*-2,6-Dimethylocta-3,7-diene-2,6-diol	A	25
48	A 1,16-Trimethyldihydronaphthalene	B,D	23
49	3,7-Dimethyloct-1-ene-3,7-diol	A	25
50	Megastigma-4,7,9-trien-3-one	B	26
51	*Z*-4-(2,3,6-Trimethylphenyl)but-3-en-2-one	B,D	27
52	3,7-Dimethylocta-1,7-diene-3,6-diol	A	25
53	A megastigma-4,6,8-trien-3-one	B	26
54	4-(2,3,6-Trimethylphenyl)butan-2-one	B	27
55	*E*-4-(2,3,6-Trimethylphenyl)but-3-en-2-one	B	27
56	4-(2,3,6-Trimethylphenyl)butan-2-ol	B	28

* Many components from the hydrolyses in Figs. 1 and 2 remain unidentified, and where no interpretative information from the mass spectrum was available, peaks were left unassigned. However, where the class of compounds could be distinguished, it has been so designated.

** A = proven previously in this laboratory by spectral and chromatographic comparison with reference material; B = mass spectrum consistent with that of published data; C = retention time consistent with that of published data; D = tentative assignment based on similarity of mass spectral data with those of related compounds.

the washing procedure did remove all the major interfering juice constituents, *i.e.* free sugars and organic acids. Finally, elution of the column with methanol yielded a fraction which, on solvent removal and desiccation, gave a dark residue. This material, after dissolving in water and Freon extraction, was found to contain no free terpenoids or other volatile compounds. Hydrolysis at pH 3, followed by extraction and GC analysis, demonstrated that the C_{18} reversed-phase material liberated monoterpenes with a pattern similar to that seen in whole juice[17] (see Fig. 1a). Thus precursors of those monoterpenes which occur free in muscat juice were isolated and concentrated by a factor of typically 20,000. Furthermore, examination of the products indicated that compounds at both the linalool and linlool oxide oxidation levels were present. This implied that more than one monoterpene precursor was in the juice initially.

The important nor-isoprenoid grape volatiles vitispirane (24)[13] and damascenone (38)[16] were also identified in this pH 3 hydrolysate of the C_{18} reversed-phase material (see Table I). Previous work[29] had shown that vitispirane concentration increased with maturation in wines. Vitispirane formation appeared to be hydrolytic rather than oxidative, implying the presence of a precursor of this compound in grapes and wines. Similarly, work by Masuda and Nishimura[15] indicated that damascenone (38) also has a precursor in grapes, but this latter compound has remained unisolated. The present study has revealed an additional pair of isomeric compounds (peaks 39 in Fig. 1a) related to the above C_{13}-constituents. These unknown new components, which were detected in this pH 3 hydrolysis, have also been observed in heated muscat grape juice headspace samples[30].

The extent of occurrence of these C_{13} and related nor-isoprenoid grape con-

stituents was not apparent however until the C_{18} reversed-phase fraction was hydrolysed at pH 1 (Fig. 1b). Extraction and GC analysis showed that a significant proportion of the volatiles produced was of this nor-isoprenoid category (Table I). Whilst some of these compounds have only been tentatively identified at present, excellent MS evidence for the isomeric megastigmatrienones (50) and (53)[26] and the aromatic compounds (54)[27], (55)[27] and (56)[28] was obtained. In addition, the presence of hydrocarbon TDN[14] was confirmed and other closely related trimethyl dihydronaphthalenes indicated (peaks 48), along with what appears to be a C_{14} homologue (peak 44). These nor-isoprenoid compounds are usually regarded as degradation products of carotenoids[31] and such a genesis may well hold in grapes. Nevertheless, it is possible that the formation of aromatic compounds like TDN, ketones (54) and (55) and alcohol (56) involved extensive rearrangement under acidic conditions and their presence may not be diagnostic of specific precursors.

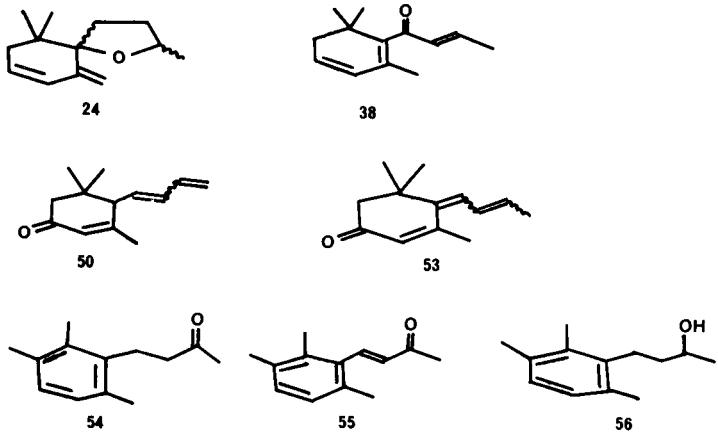

Work on these grape nor-isoprenoid compounds and their precursors, as well as the mechanisms by which the volatile constituents listed in Table I are derived from their precursors, is in progress. It will be particularly interesting to determine if the grape nor-isorpenoid precursors are glycosidic derivatives similar to those recently isolated from tobacco[32].

In addition to the nor-isoprenoid compounds in the reversed-phase material, other constituents, such as 2-phenylethanol and benzyl alcohol, were also liberated from non-volatile precursors by hydrolysis at pH 1. These compounds, which are often abundant in wines[33], are now recognised as having a derivation from grapes directly.

Significant differences can be seen in the pattern of volatile monoterpenoids produced from the reversed-phase material by hydrolysis at pH 1 and 3. It is apparent that the more acidic conditions bring about extensive rearrangement of monoterpenoids at both oxidation levels. Many of these rearrangement products have yet to be firmly identified. The influence of hydrolytic conditions on the pattern of volatiles obtained from grape monoterpene glycosides will be the subject of a separate study.

To examine further the potential of the C_{18} reversed-phase chromatographic technique to fractionate precursors of grape flavourants, material concentrated from Rhine Riesling grape juice by the method described above was rechromatographed

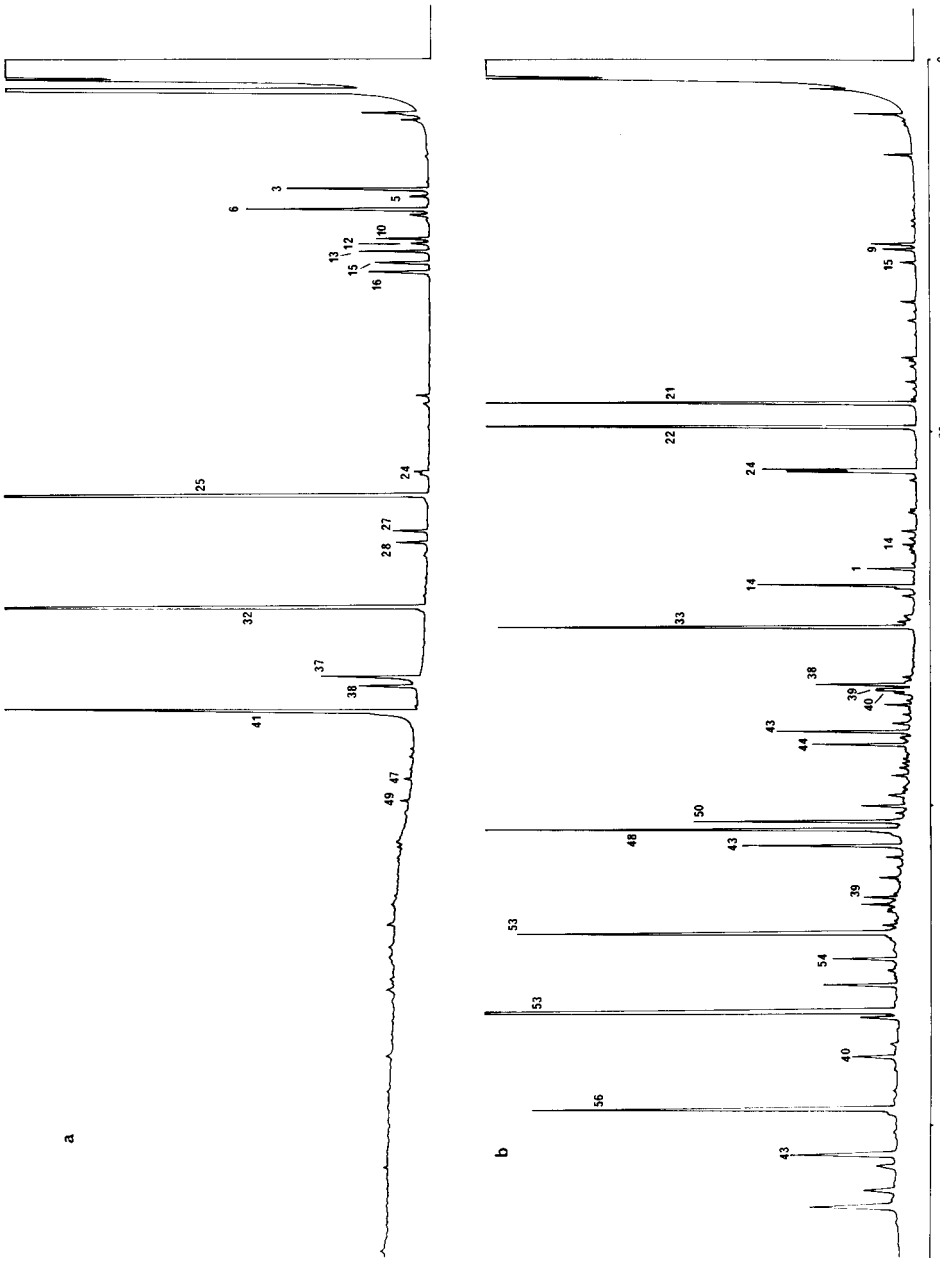

Fig. 2. Analytical gas chromatograms of Freon extracts of material selectively retained by C_{18} reversed phase from Rhine Riesling grape juice, after (a) final elution of the column with methanol and hydrolysis at pH 3, and (b) pre-elution of the column with 30% acetic acid and hydrolysis at pH 1. Peak identities are in Table I, and analytical GC conditions in the Experimental section.

on a small column of the bonded phase. After application of an aqueous solution of precursor concentrate to a short column of C_{18} reversed phase, the column was washed with water and then eluted with aqueous acetic acid. Fig. 2b shows the GC analysis of volatiles obtained by pH 1 hydrolysis of material eluted from the column with 30% acetic acid. It can be seen that monoterpenoids present in the chromatogram are principally at the higher (linalool oxide) oxidation level. By contrast, the chromatogram in Fig. 2a shows the products obtained by pH 3 hydrolysis of residual material eluted from the short C_{18} reversed-phase column with methanol, after the above 30% acetic acid fraction. Here monoterpenoids predominate and the majority of them are at the lower (linalool) oxidation state. Thus chromatography on the bonded C_{18} reversed phase allows class separation of glycosidic precursors of monoterpenes at different oxidation levels.

The chromatogram in Fig. 2b demonstrates that the fraction eluted with 30% acetic acid was also particularly rich in precursors of the grape nor-isoprenoids.

It is of interest that all of these precursor compounds have been isolated from both Rhine Riesling and Muscat of Alexandria grape varieties. Possibly significant differences have been observed between the patterns of volatiles produced on hydrolysis of the various C_{18} reversed-phase fractions from each variety. This is particularly true for that fraction giving the nor-isoprenoid products.

This technique of selective retention of monoterpene glycosides onto a bonded C_{18} reversed-phase column has also been applied to large volumes of dealcoholised wine concentrate prepared from Muscat of Alexandria as well as juice from this variety. The same column has been used repeatedly, by simply washing the bonded phase with water after elution of the target compounds and before application of the next batch. Thus a total of 45 l of dealcoholised wine concentrate and juice has been processed in batches of up to 15 l. This has enabled the isolation of quantities of glycosidic material giving linalool oxidation state monoterpenes on both acidic and enzymatic hydrolysis (similar to material giving the products seen in Fig. 2a). Further purification of this material, after acetylation, has allowed a complete spectral and chemical investigation of the monoterpene glycoside structures[3].

Presumably the hydrophobic inrteraction of the terpene moeity of the glycosides with the alkyl portion of the bonded phase accounts for the highly selective retention of these compounds on the C_{18} reversed phase. A similar phenomenon must also apply to the grape nor-isorpenoid, 2-phenylethanol and benzyl alcohol precursors. Application of the selective retention of terpene glycoside derivatives from aqueous solutions of polar interfering substances should be of use for the isolation of this class of compound from a variety of sources, *i.e.* other fruit juices and extracts of plant tissues, etc. This should facilitate research on this important group of plant constituents.

ACKNOWLEDGEMENT

We thank the South Australian Department of Agriculture, Lindemans Wines Pty. Ltd., and S. Smith & Sons Pty. Ltd. for generously donating samples of wines and grape juices. We are also indebted to Dr. D. J. Casimir, C.S.I.R.O. Division of Food Research for preparing wine concentrates. Bush Boake Allen Australia Ltd., Dragoco Pty. Ltd., Firmenich SA, Givaudan Pty. Ltd., and Naarden International are also thanked for gifts of several flavour chemicals used as reference compounds.

REFERENCES

1 P. J. Williams, C. R. Strauss and B. Wilson, *Amer. J. Enol. Vitic.*, 32 (1981) 230.
2 R. Cordonnier and C. Bayonove, *C.R. acad. Sci., Ser. D*, 278 (1974) 3387.
3 P. J. Williams, C. R. Strauss, B. Wilson and R. A. Massy-Westropp, *Phytochemistry*, submitted for publication.
4 R. Croteau and C. Martinkus, *Plant Physiol.*, 64 (1979) 169.
5 M. J. O Francis and C. Allcock, *Phytochemistry*, 8 (1969) 1339.
6 D. V. Banthorpe and J. Mann, *Phytochemistry*, 11 (1972) 2589.
7 I. Sakata and T. Mitsui, *Agr. Biol. Chem.*, 39 (1975) 1329.
8 F. Bohlmann and M. Grenz, *Phytochemistry*, 16 (1977) 1057.
9 R. Tschesche, F. Ciper and E. Breitmaier, *Chem. Ber.*, 110 (1977) 3111.
10 S. J. Angyal, G. S. Bethell and R. J. Beveridge, *Carbohydr. Res.*, 73 (1979) 9.
11 B. Lindberg and K. N. Slessor, *Carbohydr. Res.* 5 (1967) 286.
12 L. Larsson and O. Samuelson, *Acta Chem. Scand.*, 19 (1965) 1357.
13 R. F. Simpson, C. R. Strauss and P. J. Williams, *Chem. Ind. (London)*, (1977) 663.
14 P. J. Williams and C. R. Strauss, *J. Inst. Brew. (London)*, 84 (1978) 148.
15 M. Masuda and K. Nishimura, *J. Food Sci.*, 45 (1980) 396.
16 P. Schreier and F. Drawert, *Z. Levensm.-Unters.-Forsch.*, 154 (1974) 273.
17 P. J. Williams, C. R. Strauss and B. Wilson, *J. Agr. Food Chem.*, 28 (1980) 766.
18 M. H. Klouwen and R. Ter Heide, *J. Chromatogr.*, 7 (1962) 297.
19 A. F. Thomas and B. Willhalm, *Helv. Chim. Acta*, 47 (1964) 475.
20 W. Jennings and T. Shibamoto, *Qualitative Analysis of Flavor and Fragrance Volatiles by Glass Capillary Gas Chromatography*, Academic Press, New York, 1980.
21 S. R. Heller and G. W. A. Milne, *EPA/NIH Mass Spectral Data Base*, Vols. 1–4, U.S. Department of Commerce and The National Bureau of Standards, Washington, DC, 1978.
22 K. H. Schulte-Elte, B. L. Müller and G. Ohloff, *Helv. Chim. Acta*, 54 (1971) 1899.
23 H. M. Liebich, W. A. Koenig and E. Bayer, *J. Chromatogr. Sci.*, 8 (1970) 527.
24 E. Demole, P. Enggist, U. Säuberli, M. Stoll and E. sz. Kovats, *Helv. Chim. Acta*, 53 (1970) 541.
25 P. J. Williams, C. R. Strauss and B. Wilson, *Phytochemistry*, 19 (1980) 1137.
26 A. J. Aasen, B. Kimland, S. Almqvist and C. R. Enzell, *Acta Chem. Scand.* 26 (1972) 2573.
27 A. F. Thomas, B. Willhalm and R. Müller, *Org. Mass Spectrom.*, 2 (1969) 223.
28 R. Kaiser and D. Lamparsky, *Helv. Chim. Acta*, 61 (1978) 373.
29 R. F. Simpson, *Vitis*, 18 (1979) 148.
30 P. J. Williams, C. R. Strauss and B. Wilson, unpublished results.
31 C. R. Enzell, I. Wahlberg and A. J. Aasen, in W. Herz, H. Grisebach and G. W. Kirby (Editors) *Progress in the Chemistry of Organic Natural Prpdoucts*, Vol. 34, Springer, New York, 1977, p. 1.
32 H. Kodama, T. Fujimori and K. Kato, *Agr. Biol. Chem.*, 45 (1981) 941; and references cited therein.
33 A. D. Webb and C. J. Muller, in D. Perlman (Editor) *Advances in Applied Microbiology*, Vol. 15, Academic Press, New York, 1972, p. 75.

Journal of Chromatography, 235 (1982) 481–488
Elsevier Scientific Publishing Company, Amsterdam — Printed in The Netherlands

CHROM. 14,314

SEPARATION OF SATURATED, MONO-UNSATURATED AND DI-UNSATURATED ALDEHYDES AS 2,4-DINITROPHENYLHYDRAZONES USING HIGH-PERFORMANCE LIQUID CHROMATOGRAPHY AT INCREASED TEMPERATURE*

B. REINDL*
Institut für Sozialmedizin und Epidemiologie, Bundesgesundheitsamt, Unter den Eichen 82–84, 1000 Berlin 33 (G.F.R.)
and
H.-J. STAN
Institut für Lebensmittelchemie, Technische Universität, Müller-Breslau-Str. 10, 1000 Berlin 12 (G.F.R.)
(First received August 5th, 1981; revised manuscript received August 26th, 1981)

SUMMARY

Saturated and mono- and di-unsaturated aldehydes (C_5–C_{10}) were converted into their 2,4-dinitrophenylhydrazones. The separation of nanogram amounts of these hydrazones was performed by high-performance liquid chromatography with C_{18} reversed-phase columns in an isocratic elution. Separation of all aldehydes tested could only be achieved at an elevated temperature (50°C). A linear relationship between log k' and the carbon number for a series of homologous compounds could be observed also at an elevated temperature. An optimal separation was achieved utilizing the methylene group selectivity which was found to be temperature dependent.

Application of this method shows the advantage of an optimized separation for the determination of carbonyl compounds from the oxidation of fatty acids in meat.

INTRODUCTION

Aldehydes and other carbonyl compounds are ubiquitous in the environment. In addition to the presence of carbonyl compounds in air and water, their presence in foods is of considerable interest. Owing to their extremely low olfactory and gustatory threshold concentrations they contribute essentially to the aroma of foods even if present in trace amounts only. This is particularly true in respect of fat-containing foods in which the oxidation of fatty acids will result in the formation of carbonyls and other compounds. For the demonstration of such trace concentrations, a sensitive method of measurement is required.

* Parts of this work were presented at the 1st International Symposium on Chromatography in Biochemistry, Medicine and Environmental Research, Venice, June 16–17, 1981.

0021-9673/82/0000–0000/$02.75

Two different methods are commonly used for the analytical detection of aldehydes in low concentrations as present in foods. One consists of isolation of the carbonyl compounds by extraction or distillation and subsequent gas chromatographic determination without derivative formation[1–3]. The other consists of reaction with 2,4-dinitrophenylhydrazine (2,4-DNP) and chromatographic determination of the hydrazones.

Gas chromatographic determination also records numerous volatile accompanying substances since the flame-ionization detector which is commonly used does not indicate carbonyl compounds in a selective or specific way. Beyond this, its sensitivity is mostly insufficient for trace analysis. The spectrum of aldehydes may be reliably determined from a biological matrix only by a combination of gas chromatography and mass spectrometry. By reacting with 2,4-DNP, the carbonyl compounds are converted into derivatives which owing to their characteristic absorption at 340–410 nm can be clearly distinguished from the accompanying substances. Because of their high molar absorptivities, 2,4-dinitrophenylhydrazones (2,4-DNPHs) are well suited for the detection of traces[4].

A number of chromatographic methods for the separation of 2,4-DNPHs of carbonyl compounds have been described. Gas chromatographic separation of 2,4-DNPHs has been performed by a number of authors[5–8]. When compared to separation methods using thin-layer and liquid chromatography, this method will, however, show obvious disadvantages. Separation of aldehydes by multiple thin-layer chromatography (TLC) on various coating materials has been described[9]. Separation of aldehyde classes has been achieved on Kieselguhr hydrophobized with Carbowax 400[10–12]. Separation of 2,4-DNPHs by liquid chromatography has been conducted on Corasil[13,14]. The use of high-performance liquid chromatography (HPLC) with reversed-phase columns results in a better separation. Selim[15] and Fung and Grosjean[4] have reported a determination of C_1–C_6 aldehyde hydrazones in C_{18} reversed-phase columns with acetonitrile–water mixtures using isocratic elution. Demko[16] and Nakamura *et al.*[17] used gradient elution for the separation of straight-chain saturated C_1–C_{10} aldehyde hydrazones with acetonitrile–water mixtures. Vigh *et al.*[18] have described the separation of saturated (C_1–C_{12}) as well as of mono-unsaturated (C_3–C_8) aldehyde hydrazones using methanol–water mixtures with isocratic elution. The resolution of the separation achieved between saturated and mono-unsaturated aldehyde hydrazones did not appear to be satisfactory.

In this paper, an HPLC method is described which permits a separation of hydrazones from saturated and mono- and di-unsaturated aldehydes. In particular it permits a quantitative determination of all the aldehydes characteristic of the formation of off-flavour in foods at the relevant trace level.

EXPERIMENTAL

Materials

Chemicals were of analytical-reagent grade unless indicated otherwise. Pure water was obtained using Millipore equipment.

2,4-Dinitrophenylhydrazine (2,4-DNP), 95% ethanol and 98% sulphuric acid were purchased from E. Merck. Hexanal was obtained from Fluka, pentanal, 2-*trans*-hexenal, 2,4-heptadienal, 2-*trans*-heptenal, heptenal, 2-octenal, octanal, 2,4-non-

adienal, 2-nonenal, nonanal, 2,4-decadienal and 2-*trans*-decenal from Atlanta and decanal from Chrompack. Acetonitrile, tetrahydrofuran and methanol were obtained from E. Merck. ChromAR water for HPLC was purchased from Prochem. G.F.R.). All solvents were filtered using a 0.7-μm fibre glass filter.

Preparation of 2,4-DNPH standards

2,4-DNP (4 g) was dissolved in 10% sulphuric acid and the aldehyde (1.5 ml) was then added. The precipitated 2,4-DNPH was separated after 1 h and recrystallized twice from ethanol. Purity was checked by HPLC.

HPLC

The HPLC equipment consisted of a Spectra-Physics 8700 HPLC pump with helium eluent degassing, a Kipp Model 9209 automatic sample injector with a Rheodyne No. 70-10 sample valve, a Knauer type 89.00 column oven and a Perkin-Elmer LC 55 variable-wavelength detector. An HP 3390 A integrator was used for the calculation of peak areas.

The 2,4-DNPHs were separated on a 250 × 4.6 mm I.D. Supelcosil LC 18 column, 5 μm (C_{18} reversed-phase) with isocratic elution at 1.0 ml/min. Between the injector and main column a 30 mm guard column with LiChrosorb RP-18, 5 μm, was used. The eluent was acetonitrile–water–tetrahydrofuran (75:24:1, v/v/v). The eluent was pre-heated in a 100-mm LiChroprep RP-18 column installed between the pump and the injector. The temperature of all columns was 50°C. The injected volume was 20 μl and detection took place at 360 nm.

RESULTS AND DISCUSSION

The chromatographic system was designed for a complete separation of all the aldehydes expected as products of the autoxidation of lipids. The aldehydes with carbon numbers 1–4 were not included as these are less indicative of autoxidation of fatty acids and are less important as components of the off-flavour. On the other hand, the solvents used are largely contaminated with these low-chain aldehydes, which may interfere if not removed completely during the purification procedure.

Fig. 1 shows the chromatogram of the test mixture containing the 2,4-DNPHs of all the relevant aldehydes. All the aldehydes could be separated, allowing identification by means of retention times. The separation of pentanal (C_5), hexanal (C_6), 2-heptenal ($C_{7:1}$) and heptanal (C_7) was complete, with a resolution of $R \geq 1.4$. The group 2-octenal ($C_{8:1}$) 2,4-nonadienal ($C_{9:2}$) and octanal (C_8) and the pair 2-nonenal ($C_{9:1}$) and 2,4-decadienal ($C_{10:2}$) were separated with a resolution $R \approx 0.8$. This means for practical purposes that the aldehydes can be determined quantitatively with an electronic integrator. This has been confirmed by many routine analyses measuring autoxidation in meat samples.

The chromatographic system as presented in Fig. 1 is the result of an optimization with regard to resolution and time needed for analysis by changing the eluent and the temperature. All fractions are eluted with capacity factors k' between 1.8 and 8.6. Addition of 1% of tetrahydrofuran as a modifier resulted in a considerable sharpening of the eluting peaks. An increase in temperature from room temperature

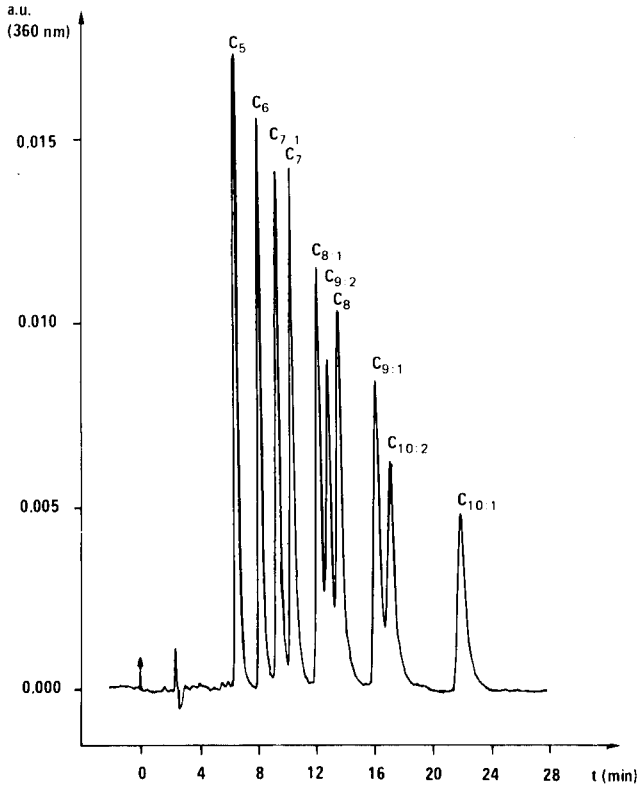

Fig. 1. HPLC trace for 2,4-DNPHs of ten aliphatic aldehydes on a C_{18} reversed-phase column (pentanal 100 ng, all others 80 ng).

(25°C) to 50°C resulted in a decisive improvement of the separation between C_8 and $C_{9:2}$ and a shortening of the time needed for a run, as shown in Fig. 2.

As can be seen from Fig. 1, mono-unsaturated aldehydes are eluted before saturated aldehydes of the same chain length. This effect increases when there is a second double bond in the molecule and can be explained by the unsaturated compounds being more polar than the saturated ones. It is obvious that this can lead to interferences in complex mixtures.

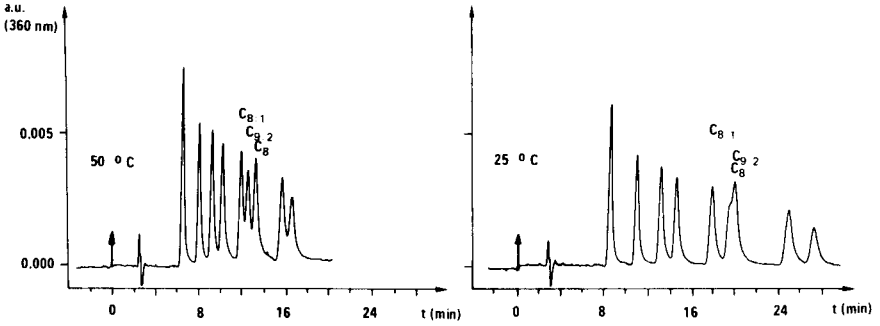

Fig. 2. HPLC trace for 2,4-DNPHs of nine aliphatic aldehydes at two column temperatures.

In Fig. 3, the relationship between chain length, degree of unsaturation and retention volume is plotted in a semi-logarithmic diagram. The members of the homologous series of saturated, mono-unsaturated and di-unsaturated aldehydes demonstrate a logarithmic increase in the capacity factor k' as a function of the carbon number. The correlation between the carbon number and log k' is found to be linear for all series. The lines in Fig. 3a and b obtained from data at both temperatures are parallel with each other within the accuracy of the measurements. These log k' graphs are suitable for predicting the retention value of other not readily available members of the homologous series. These can be further characterized by their absorption spectra which for various homologous series exhibit maxima dependent on the degree of unsaturation.

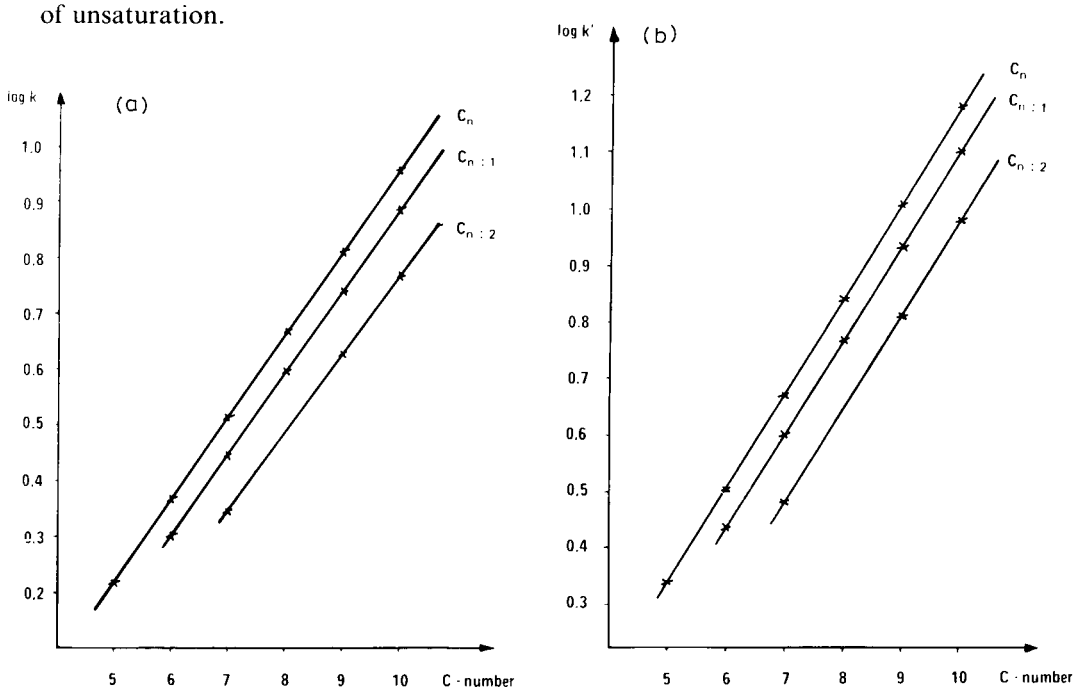

Fig. 3. Relationship between carbon number of aliphatic, straight-chain, saturated and mono- and di-unsaturated aldehydes and log k' at column temperatures (a) 50 and (b) 25°C.

At 25°C, the di-unsaturated aldehydes are eluted very close to the saturated aldehydes with one carbon less. At 50°C, all aldehydes were eluted separately. The different elution patterns at the two temperatures can be regognized from the two graphs in Fig. 3a and b. A more extended study of the influence of the column temperature on log k' and the separation of critical triplets formed by aldehydes of the saturated and mono- and di-unsaturated series is summarized in Fig. 4. From the diagram it is obvious that at higher temperatures di-unsaturated aldehyde hydrazones are accelerated more than the two other groups. This was found to be true for three critical triplets studied, of which two are shown in Fig. 4. Another effect of raising the temperature is an increase in column efficiency resulting in sharper peaks and shorter analysis times. These observations make it clear that separation of the critical triplets of aldehydes may be achieved by optimization of the temperature. For the case of

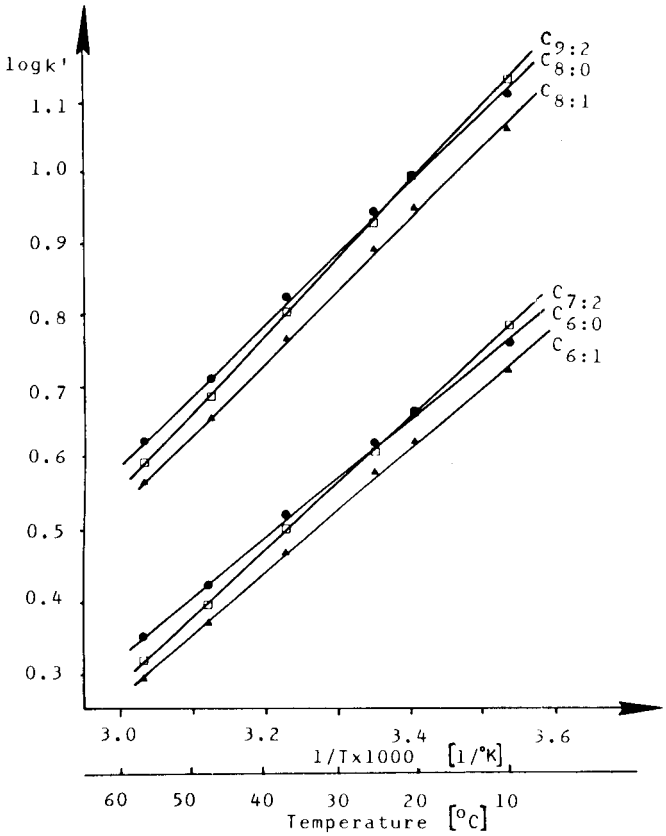

Fig. 4. Influence of the column temperature on log k' of critical triplets of aldehydes (log k' values in this figure are not the same as those in Fig. 3a and b because another column with the same packing material was used).

autoxidation of lipids, the critical triplet of practical importance is C_8, $C_{8:1}$ and $C_{9:2}$, which is separated best at 50°C (Figs. 2 and 4).

As mentioned previously, the separation system was optimized to determine the aldehydes formed during autoxidation of food samples. In Fig. 5, two chromatograms are reproduced to demonstrate the practical utility of the method. The chromatogram in Fig. 5a clearly shows the absence of aldehydes in a fresh pork liver sample with the exception of a small amount of hexanal. The chromatogram in Fig. 5b, in contrast, was obtained from a sample of identical origin after storage for 6 months at −8°C. A large hexanal peak dominates the chromatogram accompanied by the whole series of aldehydes at low concentrations as would be expected for autoxidation of animal lipids. This chromatogram indicates clearly strong rancidity. In order to give some idea about the sensitivity of detection in food samples it should be noted that the hexanal peak in Fig. 5a corresponds to 40 ppb and the peaks for octenal and heptenal in Fig. 5b represent concentrations of 90 and 20 ppb, respectively. This shows that under routine conditions aldehydes can be detected in meat samples in the lower ppb range.

The method described has been developed for the investigation of the progress

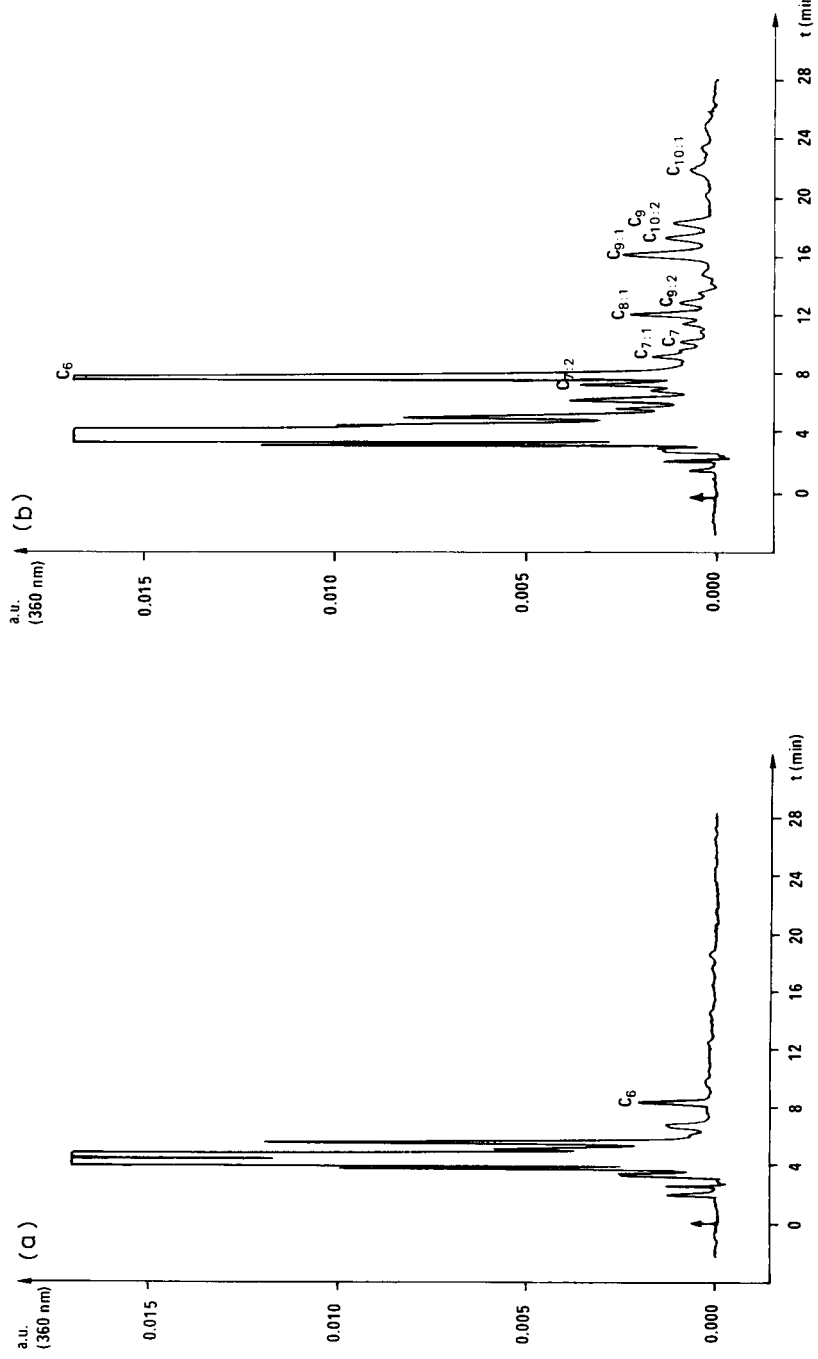

Fig. 5. HPLC trace of 2,4-DNPHs of carbonyl compounds from stored pork liver. (a) 1 week at −28°C; (b) 6 months at −8°C.

of rancidity in meat samples during storage at low temperatures. It includes an improved derivatization procedure for 2,4-dinitrophenylhydrazones which will be published elsewhere. The complete method may be of value also for carbonyl determination at trace levels in the fields of biological, medical and environmental research.

ACKNOWLEDGEMENTS

This work was supported by funds of the Minister of Youth, Family Affairs and Health of the Federal Republic of Germany. The authors thank Dr. R. Grossklaus for helpful discussions.

REFERENCES

1 A. J. St. Angelo, M. G. Legendre and H. P. Dupuy, *Lipids*, 15 (1980) 45.
2 C. W. Fritsch and J. A. Gale, *J. Amer. Oil Chem. Soc.*, 54 (1977) 225.
3 S. S. Chang, R. J. Peterson and Chi-Tang Ho, *J. Amer. Oil Chem. Soc.*, 55 (1978) 718.
4 K. Fung and D. Grosjean, *Anal. Chem.*, 53 (1981) 168.
5 H. Kallio, R. R. Linko and J. Kaitaranta, *J. Chromatogr.*, 65 (1972) 355.
6 R. J. Soukup, R. J. Scarpellino and E. Danielczik, *Anal. Chem.*, 36 (1964) 2255.
7 Y. Hoshika and Y. Takata, *J. Chromatogr.*, 120 (1976) 379.
8 V. P. Uralets, R. A. Rijks and P. A. Leclercq, *J. Chromatogr.*, 194 (1980) 135.
9 G. Urbach, *J. Chromatogr.*, 12 (1963) 196.
10 K. E. Moerck and H. R. Ball, Jr., *J. Agr. Food Chem.*, 27 (1979) 514.
11 P. W. Meijboom, *Fette, Seifen, Anstrichm.*, 70 (1968) 477.
12 J. Schormüller, M. Walther and W. Wachs, *Z. Lebensm.-Unters.-Forsch.*, 139 (1969) 273.
13 M. A. Carey and H. E. Persinger, *J. Chromatogr. Sci.*, 10 (1972) 537.
14 R. S. Deelder and P. J. H. Hendricks, *J. Chromatogr.*, 83 (1973) 343.
15 S. Selim, *J. Chromatogr.*, 136 (1977) 271.
16 P. R. Demko, *J. Chromatogr.*, 179 (1979) 361.
17 K.-I. Nakamura, M. Asami, S. Orita and K. Kawada, *J. Chromatogr.*, 168 (1979) 221.
18 G. Vigh, Z. Varga-Puchony, J. Hlavay, M. Petró-Turcza and I. Szárföldi-Szalma, *J. Chromatogr.*, 193 (1980) 432.

Journal of Chromatography, 235 (1982) 489–500
Elsevier Scientific Publishing Company, Amsterdam — Printed in The Netherlands

CHROM. 14,310

DETERMINATION OF CARBOFURAN AND ITS METABOLITES BY HIGH-PERFORMANCE LIQUID CHROMATOGRAPHY USING ON-LINE TRACE ENRICHMENT

PAUL H. CRAMER*, ARBOR D. DRINKWINE and JOHN E. GOING
Midwest Research Institute, 425 Volker Boulevard, Kansas City, MO 64110 (U.S.A.)
and
ANN E. CAREY
U.S. Environmental Protection Agency, Washington, DC (U.S.A.)
(First received August 4th, 1981; revised manuscript received August 29th, 1981)

SUMMARY

The concentration technique known as on-line trace enrichment was applied to the analysis of over 100 drinking water samples for carbofuran and five of its carbamic and phenolic metabolites. Levels of 1 ppb* could be determined from 5 ml of sample. The proposed method demonstrates shorter total analysis time than previous methods but is readily applicable only to relatively clean samples. A gas chromatographic method used as a confirmatory technique for detecting carbofuran and 3-hydroxycarbofuran is also presented. External standards data, detection limits, relative retention volumes, and sample spike compound recoveries are presented for the trace enrichment method.

INTRODUCTION

Carbofuran (2,2-dimethyl-2,3-dihydrobenzofuranyl-7-N-methylcarbamate) is a broad-spectrum insecticide–nematocide used for the control of insects in such crops as alfafa, peanuts, rice, corn, rapeseed, and potatoes. Although less persistent than organochlorine pesticides, carbofuran (I, Fig. 1) is more toxic (rat oral LD_{50} of 11 mg/kg)[1] and is a cholinesterase inhibitor. Recent findings of carbofuran and Aldicarb in groundwater supplies of Long Island, New York, have raised concern over the compounds' migration and transport characteristics after their application to crops. The carbamic (II, III) and phenolic (IV–VI) metabolites (Fig. 1) are also of interest because of their toxicity, and they may serve as indicators of previous carbofuran contamination. As part of a U.S. Environmental Protection Agency (EPA) project surveying groundwater for selected pesticides, Midwest Research Institute (MRI) sought a method to analyze some 130 samples for carbofuran and its metabolites.

Previous methods of analysis for the determination of carbofuran and its me-

* Throughout this article, the American billion (10^9) is meant.

0021-9673/82/0000–0000/$02.75

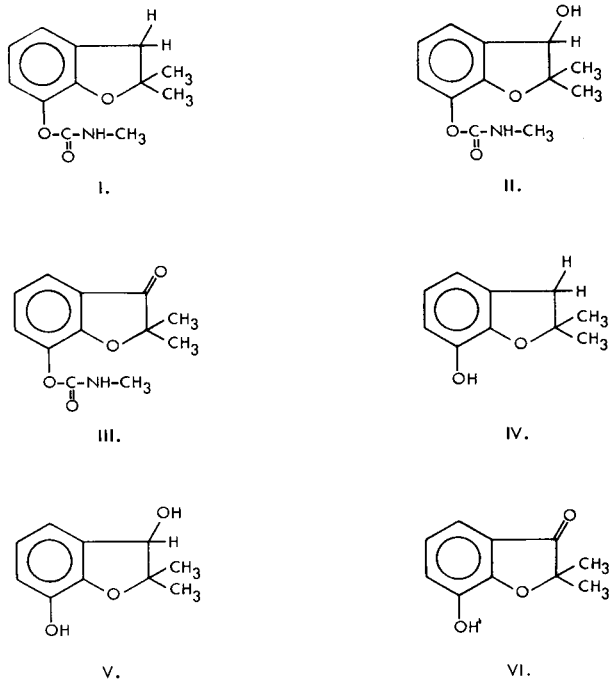

Fig. 1. Structures of carbofuran (I), 3-hydroxycarbofuran (II), 3-ketocarbofuran (III), carbofuran phenol (IV), 3-hydroxycarbofuran-7-phenol (V), and 3-ketocarbofuran-7-phenol (VI).

tabolites have been directed towards various plant and animal tissues. These methods generally have employed extensive cleanup procedures to separate the compounds of interest from interfering lipids and other hydrophobic materials and have frequently employed derivatization procedures to enhance chromatography and sensitivity. Gas chromatographic (GC) methods have used both derivatization procedures[2–5] and direct chromatography with nitrogen specific detection[6–8] to achieve the needed sensitivity. Additional direct GC methods have been applied to water and soil matrices[9–11]. Recent methods have employed high-performance liquid chromatography (HPLC) as a means of separation and detection utilizing both derivatization[12–14] and non-derivatization[15–17] procedures. All of these methods, however, require an extraction step, if not also a cleanup and derivatization step, somewhere in the procedure.

The selection of an analytical procedure was constrained by the requirements of (a) 1-ppb sensitivity, (b) an interest in all forms, (c) the limited sample volume of 200–400 ml, and (d) the preference for a single procedure. These criteria eliminated the published GC and HPLC methods in that no single procedure was applicable to the wide range of compounds. A new procedure was developed using on-column trace enrichment[18–21] to meet all the criteria.

EXPERIMENTAL

Reagents

Solvents were purchased as distilled-in-glass grade from Burdick & Jackson

Labs. (Muskegon, MI, U.S.A.) and degassed by vacuum filtration through a membrane filter. Chromatographic grade water was obtained from a Milli-Q-Reagent grade water system (Millipore, Bedford, MA, U.S.A.), which was modified to produce a lower concentration of organic contaminants by installing two charcoal cartridges at the end of the train. Aqueous filters (0.45 μm) were also obtained from Millipore. The sodium sulfate was obtained from Mallinkrodt (St. Louis, MO, U.S.A.). Chromatographic standards were obtained from the EPA Health Effects Research Laboratory (Research Triangle Park, NC, U.S.A.).

Apparatus

A Varian Model 3700 gas chromatograph equipped with a thermionic specific detector (TSD) and a Varian Model CDS-111 integrator was used in this study. The column utilized was a 0.91 m × 2 mm I.D. glass column packed with 3% OV-101 (Supelco, Bellefonte, PA, U.S.A.). After the initial temperature of 150°C was held for 1 min, the temperature was increased at a rate of 10°C/min to 180°C. The injector and detector temperature were 190°C and 200°C, respectively. The detector flow-rates were 3 ml/min for hydrogen and 175 ml/min for air, and the detector bead current was 4.5 A.

The liquid chromatograph consisted of two Waters series 6000A solvent delivery systems controlled by a Model 660 solvent programmer, a single-channel Model 440 detector operated at 280 nm, and a modified U6K injector (Waters Assoc., Milford, MA, U.S.A.). The U6K injector was adapted for this work by replacing the original 2-ml injection loop with a 1 m × 2.64 mm I.D. × 3.18 mm O.D. length of stainless-steel tubing. A μBondapak C_{18} (300 × 3.9 mm I.D.) column obtained from Waters Assoc. was used. The peaks were integrated by a Varian Model CDS-111 integrator. The standard operating procedures selected for trace enrichment reversed-phase elution analysis utilized a flow-rate of 2 ml/min starting at 100% water and stepping up to 50% methanol by setting the profile selector to the 1 position with a program length (delay) of 5 min.

Sample preparation

For GC analysis, a 100-ml aqueous sample was placed in a 250-ml separatory funnel and extracted with three 50-ml portions of dichloromethane for 1 min each time. The extracts were each drained into a 250-ml Kuderna–Danish apparatus through a 10-g column of Na_2SO_4. A Snyder column was attached and the extract concentrated to *ca.* 5 ml on a stream bath. The concentrated extract was transferred to a 7-ml vial and evaporated to dryness under a stream of nitrogen. Acetone (1 ml) was added, and the extract was stored in a refrigerator until analyzed by GC–TSD.

For the trace enrichment method, the general procedure was to measure the sample into a 10-ml volumetric flask and inject 10 μl of a 5-ng/μl solution of carbaryl internal standard into the solution. The spiked sample was transferred to a 10-ml glass/Teflon syringe equipped with a 0.45-μm aqueous filter, and 5 ml were injected into the sample loop of the U6K injector. The sample was then loaded onto the column by switching the inject lever to inject and simultaneously starting the recorder, integrator, and solvent programmer.

Sample collection and storage

Samples were collected from either private or community well sources. Water was taken directly from a household tap after allowing the water to run for 1 min, and placed in a 1-l bottle containing 1 g of sodium thiosulfate. The bottle was sealed with a PTFE-lined cap and maintained at 4°C during shipment and storage. Sampling began October 29th, 1979, and ended December 22nd, 1979.

RESULTS AND DISCUSSION

The trace enrichment method discussed here was originally developed to quantitate and verify the base hydrolysis of carbofuran (I) to carbofuran phenol (IV). Preliminary GC studies indicated that almost no carbofuran or 3-hydroxycarbofuran (II) was recovered after 1 week in tap water at a pH of 9.5. The GC method, however, could not show the concurrent increase in the phenolic hydrolysis products, and it was this fact that prompted the development of the trace enrichment method.

Monitoring the stability of carbofuran in water (spiked at 100 ppb) by the trace enrichment method gave the results shown in Fig. 2. This agrees with previous findings[1], which show the hydrolytic instability of carbofuran and its carbamic metabolites. Base hydrolysis of carbofuran begins immediately in tap water at pH 9.5, and its hydrolysis product, carbofuran phenol, is formed concurrently with mass balance of the two compounds varying between 80 and 113% recovery. At pH 6.5, no formation of the phenolic product from carbofuran was observed over the period of the 1-week study. Similar results might be expected for the hydrolysis of 3-hydroxycarbofuran (II) to 3-hydroxycarbofuran-7-phenol (V) and 3-ketocarbofuran (III) to 3-ketocarbofuran-7-phenol (VI)[1], but results were not quantitated due to lack of standards at the time the stability studies were being carried out.

Since hydrolysis occurs in basic solution and since many of the samples to be analyzed could be expected to be basic, the presence of carbofuran or its major plant metabolite, 3-hydroxycarbofuran, in drinking water would be highly unlikely[22–25]. Because of the limited sample volume (less than 100 ml in some cases), the proposed GC method utilized a very sensitive and specific detector, the TSD. This fact, however, eliminated the method's usefulness for the more probable phenolic metabolites. It was these facts, then, that led to the use of the less selective but equally sensitive HPLC method for the analysis of carbofuran and its metabolites.

The initial selection of the HPLC solvent system for the separation of carbofuran and metabolites was based on earlier work completed at MRI which analyzed for carbofuran in wastewater utilizing a simple dichloromethane extraction method with solvent exchange into acetonitrile. The solvent system used for the earlier work was acetonitrile–water (1:1). When this system was used to chromatograph carbofuran phenol, it was found that the phenol and its precursor (carbofuran) coeluted. Different ratios of acetonitrile to water did not affect resolution, but when the solvent system was changed to methanol–water, resolution was achieved. Initially the methanol–water solvent system included 1% (v/v) acetic acid in the aqueous phase to ensure protonation of the phenolic metabolites. The acetic acid was soon eliminated, however, because it did not affect resolution of these metabolites.

When the final step gradient system to methanol–water (1:1) was being chosen, it was shown that up to 50 ml of water could be passed through the analytical C_{18}

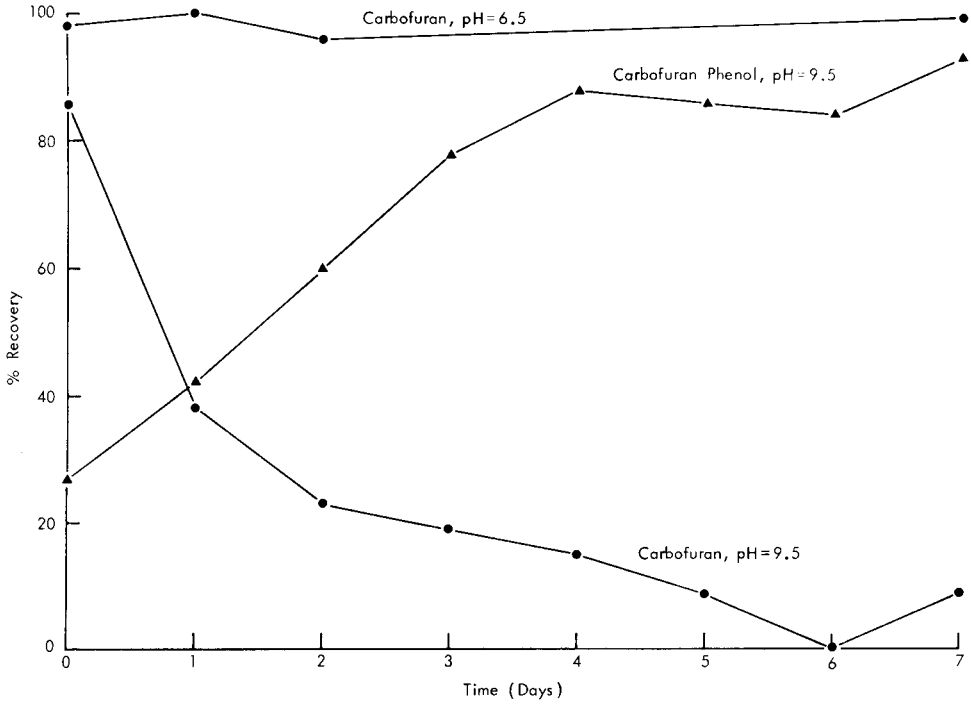

Fig. 2. Carbofuran stability in tap water at pH 9.5 and 6.5.

column, after a 10-μl injection of the compounds of interest in methanol, without altering the shape or resolution of the peaks. This fact assured us of being able to inject sizeable amounts (1–5 ml) of drinking water directly onto the analytical column. The Waters U6K injector was modified to accept a 5-ml sample volume by removing the standard 2-ml sample loop and replacing it with *ca.* 6-ml volume loop for the sample. The use of the step gradient to methanol–water (1:1) after 5 min of pumping 100% water at 2 ml/min allowed the 5-ml sample to be concentrated on the head of the column and gave an additional 2.5 min for any non-retained polar constituents to be eluted from the column before the step to methanol–water.

Detection limits based on 5 ml of sample as well as retention time windows relative to Carbaryl are given in Table I. The detection limits amounts for these compounds produced a signal which was twice the noise level at 0.005 a.u.f.s. For an individual sample, the detection limits could be higher due to interfering peaks. This was especially true for the first four metabolites, but virtually no peaks were seen to interfere with carbofuran or carbofuran phenol.

Retention time windows were used to identify carbofuran and its metabolites since the absolute retention times of the compounds and the internal standard varied slightly with the differences of sample matrices. The earlier eluting metabolites, which were most affected by changes in polarity and system anomalies, were assigned larger retention time windows than the later eluting compounds because of their greater variability.

All samples were screened for carbofuran and its metabolites (except 3-keto-

TABLE I

RELATIVE RETENTION TIMES AND DETECTION LIMITS FOR CARBOFURAN AND METABOLITES

Compound	*Detection limit (ppb)**	*Relative retention time window***
3-Hydroxycarbofuran-7-phenol	1	0.67 ± 0.01
3-Hydroxycarbofuran	1	0.71 ± 0.01
3-Ketocarbofuran	5	0.80 ± 0.005
3-Ketocarbofuran-7-phenol	5	0.81 ± 0.005
Carbofuran	1	0.91 ± 0.005
Carbofuran phenol	1	0.95 ± 0.005
Carbaryl (internal standard)	–	1.00

* Determined at 280 nm in a 5-ml sample.

** Determined on a C_{18} column using a step gradient from 100% water to 50% methanol after 5 min. Flow-rate 2 ml/min.

carbofuran) by comparison with external standards. Standard curves were generated daily from three to four mixed standards by using linear regression. A compilation of the average areas for each compound and the relative standard deviations for each compound at a given level over the period of analysis (*ca.* 5 weeks) are given in Table II. Also given in Table II are correlation coefficients for standard curves constructed from the average areas for each compound.

Limited data were obtained for 3-ketocarbofuran-7-phenol because of its relatively low sensitivity and its tendency to coelute with a compound present in the methanol as the column began to lose resolution. Although the relative standard deviations for the compound responses were large, especially at the lower levels, the correlation coefficients for the standard curves show good agreement. 3-Ketocarbo-

TABLE II

EXTERNAL STANDARD SUMMARY

Statistics	*Standard levels (ppb)*	*Compounds*				
		3-Hydroxy-carbofuran-7-phenol	*3-Hydroxy-carbofuran*	*3-Keto-carbofuran-7-phenol*	*Carbofuran*	*Carbofuran phenol*
Number of data points	1	15	15	2	21	21
	5	25	24	10	26	25
	25	20	16	5	19	21
Average area	1	29.4	14.9	3.0	9.8	9.2
	5	88.5	50.0	22.7	39.0	41.2
	25	313.9	251.4	119.4	229.4	246.4
Relative standard deviation	1	40.5	44.0	–*	29.8	29.4
	5	25.6	29.0	27.3	22.6	21.5
	25	12.1	16.4	20.8	17.5	8.7
Correlation		0.9991	0.9998	0.9999	0.9994	0.9995

* Insufficient data to calculate relative standard deviation.

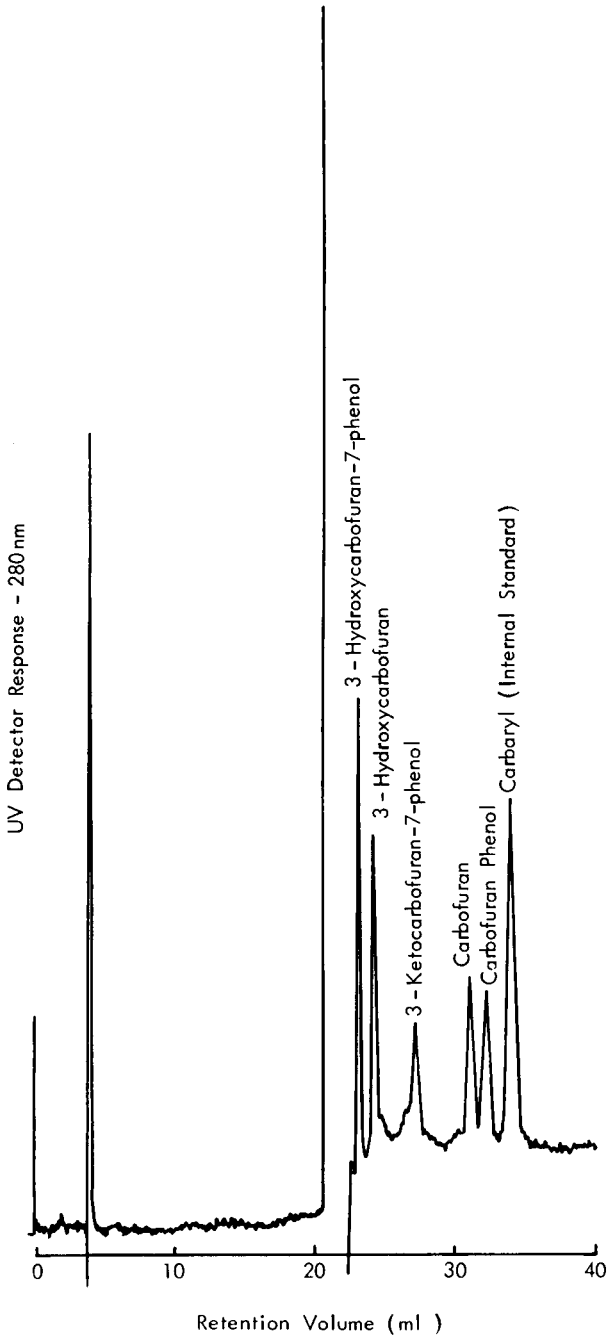

Fig. 3. Mixed 5-ppb standard. Column, μBondapak C_{18}; solvent program, step gradient to 50% methanol in water after 5 min; flow-rate 2 ml/min.

TABLE III
SAMPLE SPIKE RECOVERIES

Sample code	*Compounds*									
	3-Hydroxy-carbofuran-7-phenol		*3-Hydroxy-carbofuran*		*3-Keto-carbofuran-7-phenol*		*Carbofuran*		*Carbofuran phenol*	
	*Spiking level**	*% R***	*Spiking level*	*% R*	*Spiking level*	*% R*	*Spiking level*	*% R*	*Spiking level*	*% R*
01-069-0500C***	5	94	5	77	5	105	5	90	5	90
01-069-206C	5	85	5	93	5	82	5	93	5	111
01-109-1701C	5	49	5	82	10	obs	5	62	5	73
04-019-301C	5	114	5	67	10	obs	5	85	5	82
04-021-0355-01	1	obs§§§	1	297	2	obs	1	107	1	100
04-027-102C	5	64	5	74	5	118	5	96	5	102
06-029-0180C	5	76	5	93	5	105	5	79	5	81
06-039-201C§	10	obs	10	60	20	obs	10	67	10	90
06-039-203C	1	71	1	105	2	obs	1	53	1	74
06-039-203C	2	82	2	92	4	obs	2	168	2	150
06-039-203C	5	obs	5	48	10	obs	5	76	5	105
06-039-203C	10	121	10	60	20	obs	10	65	10	99
06-099-1395C	5	90	5	152	5	90	5	94	5	95
06-099-305C	5	86	5	80	5	111	5	123	5	79
13-321-201C	5	97	5	96	5	110	5	103	5	101
13-321-201C§§	5	99	5	105	5	100	5	97	5	119
13-321-2740C	5	94	5	84	5	75	5	85	5	88
26-049-306C	5	68	5	74	10	105	5	63	5	63
27-119-102-001	5	46	5	87	10	84	5	82	5	105
28-133-0345C	5	88	5	77	10	obs	5	obs	5	obs
28-133-103C	5	90	5	82	10	obs	5	obs	5	obs
36-051-301C	5	137	5	74	10	obs	5	72	5	63
45-089-304C	5	obs	5	74	10	obs	5	77	5	91
48-279-106C	5	obs	5	97	10	obs	5	77	5	91
Average recovery		87		93		99		87		93
Relative standard deviation		26		52		14		28		21

* Spiking levels are given in ppb.
** Percentage recovery.
*** C indicates this sample was a composite.
§ Sample has pH of 9.6; was spiked and stored 24 h before analysis.
§§ Sample spiked after filtration in this instance.

furan was not screened in the samples because of its hydrolytic instability and because it virtually coelutes with its hydrolysis product. Since it hydrolyzes *ca.* 165 times more rapidly than carbofuran[1], it was more likely to be found as 3-ketocarbofuran-7-phenol.

The trace enrichment method was applied to the analysis of 132 well-water samples or sample composites. The results of the analyses of all well-water samples were negative (below the detection limits). Those samples suspected of containing carbofuran or any of its metabolites were subjected to either spiking at 5 ppb and reanalysis by trace enrichment or extraction and GC–TSD confirmation.

Interpretation of the sample chromatograms was facilitated by spiking one sample out of a group of samples which showed the same pattern of peaks. The addition of the compounds of interest to a sample such as this eliminated any doubt as to the identity of a given peak in the unspiked samples and also gave method recovery values for those compounds in that sample matrix. Table III gives percent recoveries and spiking levels for 20 samples.

Carbofuran recoveries at all levels tested were 87%, with a relative standard deviation of 28% (Table III). In general, recoveries for all metabolites were better than 85%. Sample 06-039-203 composite (see Table III) was spiked at four different levels in an attempt to observe any patterns in recoveries at different spiking levels. No trends were observed and recoveries at the 1-ppb level were good except for 3-ketocarbofuran-7-phenol and carbofuran, both of which were partially or totally obscured by interfering peaks. Sample 13-321-201 composite was spiked at the 5-ppb level both before and after filtration to see if any losses were incurred by filtration; no difference in recoveries was observed. Sample 06-039-201 composite (pH 9.6) was spiked at 10 ppb and allowed to stand for 24 h before analysis. The low recoveries for carbofuran (67%) and 3-hydroxycarbofuran (60%) in this situation can probably be attributed to the base hydrolysis of those compounds to the corresponding phenols although an increase in the phenol recoveries was not observed.

Figs. 3–5 show chromatograms of a 5-ppb mixed standard, a typical sample, and the same sample spiked at 5 ppb. Only five samples were suspected to contain carbofuran or 3-hydroxycarbofuran. These samples were subjected to the GC method, but none were found to contain either carbamate residue. The detection limits were 1 ppb for carbofuran and 5 ppb for 3-hydroxycarbofuran by this method. Poor chromatography for 3-hydroxycarbofuran contributed to its high detection limit.

CONCLUSIONS

On-line trace enrichment for the analysis of carbofuran and metabolites in drinking water without the use of a precolumn is an effective means of analysis. The advantages of this method lie in its simplicity and its sensitivity. Instrument modification requires no special valves or fabricated parts and could be easily done in any laboratory with a similar instrument. Since there is virtually no sample preparation other than spiking the sample with the internal standard and filtering, the total analysis time for each sample is essentially the HPLC run time, or *ca.* 30 min (including re-equilibration of the HPLC system). A detection limit of 1 ppb (in 5 ml of sample) is easily achievable for carbofuran and most of its metabolites without benefit of solvent

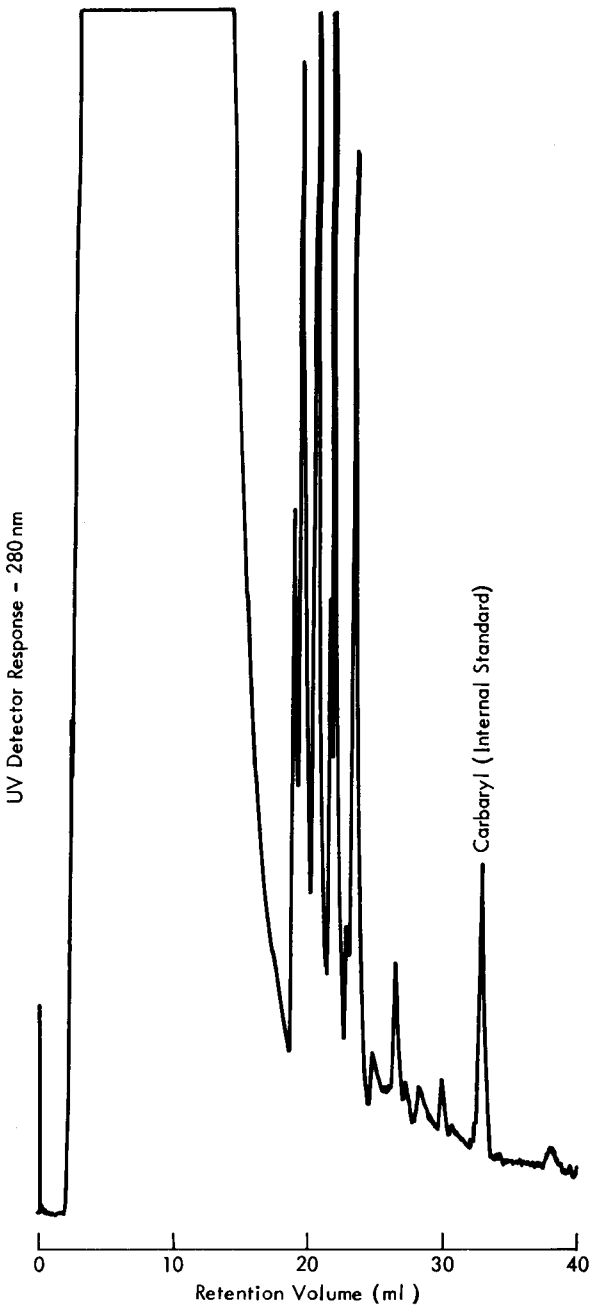

Fig. 4. Sample 06-029-0180 composite; taken from Kern County, CA, U.S.A.

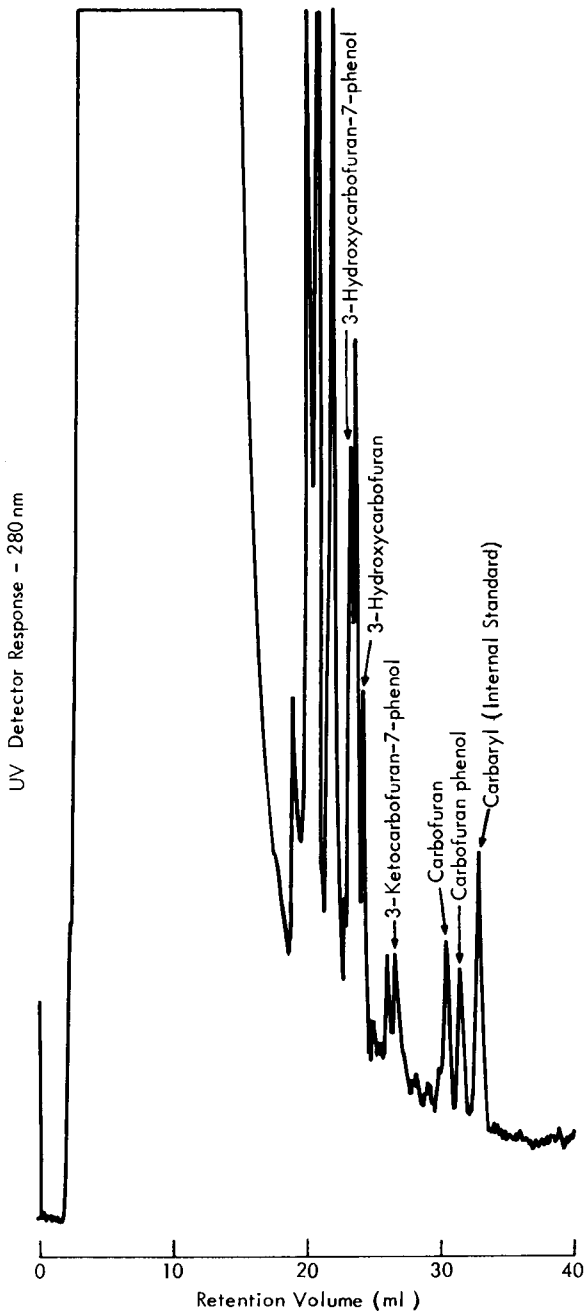

Fig. 5. Sample 06-029-0180 composite spiked at 5 ppb with carbofuran and metabolites.

extraction or derivatization procedures. If the volume of sample concentrated on the head of the column is increased, and this is highly possible, then even lower detection limits can be attained. The basic concept should be applicable, with some modifications, to other compounds with similar polarities and hydrophobic properties.

ACKNOWLEDGEMENT

This work was performed for the Field Studies Branch, Office of Toxic Substances, U.S. Environmental Protection Agency, in partial fulfillment of Contract No. 68-01-5915, Ms. Ann E. Carey, Task Manager, Dr. R. Kutz, Project Officer.

REFERENCES

1 R. L. Metcalf, T. R. Fukuto, C. Collins, K. Borck, S. Abd El-Aziz, R. Munoz and C. C. Cassil, *J. Agr. Food Chem.*, 16 (1968) 300.
2 T. E. Archer, J. D. Stokes and R. S. Bringhurst, *J. Agr. Food Chem.*, 25 (1977) 536.
3 R. A. Chapman and J. R. Robinson, *J. Chromatogr.*, 140 (1977) 209.
4 R. F. Cook, J. E. Jackson, J. M. Shuttleworth, O. H. Fullmer and G. K. Fujie, *J. Agr. Food Chem.*, 25 (1977) 1013.
5 L. Wong and F. M. Fisher, *J. Agr. Food Chem.*, 23 (1975) 315.
6 T. A. Nelsen and R. F. Cook, *J. Agr. Food Chem.*, 28 (1980) 981.
7 I. H. Williams and M. J. Brown, *J. Agr. Food Chem.*, 21 (1973) 399.
8 R. F. Cook, R. P. Stanovick and C. C. Cassil, *J. Agr. Food Chem.*, 17 (1969) 277.
9 A. M. Kadoum and D. E. Mock, *J. Agr. Food Chem.*, 26 (1978) 45.
10 R. C. Hall and D. E. Harris, *J. Chromatogr.*, 169 (1979) 245.
11 K. M. S. Sundaram, S. Y. Szeto and R. Hindle, *J. Chromatogr.*, 177 (1979) 29.
12 J. F. Lawrence, D. A. Lewis and H. A. McLeod, *J. Chromatogr.*, 138 (1977) 143.
13 J. F. Lawrence and R. Leduc, *J. Chromatogr.*, 152 (1978) 507.
14 T. R. Nelsen and R. F. Cook, *J. Agr. Food Chem.*, 27 (1979) 1186.
15 J. F. Lawrence and R. Leduc, *J. Agr. Food Chem.*, 25 (1977) 1362.
16 Y. M. Lee and N. D. Westcott, *J. Agr. Food Chem.*, 28 (1980) 719.
17 H. Sonobe, R. A. Carver and L. R. Kamps, *J. Chromatogr.*, 210 (1981) 356.
18 H. P. M. Van Vliet, Th. C. Bootsman, R. W. Frei and U. A. Th. Brinkman, *J. Chromatogr.*, 185 (1979) 483.
19 J. N. Little and G. J. Fallick, *J. Chromatogr.*, 112 (1975) 389.
20 D. C. Paschal, R. Bicknell and D. Dresbach, *Anal. Chem.*, 49 (1977) 1551.
21 R. W. Edwards, K. A. Nonnemaker and R. L. Cotter, *NBS Spec. Public.*, 519 (1979) 87.
22 C. C. Yu, G. M. Booth, D. J. Hansen and J. R. Larsen, *J. Agr. Food Chem.*, 22 (1974) 431.
23 J. H. Caro, H. P. Freeman, D. E. Glotfelty, B. C. Turner and W. M. Edwards, *J. Agr. Food Chem.*, 21 (1973) 1010.
24 T. E. Archer, *J. Agr. Food Chem.*, 24 (1976) 1057.
25 S. K. Kapoor and R. L. Kalra, *J. Food Sci. Technol.*, 12 (1975) 227.

Journal of Chromatography, 235 (1982) 501–506
Elsevier Scientific Publishing Company, Amsterdam — Printed in The Netherlands

CHROM. 14,346

CHROMATOGRAPHIC ASSAY OF STEROIDS ON IMMUNO-AFFINITY PAPER STRIPS; A RAPID METHOD FOR THE QUANTITATION OF DIGOXIN AND OESTRIOL-16α-GLUCURONIDE CONCENTRATIONS*

E. C. METCALF, M. R. A. MORGAN** and P. D. G. DEAN*
Department of Biochemistry, University of Liverpool, P.O. Box 147, Liverpool L69 3BX (Great Britain)
(Received September 9th, 1981)

SUMMARY

The combination of affinity chromatography and immunoassay provides a novel method for the quantitation of steroids in biological fluids.

Anti-digoxin and anti-oestriol-16α-glucuronide antibodies were immobilised to cellulose strips, and used for ascending paper chromatography. Labelled digoxin and oestriol-16α-glucuronide were selectively retarded on strips containing the appropriate immobilised antibodies. The degree of retardation was quantitatively affected by the addition of non-labelled steroid to the sample. Calibration curves could, therefore, be constructed. The sensitivity of the assay system can be altered by changing the concentration of immobilised antibody on the cellulose strip. Calibration curves over the range 50–800 pg for digoxin and 50–250 pg for oestriol-16α-glucuronide are presented.

INTRODUCTION

Recent advances in immunoassay techniques have focused on labelling methods including enzyme-linked immunosorbent assay[1], fluoroimmunoassay[2] and luciferase-dependent enzyme-multiplied immunoassay technique systems[3]. Whilst many of these methods have improved sensitivity and have reduced biohazards by avoiding radioisotopes, nevertheless, expensive detectors and carcinogenic substrates are still commonplace. Mass screening by traditional methods of immunoassay is time-consuming and expensive. It is desirable to be able to screen a wide cross-section of newborn for a number of conditions, *e.g.*, phenylketonuria, thyroid and steroid deficiences.

We have sought to develop an assay system which is (i) cheap, (ii) capable of widespread application, (iii) requires little skill by the user, (iv) is rapid and (v) which involves low cost apparatus. The commonplace use of batch techniques in immunoassay limits the ligand–protein interaction to high K_A systems. The disadvantages of

* Dedicated to Professor J. Porath on the occasion of his 60th birthday.
** Present address: A.R.C., Food Research Institute, Colney Lane, Norwich NR4 7UA, Great Britain.

0021-9673/82/0000–0000/$02.75

batch methods have been previously outlined[4]. However, the application of sequential exposures of ligand to immobilised macromolecules does not seem to have been exploited in immunoassay, although recently Glad and Grub[5–7] have described the determination of plasma proteins using a similar technique.

In this paper we describe the use of cellulose-immobilised anti-steroid antisera for the assay of oestriol-16α-glucuronide and digoxin. We chose these two small hapten systems because of the known difficulties of operating some affinity chromatographic separations when the ligands are bound to cellulose matrices.

MATERIALS

[G-^{3}H]Digoxin (specific activity 10.6 Ci/mmol) and [6,9(n)-^{3}H]oestriol-16α-glucuronide (specific activity 30 Ci/mmol) were obtained from the Radiochemical Centre (Amersham, Great Britain). Oestriol-16α-glucuronide was purchased from Steraloids (Wilton, NH, U.S.A.).

Anti-digoxin, code R2BI (titre 1:2500), and anti-oestriol-16α-glucuronide, code R2BI (titre 1:500), were prepared by standard procedures[8]. Digoxin, bovine serum albumin (Cohn Fraction V) and cyanogen bromide were obtained from Sigma (London, Great Britain). Rabbit serum was a gift from Dr. C. D. Green (Department of Biochemistry, University of Liverpool). NE260 micellar scintillant was purchased from Nuclear Enterprises (Edinburgh, Great Britain). Chromatography paper (Grade No. 1 or 3 MM) was obtained from Whatman (Maidstone, Great Britain). All other reagents (Analar grade) were purchased from BDH (Poole, Great Britain).

METHODS

Immobilisation of antisera

Method 1. Whatman 3 MM filter-paper (50 strips, 1 × 8 cm) were suspended in distilled water (200 ml) at 18°C and the pH of the solution raised to 10.8 by the addition of 4 *M* NaOH. Cyanogen bromide (2 g) was added and the solution titrated to pH 10.8 with 4 *M* NaOH. The temperature was maintained at 18–20°C by the addition of crushed ice. After 15 min the papers were transferred to a cooled sinter and washed rapidly with 5% (v/v) acetone–water (1 l) followed by ice-cold 0.1 *M* sodium carbonate–bicarbonate buffer, pH 9.5 (1 l). The paper strips were then immersed in antiserum (1 ml antiserum diluted with 19 ml 0.1 *M* carbonate–bicarbonate buffer, pH 9.5) and incubated on a Coulter rotary mixer for 18 h at 4°C. When dilutions of antisera were required, antisera were diluted to 1 ml with normal rabbit serum followed by dilution to 20 ml with 0.1 *M* bicarbonate buffer. After immobilisation, the paper strips were washed extensively in 100 m*M* phosphate-buffered saline pH 7.0 (5 l), dried and stored at room temperature.

Method 2. The filter-paper (Whatman No. 1, 10 strips, 8 × 0.5 cm) was immersed in 2 *M* potassium carbonate–bicarbonate buffer, pH 11.0, and kept at 4°C. Cyanogen bromide (0.5 g) was dissolved in the minimum volume of N-methylpyrrolidone, and added dropwise to the paper strips without allowing the temperature to rise. The reactants were left for 15 min with occasional mixing before decanting the liquid and washing the activated strips with ice-cold 0.1 *M* sodium bicarbonate, and 5% (v/v) acetone solution. The washing cycle was repeated three times, finishing with

a further bicarbonate wash. The papers were then placed in the antiserum (10 ml) to which 0.1 *M* sodium bicarbonate solution (5 ml) had been added, and rotated on a Coulter mixer for 4 days at 4°C. The papers were washed with 6 × 20 ml 0.1 *M* phosphate-buffered saline pH 7.4, incorporating thiomersal (1 g/l) and bovine serum albumin (1 g/l), and allowed to dry at room temperature, prior to storage at 4°C in a screw-capped bottle.

Chromatography

Each paper strip (8 × 1 cm) was cut in half (8 × 0.5 cm) and marked (pencil) at 0.5-cm intervals down its length. The sample and the labelled steroid (in ethanol) were spotted onto the paper strips 1 cm from the bottom. In the case of [G-^{3}H]digoxin, 32 pg of labelled material were applied; for labelled oestriol-16α-glucuronide, 15 pg were applied. The strips were then developed by ascending chromatography in (i) 0.1 *M* phosphate-buffered saline, pH 7.0 containing 10% (v/v) glycerol until the solvent front was 1 cm from the top of the strip; or (ii) 0.1 *M* phosphate-buffered saline, pH 7.4 for 1 h. Preliminary experiments indicated that the presence of glycerol improved binding to the immobilised antibody. The strips were dried, cut into 0.5-cm segments and radioactivity determined in NE260 scintillant (4 ml) on a Nuclear Chicago Isocap 300 scintillation counter.

RESULTS AND DISCUSSION

Figs. 1 and 2 show the distribution of labelled steroids (digoxin and oestriol-16α-glucuronide, respectively) on paper strips containing the appropriate immobilised antiserum in the presence of increasing amounts of unlabelled steroid. In the absence of unlabelled steroid, the maximum amount of radioactivity was found in segment 3, *i.e.*, the point of application of the steroid. As a control, immobilised normal rabbit serum was used instead of anti-steroid antiserum (Figs. 1 and 2). The maximum radioactivity was observed in segment 12, *i.e.*, immediately prior to the solvent front (segment 14). This indicates that retardation was due to the steroid binding specifically to the immobilised antibody, irrespective of the method of immobilisation used. In both systems, increasing the amount of unlabelled steroid applied to the strips displaced the peak of radioactivity further up the strip (Fig. 1). Thus the application of unlabelled digoxin (10 ng) to anti-digoxin paper strips displaced the peak of radioactivity from segment 3 to segment 11. Preliminary experiments indicated that the presence of human serum in the applied sample did not interfere with the displacement of tritiated steroid by unlabelled steroid.

Calibration curves were constructed relating the displacement of label to the amount of unlabelled steroid applied by measuring either (i) the position of maximum radioactivity (Fig. 3) or (ii) percentage of the total radioactivity found in a particular segment (Fig. 4). In both these plots the major portion of the curve is linear, deviating only at the upper limits of the range. Under the conditions described the sensitivity of this chromatographic method for detecting unlabelled steroid lies within the range 1–5 ng (for digoxin, Fig. 3) and 50–250 pg (for oestriol-16α-glucuronide, Fig. 4).

Because this chromatographic assay system depends on the competition of labelled and unlabelled steroid for immobilised antibody, it is suggested that the repeated exposure of antigens (and cross-reacting substances) in the sample to im-

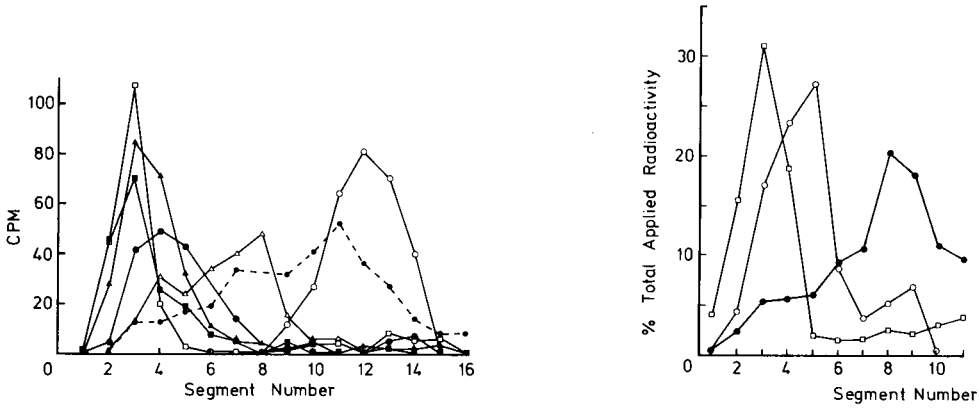

Fig. 1. The movement of [G-^{3}H]digoxin on cellulose strips containing immobilised rabbit anti-digoxin antisera in the presence of increasing amounts of unlabelled digoxin. Unlabelled digoxin (0–10 ng in 5–25 μl ethanol) was applied 1 cm from the end of cellulose strip (0.5 × 8 cm), containing immobilised anti-digoxin antisera or immobilised normal rabbit serum prepared by *Method 1* (see Methods). Tritiated digoxin (36 pg in 5 μl ethanol) was then applied. The cellulose strips were developed by ascending chromatography in 0.1 *M* phosphate-buffered saline, pH 7.0 containing 10% (v/v) glycerol (500 μl) until 1 cm from the top of the strips. The strips were dried, cut in 0.5-cm segments and counted in vials containing scintillant (4 ml). □ – □, 0 ng; ■ – ■, 0.2 ng; ▲ – ▲, 0.6 ng; ● – ●, 1 ng; △ – △, 5 ng; ●--- ●, 10 ng unlabelled digoxin applied; ○--○, immobilised rabbit serum.

Fig. 2. The migration of [6,9(n)-^{3}H]oestriol-16α-glucuronide on paper strips containing immobilised rabbit anti-oestriol-16α-glucuronide antisera in the presence of increasing amounts of unlabelled steroid. Radioactive oestriol-16α-glucuronide (15 pg) was applied as described in Fig. 1 to immobilised antibody strips prepared by *Method 2*. Unlabelled steroids (100 and 400 pg) were applied and the strip developed with 0.1 *M* phosphate-buffered saline, pH 7.4 for 1 h. The strips were dried and assayed for labelled steroid as described in Fig. 1. Radioactivity per segment is expressed as a percentage of that applied to the strip. □ – □, 0 ng; ○ – ○, 100 pg; ● – ●, 400 pg unlabelled oestriol-16α-glucuronide applied.

mobilised antibodies is likely to lead to improved selectivity. Furthermore, it is suggested that the assay sensitivity can be manipulated by the judicious choice of the concentration of the immobilised antibody. Fig. 5 shows the effect of chromatography of 36 pg of tritiated digoxin on paper strips containing decreasing concentrations

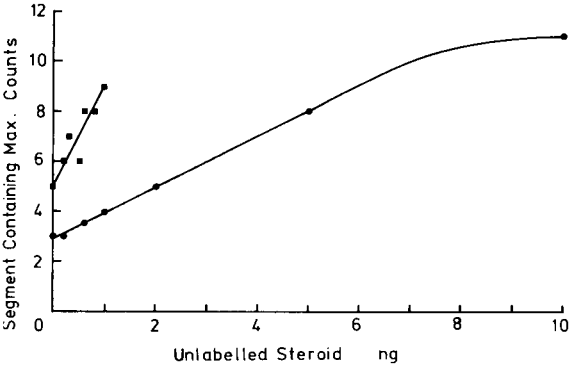

Fig. 3. Calibration curve relating the displacement of [G-^{3}H]digoxin on immobilised anti-digoxin cellulose strips with the amount of unlabelled digoxin applied. Methods see Fig. 1. ● – ●, Undiluted antiserum-paper; ■ – ■, sixty-fold diluted antiserum-paper.

of the immobilised antiserum: as the concentration of immobilised antibody decreased so radioactivity migrated further up the strip. Thus 36 pg of digoxin gave zero migration on R2BI antibody paper strips but gave a peak of maximum radioactivity at segment 7 for a fifty-fold dilution of the original immobilised antibody concentration. Indeed, this displacement is also reflected in the increased sensitivity to cold digoxin. In the "diluted" strip the working range was 50–800 pg (Fig. 3), compared with 1–5 ng in the "undiluted" strip. These data suggest that with a range of immobilized antibody concentrations, a range of assay sensitivities can be produced.

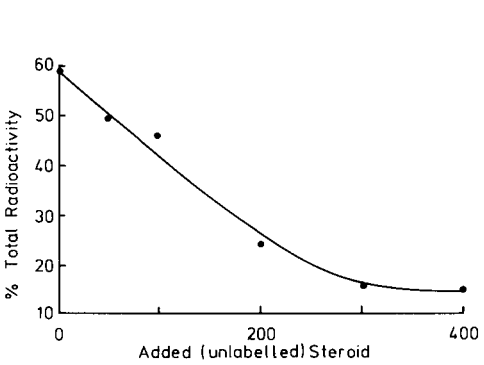

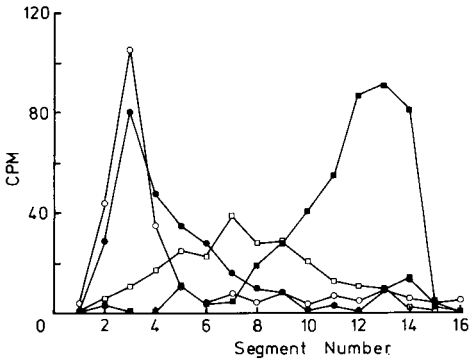

Fig. 4. Calibration curve relating the radioactivity found in segment 3 to the amount of unlabelled oestriol-16α-glucuronide applied to paper strips containing immobilised anti-oestriol-16α-glucuronide. Methods see Fig. 2.

Fig. 5. The effect of antibody concentration on the migration of tritiated digoxin on paper strips containing immobilised anti-digoxin antisera. 36 pg of [G-^{3}H]digoxin were applied to strips containing different dilutions of antisera and the strips treated as Fig. 1. ○ – ○, Undiluted sera; ● – ●, sera diluted by ten-fold; □ – □, sera diluted by fifty-fold; ■ – ■, sera diluted by a hundred-fold prior to immobilisation.

A further interesting possibility exists: the concept of combining chromatography with the separation of free and bound species in immunoassay suggests that the assay of samples need involve measuring only the distance migrated by the label. This idea could be easily applied to a device which discriminates between "high" and "low" samples by whether the label triggers the detector positioned at a fixed location in relation to the point of application. The label could be fluorescent, luminescent or a radioisotope.

CONCLUSION

This paper describes a method which combines the advantages of the chromatographic process and immunoassay: the sequential exposure to antibody as the sample moves through the strip increases sensitivity, specificity and allows rapid quantitation which is suitable for automation.

ACKNOWLEDGEMENTS

The authors wish to thank Powell & Scholefield, Liverpool, Great Britain for financial support and J. Ireland for stimulating discussions.

REFERENCES

1 E. Engvall and P. Perlmann, *Immunochemistry*, 8 (1971) 871.
2 K. E. Rubenstein, R. S. Schneider and E. F. Ullman, *Biochem. Biophys. Res. Commun.*, 47 (1972) 846.
3 H. Arakawa, M. Maeda and A. Tsuji, *Anal. Biochem.*, 97 (1979) 248.
4 C. R. Lowe, M. J. Harvey and P. D. G. Dean, *Eur. J. Biochem.*, 42 (1974) 1.
5 C. Glad and A. O. Grub, *Biochem. Soc. Trans.*, 5 (1977) 712.
6 C. Glad and A. O. Grub, *Anal. Biochem.*, 85 (1978) 180.
7 C. Glad and A. O. Grub, *Acta Chem. Scand., Ser. B*, 34 (1980) 449.
8 P. D. G. Dean, M. J. Johnson and D. Exley, *Steroids*, 18 (1971) 593.

Journal of Chromatography, 235 (1982) 507–512
Elsevier Scientific Publishing Company, Amsterdam — Printed in The Netherlands

CHROM. 14,360

MARIJUANA METABOLITES IN URINE OF MAN

XI. DETECTION OF UNCONJUGATED AND CONJUGATED Δ^9-TETRAHYDROCANNABINOL-11-OIC ACID BY THIN-LAYER CHROMATOGRAPHY

SAUL L. KANTER*, LEO E. HOLLISTER and JOSE U. ZAMORA
Veterans Administration Medical Center, Palo Alto, CA 94304 (U.S.A.)
(Received September 11th, 1981)

SUMMARY

A method for separating unconjugated and conjugated Δ^9-tetrahydrocannabinol-11-oic acid, the major urinary metabolite of Δ^9-tetrahydrocannabinol in man, by liquid–liquid extraction and detection of both forms by thin-layer chromatography is described. The unconjugated form of the metabolite is extracted with hexane–diethylether (65:35), and the conjugated form (which remains in the aqueous phase) is extracted with ether after enzymic hydrolysis. The residue of each extract is chromatographed in an alkaline and an acidic solvent sequence, and the metabolites are detected with Fast Blue Salt B.

INTRODUCTION

The principal aim in studies of drug metabolism is to identify the pathways by which drugs are transformed in the body, and to ascertain quantitatively the importance of each pathway and intermediate[1]. In order to identify these pathways, recovery and identification of metabolites are usual early steps. Thus, analytical procedures that separate metabolites, either individually or into groups of compounds, are of primary importance in the technology of methods used for identification.

In our studies of the metabolism of Δ^9-tetrahydrocannabinol (THC) we have used a multi-step extraction procedure by which, after enzymic hydrolysis and liquid–liquid extraction with hexane and anhydrous diethyl ether (ether) under various pH conditions, urinary metabolites were seaparated into four fractions, *viz.*, non-polar and polar neutral compounds, and weakly polar and more polar acids[2–5]. Recently, we found that the conjugated neutral metabolites and conjugated Δ^9-tetrahydrocannabinol-11-oic acid (THC-11-oic acid) were extracted (with the unconjugated forms of these metabolites) into ether from unhydrolyzed urine when it was acidified[6]. Until this observation, the assumption had been that conjugated metabolites of THC were not extracted from unhydrolyzed urine with ether[7,8].

We now report a method for separating unconjugated and conjugated THC-

0021-9673/82/0000-0000/$02.75

11-oic acid, the major urinary metabolite of THC in man, by liquid–liquid extraction and detecting both forms by thin-layer chromatography (TLC).

EXPERIMENTAL

Method

Extraction of unconjugated THC-11-oic acid. A volume of urine containing up to 50 mg of creatinine is adjusted to pH 4.7 to 6.3 and concentrated by evaporation in a Buchi rotary evaporator[3]. The concentrate is transferred to a 25 × 150 mm screw-capped culture tube (scct) and diluted to 10 ml with water, and the tube is stoppered with a PTFE-lined screw-cap. The liquid is extracted twice with 15 ml hexane–anhydrous diethyl ether (65:35) by shaking vigorously at 225 rpm for 2 min each time on a reciprocating shaker with the long axis of the tube in the direction of shaking. After each extraction, the tube is centrifuged at 2000 RCF for 3 min, and the hexane–ether extract is transferred with a pipet and a 3-ball-valve pipet filler to another 25 × 150 mm scct; the aqueous phase is reserved to be processed for conjugated THC-11-oic acid. The combined hexane–ether extracts are evaporated to dryness in a stream of nitrogen in a water bath at 50°C, and the residue is dissolved in 15 ml of ether. The solution is washed once with 10 ml of 5% $NaHCO_3$ solution by shaking as described above for 1 min. The tube is centrifuged briefly to separate the two phases quickly, and the $NaHCO_3$ layer is removed with a pipet and pipet filler and discarded. Approximately 1 g of anhydrous granular Na_2SO_4 is added to the ether solution, and the tube is stoppered, inverted three or four times and centrifuged briefly. The dried ether solution is poured through a small glass funnel into a 20 × 125 mm scct in a manner such as to avoid transfer of any Na_2SO_4. The Na_2SO_4 is washed once with 5 ml of ether, which is added to the contents of the scct, and the ether solution is evaporated as previously described. The inner wall of the scct is washed down with 0.5 ml of ethanol, which is then evaporated, and the residue is dissolved in 30 μl of absolute ethanol and stored at freezer temperature until chromatographed as described below.

Extraction of conjugated THC-11-oic acid. Without further adjustment of pH, the aqueous phase from the extraction of the unconjugated metabolite is incubated with 0.1 ml of β-glucuronidase–arylsulphatase at 55–60°C for 30 min[9]. The hydrolysate is cooled to room temperature and extracted with ether (15 ml × 2) by shaking vigorously as previously described for 1 min. After each extraction, the tube is centrifuged at approximately 2000 RCF for 3 min to separate the two phases quickly, and the ether extracts are transferred to another 25 × 150 mm scct. Between extractions, the ether of of the first extract is evaporated in a stream of nitrogen in a water bath at 50°C. The ether extract is washed twice with 5% $NaHCO_3$ as previously described, then the processing is continued as described above.

The residues of the unconjugated and conjugated fractions are transferred, as a streak, to a pre-coated silica gel G TLC plate (Analtech, 250 μm) with 30 and 20 μl of absolute ethanol. The origin is 2.5 cm from the bottom of the plate, and the solvent path is 10 cm. Chromatography is carried out in two tanks each saturated with its solvent mixture[9]. The first development is with acetone–chloroform–triethylamine (80:20:1) and the second is with light petroleum (b.p. 30–60°C)–diethyl ether–glacial acetic acid (50:50:1.5). After the first development, the TLC plate is placed in a fume

hood for 5 min, and approximately 5 min after the second development, it is sprayed with a cold 0.1% solution of Fast Blue Salt B in 2 *N* NaOH. A positive response is indicated by a magenta-colored zone of R_F 0.1 or corresponding to a reference standard of THC-11-oic acid. The reference standard, in absolute ethanol, is stored at freezer temperature.

Experiments

Extraction of unconjugated THC-11-oic acid. Although hexane did not extract conjugated THC-11-oic acid from acidified unhydrolyzed urine, it did extract unconjugated THC-11-oic acid, but not quantitatively. Thus, we examined the possibility of finding a hexane–ether mixture that would extract unconjugated THC-11-oic acid completely from acidified unhydrolyzed urine and not extract any conjugated THC-11-oic acid.

We first determined the minimum concentration of ether in a hexane–ether mixture that would completely extract unconjugated THC-11-oic acid from urine. A concentrate of a urine (from a user of cannabis) containing THC-11-oic acid was enzymically hydrolyzed at pH 5.5 in order to have a large amount of the metabolite in the unconjugated form. Aliquots were extracted with various hexane–ether mixtures as described for extracting unconjugated THC-11-oic acid. The aqueous phases were then checked for residual THC-11-oic acid by the procedure described for extraction of conjugated THC-11-oic acid, except that hydrolysis was not repeated. TLC showed that a hexane–ether mixture containing at least 30% of ether was needed for complete extraction of unconjugated THC-11-oic acid.

We then determined the maximum concentration of ether in a hexane–ether mixture that would not extract conjugated THC-11-oic acid from unhydrolyzed urine at pH 4. A concentrate of the same urine previously used was adjusted to pH 7.5 and the unconjugated THC-11-oic acid (as well as a small amount of conjugated THC-11-oic acid) was completely extracted with ether. The aqueous phase was adjusted to pH 4, and aliquots of it were extracted with various hexane–ether mixtures as described for extracting unconjugated THC-11-oic acid. The hexane–ether extracts were evaporated, and each residue was mixed with 10 ml of a "blank" urine adjusted to pH 5.5. Enzyme was added, and all mixtures were processed as described for conjugated THC-11-oic acid; TLC showed that a hexane–ether mixture containing 40% ether was the maximum concentration of ether that did not extract conjugated THC-11-oic acid from unhydrolyzed urine at pH 4.

On the basis of these experiments, hexane–ether (65:35) was selected as optimum for the procedure.

We determined that residues of hexane–ether extracts that were prepared with as little as 5% ether could not be chromatographed without being washed with $NaHCO_3$ solutions, as, after chromatography, the THC-11-oic acid could not be distinguished from background material. We also determined that THC-11-oic acid was extracted by $NaHCO_3$ solution from hexane–ether extracts containing more than 20% hexane. Thus, the hexane–ether extract containing unconjugated THC-11-oic acid was replaced with ether before the treatment with $NaHCO_3$.

We also established that the presence of either residual ether or residual hexane had no evident effect on enzyme activity.

RESULTS

Clinical

Two subjects, each of whom smoked cannabis as well as having THC administered intravenously, provided the urine samples analyzed in Fig. 1 and 2. Fig. 1 shows the pattern of conjugated to unconjugated metabolites in these subjects after smoking. Subject BU showed an early predominance of conjugated THC-11-oic acid, with a later predominance of unconjugated metabolite. Subject WF showed no conjugated metabolite early, but a majority of conjugated THC-11-oic acid later. Fig. 2 shows that these same inter-individual differences in the pattern of metabolite excretion obtained following intravenous administration of THC. A third subject differed from either of these two in that his urine showed both an early and a later predominance of conjugated metabolite.

We have applied these analyses to eight additional experimental subjects and to a number of suspected users of cannabis. From the results, some tentative observations can be made. (1) In spite of the difference in the excretion patterns noted between ingestion by smoking and intravenous administration for subject WF, the excretion patterns within a subject tended to be similar for both modes of ingestion. (2) If unconjugated THC-11-oic acid was present, conjugated THC-11-oic acid was almost always present also; the reverse was noted far less often. (3) Based on the

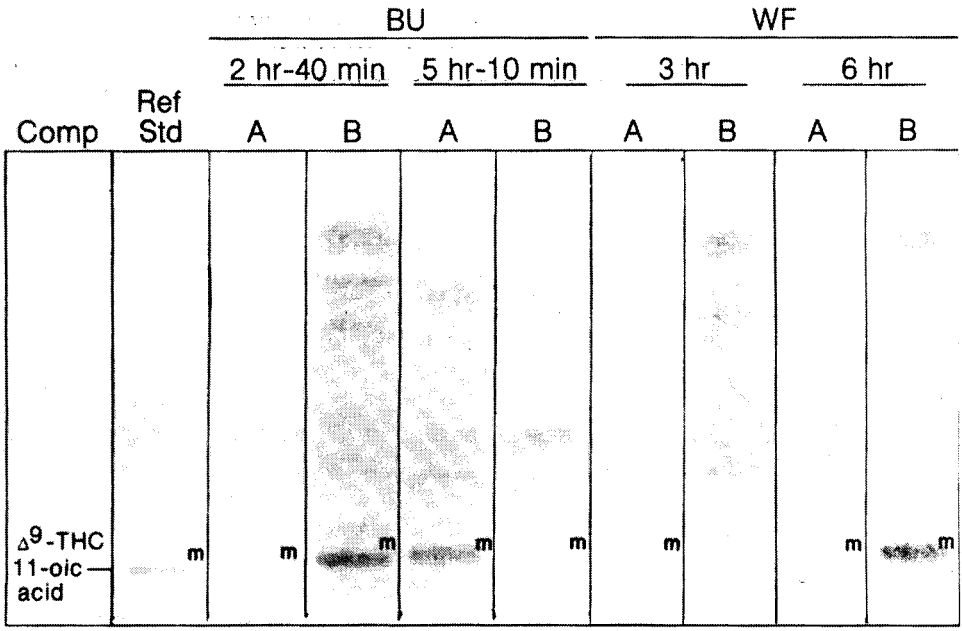

Fig. 1. Detection of THC-11-oic acid in urine after ingestion of THC by smoking: chromatograms of post-THC urines. Collection times noted by numbers at top of each chromatogram. A, unconjugated, extracted with hexane–ether (65:35) from unhydrolyzed urine; B, conjugated, extracted with ether after enzymic hydrolysis; m = magenta; Only the spot of THC-11-oic acid is identified. The other spots are either not characteristic of the reaction between cannabinoids and Fast Blue Salt B or are not identifiable. For details of TLC, sample size, see text.

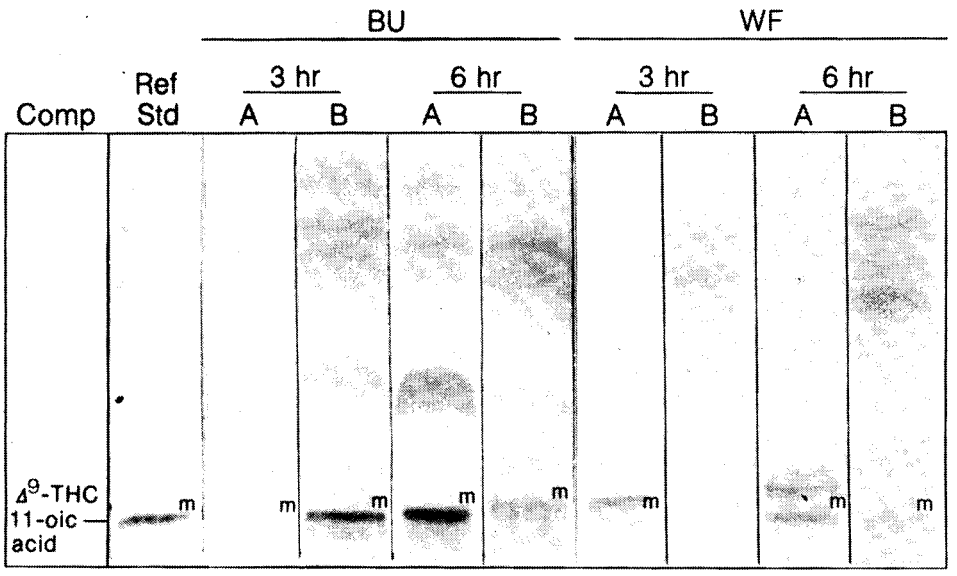

Fig. 2. Detection of THC-11-oic acid in urine after intravenous administration of THC; see Fig. 1 for details. Sample size, volume of urine containing 30 mg of creatinine.

results obtained after intravenous administration (by which procedure the amount of THC ingested between subjects varies least), individual metabolism appears to be a factor. (4) As the interval between ingestion of THC and collection of urine increased, the conjugated form tended to increase or persist, while the unconjugated form tended to decrease and become undetectable. Additionally, of twelve positives among the group of suspected users, urine from seven contained both forms of the metabolite.

DISCUSSION

Experimental

A volume of urine containing 50 mg of creatinine approximates the maximum that can be used for analysis of conjugated THC-11-oic acid. Larger amounts frequently yield emulsions during extraction and "overloading" on the TLC plate.

The concentration of ether in the hexane–ether mixture that was required for complete extraction of unconjugated THC-11-oic acid was established at the pH of hydrolysis to avoid, if possible, a second pH adjustment. At this pH, a greater concentration of ether would be required to extract unconjugated THC-11-oic acid quantitatively than at a more acid pH.

Tests to establish the maximum concentration of ether in the hexane–ether mixture that would not extract any conjugated THC-11-oic acid were carried out at pH 4, as, at this pH, less ether is needed to extract conjugated THC-11-oic from unhydrolyzed urine than at higher pH values. Thus, the hexane–ether mixture developed was optimum. It completely extracted unconjugated THC-11-oic acid from unhydrolyzed urine at the pH needed for hydrolysis, without extracting conjugated THC-11-oic acid.

Ether, instead of hexane–ether, was used to extract the hydrolyzed conjugated THC-11-oic acid as it is more efficient, and the need to change the solvent before the treatment with $NaHCO_3$ solution is avoided.

Conditions for hydrolysis, purification of the extracts with 5% $NaHCO_3$ solution and TLC on one plate with two solvent systems were developed earlier and have been used in other work[9].

A blank urine instead of an aqueous buffer solution was used in the experimental work because our previous experience indicated that the solute content of the aqueous phase significantly affected the extraction of THC-11-oic acid by ether[5].

Clinical

Clinical results showing that both unconjugated and conjugated THC-11-oic acid are excreted in urine after ingestion of THC (with the conjugated form usually predominant) agree with the recently published work of Williams *et al.*[10]. The observations that the conjugated form increased proportionately as the interval between ingestion of THC and collection of urine increased could not be compared, as Williams *et al.* did not report such fractionation for successive samples, but it does agree with the work of Wall *et al.*[11].

A procedure that can be used to detect both unconjugated and conjugated THC-11-oic acid in urine by TLC has been described. It is sensitive to as little as one standard marijuana cigarette containing approximately 16 mg of THC or the intravenous administration of 5 mg of THC. Both forms of the metabolite have also been detected in spontaneously collected urines from psychiatric patients suspected of illicitly using marijuana.

ACKNOWLEDGEMENTS

This work was supported by a grant from the National Institute of Drug Abuse, No. DA 00424, and from the Research Services of the Veterans Administration. The THC, THC-11-oic acid and standard marijuana cigarettes were provided by the National Institute of Drug Abuse, Public Health Service, NIMH.

REFERENCES

1 A. Goldstein, L. Aronow and S. M. Kalman, *Principles of Drug Action; the Basis of Pharmacology*, Wiley, New York, 2nd ed., 1974, p. 230.
2 L. E. Hollister, S. L. Kanter, F. Moore and D. E. Green, *Clin. Pharmacol. Ther.*, 13 (1972) 849.
3 S. L. Kanter, L. E. Hollister, F. Moore and D. E. Green, *Res. Commun. Chem. Pathol. Pharmacol.*, 9 (1974) 205.
4 S. L. Kanter, L. E. Hollister and F. Moore, *Res. Commun. Chem. Pathol. Pharmacol.*, 10 (1975) 215.
5 S. L. Kanter and L. E. Hollister, *Res. Commun. Chem. Pathol. Pharmacol.*, 17 (1977) 421.
6 S. L. Kanter, L. E. Hollister and M. Williams, *J. Chromatogr.*, 234 (1982) 255.
7 D. E. Green, in R. E. Willette (Editor), *NIDA Res. Mon.*, No. 7, 1976, p. 70.
8 S. Agurell, I. M. Nilsson, A. Ohlsson and F. Sandberg, *Biochem. Pharmacol.*, 19 (1970) 1333.
9 S. L. Kanter, L. E. Hollister and M. Musumeci, *J. Chromatogr.*, 234 (1982) 201.
10 P. L. Williams, A. C. Moffat and L. J. King, *J. Chromatogr.*, 186 (1979) 595.
11 M. E. Wall, D. R. Brine and M. Perez-Reyes, in M. C. Braude and S. Szara (Editors), *Pharmacology of Marihuana*, Raven Press, New York (1976) p. 93.

Journal of Chromatography, 235 (1982) 513–516
Elsevier Scientific Publishing Company, Amsterdam — Printed in The Netherlands

CHROM. 14,309

Note

Retention plots of aliphatic esters

J. K. HAKEN
Department of Polymer Science, The University of New South Wales, P.O. Box 1, Kensington, N.S.W. 2033 (Australia)
(Received August 24th, 1981)

The introductory work of James and Martin[1] demonstrated the linear relationship between retention and carbon number of homologous compounds. These workers extended the development of retention plots to allow the detection of polarizable groups by the study of the retention behaviour on two or more phases of differing polar character[2,3]. With unsaturated fatty esters[4] a plot of retention on a polyester stationary phase against values on a non-polar stationary phase produced a grid of parallel lines lines from which the number of double bonds or carbon atoms in an unknown ester could be established.

While the retention behaviour of the total carbon number, *i.e.* the complete molecule, was considered in these procedures it was evident that because of their structure various series could be plotted as members of two or three homologous series to produce near-linear relationships. In these cases a correlation was possible between retention behaviour and structural parameters and the procedures were demonstrated with several series of carbonyl compounds[5–7]. On a non-polar stationary phase a grid-type plot was produced when either the carbon number of the alcohol (R') or acid chain (R) was used as the abscissa. A second set of nearly linear lines linked points of esters of constant $R + R'$. Fig. 1 shows the plot for *n*-alkylacrylic esters with the acid chain (R) as the abscissa and the secondary plots formed by linking points having constant values of $R + R'$ in increasing order from 1 to 12. Further studies[8] have shown that ester plots with R', and particularly R, as abscissa exhibit marked deviations from linearity with polar stationary phases, and regular networks as shown in Fig. 1 are not produced.

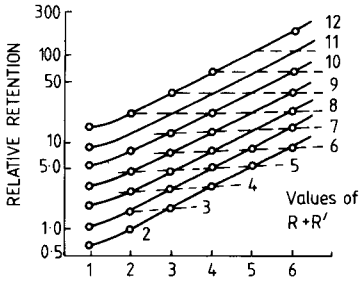

Fig. 1. Retention plot for *n*-alkylacrylic esters using acid chain length (R) as abscissa[5].

0021-9673/82/0000–0000/$02.75

Calixto and Raso[9] have recently shown the same type of plot (Fig. 2) for retention of aliphatic esters with $R + 1/R'$ as the abscissa where the ester is represented by RCOOR'. Linking points which the same total carbon number (n), *i.e.* $n = R + R' + 1$ according to the convention used above, produced a series of curved relationships, with the curvature increasing as n decreased. It is evident that the retention is minimized where the $R + 1/R'$ ratio is near unity, where it is stated that the charge and mass centres are as close as possible.

With such a suggestion it would be prudent to extend the plot to include esters of lower total carbon number, *i.e.* less than seven, and to indicate the effect of polarity, *i.e.* that linearity decreased with increasing phase polarity.

From Fig. 2 it is evident that a set of plots is possible linking points of equal R' and producing a series of lines whose slope increases as R' increases. Such a situation is similar to that shown in Fig. 1 except that the abscissa is an increasing carbon number multiplied by a constant, *i.e.* depending on the carbon number of R' forming the divisor, the value of the constant decreases with increasing value of R' and is largely responsible for the slopes increasing as R' increases from 1 to 6 as shown, rather than the differences obtained on using the total carbon number[8].

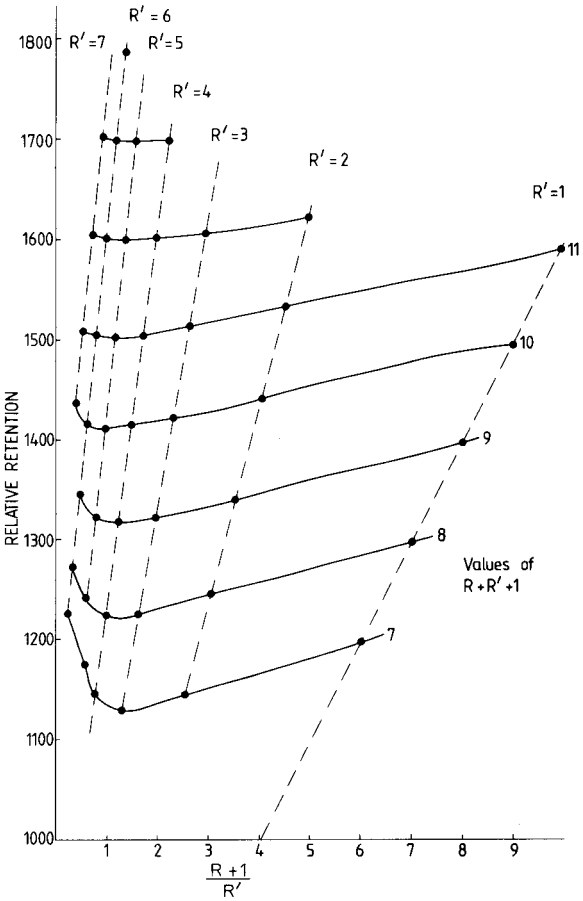

Fig. 2. Retention plot for aliphatic esters with $R + R' + 1 = 7$–13 (ref. 9).

For the data used in Fig. 1 a polynomial expression was produced whereby the retention of aliphatic esters might be calculated. While this relationship may hold for esters where $n < 7$ it is obvious from several data points from the tabulations of Calixto and Raso[9] that as the plots proceed towards the origin they become markedly curved. As this behaviour has been previously reported[8] it is expected that the equation shown is not applicable to many of the common simpler esters.

A plot for all of the simpler esters on SILAR 5CP is shown in Fig. 3 which shows a series of curves. A new polynomial expression is not shown as such an approach is of restricted value. If required the data may be better presented by the construction of a nomogram which, as shown earlier[5], may be drawn to accomodate deviations occuring with the various esters.

The plot shown in Fig. 2 considers the retention of both the methylene and the C = O group to be essentially equivalent, which of course does not occur. A methylene group, irrespective of the stationary phase, exhibits a retention of *ca.* 100 units with a variation of possibly 10 units while the contribution of a carbonyl group has

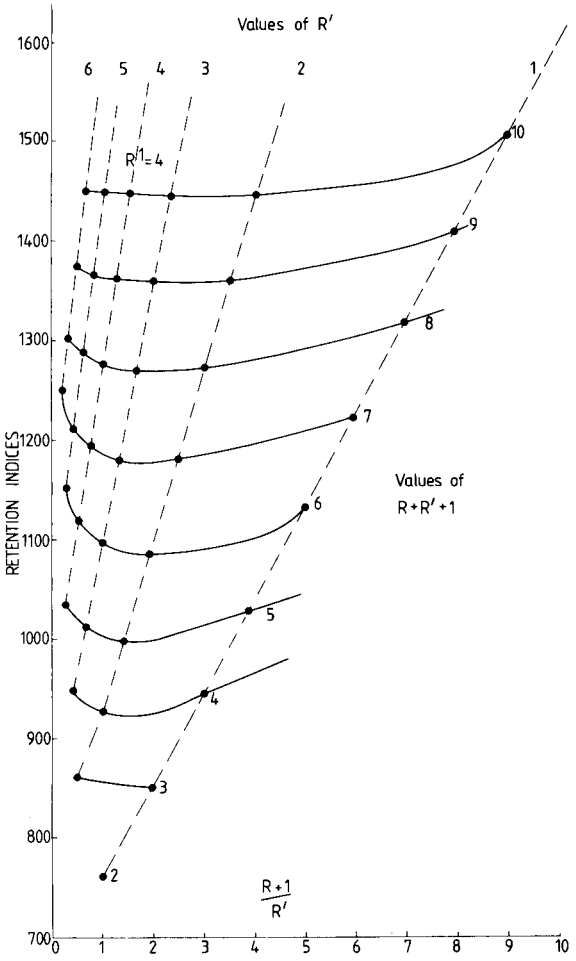

Fig. 3. Retention plot for aliphatic esters with $R + R' + 1 = 2$–10.

been shown elsewhere to vary by possibly 100% depending on the stationary phase used. The contribution of the carboxy group has been determined by graphical procedures for aliphatic esters on a variety of stationary phases[10,11].

A number of other variations of the retention plot are possible depending on the abscissa used while the shape of the plots may be varied by the relative magnitudes of the coordinate scales used. The effects are readily demonstrated by the use of a programmable data plotter.

REFERENCES

1 A. T. James and A. J. P. Martin, *Biochem. J.*, 50 (1952) 679.
2 A. T. James, *Biochem. J.*, 52 (1952) 242.
3 A. T. James and A. J. P. Martin, *J. Appl. Chem.*, 6 (1956) 105.
4 A. T. James, *J. Chromatogr.*, 2 (1959) 552.
5 J. K. Haken and T. R. McKay, *J. Gas Chromatorgr.*, 3 (1965) 61.
6 J. K. Haken and P. Souter, *J. Gas Chromatogr.*, 3 (1965) 348.
7 J. K. Haken, *J. Gas Chromatogr.*, 4 (1966) 85.
8 J. R. Ashes and J. K. Haken, *J. Chromatogr.*, 101 (1974) 103.
9 F. S. Calixto and A. G. Raso, *Chromatographia*, 14 (1981) 143.
10 I. D. Allen and J. K. Haken, *J. Chromatogr.*, 49 (1970) 409.
11 J. R. Ashes and J. K. Haken, *J. Chromatogr.*, 60 (1971) 33.

Journal of Chromatography, 235 (1982) 517–522
Elsevier Scientific Publishing Company, Amsterdam — Printed in The Netherlands

CHROM. 14,432

Note

Comparison of molecular connectivity and a chromatographic correlation factor in reversed-phase high-performance liquid chromatography for polycyclic aromatic hydrocarbons

ROBERT J. HURTUBISE* and TODD W. ALLEN
Chemistry Department, University of Wyoming, Box 3838, Laramie, WY 82071 (U.S.A.)
and
HOWARD F. SILVER
Chemical Engineering Department, University of Wyoming, Box 3828, Laramie, WY 82071 (U.S.A.)
(Receiving August 3rd, 1981)

Molecular connectivty (χ) has been used to correlate molecular structure with various physical and biological properties[1–7]. Randić[8] developed the concept of molecular connectivity and discussed the relationship of molecular branching to molecular connectivity. Molecular connectivity has been used to predict retention indices of polycyclic aromatic hydrocarbons (PAHs) and other compounds in gas chromatography[9–11]. Karger *et al.*[12] employed molecular connectivity for estimating non-polar group contributions to retention in reversed-phase liquid chromatography.

To determine the usefulness of molecular connectivity for PAHs and hydroaromatics on a reversed-phase high-performance liquid chromatographic (HPLC) column, the retention of thirty-four compounds was measured on a μBondapak C_{18} column with a methanol–water mobile phase. Alkyl-substituted and hydroaromatic compounds were included. Log capacity factor (k') was plotted as a function of χ and compared with graphs of log k' as a function of F (F is a chromatographic correlation factor developed by Schabron *et al.*[13] which relates compound structure to k' on a μBondapak C_{18} column).

EXPERIMENTAL

Instrumentation

The liquid chromatograph used was a Waters model ALC/GPC 244 equipped with a Model 6000A pump, a U6K injector, a Model 440 absorbance detector set at 254 nm and 280 nm, and a strip chart recorder. A 10-μm particle size μBondapak C_{18} column (30 cm × 3.9 mm I.D.) from Waters was used with methanol–water (65:35) at 1.0 ml/min and ambient temperature.

Reagents

Baker HPLC-grade methanol was filtered through a Millipore type F-H 0.45-μm filter. Distilled water was filtered through a Millipore type G-S 0.22-μm filter. Cyclohexane (99 + % from Aldrich, Milwaukee, WI, U.S.A.) or pure-grade *n*-hexane

0021-9673/82/0000–0000/$02.75

(99% minimum from Phillips, Borger, TX, U.S.A.) were used to dissolve standard compounds. 1,2-Dihydropyrene was obtained from Laramie Energy Technology Center and 1,2,6,7-tetrahydropyrene was obtained from Pittsburgh Energy Technology Center. All other compounds were obtained from commercial sources and purified when necessary.

Cyclohexane or *n*-hexane standard solutions were injected into the HPLC system. Amounts injected were 1–12 μg depending on the compound. Each solution was injected at least twice. The void volume of the μBondapak C_{18} column was determined to be 2.75 ml by eluting methanol.

Calculations

Molecular connectivity was calculated with the equation below.

$$\chi = \Sigma (\delta_i \cdot \delta_j)^{-1/2}$$

The values of δ can be 1, 2, 3, or 4 corresponding to the number of bonds associated with atoms i and j. The hydrogen atom bonds are neglected. An example calculation is shown below for 2,3-dimethylnaphthalene.

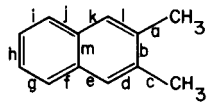

$$\chi = \underset{(a)}{\frac{1}{(1\cdot4)^{1/2}}} + \underset{(b)}{\frac{1}{(4\cdot4)^{1/2}}} + \underset{(c)}{\frac{1}{(1\cdot4)^{1/2}}} + \underset{(d)}{\frac{1}{(4\cdot3)^{1/2}}} + \underset{(e)}{\frac{1}{(3\cdot4)^{1/2}}} +$$

$$\underset{(f)}{\frac{1}{(4\cdot3)^{1/2}}} + \underset{(g)}{\frac{1}{(3\cdot3)^{1/2}}} + \underset{(h)}{\frac{1}{(3\cdot3)^{1/2}}} + \underset{(i)}{\frac{1}{(3\cdot3)^{1/2}}} + \underset{(j)}{\frac{1}{(3\cdot4)^{1/2}}} +$$

$$\underset{(k)}{\frac{1}{(4\cdot3)^{1/2}}} + \underset{(l)}{\frac{1}{(3\cdot4)^{1/2}}} + \underset{(m)}{\frac{1}{(4\cdot4)^{1/2}}} = 4.23$$

The chromatographic correlation factor, F, was calculated using the equation below[13].

F = number of double bonds + the number of primary and secondary carbons − 0.5 for a non-aromatic ring

An example calculation for 9,10-dihydroanthracene is

$$F = 6 + 2 - 0.5 = 7.5$$

RESULTS AND DISCUSSION

A comparison of log k', χ, and F values is given in Table I for the thirty-four compounds investigated. Fig. 1 gives a graph of log k' *versus* χ. Least-squares analysis gave an intercept of -0.55, a slope of 0.30, and a correlation coefficient of 0.97. Fig. 2 shows a graph of log k' *versus* F. Least-squares analysis gave an intercept of -0.58, a slope of 0.21, and a correlation coefficient of 0.99.

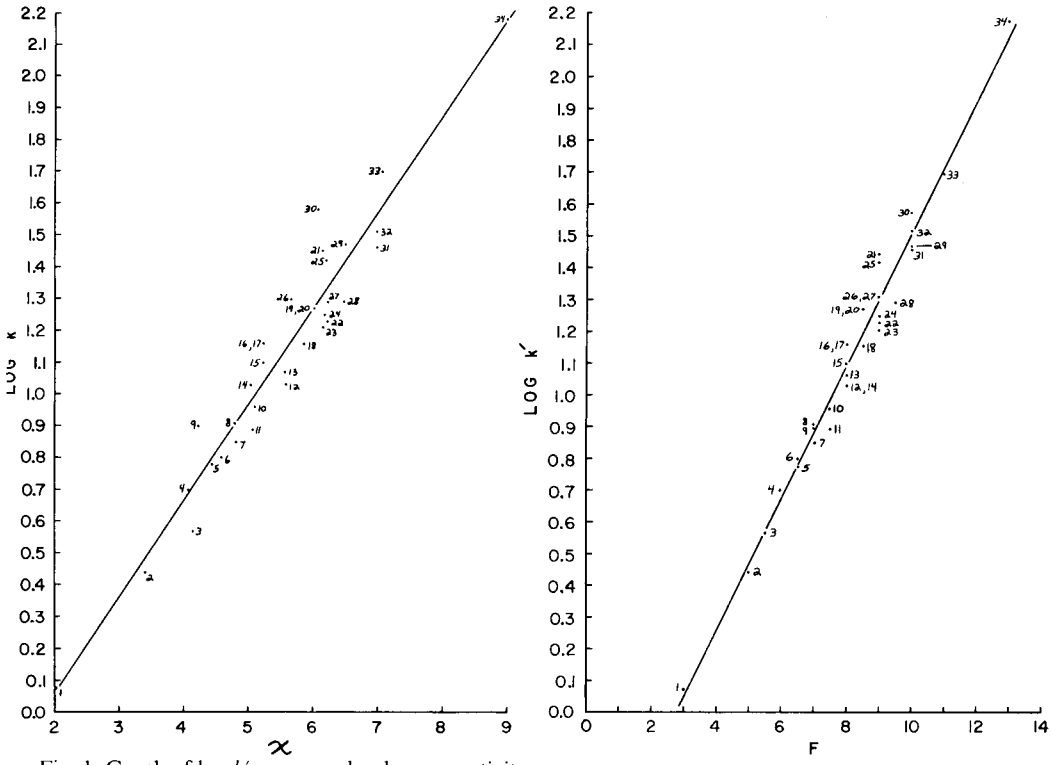

Fig. 1. Graph of log k' *versus* molecular connectivity.

Fig. 2. Graph of log k' *versus* chromatographic correlation factor.

Comparison of Figs. 1 and 2 shows that less scatter was obtained with F, indicating that a better correlation was achieved with the chromatographic correlation factor than with molecular connectivity, χ. The alkyl-substituted PAHs, hydroaromatics and the parent PAHs all show a good correlation with F. F has also been shown to give good correlation with log k' for other substituted PAHs and hydroaromatics on a similar reversed-phase system[13]. Fig. 1 shows that 1,2,3,4,5,6,7,8-octahydroanthracene (compound 30) lies far from the least-squares line, whereas in Fig. 2 it is very close to the least-squares line. Also, acenaphthylene (compound 3) is far from the least-squares line in Fig. 1 but very close to the least-squares lines in Fig. 2. Several other comparisons like the previous two can be made, indicating F should be more useful in predicting log k' values than χ. The previous conclusion is important because of the variety of chemical structures investigated, namely PAHs, alkyl-substituted PAHs, and hydroaromatics. It seems that the chromatographic corre-

TABLE I

log k', F AND χ VALUES FOR THE COMPOUNDS INVESTIGATED

Compound	*Structure*	*log k'*	*F*	χ
1 Benzene		0.073	3.0	2.00
2 Naphthalene		0.44	5.0	3.40
3 Acenaphthylene		0.57	5.5	4.15
4 Biphenyl	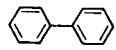	0.70	6.0	4.07
5 Acenaphthene		0.78	6.5	4.45
6 Fluorene	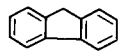	0.80	6.5	4.61
7 Phenanthrene	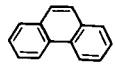	0.85	7.0	4.82
8 Anthracene	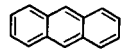	0.91	7.0	4.81
9 2,3-Dimethylnaphthalene	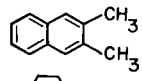	0.90	7.0	4.23
10 9,10-Dihydrophenanthrene	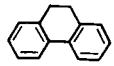	0.96	7.5	5.11
11 9,10-Dihydroanthracene	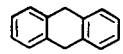	0.89	7.5	5.07
12 Fluoranthene	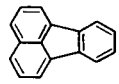	1.03	8.0	5.56
13 Pyrene	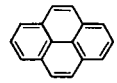	1.07	8.0	5.56
14 Bibenzyl	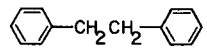	1.03	8.0	5.03
15 9-Methylanthracene	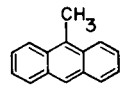	1.10	8.0	5.23
16 2-Methylphenanthrene	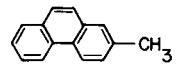	1.16	8.0	5.23

TABLE I *(continued)*

Compound	*Structure*	*log k'*	*F*	*χ*
17 2-Methylanthracene	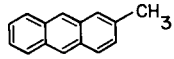	1.16	8.0	5.22
18 1,2-Dihydropyrene	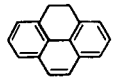	1.16	8.5	5.86
19 1,2-Benzofluorene	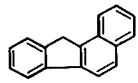	1.27	8.5	6.02
20 2,3-Benzofluorene	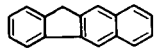	1.27	8.5	6.02
21 *p*-Terphenyl	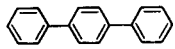	1.45	9.0	6.14
22 Triphenylene	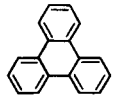	1.23	9.0	6.23
23 1,2,6,7-Tetrahydropyrene	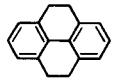	1.21	9.0	6.15
24 1,2,3,4-Tetrahydrofluoranthene	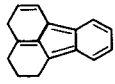	1.25	9.0	6.17
25 Tetracene	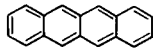	1.42	9.0	6.21
26 9,10-Dimethylanthracene	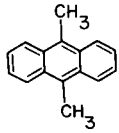	1.30	9.0	5.66
27 Chrysene	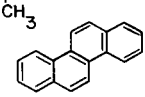	1.29	9.0	6.23
28 5,12-Dihydrotetracene	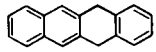	1.29	9.5	6.47
29 1,2,3,6,7,8-Hexahydropyrene	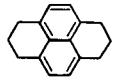	1.47	10.0	6.49
30 1,2,3,4,5,6,7,8-Octahydroanthracene	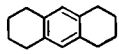	1.58	10.0	6.07
31 Perylene	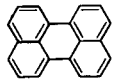	1.46	10.0	6.98

(Continued on p. 522)

TABLE I *(continued)*

Compound	*Structure*	*log k'*	*F*	χ
32 3,4-Benzofluoranthene	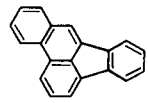	1.51	10.0	6.98
33 7,12-Dimethylbenz[*a*]anthracene	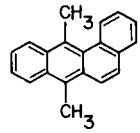	1.70	11.0	7.06
34 9,10-Diphenylanthracene	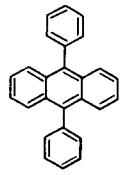	2.18	13.0	8.98

lation factor, F, should have considerable applicability in reversed-phase chromatography work with PAHs, alkyl-substituted PAHs, and hydroaromatics. For example, F could be used to predict k' values for several compounds using graphs similar to the one in Fig. 2. Also, if the k' value of an unknown compound is known, then F for the compound can be determined and used to predict various structural features of the compound. Schabron *et al.*[13] have already presented several examples of these approaches.

ACKNOWLEDGEMENTS

Appreciation is expressed to John McKay of the Laramie Energy Technology center and Charles Schmidt of the Pittsburgh Energy Technology Center for standard compounds.

Financial support was provided by the U.S. Department of Energy under contract number DE-AC22-79ET14874.

REFERENCES

1 L. B. Kier, L. H. Hall, W. J. Murray and M. Randić, *J. Pharm. Sci.*, 64 (1975) 1971.
2 L. H. Hall, L. B. Kier and W. J. Murray, *J. Pharm. Sci.*, 64 (1975) 1974.
3 W. J. Murray, L. H. Hall and L. B. Kier, *J. Pharm. Sci.*, 64 (1975) 1978.
4 L. B. Kier, W. J. Murray, M. Randić and L. H. Hall, *J. Pharm. Sci.*, 65 (1976) 1226.
5 W. J. Murray, L. B. Kier and L. H. Hall, *J. Med. Chem.*, 19 (1976) 573.
6 T. Di Paolo, L. B. Kier and L. H. Hall, *Mol. Pharmacol.*, 13 (1977) 31.
7 L. B. Kier and L. H. Hall, *Molecular Connectivity in Chemistry and Drug Research*, Academic Press, New York, 1976.
8 M. Randić, *J. Amer. Chem. Soc.*, 97 (1975) 6609.
9 R. Kaliszan and H. Lamparczyk, *J. Chromatogr. Sci.*, 16 (1978) 246.
10 A. Radecki, H. Lamparczyk and R. Kaliszan, *Chromatographia*, 12 (1979) 595.
11 T. R. McGregor, *J. Chromatogr. Sci.*, 17 (1979) 314.
12 B. L. Karger, J. R. Gant, A. Hartkopf and P. H. Weiner, *J. Chromatogr.*, 128 (1976) 65.
13 J. F. Schabron, R. J. Hurtubise and H. F. Silver, *Anal. Chem.*, 49 (1977) 2253.

Journal of Chromatography, 235 (1982) 523–526
Elsevier Scientific Publishing Company, Amsterdam – Printed in The Netherlands

CHROM. 13,376

Note

Detection of trace amounts of oestrogens by radio-gas–liquid chromatography on glass capillary columns

HORST WEBER*, MICHAEL HÖLLER and HEINZ BREUER
Institut für Klinische Biochemie, Universität Bonn, Sigmund-Freud-Strasse 25, D-5300 Bonn 1 (G.F.R.)
(Received August 25th, 1981)

It is difficult to separate, identify and quantitate trace amounts of radioactive oestrogens (8–10 pmol) in the presence of contaminants from biological material. To overcome these difficulties, radio-gas–liquid chromatography (RGLC) was found to be the method of choice; by the use of glass capillary columns, the efficiency of RGLC was significantly improved. The applicability and efficacy of the method described here is demonstrated by the identification of a metabolite of [4-^{14}C]oestradiol-17β after perfusion of isolated rat brain.

EXPERIMENTAL

Apparatus

A schematic representation of the radio-gas chromatograph, consisting of a Pye 104 gas chromatograph and a radiodetector assembly (Panax Nucleonics, Mitcham, Great Britain), is given in Fig. 1. A solid injector with a moveable needle (WGA, Düsseldorf, G.F.R.) is used. A 12-m glass capillary column, coated with OV-101 or QF-1, was purchased from WGA. The carrier gas flow-rate is 1 ml/min. At the end of the capillary column (6 in Fig. 1), argon is added as make-up gas at a rate of 10 ml/min. The gas flow is split (7 in Fig. 1) in a ratio of 2:1; the minor portion passes through the flame-ionization detector, and the major portion is transferred (9 in Fig. 1) to the radiodetector interface. Before entering the transfer line, about 20 ml/min of humidified argon is added to the gas stream (8 in Fig. 1). Between the first and the second oven (11 and 12 in Fig. 1) 3 ml/min of hydrogen is added, but only if tritiated steroids are to be determined. Before the gas stream enters the counting tube, about 2 ml/min of carbon dioxide is added to the gas stream. Under these conditions, a total gas flow of about 32 ml/min passes the counting tube. The stationary volume of the counting tube is 18 ml (for the working conditions of the proportional counter, see the Panax Nucleonics manual).

The working temperature of the column oven is 230°C, that of the transfer line 300°C and that of the two ovens of the radiodetector interface 650°C.

Preparation of samples

Hypothalamic regions from rat brain which had been perfused (details will be published elsewhere) with [4-^{14}C]oestradiol-17β (specific radioactivity 30 nCi/nmol)

0021-9673/82/0000–0000/$02.75

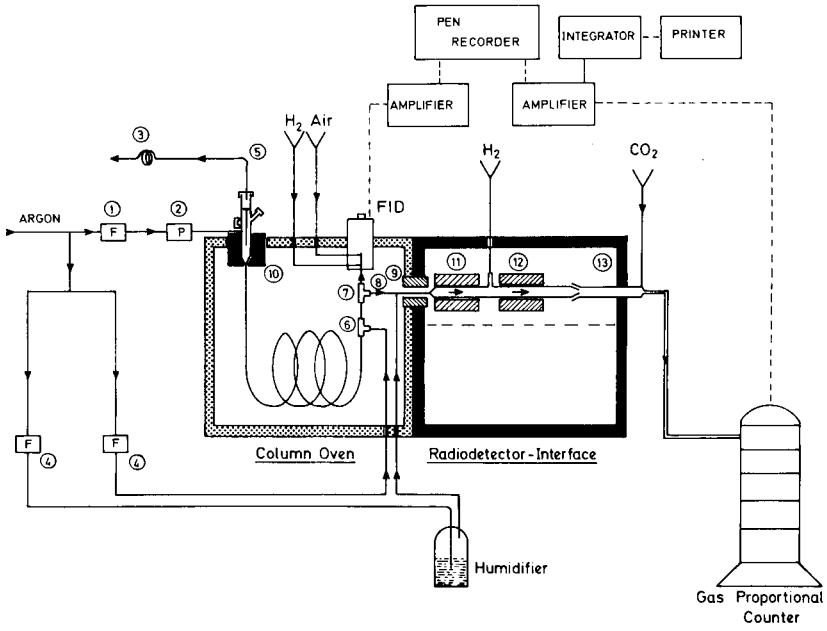

Fig. 1. Schematic diagram of the radio-gas chromatograph. For operating conditions, see text. 1 = Flow controller (carrier gas); 2 = pressure controller (carrier gas); 3 = variable purge restrictor; 4 = flow controller (make-up gas); 5 = solid injector; 6 = addition of make-up gas; 7 = column effluent splitter; 8 = addition of humid make-up gas; 9 = transfer line; 10 = inlet overheating coil; 11 = catalytic oxidation (CuO); 12 = catalytic reduction (Fe); 13 = removable drier [$Mg(ClO_4)_2$].

are homogenized in water–methanol (3:1). A solution of butylated hydroxytoluene (Ionol, Deutsche Shell, Düsseldorf, G.F.R.) is added to the homogenate to prevent oxidation of labile oestrogens (*e.g.*, catecholoestrogens). The homogenate is centrifuged at 3000 *g* and the sediment washed with water–methanol until all radioactivity is removed. The combined supernatants are purified by adsorption chromatography on Sephasorb HP (Deutsche Pharmacia, Freiburg, G.F.R.), using water and subsequently methanol as the mobile phase. The eluate from the column is evaporated and the residue submitted to thin-layer chromatography on silica gel F254 (Merck, Darmstadt, G.F.R.) using chloroform–methanol (9:1). Radioactive steroids are localized using a radioscanner (Model II; Berthold, Wildbad, G.F.R.). The area corresponding in mobility to 7α-hydroxyestradiol-17β (7α-OHE_2) is eluted with methanol–acetone (3:1).

The eluted radioactive oestrogen fraction is incubated with 50 μl of N-methyl-N-trimethylsilyltrifluoroacetamide (MSTFA; Macherey, Nagel & Co., Düren, G.F.R.) for 1 h at 60°C. The incubation mixture is evaporated to dryness and the residue dissolved in 20 μl of MSTFA. Aliquots of 3 μl are injected in the radio-gas chromatograph.

RESULTS AND DISCUSSION

The method described here permits the quantitative determination of about 4 pmol of ^{14}C-labelled oestrogens extracted from biological materials. As the detection

limit depends on the specific radioactivity of the steroid chromatographed, ^{3}H-labelled oestrogens can be determined even in femtomole amounts. In addition to the high sensitivity, RGLC with capillary columns also exhibits a high separation efficiency. However, a prerequisite for maintaining this high efficiency is the reduction of the residence time of the substance eluted from the column inside the detector. A long residence time, which decreases considerably the separation efficiency, results from the combination of a low gas flow-rate with a high dead volume of the proportional counter. To reduce the residence times of the eluted substances in the radio detector, make-up gas is added at two points behind the chromatographic column. First, argon is added immediately behind the column, which makes it possible to split the column effluent at a constant ratio. Second, humidified argon is added before the gas stream enters the transfer line. Humidification of argon proves to be very useful if tritiated steroids are to be chromatographed; it reduces the non-specific adsorption of tritiated water which otherwise would lead to peak tailing and reduced recovery.

On the other hand, an increase in the resolving power by shortening the residence time of the labile isotope in the counting tube reduces the sensitivity. Depending on the analytical problem to be solved, an optimal flow-rate of make-up gas with

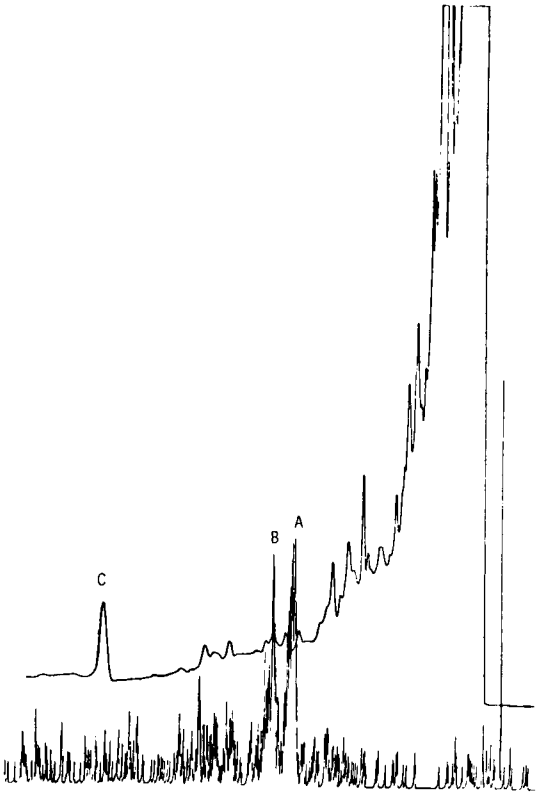

Fig. 2. Radio-gas chromatogram of a purified fraction from the hypothalamic region after perfusion of [4-^{14}C]oestradiol-17β through isolated rat brain. The two radioactive peaks exhibit relative retention times of 0.53 and 0.58 compared with simultaneously injected oestriol. OV-101 was used as the stationary phase. A = Oestradiol-17β; B = 7α-hydroxyoestradiol-17β; C = oestriol.

respect to both sensitivity and resolving power has to be established. A typical example is given below.

As shown in Fig. 2, 16 pmol of 7α-OHE_2 can easily be separated from an equal amount of oestradiol-17β and quantitated. It is obvious that even smaller amounts of the two oestrogens can be separated from each other, particularly if steroids with a higher specific activity are studied. It should be mentioned that RGLC with packed columns leads to incomplete chromatographic separation of the two oestrogens in question; therefore, quantitation of each individual peak is possible only by using glass capillary columns.

The definitive identification of the metabolite was achieved, using gas chromatography–mass spectrometry (GC–MS). To obtain a sufficient concentration, the metabolite extracted from various brain regions was purified by preparative GLC.

The results obtained with the method described here show that, after 120-min perfusion of [4-^{14}C]oestradiol-17β through isolated rat brain, 7% of the phenolic steroids in the hypothalamic region consist of 7α-OHE_2, a metabolite which so far has not been found in the brain.

ACKNOWLEDGEMENT

The authors thank Professor L. Siekmann, Bonn, G.F.R., for the identification of 7α-hydroxyoestradiol-17β by GC–MS.

Journal of Chromatography, 235 (1982) 527–531
Elsevier Scientific Publishing Company, Amsterdam — Printed in The Netherlands

CHROM. 14,381

Note

Gas chromatographic quantification of a new antitumour agent, pentaziridinocyclophosphathiazene

TOSHIRO UCHIDA* and YUZURU OGATA
The Fourth Section of Research, Otsuka Chemical Co., Ltd., 463 Kagasuno, Kawauchi-Cho, Tokushima 771-01 (Japan)
and
YUKIHIKO UMENO, YOSHINORI MINAMI and TERUYOSHI MARUNAKA
Research Laboratory, Taiho Pharmaceutical Co., Ltd., 224-2 Hiraishi-Ebisuno, Kawauchi-Cho, Tokushima 771-01 (Japan)
(Received September 15th, 1981)

The insect chemosterilant, apholate, has been reported to have an antitumour activity on murine L 1210 and P 388 leukaemias and on B 16 melanoma[1]. A gas chromatographic (GC) detection of this compound has been reported by Bowman[2], who utilized a phosphorus flame detector and six different columns including Dexsil 300 and silicone OV-17. An analogue, pentaziridinocyclophosphathiazene (SOAz), has recently been shown to have a remarkable antitumour activity on the tumours described above[3,4]. However, we have been unable to find any report on the detection of this compound, which urged us to devise an analytical method. We have previously reported a high-performance liquid chromatographic (HPLC) determination of the compound in biological fluids[5]. In the present paper, a GC analysis is described.

EXPERIMENTAL

Chemical synthesis

SOAz was synthesized by Otsuka Chemical Co. (Tokushima, Japan) according to the procedure of Van de Grampel *et al.*[4].

Gas chromatography

A Shimadzu GC-R1A gas chromatograph equipped with a flame thermionic detector (Shimadzu FTD-R1A) was used to detect SOAz, which contains five aziridino groups. Chromatograms were recorded on a Shimadzu RPR-G1 processor. The glass columns (1 m or 2 m × 3 mm I.D.) were packed with 2% Dexsil 300 GC on Chromosorb W AW DMCS (80–100 mesh) (Wako, Osaka, Japan), 1% silicone OV-17 on Gas-Chrom Q (80–100 mesh) (Gasukuro Kogyo, Tokyo, Japan) or 1% silicone OV-17 on Chromosorb W AW DMCS (Wako). They were conditioned overnight before use at 340, 310 and 260°C, respectively.

The carrier gas (helium) flow-rate was 50 ml/min for the 1-m column and 60 ml/min for the 2-m column; hydrogen flow-rate 11 ml/min, air flow-rate 250 ml/min.

0021-9673/82/0000–0000/$02.75

TABLE I

GAS CHROMATOGRAPHIC ANALYSIS OF SMALL AMOUNTS OF SOAz USING A FLAME THERMIONIC DETECTOR

Columns	*Column length (M)*	*Temperatures (°C)*		*Retention time (min)*	*FTD output*	*Areas* ($\times 10^3$) at range 10*	
		Inj. port	*Oven*			*20 ng*	*5 ng*
2% Dexsil 300 GC on Chromosorb W AW DMCS	1	280	245	3.64	6.30	217.9 ± 39.3	51.7 ± 3.1
1% OV-17 on Gas-Chrom Q	2	300	270	7.18	6.00	101.5 ± 4.3	18.0 ± 3.7
	1	290	260	3.44	6.70	243.9 ± 10.0	52.7 ± 10.1
1% OV-17 on Chromosorb W AW DMCS	1	290	260	3.37	6.70	490.5 ± 11.0	103.3 ± 4.3

* Averages from three runs ± S.D.

The solvents dichloromethane and acetone, of analytical grade (Wako), were used to dissolve SOAz.

Standard solutions

SOAz (5 mg) was dissolved in acetone (25 ml) to produce a stock standard solution. Portions of this solution were diluted with acetone to obtain calibration solutions. The stock solution contained 200 ng/μl and could be used for at least 1 month if stored in a cool place.

Procedures

The operational parameters of the apparatus were as shown in Table I. The injection volume was 1 μl. Before analysis, several injections of 200–1000 ng of SOAz were required to produce constant FTD responses. Standards were preferably injected after each analysis. If the response sensitivity dropped after several successive analyses of amounts of less than 10 ng, 200 ng were injected to regain the initial response.

RESULTS AND DISCUSSION

Typical chromatograms are shown in Fig. 1, and a calibration curve is presented in Fig. 2. Although the peak area–concentration plot generally gave a smooth curve, especially at concentrations lower than 10 ng, the response of the FTD to SOAz was approximately proportional to concentration in the range of 0.5–200 ng/μl as shown in Fig. 2 and in Table II. Injections as large as 3 μl may be made for improvement of the detection limit.

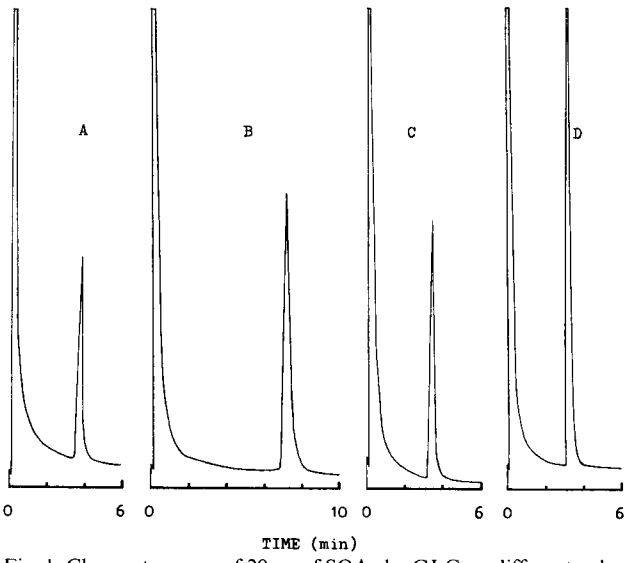

Fig. 1. Chromatograms of 20 ng of SOAz by GLC on different columns using a flame thermionic detector. A, 2% Dexsil (attenuation 32); B, 1% OV-17 on Gas-Chrom Q (2 m, attenuation 8); C, 1% OV-17 on Gas-Chrom Q (1 m, attenuation 32); D, 1% OV-17 on Chromosorb W AW DMCS (attenuation 32).

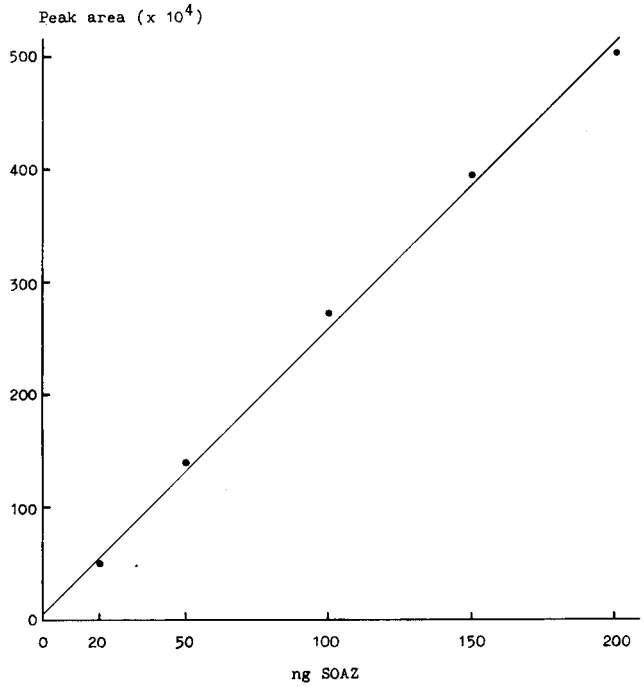

Fig. 2. Calibration curve for quantitation of SOAz obtained from 1% OV-17 on Chromosorb W AW DMCS.

TABLE II

PRECISION AND ACCURACY OF GC USING AN FTD FOR ANALYSIS OF SOAz

Injected amount (ng)	*Area counted* ($\times 10^3$) ± S.D.*	*Coefficient of variation (%)*
0.5	8.1 ± 1.1	13.6
5.0	103.3 ± 4.3	4.2
20.0	490.5 ± 11.0	2.2
50.0	1408.4 ± 43.2	3.1
100.0	2721.3 ± 113.4	4.2
150.0	3937.5 ± 52.2	1.3
200.0	5028.3 ± 102.1	2.0

* Values are averages from three runs, yielding a correlation coefficient of 0.999.

The column materials used were practically equivalent in their analytical function as shown in Table I. Low loading and proper conditioning by periodical injections of large amounts of SOAz seemed essential to obtain a constant reproducibility and a high sensitivity. Short columns with low loadings provided a higher sensitivity and were more time-saving than the long column tried. It seemed that the column of

1% OV-17 on Chromosorb W AW DMCS was least adsorptive and most suitable for the quantification of the compound.

The main problem is the column conditioning before and during analysis in order to maintain the sensitivity. This is considerably time-consuming and requires the injection of standards after several, preferably each, analyses to achieve precise quantitation. However, the present method requires no clean-up of biological samples such as plasma and urine, since the FTD is highly sensitive and specific for nitrogen-containing compounds and very insensitive to raw contaminants in extracts of such samples.

SOAz readily dissolves in dichloromethane, but this solvent should be avoided for it causes a severe negative response immediately after the injection into the FTD. Acetone is preferred because of the high solubility of the compound and the lack of a negative response.

We have previously reported the detection of SOAz in rat plasma and urine by HPLC[5]. The detection limit was 500 ng/ml of plasma, the injection volume being 40 μl. The detection limit by GC using an FTD was 0.5 ng/μl, identical to that by HPLC. However, the injection volume used was 40 times smaller. Thus, the present method should be superior to HPLC for the analysis of SOAz in biological samples if these contain a large amount of raw contaminants that might cause failure of HPLC columns. Moreover, the GC retention time is half as that of HPLC.

REFERENCES

1 J.-F. Labarre, J.-P. Faucher, G. Levy, F. Sournies, S. Cros and G. François, *Eur. J. Cancer*, 15 (1979) 637.
2 M. C. Bowman, *J. Chromatogr. Sci.*, 13 (1975) 307.
3 J.-F. Labarre, F. Sournies, S. Cros, G. François, J. C. van de Grampel and A. A. van der Huizen, *Cancer Lett.*, 12 (1981) 245.
4 J. C. van de Grampel, A. A. van der Huizen, A. P. Jekel, D. Wiedijk, J.-F. Labarre and F. Sournies, *Inorg. Chim. Acta*, 53 (1981) L169.
5 E. Matsushima, Y. Umeno, T. Marunaka and H. Akagi, *J. Chromatogr.*, 226 (1981) 333.

Journal of Chromatography, 235 (1982) 532–535
Elsevier Scientific Publishing Company, Amsterdam — Printed in The Netherlands

CHROM. 14,423

Note

High-performance semi-preparative liquid chromatography of diesel engine emission particulate extracts

S. P. LEVINE*,* and L. M. SKEWES
Ford Motor Company, Scientific Research Staff, Analytical Sciences Department, Dearborn, MI 48121 (U.S.A.)

(Received August 17th, 1981)

INTRODUCTION

A variety of techniques have been utilized to identify the constituents and assess the biological activity of the soluble organic fraction (SOF) of diesel engine exhaust particulate material[1,2]. Preparative liquid chromatography (PLC) has been used to fractionate and concentrate mixtures containing polycyclic aromatic hydrocarbons (PAHs) prior to analysis[1–8]. PLC techniques such as open-column LC[4–7], analytical (Type 1)[9] high-performance liquid chromatography (HPLC)[3], and automated coupled-column HPLC[8] have been used for the fractionation of SOF and of fuel feedstocks. Recent trends in HPLC column packings have emphasized the use of microparticles which provide 10,000–20,000 theoretical plates per meter for certain analytical and preparative applications[9–11]. In our study, the use of a silica microparticulate packing in conjunction with a large diameter (8 mm) separation column and commercially available HPLC instrumentation has resulted in a maximum allowable sample size of 15–25 mg, with little or no reduction of resolution when compared to analytical HPLC separations. This method fits into the semi-preparative, or Type 2 PLC classification (as defined by Verzele and Geeraert[9]), which is best suited for the fractionation of compounds present in complex mistures. The solvent program used was designed to provide separation of paraffins from PAHs, of nitro-PAHs, and of the oxygenated-PAH sub-fractions.

MATERIALS AND METHODS

All PAH standards were obtained from Aldrich, except for 1-nitropyrene and dinitropyrene which were obtained from C. King (Michigan Cancer Center) and R. Mermelstein (Xerox Corp.), respectively. All solvents were distilled-in-glass and quality-controlled to ensure less than 5 ppb (10^9) phthalate-type impurities (Burdick and Jackson)[12,13]. Chromatography was done with a Varian 5060 HPLC apparatus using Perkin-Elmer 75 AC UV (254 nm) and Schoeffel FS 970 fluorescence (254 nm excitation, 320 nm cut off) detectors. A Spectrum 101 signal amplifier/noise filter was

* Present address: O.H. Materials Company, Box 551, Findlay, OH 45840, U.S.A.

0021-9673/82/0000-0000/$02.75

used to condition the output of the fluorescence detector. Detector monitoring was performed with strip chart recorders and/or with a Varian 401 data system. The chromatographic column was 25 cm × 7.9 mm packed with 10-μm μPorasil (Waters Assoc.)[10]. The solvent gradient was as follows: hold 100% hexane for 5 min after injection, linear change for 5 min to 5% methylene chloride, linear change for 25 min to 100% methylene chloride, hold with 100% methylene chloride for 10 min, linear change for 10 min to 100% acetonitrile, hold with acetonitrile for 5 min, step change to tetrahydrofuran (THF) and hold for 10 min, step change back to acetonitrile and hold for 5 min (end of chromatographic run), step change from acetonitrile to methylene chloride back to hexane at 10-min intervals, re-equilibrate for 15 min before the next injection. The solvent flow-rate was 4.5 ml/min. All preparative injections were made using a Waters U6K injector and 200 μl of methylene chloride solutions containing 50–100 mg of SOF/ml.

RESULTS AND DISCUSSION

The analytical procedure is illustrated in Fig. 1, along with the UV and fluorescence profiles obtained from the PLC of a typical Diesel SOF sample. The aliphatic compounds and alkylbenzenes, which make up 40–80% of a typical SOF sample[2,3], are separated into the hydrocarbon (HC) fraction with 90–95% efficiency (as determined mass spectrometrically). (All fraction designations follow the nomenclature given in refs. 2 and 3, and are illustrated in the Figure.) An injection in which there is column overloading usually by the HC fraction, is characterized by decreased column efficiency which results in reduced detail in the alpha-fraction envelope, and by the pyrene and benzo[*a*]pyrene components eluting at shorter retention times. The efficient separation of the HC and α fractions, which is achieved by the use of the initial hexane hold period, permits an approximately 4- to 5-fold improvement in maximum allowable sample size up to the 20 mg level. Work is underway to increase the maximum allowable sample size to the 50–100 mg range through the use of 20-mm diameter columns.

The γ regions of the fractionation scheme are potentially the most important due to the presence of 1-nitropyrene and related nitro-PAH compounds. These substances characteristically have high mutagenic activity on the Ames bioassay test[2,15], and must therefore be separated cleanly from both the $\alpha + \beta$ and from the δ fractions, as well as from bis(2-ethylhexyl) phthalate which emerges late in the γ_2 region. (Phthalates are ubiquitous contaminants of solvents and glassware and will therefore be present under even the most carefully controlled conditions.) The Ames-active constituents are resolved from each other and from interfering compounds using this PLC technique.

The retention times of components in the γ_2 and δ regions vary according to the immediate past history of the column. Specifically, the degree of activity of the silica and the silica-solvent interface layers can greatly affect the retentivity of the silica towards polar compounds[14], *e.g.*, 9-hyroxyfluorene. For this reason, a mixture of retention time standards must be chromatographed daily, and the column activity adjusted with dry hexane, THF, or a solution of 1% water in acetonitrile. (The use of water should be kept to an absolute minimum to avoid column degradation.)

The recovery of the sample after PLC fractionation is not readily determined

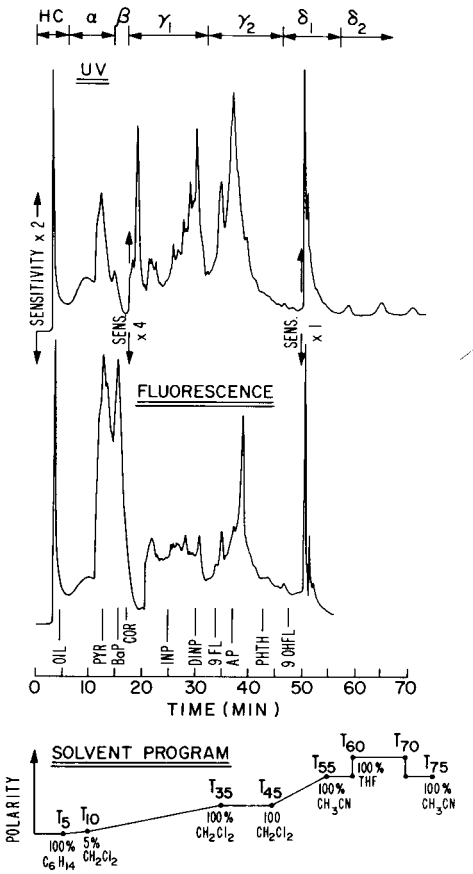

Fig. 1. Typical PLC profile of SOF sample. Top: Fraction designations (HC–δ)[2,3]. Middle: UV and fluorescence detector output tracings with *approximate* retention times of standards noted (PYR = pyrene; BaP = benzo[*a*]pyrene; COR = coronene; 1NP = 1-nitropyrene; DINP = dinitropyrene; 9FL = 9-fluorenone; AP = aminopyrene; PHTH = bis(2-ethylhexyl) phthalate; 90HFL = 9-hydroxyfluorene). Bottom: Solvent program and time scale (T_5 = 5 min, etc.).

because of the wide variation in sample type, ranging from 75% (w/w) unoxidized hydrocarbons (oil and unburned fuel) in diesel emission samples to 65% (w/w) highly oxygenated PAH compounds in ambient air samples. Furthermore, three separate but related criteria for recovery should be used: recovery as Ames activity[15], recovery of injected mass, and recovery of individual components. Typically, mass recoveries in the range of 60–80% have been achieved without the final THF elution step. THF elution results in mass recoveries of up to 100% probably due to increased recovery of highly polar species[16]. The use of methanol has been discussed with respect to increased recovery of polar species[2]. This solvent must be used with care to avoid significant changes in retention times of polar components in subsequent runs, and to avoid slow degradation of column efficiency. The recoveries of nitropyrene, 9-fluorenone, and 9-hydroxyfluorene were determined through the injection either of a standard or of a standard mixed with engine oil (a simulated SOF matrix), collection of the appropriate peak fraction, and reinjection of that fraction. In all cases, compar-

ison of the peak areas indicated a 100% recovery (within experimental error) for these PAH derivatives. The questions of recovery of other constituents of diesel SOF, and of the Ames activity, are presently being investigated and will be reported at a later date.

The use of simultaneous UV and fluorescence monitoring of HPLC separations of PAH-containing mixtures has been advocated[17]. This procedure is used in these PLC separations, but interpretation is difficult because of the large number of unidentified constituents in the SOF. However, it was observed that typical compounds that elute in the γ and δ regions have strong UV absorbance characteristics but little or no fluorescence emissions. The fluorescence trace shows more individual peaks in the delta region than does the UV trace. Nitro-PAH standards can be monitored using a UV detector, but there is insufficient selectivity and sensitivity to monitor these compounds during an actual analysis.

CONCLUSIONS

Semi-preparative (Type 2) HPLC has been applied successfully to the fractionation of the SOF of Diesel engine exhaust particulate material. A capacity of 15–25 mg has been achieved along with a clean separation of HC, PAHs, mildly oxygenated PAHs, and highly polar oxygenated fractions.

ACKNOWLEDGEMENTS

We thank R. Gorse and F. Ferris for providing the sample extracts, M. Paputa and A. Durisin for assistance in the PLC experiments, W. Pierson, D. Schuetzle, and R. Gorse for helpful suggestions during the course of this work, and T. Riley and T. Prater for mass spectrometric analyses.

REFERENCES

1 P. C. Uden, S. Siggia and H. B. Jensen (Editors), *Analytical Chemistry of Liquid Fuel Sources, (Advances in Chemistry Series 170)*, American Chemical Society, Washington, DC, 1978.
2 D. Schuetzle, F. S. C. Lee, T. J. Prater and S. B. Tejada, *Int. J. Environ. Anal. Chem.*, 9 (1981) 93, and references cited therein.
3 D. Schuetzle and J. M. Perez, *Proc. 74th Air Poll. Control Assoc. Conference, Philadephia, PA, 1981*, Paper 81-56.4.
4 R. K. Sorrell and R. Reding, *J. Chromatogr.*, 185 (1979) 655.
5 L. Szepesy, K. Lakszner, L. Ackermann, L. Podmaniczky and P. Literáthy, *J. Chromatogr.*, 206 (1981) 611.
6 E. F. Funkenbush, D. G. Leddy and J. H. Johnson, *Society of Automotive Engineers Congress, 1979*, Paper 790418.
7 F. P. Disanzo, P. C. Uden and S. Siggia, *Anal. Chem.*, 53 (1981) 721.
8 K. Ogan and E. Katz, *Perkin-Elmer Analytical Study 78*, Perkin-Elmer Corp., Norwalk, CT, 1980.
9 M. Verzele and E. Geeraert, *J. Chromatogr. Sci.*, 18 (1980) 559.
10 R. E. Majors, *J. Chromatogr. Sci.*, 18 (1980) 488.
11 D. L. Strack and M. L. Abbot, *Waters Bulletin B24*, Waters Associates, Milford, MA, 1979, p. 10.
12 W. D. Bowers, M. L. Parsons, R. E. Clement, G. A. Eiceman and F. W. Karasek, *J. Chromatogr.*, 206 (1981) 279.
13 J. Huber, Burdick and Jackson Labs., Muskegon, MI, personal communication, May 1981.
14 R. P. W. Scott, *J. Chromatogr. Sci.*, 18 (1980) 297.
15 I. Salmeen, A. M. Durisin, T. J. Prater, T. Riley and D. Schuetzle, *Mutation Res.*, March (1982) in press.
16 M. Selucky, T. Ruo, Y. Chu and O. P. Strausz, in P. C. Uden, S. Siggia and H. B. Jensen (Editors), *Analytical Chemistry of Liquid Fuel Sources (Advances in Chemistry Series 170)*, American Chemical Society, Washington, DC, 1978, Ch. 8.
17 S. Marsh and C. Grandjean, *J. Chromatogr.*, 147 (1978) 411.

Journal of Chromatography, 235 (1982) 536–538
Elsevier Scientific Publishing Company, Amsterdam — Printed in The Netherlands

CHROM. 14,425

Note

Cation-exchange chromatography of histamine in the presence of ethylammonium chloride

C. L. METT and R. J. STURGEON*,*
American McGaw, Irvine, CA 92714 (U.S.A.)
(First received April 27th, 1981; revised manuscript received September 29th, 1981)

The potent vasopressor substance histamine has been characterized by a number of methods including thin-layer chromatography[1], ion-exchange chromatography using a fluorescent derivative[2], and several reversed-phase high-performance liquid chromatographic (HPLC) methods[3,4] using derivatization after extraction. Since intravenous injection of small quantities of histamine can cause undesirable physiological responses in humans[5], it is desirable to have an easy, fast and accurate means of analysis for histamine.

In this paper we describe a fast, accurate method of analyzing histamine which requires no derivatization or extraction and is applicable to commercial amino acid solutions, whole blood and other biological fluids. The use of small amounts of ethylammonium ions to decrease retention and the effects of pH of the mobile phase on separation are discussed.

EXPERIMENTAL

Cation-exchange HPLC was carried out on a 25 cm × 4.6 mm I.D. Partisil 10 SCX column (Whatman, Clifton, NJ, U.S.A.) using a Waters liquid chromatographic system equipped with a Model 6000 A pump, a Model U6K sample injector and a Schoeffel Model SF-770 variable-wavelength detector operated at 210 nm. All measurements and chromatography were at room temperature. The mobile phase consisted of 0.03 *M* K_2HPO_4 in distilled water at pH 4.5. Ethylamine hydrochloride at 0.2%, 0.25% and 0.5% was added to the mobile phase to decrease retention of histamine. The mobile phase was filtered through a 0.45-μm Millipore Type HA filter before use.

Histamine dihydrochloride (Eastman Kodak, Rochester, NY, U.S.A.) and tryptamine hydrochloride (Aldrich, Milwaukee, WI, U.S.A.) were purchased as analytical reagent grade and used without further purification.

Nephramine® and FreAmine® (American McGaw, Irvine, CA, U.S.A.) are amino acid solutions containing ten (5.4%, w/v) and fifteen (8.5%, w/v) individual amino acids respectively.

Whole blood was lysed by an ultrasonic device and centrifuged to obtain a clear supernate. Saliva was centrifuged and the supernate used for analysis.

* Present address: Merck Sharp & Dohme, West Point, PA 19486, U.S.A.

0021-9673/82/0000–0000/$02.75

RESULTS AND DISCUSSION

Table I contains the effects of ethylammonium chloride concentration on k' for histidine, histamine and tryptamine. As can be seen, increasing the ethylammonium ion concentration substantially alters the k' value for the three components. The addition of ethylammonium ions also greatly improves peak symmetry of histamine and tryptamine. The best separation and a reasonable time of analysis were accomplished using 0.35% ethylammonium chloride. Fig. 1 shows typical chromatograms of histamine in water, an amino acid solution, and plasma. Tryp-

TABLE I

EFFECTS OF ETHYLAMMONIUM CHLORIDE CONCENTRATION ON k' FOR HISTIDINE, HISTAMINE AND TRYPTAMINE IN WATER

Ethylammonium chloride (%, w/v)	k'		
	Histidine	*Tryptamine*	*Histamine*
0	2.92	4.80	6.85
0.20	2.58	4.25	5.45
0.25	2.33	4.15	5.14
0.50	2.16	3.09	3.48

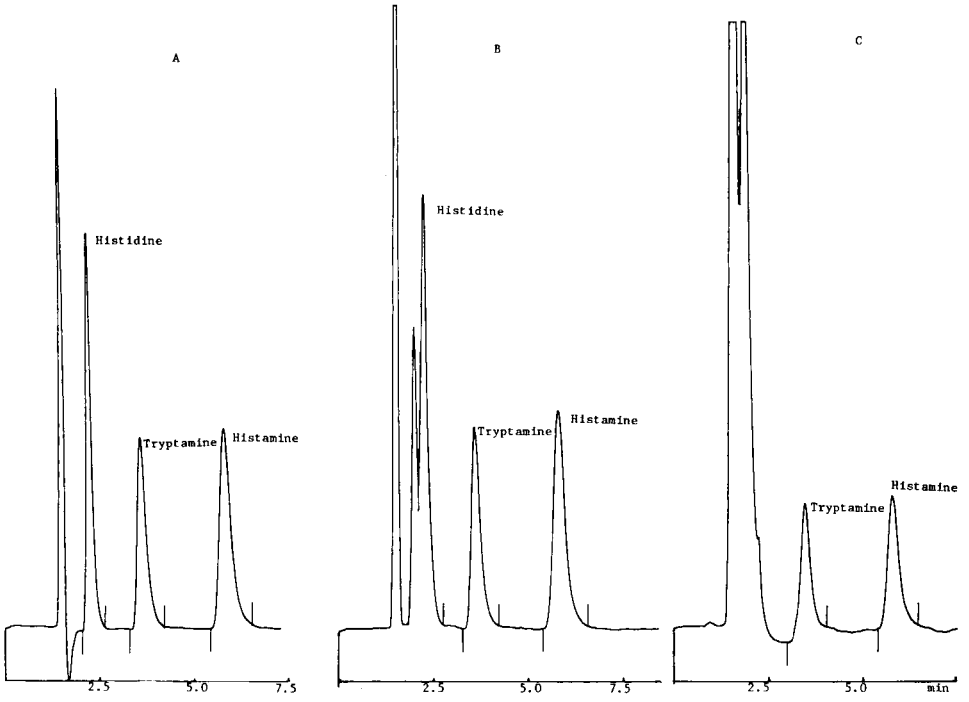

Fig. 1. Chromatograms for the separation of histamine spiked at 25 μg/ml using 2.5 μg/ml of tryptamine hydrochloride as an internal standard and 0.25% ethylammonium chloride in (A) water, (B) FreAmine III and (C) plasma.

tamine was chosen as an internal standard due to its retention lying between that of histidine and histamine.

The common interferences in the analysis of histamine using derivatization methods such as *o*-phthaldehyde are amino acids, proteins and primary and secondary amines[6]. By choosing the mobile phase at pH 4.5, the amino acids, proteins, amines and ethylammonium chloride are completely ionized. The interferences from amino acids and most proteins are eliminated due to their lack of retention in their completely ionized state. A lower pH (2.9) gave longer retention and a higher pH (7.0) gave shorter retention for histamine, but in both cases increased interferences from amino acids and proteins.

Table II contains the limits of detection and actual quantities found for histamine in water, two amino acid solutions, whole blood and saliva. The amino acid solutions showed no detectable quantities of histamine as supplied by the manufacturer.

TABLE II

LIMITS OF DETECTION OF HISTAMINE IN WATER, AMINO ACID SOLUTIONS, PLASMA AND SALIVA USING 0.25% ETHYLAMMONIUM CHLORIDE

Solution	*Limit of detection (μg/ml)*	*Actual quantity found (μg/ml)**
Water	0.020	0
FreAmine	0.020	0
Nephramine	0.020	0
Whole blood	0.050	0.090 ± 0.006
Saliva	0.042	0.150 ± 0.010

* Mean (n = 5) ± S.D.

The results of this investigation indicate that this technique can successfully and conveniently determine histamine in a variety of solutions without extraction and/or derivatization. It is also anticipated that the use of ethylammonium ions can decrease retention and improve peak shape of selected amines when using cation-exchange chromatography under isocratic conditions.

REFERENCES

1 W. Diemair and S. Diemair, *Deut. Wein Ztg.*, 102 (1966) 1146.
2 G. deSaint-Blanquat and R. Derache, *Trav. Soc. Pher. Montpellier*, 28 (1968) 23.
3 R. E. Subden, R. G. Brown and A. C. Noble, *J. Chromatogr.*, 166 (1978) 310.
4 Y. Tsuruta, K. Kohashi and Y. Ohkura, *J. Chromatogr.*, 146 (1978) 490.
5 J. Schneyder, *Mitt. Rebe Wein*, 22 (5) (1972) 313.
6 F. Engbaek and I. Magnussen, *Clin. Chem.*, 24 (1978) 376.

Journal of Chromatography, 235 (1982) 539–543
Elsevier Scientific Publishing Company, Amsterdam — Printed in The Netherlands

CHROM. 14,283

Note

High-speed aqueous gel permeation chromatography of cationic polymers

YOSHIO KATO* and TSUTOMU HASHIMOTO
Central Research Laboratory, Toyo Soda Mfg. Co., Ltd., Tonda, Shinnanyo, Yamaguchi (Japan)
(Received August 12th, 1981)

Although substances are separated on the basis of their molecular sizes in gel permeation chromatography (GPC), they are sometimes eluted earlier or later than predicted due to their interactions with the gel matrices. The solute–gel materix interactions are especially prominent in aqueous GPC[1–6]. Electrostatic adsorption and exclusion effects are well-known with cationic and anionic substances. This is because negatively charged groups are present in many gel matrices. Aromatic substances also have a tendency to adsorb on many gel matrices according to charge-transfer interactions[7]. In addition, hydrophobic interactions and hydrogen bonding interactions sometimes occur with hydrophobic and hydrophilic substances, respectively.

Although these solute–gel matrix interactions can be exploited in the analyses of low-molecular-weight compounds or in the purifications of biological substances such as proteins, they are undesirable in the determination of the molecular weight distributions of polymers. Unfortunately, however, it seems to have been rather difficult to eliminate the interactions for polycationic and polyaromatic samples, in spite of much effort so far. Talley and Bowman[8] succeeded in measuring some cationic polymers on quaternized porous beads. However, since these column packings are not commercially available, their method is easy to reproduce.

Thus, we attempted to measure cationic or cationic and yet aromatic polymers on commercially available TSK-GEL PW type columns (Toyo Soda, Tokyo, Japan) currently used extensively in high-speed GPC of water-soluble polymers[9–11]. Aqueous acetic acid solutions of low pH were employed. This is based on the findings with Sephadex that the adsorption of cationic substances can ne reduced in eluents of low pH where ionization of carboxyl groups on the gel matrices is suppressed[2], and that the adsorption of aromatic substances can be reduced in eluents containing acetic acid, pyridine, phenol or urea[1]. These eluents are expected to be effective also on TSK-GEL PW which like Sephadex contains many hydroxyl groups and small amounts of carboxyl groups.

EXPERIMENTAL

Six types of cationic polymers were studied. DEAE-Dextran, dextran containing diethylaminoethyl groups, was purchased from Pharmacia (Uppsala, Sweden). According to the manufacturer, the weight average molecular weight is *ca.* 500,000

0021-9673/82/0000–0000/$02.75

and the nitrogen content is ca. 3.2%. Glycol chitosan for colloid titration, with a degree of polymerization higher than 400, was obtained from Wako (Osaka, Japan). The iodide salt of poly(trimethylaminoethyl methacrylate) was prepared by polymerizing dimethylaminoethyl methacrylate with α,α′-azobisisobutyronitrile and then quaternizing the obtained polymer with iodomethane in methanol. Two poly(N-methyl-2-vinylpyridine) iodide salts were kindly supplied by Dr. Fukuda of our research laboratory. They were prepared by living polymerization of 2-vinylpyridine and quaternization of the obtained polymer with iodomethane in methanol. The molecular weights of the two samples calculated from the molar ratios of monomer and initiator in the living polymerizations are 90,000 and 230,000. Two poly(4-vinylbenzyltrimethylammonium chloride) samples with number average molecular weights of 40,000 and 120,000 were kindly supplied by Mr. Higo of Nagoya University. Polyamines, SP-200 (20,000) SP-018 (1,800) and SP-003 (300), were purchased from Japan Catalyst Chemicals (Osaka, Japan). The molecular weights are shown in parentheses. Ethylenediamine was purchased from Wako.

GPC measurements were performed at 25°C with a Toyo Soda HLC-803C liquid chromatograph equipped with a refractive index detector RI-8. Three column systems of different separation ranges were employed; that used in any given case depended on the molecular weight ranges of the sample. DEAE-Dextran, glycol chitosan and poly(trimethylaminoethyl methacrylate) iodide salt were measured on a column system consisting of G6000PW and G3000PW, poly(N-methyl-2-vinylpyridine) iodide salt and poly(4-vinylbenzyltrimethylammonium chloride) G5000PW and G3000PW and polyamine on two G3000PW columns. Each column was 60 cm × 7.5 mm I.D. The eluent was 0.5 *M* aqueous acetic acid containing 0.3 *M* sodium sulphate (pH = 2.9) for all the measurements, except for polyamine. Because SP-200 was insoluble in this eluent, polyamine was measured in 0.5 *M* aqueous acetic acid containing 0.5 *M* sodium acetate (pH = 4.8). The flow-rate was 0.7 ml/min. 0.1–0.2% solutions of each sample were prepared and 0.1 ml and 0.5 ml were injected in the measurements of polyamine and all other samples, respectively.

RESULTS AND DISCUSSION

The elution curves obtained are shown in Figs. 1–6. When polymer samples adsorb on the gel matrix, severely distorted elution profiles (sharp start-up and tailing) are usually observed. However, since these features are not seen in all the elution

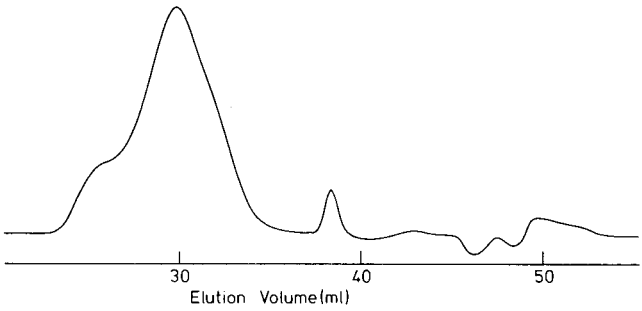

Fig. 1. Elution curve of DEAE-Dextran.

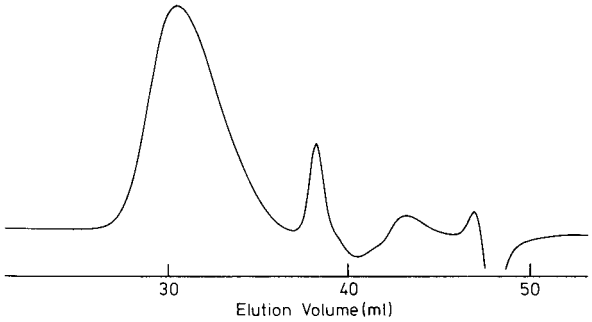

Fig. 2. Elution curve of glycol chitosan.

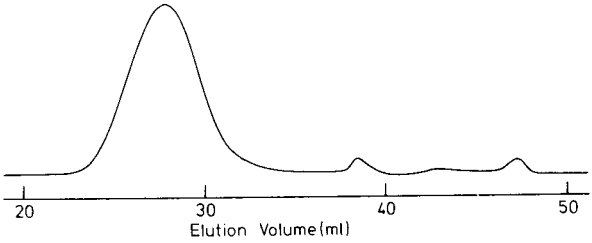

Fig. 3. Elution curve of poly(trimethylaminoethyl methacrylate) iodide salt.

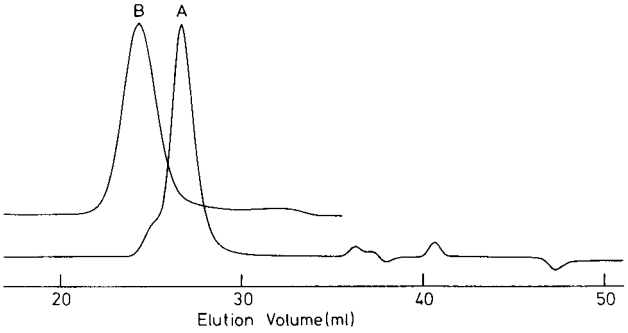

Fig. 4. Elution curves of poly(N-methyl-2-vinylpyridine) iodide salts with molecular weights of 90,000 (A) and 230,000 (B).

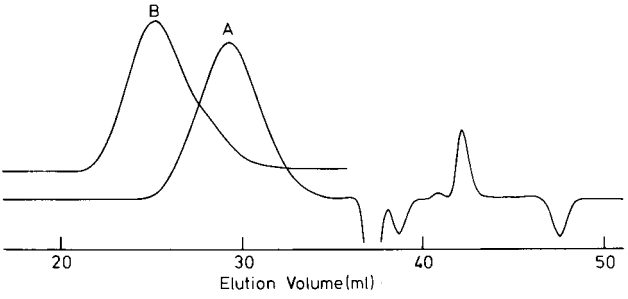

Fig. 5. Elution curves of poly(4-vinylbenzyltrimethylammonium chloride) with molecular weights of 40,000 (A) and 120,000 (B).

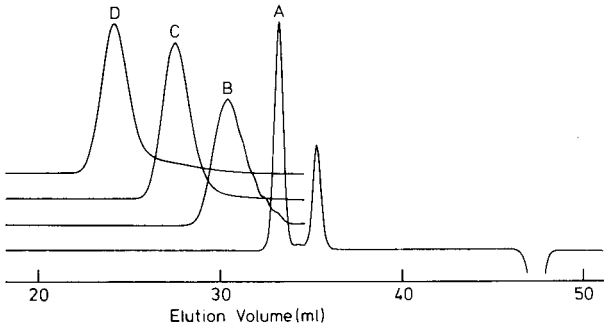

Fig. 6. Elution curves of ethylenediamine (A) and polyamines SP-003 (B), SP-018 (C) and SP-200 (D).

curves in Figs. 1–6, all samples may be considered to be separated in terms of their molecular size without adsorption. The shoulder in the elution curve of DEAE-Dextran at low elution volume can probably be attributed to the molecular weight distribution of this sample. Narrow elution curves accompanied by slight tailing or small humps were obtained with both the poly(N-methyl-2-vinylpyridine) iodide salts, indicating that living polymerizations of these samples proceeded almost ideally.

In the measurements of polyamine, aqueous acetic acid solutions containing sodium nitrate or sodium acetate were examined as eluents because the highest-molecular-weight sample, SP-200, was insoluble in aqueous acetic acid solutions containing sodium sulphate. Sodium nitrate was more effective in preventing adsorption of the samples. However, peaks of this salt and ethylenediamine overlapped as shown in Fig. 7, and could not be separated by adjusting the concentrations of salt and acetic acid. Although the injected solutions were prepared from the eluents, the salt peak always appeared. This is believed to be a result of ion inclusion[3]. At a sodium acetate concentration of 0.5 *M*, on the other hand, the peaks of the salt and ethylenediamine were separated completely, as shown in Fig. 6. However, as the sodium acetate concentration was decreased from 0.5 to 0.3 *M*, the separation became incomplete

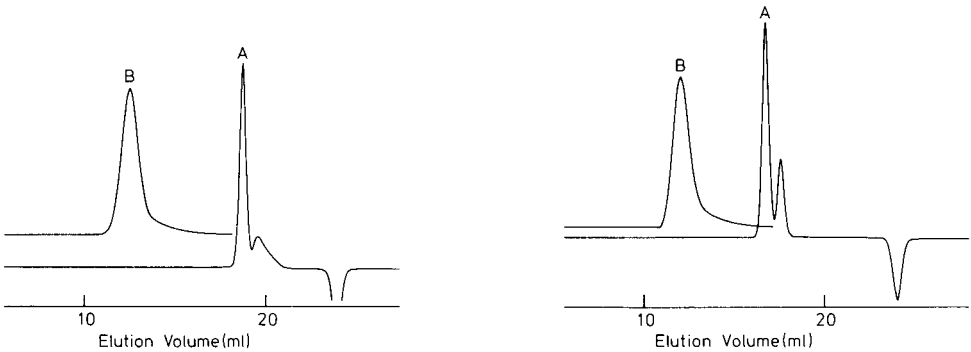

Fig. 7. Elution curves of ethylenediamine (A) and polyamine SP-200 (B) obtained on a G3000PW column with 0.5 *M* aqueous acetic acid solution containing 0.5 *M* sodium nitrate (pH = 2.5).

Fig. 8. Elution curves of ethylenediamine (A) and polyamine SP-200 (B) obtained on a G3000PW column with 0.5 *M* aqueous acetic acid solution containing 0.3 *M* sodium acetate (pH = 4.6).

and there was also a sharp start-up, which is a sign of adsorption, in the elution curve of SP-200, as shown in Fig. 8.

As shown above, aqueous acetic acid solutions containing appropriate salts were found to be very effective in GPC measurements of cationic polymers. An acetic acid concentration of 0.5 *M* was sufficient for all the samples examined. However, since the type and concentration of the salt added seem to affect the adsorption of some samples and the degree of separation between the salt and low-molecular-weight samples, they must be properly selected; 0.3 *M* sodium sulphate, which causes little corrosion of stainless steel at low pH, is recommended as a first choice.

ACKNOWLEDGEMENT

The authors thank Mr. Watanabe and Mr. Umino for valuable discussions.

REFERENCES

1 J. C. Janson, *J. Chromatogr.*, 28 (1967) 12.
2 D. Eaker and J. Porath, *Separ. Sci.*, 2 (1967) 507.
3 B. Stenlund, *Advan. Chromatogr.*, 14 (1976) 37.
4 A. R. Cooper and D. S. V. Derveer, *J. Liq. Chromatogr.*, 1 (1978) 693.
5 H. G. Barth, *J. Chromatogr. Sci.*, 18 (1980) 409.
6 E. Pfannkoch, K. C. Lu, F. E. Regnier and H. G. Barth, *J. Chromatogr. Sci.*, 18 (1980) 430.
7 J. Porath, *J. Chromatogr.*, 159 (1978) 13.
8 C. P. Talley and L. M. Bowman, *Anal. Chem.*, 51 (1979) 2239.
9 T. Hashimoto, H. Sasaki, M. Aiura and Y. Kato, *J. Polym. Sci., Polym. Phys. Ed.*, 16 (1978) 1789.
10 T. Hashimoto, H. Sasaki, M. Aiura and Y. Kato, *J. Chromatogr.*, 160 (1978) 301.
11 Y. Kato, H. Sasaki, M. Aiura and T. Hashimoto, *J. Chromatogr.*, 153 (1978) 546.

Author Index

PUBLICATION SCHEDULE FOR 1982

Journal of Chromatography (incorporating *Chromatographic Reviews*) and *Journal of Chromatography, Biomedical Applications*

MONTH		J	F	M	A	M	J	J	A	S	O	N	D
Journal of Chromatography		234/1 234/2 235/1 235/2	236/1 236/2	The publication schedule for further issues will be published later.									
Chromatographic Reviews													
Biomedical Applications		227/1	227/2										

INFORMATION FOR AUTHORS

(Detailed *Instructions to Authors* were published in Vol. 209, No. 3, pp. 501–504. A free reprint can be obtained by application to the publisher.)

Types of Contributions. The following types of papers are published in the *Journal of Chromatography* and the section on *Biomedical Applications:* Regular research papers (Full-length papers), Short communications and Notes. Short communications are preliminary announcements of important new developments and will, whenever possible, be published with maximum speed. Notes are usually descriptions of short investigations and reflect the same quality of research as Full-length papers, but should preferably not exceed four printed pages. For reviews, see page 2 of cover under Submission of Papers.

Submission. Every paper must be accompanied by a letter from the senior author, stating that he is submitting the paper for publication in the *Journal of Chromatography*. Please do not send a letter signed by the director of the institute or the professor unless he is one of the authors.

Manuscripts. Manuscripts should be typed in double spacing on consecutively numbered pages of uniform size. The manuscript should be preceded by a sheet of manuscript paper carrying the title of the paper and the name and full postal address of the person to whom the proofs are to be sent. Authors of papers in French or German are requested to supply an English translation of the title of the paper. As a rule, papers should be divided into sections, headed by a caption (e.g., Summary, Introduction, Experimental, Results, Discussion, etc.). All illustrations, photographs, tables, etc., should be on separate sheets.

Introduction. Every paper must have a concise introduction mentioning what has been done before on the topic described, and stating clearly what is new in the paper now submitted.

Summary. Full-length papers and Review articles should have a summary of 50–100 words which clearly and briefly indicates what is new, different and significant. In the case of French or German articles an additional summary in English, headed by an English translation of the title, should also be provided. (Short communications and Notes are published without a summary.)

Illustrations. The figures should be submitted in a form suitable for reproduction, drawn in Indian ink on drawing or tracing paper. Each illustration should have a legend, all the *legends* being typed (with double spacing) together on a *separate sheet*. If structures are given in the text, the original drawings should be supplied. Coloured illustrations are reproduced at the author's expense, the cost being determined by the number of pages and by the number of colours needed. The written permission of the author and publisher must be obtained for the use of any figure already published. Its source must be indicated in the legend.

References. References should be numbered in the order in which they are cited in the text, and listed in numerical sequence on a separate sheet at the end of the article. Please check a recent issue for the lay-out of the reference list. Abbreviations for the titles of journals should follow the system used by *Chemical Abstracts*. Articles not yet published should be given as "in press", "submitted for publication", "in preparation" or "personal communication".

Proofs. One set of proofs will be sent to the author to be carefully checked for printer's errors. Corrections must be restricted to instances in which the proof is at variance with the manuscript. "Extra corrections" will be inserted at the author's expense.

Reprints. Fifty reprints of Full-length papers, Short communications and Notes will be supplied free of charge. Additional reprints can be ordered by the authors. An order form containing price quotations will be sent to the authors together with the proofs of their article.

News. News releases of new products and developments, and information leaflets of meetings should be addressed to: The Editor of the News Section, Journal of Chromatography/Journal of Chromatography, Biomedical Applications, Elsevier Scientific Publishing Company, P.O. Box 330, 1000 AH Amsterdam, The Netherlands.

Advertisements. Advertisement rates are available from the publisher on request. The Editors of the journal accept no responsibility for the contents of the advertisements.

Ionic Hydration in Chemistry and Biophysics

by B.E. CONWAY,
Department of Chemistry, University of Ottawa, Ontario, Canada.

STUDIES IN PHYSICAL AND THEORETICAL CHEMISTRY 12

1981 xxx + 774 pages
Price: US $131.75/
Dfl. 270.00
ISBN 0-444-41974-0

This monograph is a comprehensive coverage of all aspects of ionic hydration. Not only is the nature of the phenomenon described, but also its importance in electrochemistry, inorganic and physical chemistry, biophysics and biochemistry. The basic background of techniques and approaches (e.g. electrostatic theory) required for the study and interpretation of ionic hydration in chemistry is included.

CONTENTS: Chapters. 1. Introduction. 2. Properties of the Water Molecule. 3. Properties of Liquid Water as a Solvent for Ions. 4. Scales for Ionic Radii in Gases, Crystals and Solutions. 5. Ionic Solvation in the Gas Phase. 6. Methods for Study of Solvation of Ions. 7. Infrared Spectral Studies on Ionic Hydration. 8. Raman Spectral Studies on Ionic Hydration. 9. Studies of Ionic Solvation by Nuclear and Electron Magnetic Resonance. 10. Elements of Electrostatics for Problems in Ionic Solutions. 11. Relation between Energetics of Ion Hydration and Ionic Processes in Solution. 12. "Real" Solvation Energies: Surface Potential Effects. 13. Solvation Effects in Electrode Processes and Homogeneous Ionic Solutions. 14. Ionic Hydration and the Dielectric Behaviour of Solutions. 15. Calculation of Ionic Hydration Energies. 16. Hydration of Individual Cations and Anions: Specificity of Ion-Solvent Interactions. 17. Hydration of the Proton. 18. Hydration Effects in the Concentration Dependence of Thermodynamic Properties of Electrolyte Solutions. 19. Ion-Pairing and Ionic Hydration. 20. Salting-Out and Salting-In by Electrolytes in Solution. 21. Steric and Stereochemical Effects in Solvation. 22. Entropies of Ions in Solution, and Hydration Entropies. 23. Solute and Solvent Structure Factors in Hydration and the Entropies of Ions in Solution. 24. Hydrophobic Interactions in Ionic Hydration. 25. Electrostriction and the Partial Molal Volumes and Compressibilities of Ions. 26. H_2O-D_2O Solvent Isotope Effects in Ionic Hydration. 27. Dynamical Aspects of Ionic Solvation. 28. Solvation Effects in Conductance of Electrolytic Solutions. 29. Hydration Numbers. 30. Ionic Solvation in Terms of Lewis Acid-Base Interactions. 31. Solvation in Non-Aqueous media. 32. Hydration of Ions at Interfaces in Chemistry and Biology, and the Nature of Liquid Surfaces. 33. Hydrated Ions in Active Transport Processes at Cell Membranes. 34. Hydration of Polyions of Synthetic and Biological Origin. Subject Index.

ELSEVIER

P.O. Box 211,
1000 AE Amsterdam,
The Netherlands,

52 Vanderbilt Ave.
New York, N.Y. 10017.

The Dutch guilder price is definitive. US $ prices are subject to exchange rate fluctuations.

7208